Cancer colorectal et viande rouge : les produits dérivés de la lipoperoxydation induisent différentes réponses d'apoptose, d'autophagie et de Nrf2 dans des cellules coliques normales et prénéoplasiques

Reggie Surya

Université de Toulouse

THÈSE

En vue de l'obtention du

DOCTORAT DE L'UNIVERSITÉ DE TOULOUSE

Délivré par:

Université Toulouse III - Paul Sabatier

Présentée et soutenue par:

Reggie SURYA
Le 5 septembre 2016

Titre:

Red Meat and Colorectal Cancer :
Lipid Peroxidation-Derived Products Induce Different Apoptosis, Autophagy and Nrf2-Related Responses in Normal and Preneoplastic Colon Cells

---

Ecole doctorale et discipline ou spécialité:

ED SEVAB : Pathologie, Toxicologie, Génétique et Nutrition

Unité de recherche :

INRA UMR 1331 TOXALIM

Directeurs de thèse :

Dr . Fabrice PIERRE
Dr. Laurence HUC

Rapporteurs :

Dr. Mojgan DJAVAHERI-MERGNY
Dr. Adrien ROSSARY

Autres membres du jury :

Pr. Catherine MULLER (Présidente)
Pr. Saadia KERDINE-RÖMER
Dr . Fabrice PIERRE
Dr. Laurence HUC

ACKNOWLEDGEMENTS

Firstly, I would like to express my sincere gratitude to my exceptional advisors Dr. Laurence Huc and Dr. Fabrice Pierre for their continuous support for my PhD study and related research, also for their patience, motivation and immense knowledge. Their guidance helped me in all the time of research and writing of this thesis. I could not have imagined having better advisors and mentors for my PhD study.

Besides my advisors, I would also like to thank the members of my thesis committee and examination panel: Dr. Dominique Lagadic-Gossmann, Dr. Nicolas Loiseau, Pr. Catherine Muller, Pr. Saadia Kerdine-Römer, Dr. Mojgan Djavaheri-Mergny and Dr. Adrien Rossary, for their guidance, insightful comments, critical analyses and encouragement, also for their questions which incented me to widen my research from various perspectives.

I thank all fellow labmates in Team E9 (Prevention and Promotion of Carcinogenesis by Food) since my arrival in the team: Dr. Cécile Héliès-Toussaint, Dr. Françoise Guéraud, Dr. Jacques Dupuy, Dr. Nathalie Naud, Dr. Sylviane Taché, Dr. Maryse Baradat, Dr. Sabine Dalleau, Dr. Océane Martin, Dr. Natalie Priymenko, Dr. Vanessa Graillot, Dr. Julia Keller and all the interns. In particular, I am grateful for Pr. Denis Corpet for supporting and recommending me doing my internship and PhD study in this incredible team. My sincere thanks also goes to Dr. Thierry Gauthier who helped me realize experiments related to confocal microscopy in his sophisticated platform for the last three years.

Last but not the least, I would like to thank sincerely my family and friends, in France, in Indonesia and all over the world, for supporting me spiritually throughout the realization of this thesis and my life in general. I am really grateful to have you all in my life.

ABSTRACT

Red meat is a factor risk for colorectal cancer, considered as probably carcinogenic to humans. Red meat is associated to colorectal cancer through the oxidative properties of heme iron released in the colon. This latter is a potent catalyst for lipid peroxidation, resulting in the neoformation of deleterious aldehydes present in the fecal water of heme-fed rats, including 4-hydroxynonenal (HNE). Fecal water of heme-fed rats preferentially induced mortality in mouse normal colon epithelial cells than in those harboring mutation on *APC* (adenomatous polyposis coli) gene, considered as preneoplastic. This relative resistance of preneoplastic cells to fecal water of heme-fed rats was associated with their higher activity of Nrf2 (Nuclear factor (erythroid-derived 2)-like 2) compared to normal cells, as evidenced by Nrf2 invalidation. To investigate the importance of secondary aldehydes derived from lipid peroxidation, depletion of carbonyl compounds in the fecal water was optimized and this turned out to abolish the difference of mortality between normal and preneoplastic cells. By using human colon epithelial cell (HCEC) lines to approach human physiology, we confirmed that HNE and fecal water of heme-fed rats also induced higher mortality in normal HCECs compared to *APC*-invalidated HCECs, and that higher Nrf2 activity in *APC*-invalidated HCECs was also associated with such a difference. Furthermore, autophagy, found to be up-regulated in *APC*-invalidated HCECs, was suggested to exert protective effects against HNE and fecal water toxicity by activating Nrf2. Taken together, these findings suggest that Nrf2 and autophagy were potentially involved in the resistance of preneoplastic cells upon exposure to HNE or fecal water of heme-fed rats. This different resistance could explain the promoting effect of red meat and heme-enriched diet on colorectal cancer, by initiating positive selection of preneoplastic cells over normal cells.

Keywords:
colorectal cancer, heme iron, lipid peroxidation, 4-hydroxynonenal, Nrf2, autophagy

RESUME

La viande rouge est un facteur de risque du cancer colorectal, considérée comme probablement cancérigène chez l'Homme. Le lien entre la viande rouge et le cancer colorectal impliquerait la lipoperoxydation induite par le fer héminique, aboutissant à la formation d'aldéhydes cytotoxiques présents dans les eaux fécales des rats ayant consommé de l'hème, dont le 4-hydroxynonénal (HNE). Ces eaux fécales ont préférentiellement induit la mort cellulaire dans des cellules coliques murines normales plutôt que dans des cellules coliques murines mutées pour le gène *APC* (adenomatous polyposis coli), considérées comme prénéoplasiques. Cette résistance des cellules prénéoplasiques est associée à une activité plus élevée du Nrf2 (Nuclear factor (erythroid-derived)-like 2) par rapport aux cellules normales, mise en evidence par l'invalidation du Nrf2. Afin de valider l'importance des aldéhydes néoformés derives de la lipoperoxydation, nous avons optimisé la depletion des composes carbonyls dans les eaux fécales qui a aboli le différentiel de mortalité entre les cellules normales et prénéoplasiques. En utilisant des cellules épithéliales coliques humaines (CECH) afin de se rapprocher de la physiologie humaine, nous avons confirmé que le HNE et les eaux fécales des rats ayant consommé de l'hème ont aussi induit une mortalité plus élevée dans les CECHs normales que dans celles invalidées pour *APC* ; et qu'une activité de Nrf2 plus élevée est aussi observée dans ces dernières. L'autophagie, dont le niveau est plus élevé dans les CECHs invalidées pour *APC*, exercerait des effets protecteurs contre la toxicité du HNE et des eaux fécales en activant Nrf2. Globalement, nos résultats suggèrent que le Nrf2 et l'autophagie seraient impliqués dans la résistance des cellules prénéoplasiques suite à une exposition aux eaux fécales des rats ayant consommé de l'hème. Ce différentiel de résistance pourrait expliquer l'effet promoteur de la viande rouge sur la cancérogenèse colorectale, en établissant une sélection positive des cellules prénéoplasiques au détriment des cellules normales.

Mots-clés:

Cancer colorectal, fer héminique, lipoperoxydation, 4-hydroxynonénal, Nrf2, autophagie

TABLE OF CONTENTS

FIGURES AND TABLES

Figures

Tables

ABBREVIATIONS

3-MA : 3-Methyladenine
5-FU : 5-Fluorouracil
aa : amino acid
ACF : Aberrant crypt foci
AGO : Argonaute
AICR : American Institute for Cancer Research
AIEC : Adherent invasive *Escherichia coli*
AIF : Apoptosis-inducing factor
AIM2 : Absent in melanoma 2
ALDH : Aldehyde dehydrogenase
AKR : Aldo-keto reductase
AKT : (see PKB)
AMP : Adenosine monophosphate
AMPK : Adenosine monophosphate kinase
AOR : Alkenal/one oxidoreductase
AP-1 : Activator protein 1
APC : Adenomatous polyposis coli
ARE : Antioxidant response element
ARF : Adenosine diphosphate ribosylation factor
ASEF : APC-stimulated guanine nucleotide exchange factor
ASK1 : Apoptosis signal-regulating kinase 1
ATF6 : Activating transcription factor 6
ATG : Autophagy-related protein
ATG16L1 : Autophagy-related 16 like 1
ATNC : Apparent total N-nitroso compound
ATP : Adenosine triphosphate
B-RAF : v-Raf murine sarcoma viral oncogene homolog B
BAX : BCL-2-associated X protein
Bf : Beef
BMPR1A : Bone morphogenetic protein receptor type 1A
BRCA1 : Breast cancer 1
BTB : Broad complex/tramtracl/bric-a-brac
BUB1 : Budding uninhibited by benzimidazole homolog 1
BVR : Biliverdin reductase
Caspase : Cysteine aspartate-specific protease
CBP : CREB-binding protein
CDC4 : Cell division control protein 4
CDC42 : Cell divison cycle 42
CDK4 : Cyclin-dependent kinase 4
CDX2 : Caudal type homeobox 2
CHD6 :Chromodomain helicase DNA-binding protein 6
CI : Confidence interval
CIMP : CpG island methylator phenotype
CIN : Chromosomal instability
CK1 : Casein kinase 1

CK2 : Casein kinase 2
CLIP-170 : Cytoplasmic linker protein 170
CMAH : CMP-N-acetylneuraminic acid hydroxylase
CO : Carbon monoxyde
CRC : Colorectal cancer
CSC : Cancer stem cell
CtBP : Carboxy-terminal binding protein
CTR : Carbonyl-trapping resine
Cul3 : Cullin 3
CUP : Continuous Update Project
CYP1A1 : Cytochrome p450 family 1 member A1
CYP1A2 : Cytochrome p450 family 1 member A2
DAMP : Damage-associated molecular pattern
DAPK : Death-associated protein kinase
Daxx : Death domain-associated protein
DHN : 1,4-dihydroxynon-2-ene
DHN-MA : 1,4-dihydroxynonane mercapturic acid
DIABLO : Direct IAP binding protein with low pI
DiMeIQx : 2-amino-3,4,9-trimethylimidazo[4,5-f]quinoxaline
DISC : Death-inducing signaling complex
DMF : Dimethylfumarate
DPP3 : Dipeptidyl peptidase 3
Dsh : Dishevelled
EB1 : End binding 1
EGCG : Epigallocatechin-3-gallate
ER : Endoplasmic reticulum
FADD : Fas-associated death domain
FasL : Fas ligand
FAP : Familial adenomatous polyposis
FeNO : Nitrosylated iron
FRA-1 : Fos-related antigene 1
GCL : Glutamate-cysteine ligase
GCLM : Glutamate-cysteine ligase, modifier subunit
Gro : Groucho
GSH : Glutathione (reduced form)
GSK3β : Glycogen synthase-3β kinase
GSSG : Glutathione (oxidized form)
GST : Glutathione *S*-transferase
GSTA4 : Glutathione *S*-transferase A4
GWAS : Genome-wide association study
H2DCF-DA : Dihydrodichlorofluorescein diacetate
H_2O_2 : Hydrogen peroxide
Hb : Hemoglobin
HCA : Heterocyclic amine
HCEC : Human colon epithelial cell
HHE : 4-hydroxyhexenal
HMGB1 : High mobility group box 1
HNA : 4-hydroxynon-2-enoic acid
HNE : 4-hydroxy-2-nonenal
HNPCC : Hereditary non-polyposis colorectal cancer

HPRT : Hypoxanthine-guanine phosphoribosyltransferase
Hrd1 : (see SYVN1)
HSC : Hematopoietic stem cell
HSC70 : Heat shock cognate 70
hTERT : Human telomerase reverse transcriptase
hTID-1 : Human timorous imaginal disc 1
HTRA2 : High temperature requirement protein A
IAP : Inhibitor of apoptosis
IARC : International Agency for Research on Cancer
IBD : Inflammatory bowel disease
Id2 : Inhibitor of DNA binding 2
IFN : Interferon
IGF1 : Insulin-like growth factor 1
IGF2R : Insulin-like growth factor 2 receptor
IL : Interleukin
IPS1 : Interferon β promoter stimulator protein 1
IRGM : Immunity-associated GTPase family M
IQGAP1 : IQ motif-containing GTPase activating protein 1
IRE1 : Inositol-requiring enzyme 1
IVR : Intervening region
JNK : c-Jun N-terminal kinase
K-RAS : Kirsten rat sarcoma viral oncogene homolog
Keap1 : Kelch-like ECH-associated protein 1
KIR : Keap1-interacting region
LAMP-2A : Lysosome-associated membrane protein 2A
LAP : LC3-associated phagocytosis
LC/HRMS : Liquid chromatography/high resolution mass spectometry
LC3 : Light chain 3
LCM : Laser capture/cutting microdissection
LIR : LC3 interacting region
LR : Linker region
LRP5/6 : Low-density lipoprotein receptor-related protein 5/6
Maf : Masculoaponeurotic fibrosarcoma
MAPK : Mitogen-activated protein kinase
MDA : Malondialdehyde
MDF : Mucin-depleted foci
MEF : Mouse embryonic fibroblast
mEH : Microsomal epoxide hydrolase
MeIQx : 2-amino-3,8-dimethylimidazo[4,5-f]quinoxaline
MHCI : Major histocompatibility complex I
Min : Multiple intestinal neoplasia
miRNA : Micro RNA
MLH1 : MutL homolog 1
MMR : Mismatch repair
MMS7 : Matrix metallopeptidase 7
MOMP : Mitochondrial outer membrane permeabilization
MRP : Multidrug resistance protein
MSH2 : MutS homolog 2
MSH6 : MutS homolog 6
MSI : Microsatellite instability

mTOR : Mammalian target of rapamycin
NANA : N-acetylneuraminic acid
NBR1 : Neighbor of breast cancer early-onset 1 gene 1
NDGA : Nordihydroguairetic acid
NDP52 : Nuclear dot protein 52
NF-κB : nuclear factor kappa-light-chain-enhancer of activated B cells
NGNA : N-glycolylneuraminic acid
NLRP3 : NOD-, leucine-rich repeats (LRR)- and pyrin domain-containing protein 3
NO_2 : Nitrite
NOC : N-nitroso compound
NOD2 : Nucleotide-binding oligomerization domain-containing protein 2
NOX : NAD(P)H oxidase
NOXA : (see PMAIP1)
NQO1 : NAD(P)H quinone oxidoreductase 1
Nrf2 : Nuclear factor (erythroid derived 2)-like 2
NTA1 : N-acetyl transferase
OPTN : Optineurin
PAH : Polycyclic aromatic hydrocarbon
PALB2 : Partner and localizer of breast cancer 2
PAMP : Pathogen-associated molecular pattern
PARP : Poly (ADP-ribose) polymerase 1
PE : Phosphatidylethanolamine
PERK : Protein kinase RNA-like ER kinase
PhIP : 2-amino-1-methyl-6-phenylimidazo[4,5-b]pyridine
PI3K : Phosphoinositide 3-kinase
PKB : Protein kinase B
PMAIP1 : Phorbol-12-myristate-13-acetate-induced protein 1
PMS2 : Post-meiotic segregation increase 2
PPARd : Peroxidome proliferator-activated receptor delta
PPIB : Peptidylpropyl isomerase B
PRR : Pattern recognition receptor
PRX1 : Peroxiredoxin
PTEN : Phosphatase and tensin homolog
PUFA : Polyunsaturated fatty acid
PUMA : p53 up-regulated modulator of apoptosis
RAC1 : Ras-related C3 botulinum toxin substrate 1
Rbx1 : Ring-box 1
RIG-I : Retinoic acid-inducible gene I
RLIP76 : RalA-binding protein 16 encoded 76-kDa splice variant
ROS : Reactive oxygen species
RPE : Retinal pigment epithelium
RPLP0 : Large ribosomal protein
RXRα : Retinoic X receptor alpha
SCF : Skp I-Cullin-F box
shRNA : small hairpin RNA
siRNA : small interfering RNA
Skp1 : S-phase kinase-associated protein 1
SLR : Sequestosome 1-like receptor
Smac : Second mitochondria-derived activator of caspase
SMAD4 : Mothers against decapentaplegic homolog 4

SOD : Superoxide dismutase
SQSTM1 : Sequestosome 1
STK : Serine/threonine kinase
SYVN1 : Synoviolin
TA : Transit amplifying
TAK1 : TGFβ-activated kinase 1
TBARS : Thiobarbituric acid reactive species
tBHQ : Tertiary butylhydroquinon
TCF/LEF : T-cell factor/lymphoid enhancer factor
TCR : T-cell receptor
TGFβ : Transforming growth factor beta
TGFBR2 : TGFβ receptor 2
T_H17 : T cell helper 17
TLR : Toll-like receptor
TNF : Tumor necrosis factor
TNFR1 : Tumor necrosis factor receptor 1
TRADD : TNF receptor-associated death domain
TRAF6 : TNF receptor-associated factor 6
TRE : TPA (12-O-Tetradecanoylphorbol-13-acetate)-responsive element
TRX : Thioredoxin
TRX1 : Thioredoxin 1
Ub : Ubiquitin
UBD : Ubiquitin binding domain
Ubx : Ultrabithorax
ULK1 : unc-51-like autophagy activating kinase 1
uPAR : Urokinase plasminogen activator surface receptor
UPR : Unfolded protein response
VPS34 : Vacuolar protein sorting 34
WCRF : World Cancer Research Fund
WHO : World Health Organization
Wnt : Wingless/Integrated
XBP1 : X-box-binding protein 1
xCT : Cystine/glutamate antiporter
Z-VAD-FMK : Benzyloxycarbonyl-Val-Ala-Asp (OMe) fluoromethylketone

Chapter I
INTRODUCTION

1.1. Introduction to colorectal cancer

1.1.1. Characteristics of colorectal cancer

Colorectal cancer (CRC) is the third most frequently diagnosed cancer worldwide, which makes up about 10% of all cancer cases. It is ranked second in women after breast cancer while in men it is ranked third after lung and prostate cancer. In terms of global mortality by cancer, CRC is ranked fourth behind breast cancer, prostate cancer and lung cancer. In 2012, 1.4 million new global cases of CRC have been identified with 694,000 reported deaths from the disease. The incidence of CRC is more common in affluent countries, where 65% of cases were found. It also tends to commonly develop in men than in women [1-3]. In France, 42,152 new CRCs and 17,722 deaths caused by CRC were reported in 2012. The survival rate of CRC patients is 79% (in 1 year), 56% (in 5 years) and 50% (in 10 years) following first diagnostics [4]. The survival rate, however, depends on how advanced the cancer is, the possibility of cancer removal through surgery, and the person's general health condition [5].

The signs and symptoms of CRC depend on the location of the tumor in the bowel and whether the cancer itself has spread elsewhere in the body (metastasis). The classic warning signs include the presence of blood in the stool, worsening constipation, decrease in stool caliber, loss of appetite, loss of weight, and sometimes, vomiting. While rectal bleeding or anemia are high-risk features in those over the age of 50, other commonly-described symptoms including weight loss and changes in bowel habit are typically only concerning if associated with bleeding [6,7].

The common diagnosis of CRC consists in obtaining a sample of the colon during a sigmoidoscopy or colonoscopy. While sigmoidoscopy only allows the observation of anus, rectum, and lower part of colon, colonoscopy enables the observation of entire colon in addition to rectum and anus. This observation is usually accompanied by removal or isolation of colon tissues which are suspicious for possible tumor development, such as polyps for further analyses [5,8].

The treatments for CRC can be aimed at cure or palliation, depending on the person's health and preferences, as well as the stage of the tumor [9]. The cancer detected at early stage can be removed during a colonoscopy [5]. For people with localized cancer, complete surgical removal attempting at achieving a cure is the most common. In case of metastasis, some parts of the organs in which the cancer has spread can also be removed if possible (in most cases, lungs and liver) [8]. Chemotherapy medications are preferred for late-stage colorectal cancer (stage III or IV). Chemotherapy drugs for this condition may include capecitabine, fluorouracil, irinotecan and oxaliplatin [10]. Palliative care may implicate non-curative surgical removal of some cancer tissues, bypassing part of the intestines, or stent placement. These procedures can be considered to improve symptoms and reduce complications such as bleeding from the tumor, abdominal pain, or intestinal obstruction [11]. Non-operative methods of palliative treatments include radiation therapy to reduce tumor size and medications to relieve pain [12].

Several risk factors regarding CRC have been identified and established. Among the known risk factors, physical activity and dietary fiber appear to be convincing factors that decrease the colorectal cancer risk whereas red meat, processed meat, alcoholic drinks (in men, considered as probable increasing risk in women) and body fatness are considered as convincing factors that increase the colorectal cancer risk. Garlic, milk and calcium are categorized as factors that probably decrease the risk of colorectal cancer [1]. Some studies revealed that people suffering from inflammatory bowel disease (Crohn's disease and ulcerative colitis) are at increased risk of CRC. The reported risks in meta-analysis studies were 2.5 (95% CI 1.3-4.7) and 2.4 (95% CI 2.1-2.7) for Crohn's disease and ulcerative colitis respectively [13,14]. However, people with inflammatory bowel disease account for less than 2% of annual CRCs [15].

1.1.2. Presentation of colon-rectum anatomy

Colon and rectum are the last part of human digestive system connecting small intestine and anus in which fecal matters are formed. With the cecum, they construct the large intestine. Unlike the small intestine, the colon does not play a major role in absorption of nutrients. Its main role is extracting water and salt from solid wastes before they are excreted from the body. It is also the site in which flora-aided fermentation of unabsorbed material ensues [16]. The average length of human colon is 155 cm (range of 80-214 cm) for women

and 166 cm (range of 80-313 cm) for men, making up about 20% of the whole length of gastrointestinal tract [17].

Human colon consists of four sections (Figure 1): 1) ascending colon (also called proximal colon) on the right side of the abdomen which is connected to the small intestine by a section of bowel called the cecum, 2) transverse colon located in the upper part of the abdomen which links ascending and descending colon, 3) descending colon (also called distal colon) on the left side of the body, and 4) sigmoid colon (called so for its S-like shape) which is linked with rectum. Rectum is about 12 cm in long and acts as temporary storage site for feces before defecation [18].

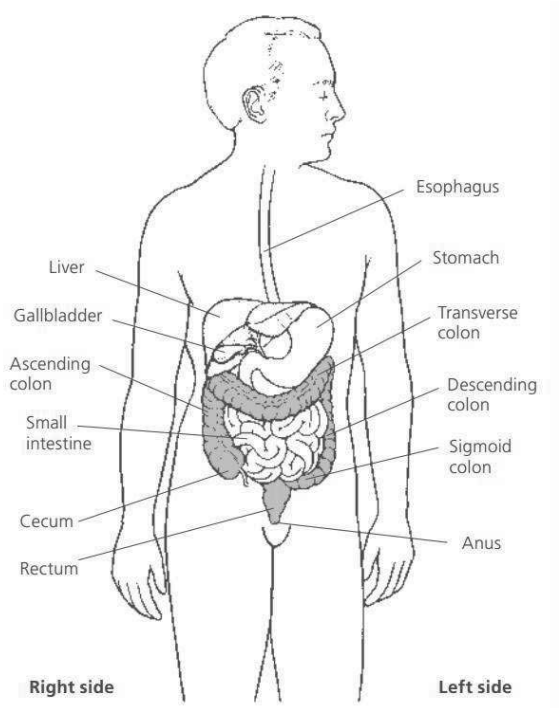

Figure 1. Anatomy of human colon and rectum [19].

The wall of colon and rectum is composed of four layers (Figure 2A): 1) mucosa, the inner layer consisting of simple columnar epithelium with invaginations called colonic crypts (crypts of Lieberkühn), 2) submucosa, a fibrous connective tissue layer containing fibroblasts, mast cells, and blood and lymphatic vessels, 3) muscularis (muscularis propria), two layers of smooth muscle mainly responsible for contractility, and 4) serosa (adventitia), the outermost layer of connective tissues [20].

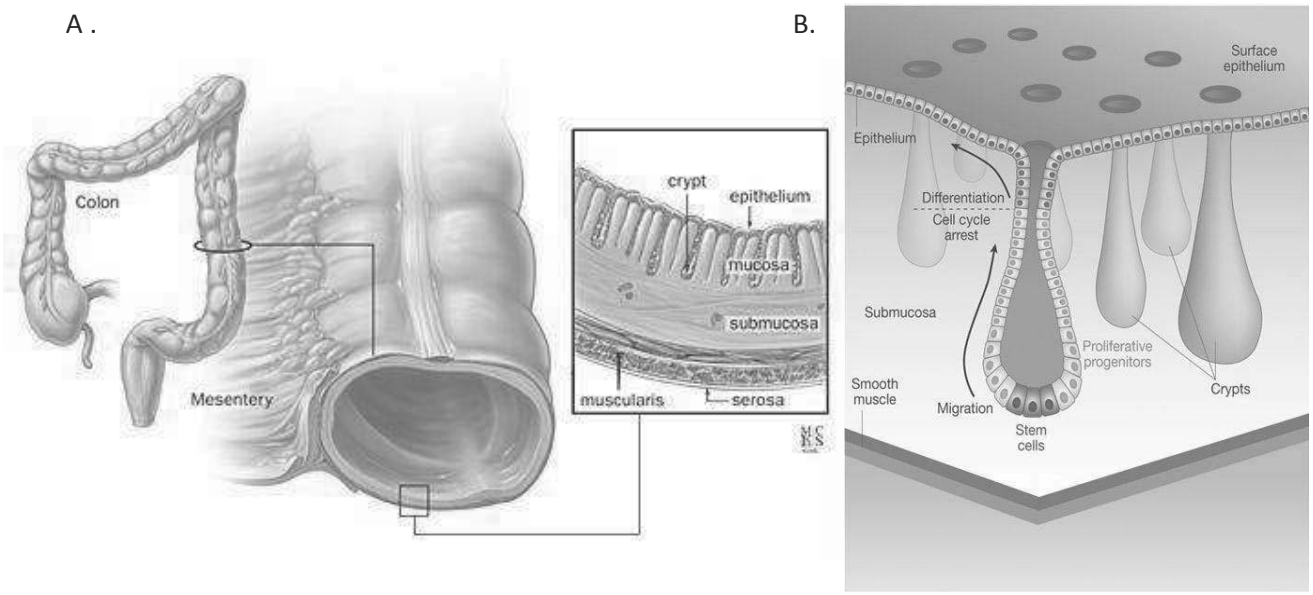

Figure 2. Structure of A) colon wall [21] and B) colon epithelium with its crypts [22].

As mentioned above, the epithelial inner surface of the colon mucosa is punctuated by invaginations, the colonic crypts. These latter are shaped like microscopic thick walled test tubes with a central hole down the length of the tube (the crypt lumen). Several types of epithelial cells construct the colonic crypts and epithelial surface: 1) colonocytes (absorptive cells) which absorb water and electrolytes, 2) mucus-secreting goblet cells, 3) hormone-secreting enteroendocrine cells, and 4) stem cells at the bottom of the crypts [23]. The average circumference of a crypt is 23 cells [24] with 1,500-4,900 cells constructing a crypt [25]. Stem cells produce proliferative progenitors (also known as transit amplifying cells or TA cells) which migrate upward along the crypt axis and differentiate into epithelial cells with specific functions before being shed into the colonic lumen (Figure 2B). The complete turnover of this process is every 4-5 days. There are 5-6 stem cells at the base of the crypts [24].

The homeostasis of colonic epithelium depends on a dynamic equilibrium between rapid stem cells proliferation and cellular differentiation. Any disruption of this equilibrium, such as uncontrolled cellular growth or proliferation might lead to cancer.

1.1.3. Types of colorectal cancer

Two major types of CRC are discussed in this chapter: 1) hereditary forms of CRC and 2) sporadic CRC.

1.1.3.1. Hereditary forms of colorectal cancer

While the majority cases of CRC are sporadic, a significant minority occur as a result of inherited genetic mutation. Two major forms of hereditary CRC are: 1) familial adenomatous polyposis (FAP) and 2) hereditary non-polyposis colorectal cancer (HNPCC). These latter account for about 5% of all CRCs [26].

1.1.3.1.1. Familial adenomatous polyposis

Familial adenomatous polyposis (FAP) represents 0.5%-1.0% of all CRCs [27]. The clinical features of FAP include hundreds to thousands of adenomatous polyps in the colon and rectum that usually appear during adolescence or the third decade of life [26]. CRC is the inevitable consequence of FAP if the condition is left untreated. The only treatment of FAP consists of surgical resection of colon or rectum by colectomy. This act aims at eliminating the risk of subsequent CRC development in the area proven to develop FAP [28]. Attenuated FAP is a phenotypic variant of FAP characterized by the presence of less than 100 adenomatous polyps [29].

The origin of FAP is a mutation on a tumor suppressor gene adenomatous polyposis coli (*APC*) located on the chromosome 5q. This mutation contributes to a loss of cellular growth control [30]. APC mutation, which occurred in 100% of FAP cases and nearly 70-80% of all colorectal tumors, is believed to be an early event in the colorectal tumorigenesis process [27,31,32].

1.1.3.1.2. Hereditary non-polyposis colorectal cancer

Hereditary non-polyposis colorectal cancer (HNPCC), also known as Lynch syndrome, is the most common form of hereditary colorectal cancer which accounts for 2%-4% of all CRCs [33]. It is characterized by the tendency of tumors to be present in the proximal colon and also in other organs (small intestine, ovary, stomach, endometrium, urinary tract, hepatobiliary tract). This syndrome is divided into Lynch syndrome I (familial colon cancer) and Lynch syndrome II (HNPCC associated with other cancers of the gastrointestinal or reproductive system). The increased cancer risk is due to inherited mutations that degrade the self-repair capability of DNA [34].

The identification of HNPCC kindreds has been facilitated by the Amsterdam criteria defined by the International Collaborative Group on HNPCC. These criteria state that: 1) CRC should be present in at least three relatives where one is a first-degree relative of others,

2) CRC should occur in at least two generations of a family, and 3) at least one CRC should be diagnosed before the age of 50 years [26,35].

HNPCC is caused by mutations in one of the mismatch repair (MMR) genes, most commonly *MLH1* (MutL homolog 1), *MSH2* (MutS homolog 2), *MSH6* (MutS homolog 6) and *PMS2* (Post-meiotic segregation increase 2). The condition is inherited as an autosomal dominant with an 80% life-time risk of colorectal cancer [36]. The MMR system is necessary for maintaining genomic stability by correcting single-base mismatches and insertion-deletion loops that form during DNA replication. Dysfunctional MMR may lead to microsatellite instability (MSI), which is observed in more than 90% of colorectal tumors from HNPCC patients [37]. Microsatellites are repeated sequences of DNA made of repeating units of one to six base pairs in length, generally in non-coding regions of genome. MSI affects the genome only in rare case where the microsatellites are located in the coding regions of DNA, such as in the case of gene *TGFβ* (transforming growth factor beta) involved in cellular proliferation or *BAX* (BCL-2-associated X protein) involved in apoptosis machinery [38].

1.1.3.1.3. Other forms of hereditary polyposis syndrome

There are other, very rare forms of inherited polyposis syndrome that are associated with an increased risk of CRC. These include: 1) juvenile polyposis characterized by polyps formation in colon and rectum which usually begins before the age of 10 years. Mutations on gene *SMAD4* (Mothers against decapentaplegic homolog 4), *PTEN* (Phosphatase and tensin homolog) and *BMPR1A* (Bone morphogenetic protein receptor type IA) are responsible for this syndrome, 2) Peutz-Jegher's syndrome characterized by polyps formation primarily in stomach and small intestine. This syndrome is related to mutations on gene *STK11* (Serine/threonine kinase 11) [26].

1.1.3.2. Sporadic colorectal cancer

The sporadic form represents about 90% of total CRCs, 15% and 70%-80% of which carry a mutation on MMR and *APC* gene respectively [39,40]. The development of CRC consists of the transition from normal colorectal epithelium to adenoma (benign tumor) to carcinoma (malignant tumor) which is associated with acquired sequential molecular events, mostly mutations [41-43]. A recent statistical study using mathematical models to compare the mutation rates and the rates of human CRC development revealed that only three driver gene mutations were required for CRC development [44]. There are two major pathways by

which alterations of molecular events can lead to colorectal cancer: chromosomal instability (CIN) and microsatellite instability (MSI) (Figure 3). These tumor progression models were deduced from comparison of genetic alterations observed in normal colon epithelium, adenomas of progressively larger size, and malignancies [45]. While the majority of CRCs are due to events resulting in CIN, 20%-30% of them display characteristic patterns of gene hypermethylation, termed CpG island methylator phenotype (CIMP), of which a portion display MSI (15%) [46-48].

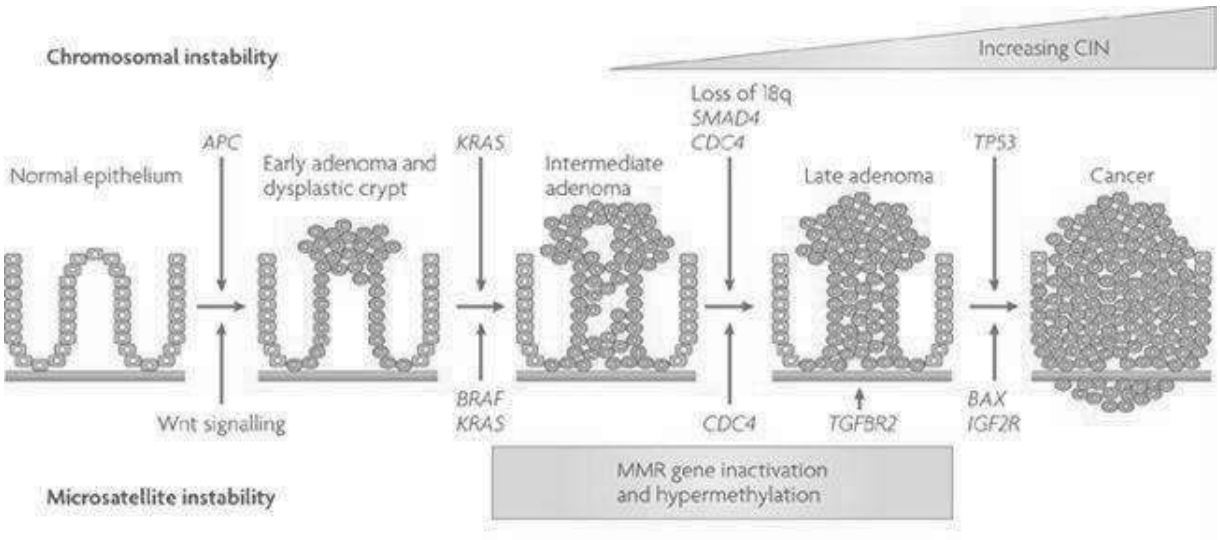

Figure 3. Adenoma-carcinoma sequence model for chromosomal and microsatellite instability in colorectal tumorigenesis [49].

Key changes in CIN cancers include widespread alterations in chromosome number (aneuploidy) and frequent detectable losses at the molecular level of portions of chromosome 5q, 18q and 17p; and mutation of the *K-RAS* (Kirsten rat sarcoma viral oncogene homolog) (Figure 3, upper panel). Among the earliest events in the colorectal tumorigenesis is the loss of *APC* gene (5q). Larger adenomas and early carcinomas acquire mutations in the small GTPase *K-RAS*, followed by loss of chromosome 18q with *SMAD4* and *CDC4* (cell division control protein 4) implicated in signal transduction and DNA replication respectively, and mutations in *p53* (17p) in frank carcinoma [49].

MSI-related CRC (Figure 3, lower panel), characterized by a deficiency of the mismatch repair system that leads to slippage in microsatellites, only carry the molecular events observed in CIN-related CRC infrequently. Therefore, the development of CRC through MSI must involve different but analogous genetic changes to those decribed in CIN-

related CRC. The initial of MSI-related colorectal tumorigenesis is thought to involve alterations in Wnt (Wingless/Integrated) signaling (discussed later, in 1.1.5.2.1), possibly involving axin. Mutations in *B-RAF* (v-Raf murine sarcoma viral oncogene homolog B), commonly observed in MSI-related CRC, are likely to occur in the place of *K-RAS* mutations although the latter do occur in a minority of cases. Mismatch repair (MMR) deficiency in sporadic CRC occurs predominantly by downregulation of *MLH1* by promoter methylation. Mutations of *MSH3* and *MSH6* which lead to their inactivation are also observed. Inactivation of MMR genes affect mutations of genes carrying microstallites in their coding region through which the tumorigenesis gets advanced. Among these genes are TGFβ receptor 2 (*TGFBR2*), insulin-like growth factor 2 receptor (*IGF2R*) and *BAX* [49].

1.1.4. Heterogeneity of colorectal cancer

In general, tumor heterogeneity describes that different tumor cells can show distinct phenotype profiles, including cellular morphology, gene expression, metabolism, motility, proliferation and metastatic potential. This phenomenon may occur both among tumor subtypes (inter-tumor heterogeneity) and among cells constituting a tumor (intra-tumor heterogeneity) [50-52]. Indeed, tumor heterogeneity has been observed in numerous cancers including colorectal cancer [53-55]. There are two existing models that are generally used to explain tumor heterogeneity: (1) cancer stem cells model and (2) clonal evolutional model. Both models are not mutually exclusive and it is believed that they both contribute to heterogeneity in varying amounts across different tumor types [52].

The cancer stem cell model posits that there is only a small portion of cells within a population of tumor cells that are tumorigenic (able to form tumors). These cells are termed cancer stem cells (CSCs) and are marked by their ability to self-renew, drive tumor growth and generate tumor cell progeny forming the tumor bulk. This model points out that the heterogeneity observed between tumor cells results from the variability of the stem cells from which they were originated. Stem cell variability is often caused by epigenetic changes or accumulation of mutations through carcinogenesis [51,52].

The clonal evolution model emphasizes that tumors arise from a single mutated cell that accumulates additional mutations as it progresses (Figure 3) [51,56]. These mutations give rise to additional subpopulations and each of these subpopulations possesses the ability to divide and undergo further mutations. This heterogeneity later gives rise to subclones that possess evolutionary advantages over the others within the tumor environment and these

subclones may become dominant in the tumor over time [57,58]. The long-term accumulation of mutations may provide selective advantages to certain pressures (such as unfavored tumor microenvironment or exposure to drugs) during tumor progression [59].

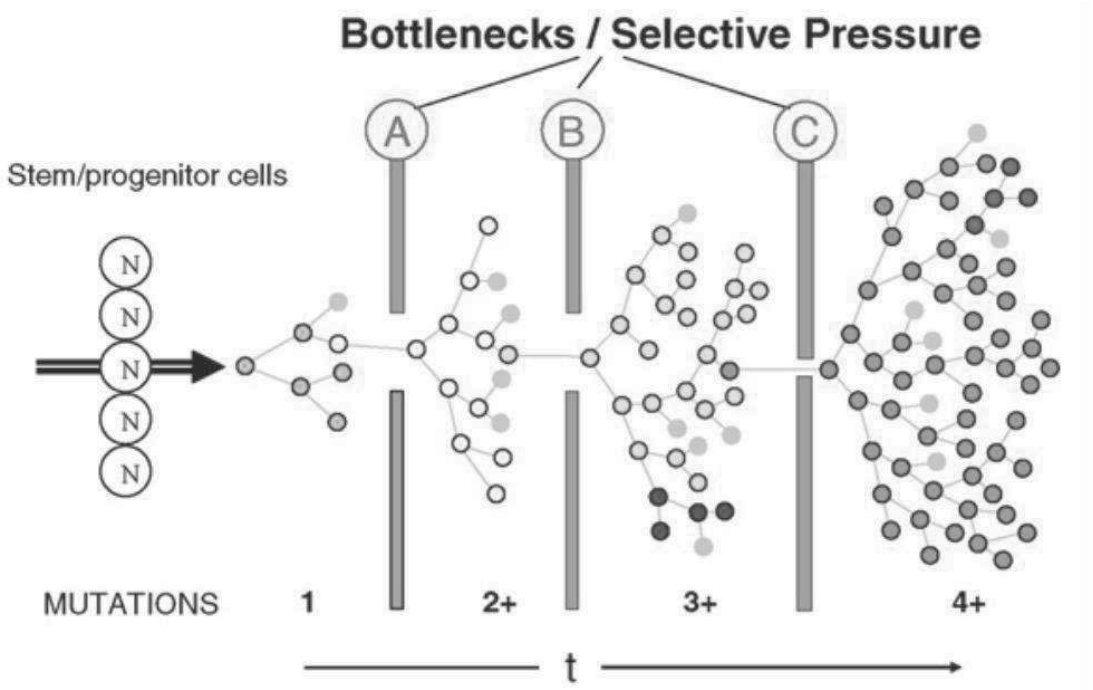

Figure 4. Clonal evolution of a cancer [51].
N: normal cells; A and B: intracellular and intercellular/microenvironmental constraints; C: decimation by drugs; t: time. Different colored cells: distinctive mutant genotypes.

A well-known implication of tumor heterogeneity is the treatment resistance following chemotherapy. Heterogenous tumors exhibit different phenotypes, including different sensitivity towards tumor microenvironment or cytotoxic drugs among different clonal populations. Tumor microenvironment is capable of altering selective pressures to which tumor cells are exposed. Drug administration in heterogenous tumors seldom kills all tumor cells. The initial heterogenous population may bottleneck in a manner that such few cells that are resistant to tumor microenvironment and cytotoxic drugs will survive (Figure 4). This mechanism, which resembles Darwin's theory of natural selection, would allow resistant tumor populations to replicate and grow new tumors that would be resistant to the initial drug therapy used. The repopulated tumors may appear to be more aggressive and this is attributed to the drug-resistant selective advantages of the tumor cells [50-52,60]. The mutation-driven resistance of cancer cells towards tumor microenvironment and drugs may also explain the tumorigenesis of CRC. Interestingly, this different resistance is also observed during the early

stages of colorectal carcinogenesis, therefore highlighting the importance of this mechanism in CRC promotion. Different resistance between normal and preneoplastic colon cells towards lipid peroxidation-derived products has been suggested to explain the mechanisms by which red meat consumption may promote CRC (discussed later in Chapter 1.3.3) [61-63].

1.1.5. Roles of adenomatous polyposis coli (*APC*) in colorectal cancer

As previously mentioned, mutations in the *APC* gene are considered as one of the earliest events in the initiation and progression of CRC. This highlights the important roles of *APC* in CRC development. While *APC* mutation directs tumor progression, *APC* restoration has been shown to regress tumor by reestablishing crypt homeostasis in CRC [64]. Here, the structure and functions of *APC* in several cellular functions including those that are directly implicated in CRC development will be discussed [65].

1.1.5.1. Structure of APC protein

APC gene in human is located in the long (q) arm of chromosome between positions 21 and 22. More precisely, the *APC* gene is located from base pair 112,707,505 to base pair 112,846,239 on chromosome 5. The *APC* gene product is a 310 kDa protein consisting of 2,843 amino acids (aa) localized in both the cytoplasm and the nucleus (Figure 5). It is expressed constitutively within normal colonic epithelium [66].

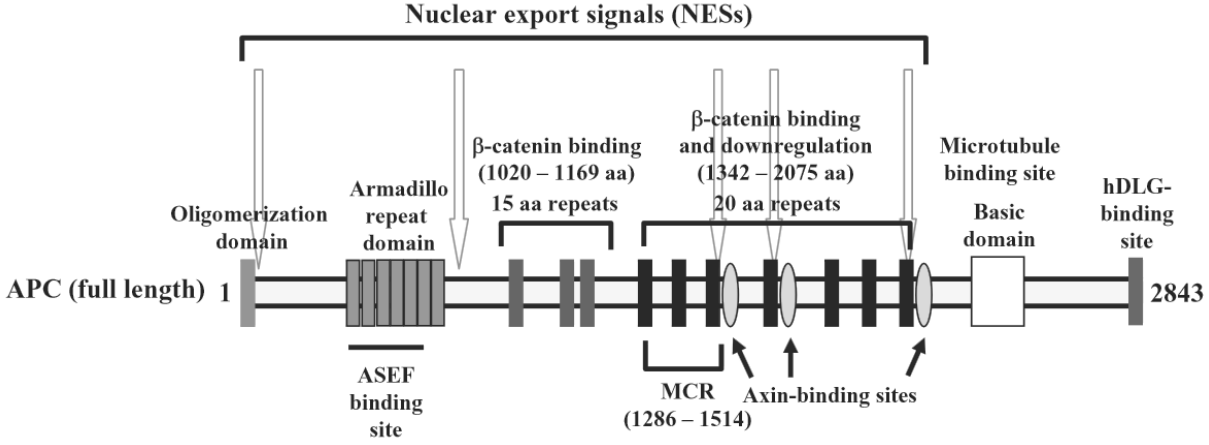

Figure 5. Structural features of APC protein [66].

The structure of APC protein with different protein interaction domains is given in Figure 5. At the N-terminal site, the APC protein contains oligomerization and armadillo repeat binding domain. Armadillo repeat binding domain allows interaction between APC and

ASEF (APC-stimulated guanine nucleotide exchange factor) which is involved in linkage with cytoskeleton. At the C-terminal site, there are EB1 (end binding 1) and tumor suppressor protein DLG binding domains, along with a microtubule binding site. APC protein also contains three 15-aa and seven 20-aa repeat regions which are involved in the binding and regulation of β-catenin in cells. Three axin-binding sites and five nuclear export signals (NESs) allowing nucleus-cytoplasm shuttle have also been identified. Mutator cluster region (MCR) is a domain where most *APC* mutation occurs and creates truncated APC proteins. For example, 30% of FAP cases carry *APC* mutations causing 1061-aa and 1309-aa truncated APC proteins [67,68] (note that the truncation of the latter takes place in MCR). In both cases, the truncated proteins contain β-catenin binding sites in the armadillo repeat binding domain but lose the β-catenin regulatory activity which is located in the 20-aa repeat domain. It is noteworthy that *APC* mutation is observed in 70-80% of sporadic CRCs and 100% of FAP [39,66].

1.1.5.2. Functions of APC protein

APC protein has been shown to be involved in several molecular pathways that regulate the sustainability of colon epithelium. Its principal role is in the regulation of β-catenin *via* Wnt signaling pathway. Apart from this role, APC is also involved in actin cytoskeletal integrity, cell-cell adhesion, cell migration and chromosomal stability [66].

1.1.5.2.1. APC regulates β-catenin levels through Wnt signaling pathway

APC acts indispensably as a negative regulator of β-catenin *via* Wnt signaling pathway in the transformation of colonic epithelial cells and in melanoma progression [69]. *Wnt* genes encode a large family of secreted molecules that have important roles in controlling the fate and proliferation of epithelial cells. In humans, there are at least 19 members of *Wnt* family and 10 members of its receptor family, Frizzled [22]. The Wnt receptor complex is made up of Frizzled and LRP5/6 (low-density lipoprotein receptor-related protein 5/6) [70]. β-catenin is a transcriptional coactivator of transcription factors belonging to the TCF/LEF family (T-cell factor/lymphoid enhancer factor) [66]. The role of Wnt signaling pathway has been described in *Drosophila*, *Xenopus* and in vertebrates; and has been shown to exert important involvement in organ development, morphology, motility, cellular proliferation and the fate of embryonic cells [66,71,72].

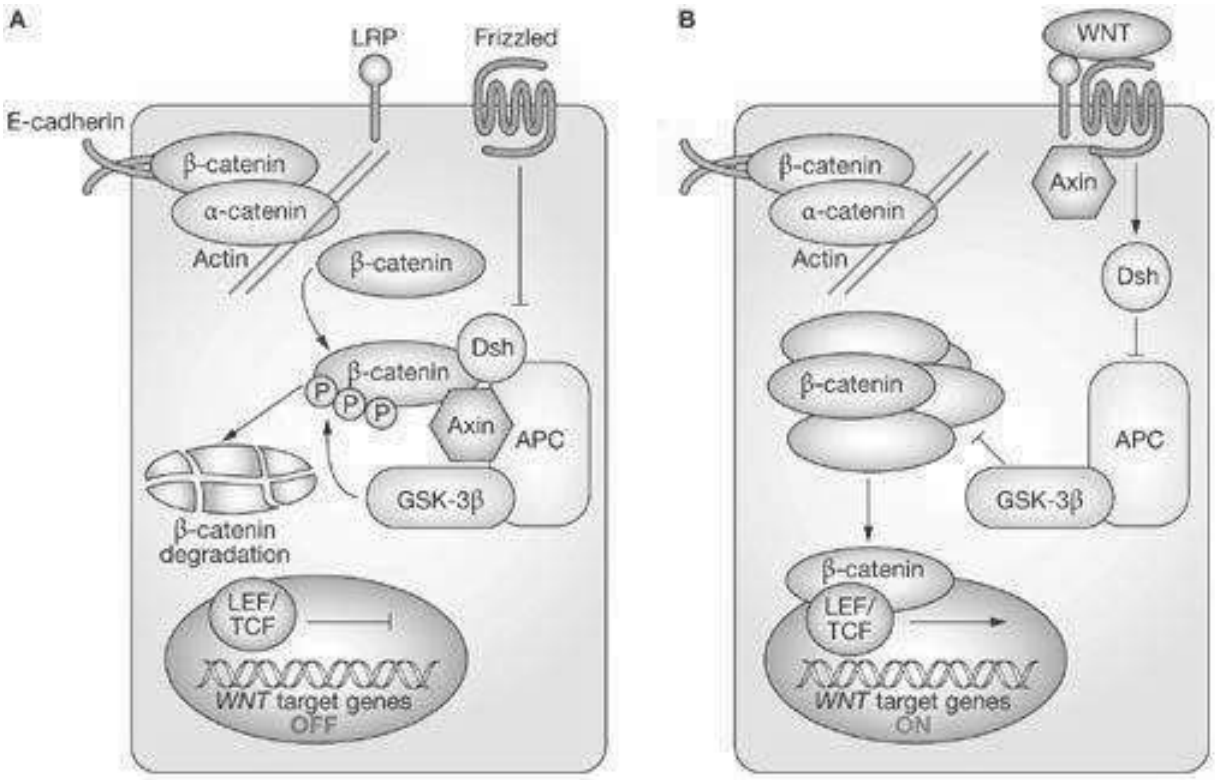

Figure 6. Model for Wnt signaling pathway A) in the absence of Wnt ligand and B) in the presence of Wnt ligand [73].

The level of β-catenin is maintained at a low level through degradation by proteasome. In the absence of Wnt ligand, cytosolic β-catenin, which is normally bound to membranous E-cadherin, interacts with "destruction complex" composed of axin, APC, β-catenin, glycogen synthase-3β kinase (GSK3β) and casein kinase 1 or 2 (CK1 or 2) (Figure 6A). GSK3β and CKA1 or 2 phosphorylate β-catenin at serine and threonine residues in the N-terminal domain. The phosphorylated β-catenin then binds to F-box protein β-TrCP (beta transducin repeat containing protein) of Skp I-Cullin-F-box (SCF) complex of ubiquitin ligases, is ubiquitinated, and undergoes proteasomal degradation. The activity of TCF/LEF transcription factor in the nucleus is inhibited by its repressors and corepressors such as carboxy-terminal binding protein (CtBP), CREB-binding protein (CBP) and Groucho (Gro) [66]. The Wnt target genes are not transcribed. This whole mechanism is important in controlling cell growth.

Wnt signaling pathway is basically a normal mechanism by which cells in the colon crypts are regulated. Stem cells in the bottom of colon crypts are very proliferative and produce proliferative progenitors (transit amplifying cells or TA cells) that will differentiate into epithelial cells such as colonocytes, enteroendocrine cells and goblet cells. In the

presence of Wnt ligand, Wnt signaling pathway is activated (Figure 6B). Axin is recruited to the Frizzled and another protein called disheveled (Dsh) is activated and uncouples β-catenin from the destruction complex. Consequently, the β-catenin is not degraded and activates TCF/LEF transcription factor to transcribe Wnt target genes that promote cellular proliferation. Indeed, Wnt signaling pathway is active in stem cells and TA cells to promote cellular proliferation. However, this pathway is gradually switched off as the cells differentiate and migrate to the top of the crypt (Figure 7). Hyperactivity of Wnt signaling pathway on the top of colonic crypt may cause uncontrolled cell growth and the formation of cellular masses on colon epithelium that are potential to develop cancerousness.

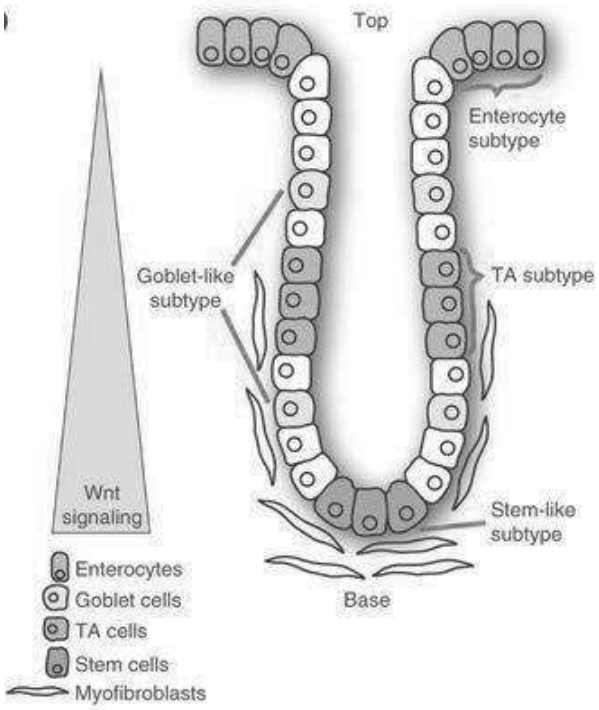

Figure 7. Wnt-signaling along the colon crypt [74].

In the case of *APC* mutation, when *APC* mutation results in the expression of truncated APC protein that does not contain β-catenin binding site (Figure 5), the β-catenin destruction complex is not formed. Therefore, β-catenin escapes its degradation and heterodimerizes with TCF/LEF transcription factor in the nucleus, where it actively transcribes cell cycle-related genes promoting cellular proliferation (*c-myc*, *cyclin D1*). The binding of β-catenin with TCF/LEF inhibits the binding of CtBP, CBP or Gro and therefore potentiates its transcriptional activity [66]. Some other genes which are known to be regulated

by β-catenin/TCF/LEF pathway are *CDH1* (cadherin 1), *TCF-1* (T-cell factor 1), *c-jun*, *FRA-1* (Fos-related antigene 1), *PPARδ* (peroxisome proliferatore-activated receptor delta), *Gastrin*, *uPAR* (urokinase plasminogen activator surface receptor), *MMP7* (matrix metallopeptidase 7), *Conductin*, *CD44*, *Id2* (inhibitor of DNA binding 2), *Siamois*, *Xbra*, *Twin* and *Ubx* (ultrabithorax) [75]. *APC* mutation, which leads to the expression of genes promoting cellular proliferation, may result in uncontrolled cell growth and furthermore, tumor development. Here, *APC* mutation results in a constitutive active Wnt signaling pathway, marked by constitutively active β-catenin activity due to the absence of the β-catenin degradation complex.

1.1.5.2.2. APC is involved in actin cytoskeletal integrity, cell-cell adhesion and cell migration

Actin cytoskeletal integrity is necessary to maintain the shape and adherence of junctions of cells. The imbalance in actin cytoskeletal integrity can cause disturbance in cell-cell adhesion and cell migration. In colon epithelium, α-catenin, through direct binding with actin, maintains intracellular actin cytoskeletal network [66,76]. β-catenin establishes a link between APC and actin by providing a bridge to α-catenin. Along with γ-catenin that is linked to α-catenin, β-catenin also maintains the integrity of E-cadherin, Ca^{2+}-dependent transmembrane protein forming adherent junctions to binds cells within tissues together (Figure 8A). Since APC is one of the building blocks of cytoskeletal integrity, its mutation is likely to disrupt the cytoskeletal network. Truncated APC is not able to bind β-catenin. Therefore, the actin and E-cadherin networks are disrupted, leading to distorted cytoskeletal network, loss of polarity and decreased cell-cell adhesion (Figure 8B).

Via its armadillo-repeated domain, APC can recruit and activate ASEF and IQGAP1 (IQ motif-containing GTPase activating protein 1) [66]. Activated ASEF leads to cascade activation of CDC42 (cell division cycle 42) and RAC1 (Ras-related C3 botulinum toxin substrate 1) which regulate actin polymerization and cell adhesion. *APC*-mutated cells with truncated APC protein have been shown to exhibit ASEF hyperactivity (which is not observed in normal cells with full-length APC protein) and active ASEF is linked to a decrease in E-cadherin-mediated cell-cell adhesion [77,78]. APC and IQGAP1 form a complex with CLIP-170 (cytoplasmic linker protein 170) that links the actin cytoskeleton and microtubule dynamics during cell polarization and directional migration [79]. In addition to these

pathways, N-terminal domain of APC contains an EB1 binding site that is also involved in APC-microtubules linkage [80].

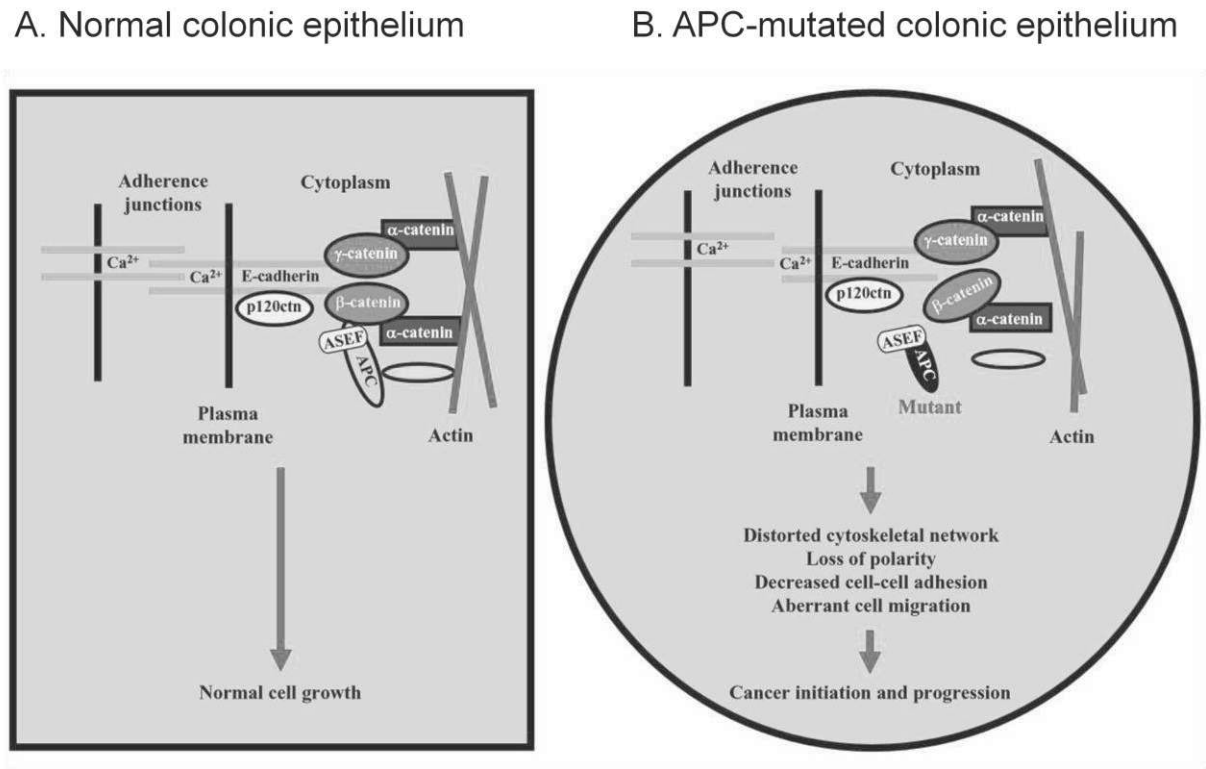

Figure 8. Model for cytoskeletal network in A) normal colonic epithelium and B) *APC*-mutated colonic epithelium ([66] with modifications).

Another important role of APC is assigned in cell migration. Colonic epithelial cells, derived from stem cells, divide in the lower two-third of the crypts and migrate rapidly to the surface to form a single-layer epithelium. *APC* mutation has been shown to affect cell migration. These cells, instead of migrating upwards towards the gut lumen, migrate aberrantly or less efficiently towards the crypt base where they accumulate and form polyps [81]. In due time, the cells acquire β-catenin stabilization and activation of genes for cell proliferation as well as becoming aneuploid due to defects in chromosome segregation (this lastly-mentioned role of APC in chromosome segregation is discussed in part 1.1.5.2.3).

1.1.5.2.3. APC is involved in normal chromosome segregation

Aneuploidy, the abnormal number of chromosomes both quantitatively and qualitatively, is proposed to be a common characteristic of CRC. It is believed that the aneuploidy in CRC arises during mitosis through a defective cell division [66]. Microtubules

possess a substantial role in mitosis by forming mitotic spindle that associates chromosomes. APC, which is able to bind to microtubules, may be involved in maintaining the proper connection of microtubules and chromosomes during cell division.

APC performs a bridging function between microtubules and chromosomes. APC binds to microtubules through EB1, stretches it to the chromosomes, and inserts them to kinetochores after binding with BUB1 (budding uninhibited by benzimidazole homolog 1) [82-84]. The successful complex formation may allow proper growth of spindle formation and helps maintain euploidy (Figure 9A). Truncated APC protein, due to *APC* mutation, may lose its ability to bind with BUB1, and it may become unable to properly maintain the attachment of microtubules at kinetochores, resulting in defective chromosome segregation (Figure 9B).

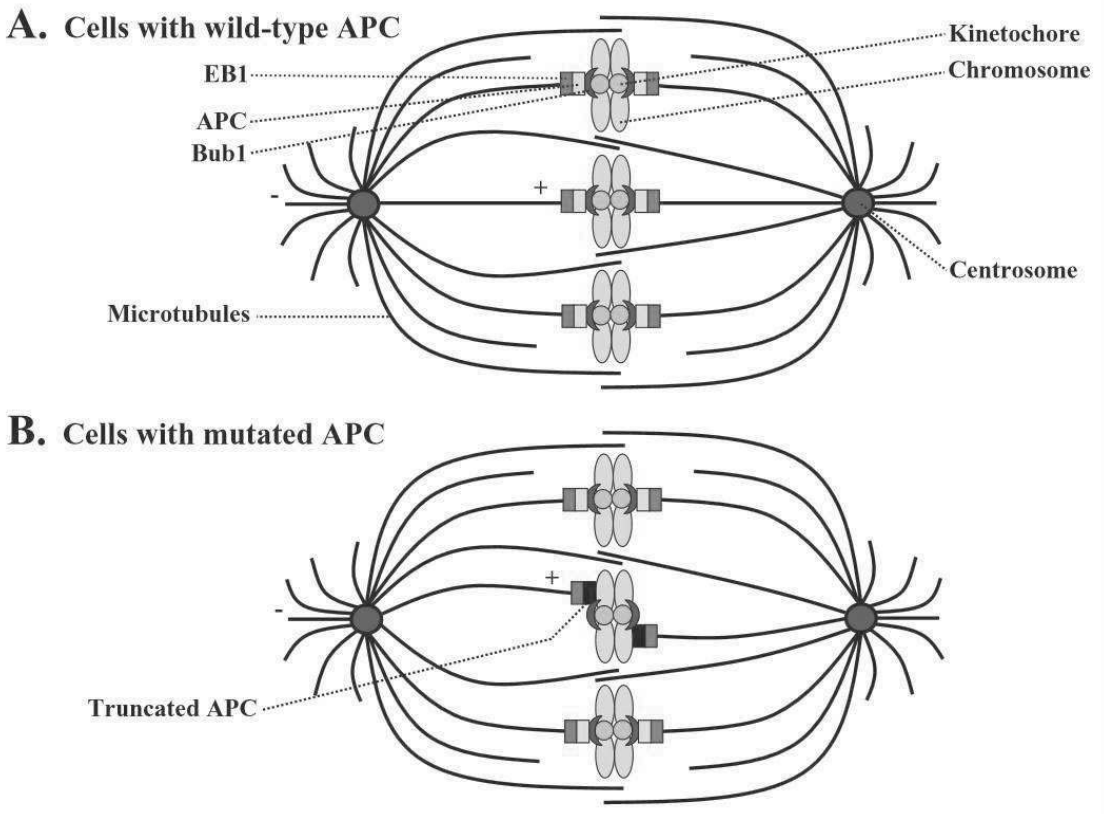

Figure 9. Model for A) normal chromosome segregation in normal cells with wild-type *APC* and B) disrupted chromosome segregation in cells with mutated *APC* [66].

1.1.6. *In vivo* and *in vitro* models for *APC* mutation

Several *in vivo* and *in vitro* models for *APC* mutation have been established and are widely used in CRC-related studies. These models, expressing truncated APC protein as a

result of *APC* mutation on specific codons, represent preneoplastic phenotype of colon epithelium since *APC* mutation is considered as one of the earliest events in colorectal carcinogenesis. The use of models for *APC* mutation is interesting since it allows the studies on the initial phenomena during colorectal carcinogenesis that would favor tumor promotion. Figure 10 displays the truncation position of APC protein in available *APC*-mutated mice for *in vivo* studies [85].

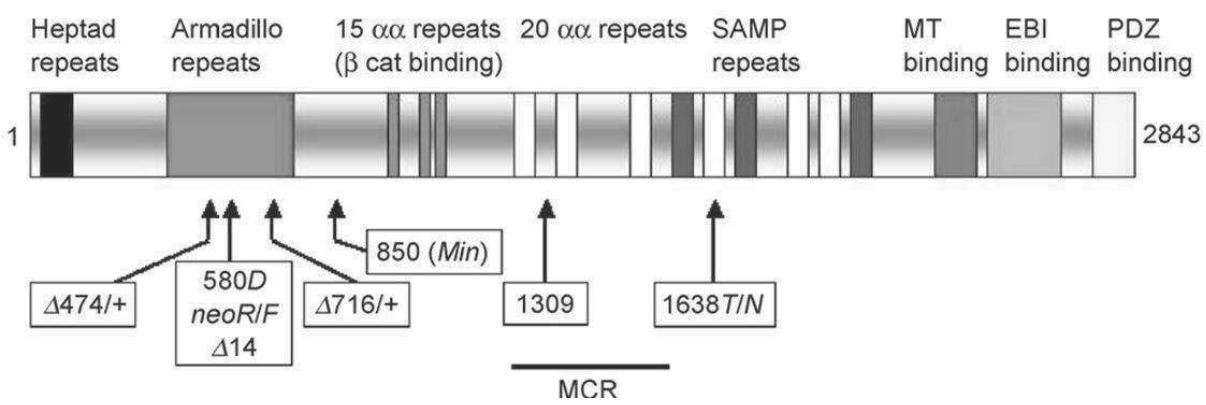

Figure 10. Schema of APC protein and the truncation positions of available *APC*-mutated mice for *in vivo* studies [85].

The most well-known and widely used *in vivo* model of *APC* mutation is Min (multiple intestinal neoplasia) mouse. Min mouse is a genetic *in vivo* model for FAP colorectal carcinogenesis developed from a colony of randomly mutagenized C57BL6/J mice with ethylnitrosourea [86]. These mice, discovered in 1990, carry constitutive *APC* mutation resulting in 850-aa truncated APC protein [87] and heterozygous APC mutation ($APC^{Min/+}$) since the mice carrying homozygous mutation are not viable. Min mice develop approximately 30 polyps in the small intestine but very rarely reach metastasis [85,88].

Later, several knock-out mutants of *APC* gene were engineered, mostly directed to produce truncating mutations that disrupt Armadillo repeat domain of APC protein. Armadillo repeat binding domain has been shown to suppress intestinal tumorigenesis in mice and the deletion of this domain in APC protein increased polyp formation in *APC*-mutated mice [89]. Min mice, that express 850-aa truncated APC protein, possess an intact armadillo repeat binding domain. Indeed, $APC^{\Delta 716/+}$ mice expressing truncated APC at codon 716 in armadillo repeat binding domain developed more than 300 polyps in small intestine [90], compared to approximately 30 polyps in Min mice with intact armadillo repeat binding domain. An additional mutation of *CDX2* (caudal type homeobox 2) in $APC^{\Delta 716/+}$ mice resulted in polyp

development in the distal colon, making it resemble human FAP and sporadic CRCs [91]. Other mice with a frameshift mutation at codon 580 ($APC^{\Delta 14}$) and an additional truncation at codon 605 ($APC^{\Delta 580}$) developed approximately 65 and 120 intestinal polys respectively [92,93]. $APC^{\Delta 474/+}$ mice harboring a frameshift mutation at codon 474 even developed intestinal tumor [94]. Finally, APC^{neoR} and APC^{neoF} mice with neomycin inserted into intron 13 expressed 80% and 90% less APC protein compared to normal C57Bl/6 rats [95].

Other mice models carry *APC* mutations that produce longer APC protein compared to Min mice and therefore possess intact armadillo repeat domains. They are $APC^{1638N/+}$ $APC^{1638T/+}$ mice with truncated APC protein at codon 1638 and $APC^{1309/+}$ mice with a frameshift mutation at codon 1309. These mice develop similar or lower polyp burden compared to Min mice (<10 polyps per mice for $APC^{1638N/+}$ $APC^{1638T/+}$ mice; and approximately 35 polyps per mice for $APC^{1309/+}$ mice) [96,97]. This highlights the importance of armadillo repeat binding domain in suppressing intestinal tumorigenesis in *APC*-mutated mice. Lastly, another mouse model named $APC^{+/\Delta e1\text{-}15}$, derived by deleting all 15 exons composing *APC* gene, exhibits a complete loss of APC protein and results in more rapid tumor development than other models with *APC* truncation [98]. These mice have reduced survival ability compared to Min mice and undergo severe polyposis.

Interestingly, a mouse model of CRC whereby *APC* can be conditionally suppressed using a doxycycline-regulated shRNA (short hairpin RNA) has been developed to study the role of *APC* disruption in tumor maintenance [64]. *APC* suppression was shown to produce adenomas in the small intestine and the colon that could progress to invasive carcinoma in the presence of *K-RAS* and *p53* mutation. In established tumors, *APC* restoration resulted in tumor regression which was accompanied by the re-establishment of crypt-villus homeostasis, such that once aberrantly proliferating cells reacquired self-renewal and differentiation ability.

Finally, it is noteworthy that: 1) Min mice with APC mutation at codon 850 tend to develop polyps in the small intestine, not in the colon-rectum as observed in human FAP and sporadic CRCs, and 2) *APC* mutation in Min mice at codon 850 results in shorter truncated APC protein than what is observed in human FAP (codon 1061 and 1309). Nevertheless, among all murine models, Min mice are still the best characterized model for human FAP and sporadic CRCs and, despite their limitations, provide the best tools for evaluation of biological consequences of APC mutation. Another promising *in vivo* model, ApcPirc rat was

established in 2007. ApcPirc rats carry APC mutation at codon 1137 and develop adenomas in the small intestine and the colon [99].

Apart from *in vivo* model for *APC* mutation, *in vitro* models are also available to study the early stages of colorectal carcinogenesis. They are: 1) mouse-origin APC +/+ and APC Min/+ cells that were established within our team (E9 Prevention and Promotion of Carcinogenesis by Food, INRA ToxAlim, Toulouse, France) [100] and 2) human-origin CT and CTA cells with shRNA-mediated invalidation of *APC* [101,102]. These models are discussed in a more detailed way in Chapter III: Experimental Models.

1.2. Colorectal cancer and red meat intake

In general, most cancer is considered as a disease that is particularly influenced by environmental (extrinsic) factors rather than genetic (intrinsic) factors [103,104]. Here, the word "environmental" defined broadly to include a wide range of often ill-defined cultural, social, and lifestyle factors. These lifestyle factors include cigarette smoking, diet (fried foods, red meat), alcohol, sun exposure, environmental pollutants, infections, stress, obesity and physical inactivity [104]. As such, cancer is believed to be preventable, especially by adopting healthy lifestyle. A recent study has reported that environmental factors contributed to 70-90% of lifetime risk to cancer development while genetic factors only contributed to 10-30% of lifetime risk to cancer development [105]. In 2015, a statistical study harvested controversy by stating that only 1/3 of most cancer cases are due to genetic and environmental factors, 2/3 of them are due to "bad luck", that is, random mutations arising during DNA replication in normal, noncancerous stem cells [106]. Interestingly, in this study, human CRC in general is categorized as cancer that is more likely to be dependent on genetic and environmental factors rather than on "bad luck".

CRC is widely considered to be an environmental disease and therefore, is preventable [107,108]. Some of the evidence of environmental risk came from studies of migrants and their offsprings. Among migrants from low-risk to high-risk countries, incidence rates of CRC tended to increase toward those typical of the population of the host country [109,110]. For example, among offsprings of southern European migrants to Australia and Japanese migrants to Hawaii, the CRC risk increased in comparison with that of populations of the country of origin. These studies showed that the incidence of CRC is greatly dependent on environmental factors, not merely on genetic factors. Several environmental factors have been identified as CRC risk factors: nutritional practices, physical activity and obesity, cigarette

smoking and alcohol consumption [1,107]. To clarify the role of environmental factors, in particular nutritional practices, World Cancer Research Fund (WCRF) and American Institute for Cancer Research (AICR) published systematic literature reviews called Expert Report in 1997 and 2007. Since 2008, the Continuous Update Project (CUP) developed the work of the first and second Expert Reports, published in 1997 and 2007 respectively [111,112]. Unlike Expert Reports, CUP is an ongoing review and captures new data, organ per organ, with the CUP report on the colon published in 2011 [1]. This report, focused on the associations between food, nutrition and physical activity and the risk of cancer, included 10 recommendations on how the general public can prevent cancer:

- Be as lean as possible within the normal range of body weight
- Be physically active as part of everyday life
- Limit consumption of energy-densed foods and avoid sugary drinks
- Eat mostly foods of plant origin
- **Limit intake of red meat and avoid processed meat**
- Limit alcoholic drinks
- Limit consumption of salt and avoid mouldy cereals (grains) or pulses (legumes)
- Aim to meet nutritional needs through diet alone
- Mothers to breastfeed; children to be breastfed
- Cancer survivors should follow the recommendations for cancer prevention

Concerning the risk of CRC, the expert panel of WCRF/AICR classified different types of factors (mostly foods) into 4 risk categories based on scientific evidence showing their role in increasing or decreasing CRC risk: convincing, probable, limited-suggestive and limited-no conclusion (Table 1).

Table 1 shows that red meat is classified as a risk factor of CRC. Indeed, numerous scientific publications have reported a positive link between colorectal cancer and red meat intake, analyzed by cohort studies, case-control studies and meta-analysis. Cohort studies compare the incidence of a disease in two groups of people: exposed and not exposed to experimental factors. Case-control studies consist in identifying a group of people with a disease (“cases”) and a similar group without the disease (“controls”) and then comparing them with respect to exposure to experimental factors. Meta-analysis is a statistical technique for combining the findings from independent studies, allowing to propose a strong conclusion. The most recent meta-analysis study conducted by the expert panel of WCRF/AICR

regrouping cohort and case control studies revealed a statistically significant dose-response relationship between CRC and red meat intake, with a 17% increased risk of CRC (95% CI 1.05-1.31), a 25% increased risk for colon cancer and a 31% increased risk for rectal cancer per 100 g per day of red meat [113]. WCRF also published a recommendation on limiting red meat intake of 500 g per week maximum and avoiding consumption of processed meat [1]. Red meat refers to beef, pork, lamb and goat from domesticated animals. Processed meat is meat that has been transformed through salting, curing, fermentation, smoking, or other processes aiming at enhancing flavor or improving preservation. Although it will not be detailed in this thesis, processed meat is also considered as risk factor of CRC with relative risk of 1.18 (95% CI 1.10-1.28) per 50 g per day of processed meat [113]. In addition, WCRF also expressed its public health goal encompassing population average of red meat consumption to be no more than 300 g a week [1]. In 2015, International Agency for Research on Cancer (IARC) under World Health Organization (WHO) categorized red meat in category 2A (probably carcinogenic to humans) and processed meat in category 1 (carcinogenic to humans) [114].

	Decreases risk	**Increases risk**
Convincing	Physical activity Foods containing dietary fiber	**Red meat** Processed meat Alcoholic drinks (men) Body fatness Abdominal fatness Adult attained height
Probable	Garlic Milk Calcium	Alcoholic drinks (women)
Limited-suggestive	Non-starchy vegetables Fruits Foods containing vitamin D	Foods containing iron Cheese Foods containing animal fats Foods containing sugars
Limited-no conclusion	Fish, glycemic index; folate; vitamin C; vitamin E; selenium; low fat; dietary pattern	

Table 1. The role of food, nutrition and physical activity in colorectal cancer [1].

1.2.1. Red meat

Red meat refers to mammalian muscle meat — for example, beef, veal, pork, lamb, mutton, horse, or goat meat — including minced or frozen meat; it is usually consumed cooked [115]. Red meat contains high biological-value proteins and important micronutrients such as vitamin B, iron and zinc. Depending on the country, the proportion of the population consuming red meat varies worldwide from less than 5% to up to 100%. The global mean intake of red meat by those who consume it is about 50-100 g per person per day, with high consumption equaling more than 200 g per person per day [116].

Meat processing, such as curing (with nitrite and nitrate) and smoking, can result in formation of carcinogenic chemicals, including N-nitroso-compounds (NOCs) and polycyclic aromatic hydrocarbons (PAHs). Cooking improves the digestibility and palatability of red meat, including prolongs its preservation, but can also produce known or suspected carcinogens, including heterocyclic amines (HCAs) and PAHs. High-temperature cooking by pan-frying, grilling, or barbecuing generally produces the highest amount of these chemicals [115].

Myoglobin is the main responsible protein for red meat's red color. It is a cytoplasmic hemoprotein consisting of a single polypeptide chain of 154 aa and solely expressed in cardiac myocytes and oxidative skeletal muscle fibers. Myoglobin contains heme (complex between porphyrin ring and iron ion) and globin protein (Figure 11A). The main function of myoglobin in muscle tissues is binding oxygen (O_2) provided by hemoglobin in blood to be used in cellular activity. Myoglobin binds oxygen by its heme residue. The iron ion in the heme interacts with six ligands, four of which are provided by nitrogen atoms in the porphyrin ring (Figure 11B). Globin imidazole side chain of His93 provides the fifth ligand, stabilizing the heme group. The sixth ligand serves as binding site with O_2 and is unoccupied in deoxymyoglobin. This ligand is stabilized by globin side chain of His64 [117].

Myoglobin shares similarities with hemoglobin (red pigment of red blood cells) in terms of structure and function. Both molecules consist of globin protein and heme residue; and are important in O_2 binding and transport. However, myoglobin has higher affinity to O_2 than hemoglobin despite the ability of hemoglobin to transport four O_2 molecules (vs. one O_2 molecule per myoglobin) [118].

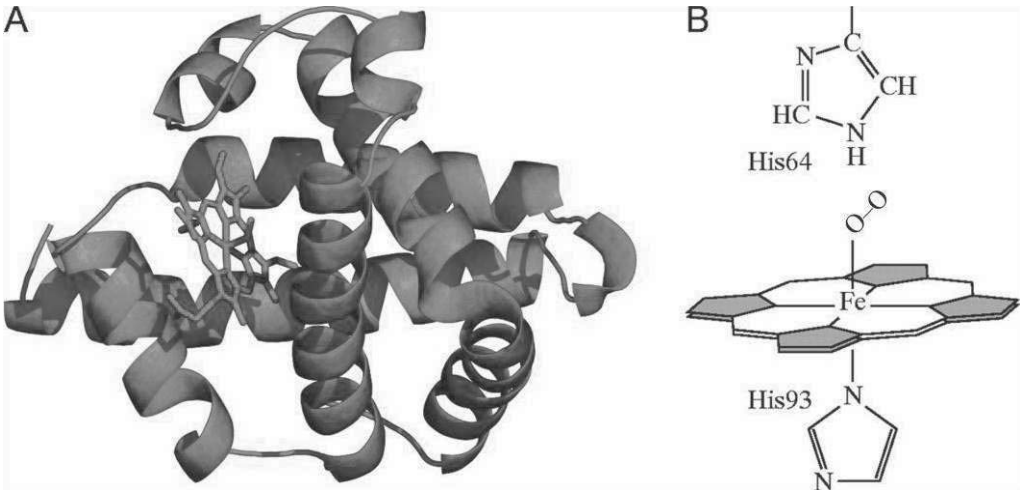

Figure 11. Structure of A) myoglobin (red: heme, blue: globin) and B) heme residue in myoglobin ([118] with modifications).

1.2.2. Hypotheses on colorectal cancer and red meat intake

Several hypotheses, which are mainly based on studies carried out on red meat, may explain the reasons for which red meat intake is linked to CRC risk: 1) high-fat diets could promote carcinogenesis *via* insulin resistance or fecal bile acids, 2) cooking meat at high temperature forms carcinogenic heterocyclic amines and polycyclic aromatic hydrocarbons, 3) carcinogenic N-nitroso compounds are formed in meat and endogenously, 4) N-glycolylneuraminic acid in red meat provokes colon inflammation and 5) heme iron in red meat can promote carcinogenesis because it increases cell proliferation in the mucosa, through lipoperoxidation and/or cytotoxicity of fecal water [119,120].

1.2.2.1. Fat

The implication of fat as a possible etiologic factor is linked to the concept of the typical Western diet. Ingested fat increases secretion of bile acids in intestinal lumen and bile acids are known to be tumor promoters. Bile acids are abrasive towards colonocytes [121] and can be degraded into carcinogenic N-nitroso compounds (NOC) in the presence of certain bacterial flora [122]. High-fat diet also increases obesity risk, which is considered as a convincing risk factor of CRC [1]. Obesity can lead to insulin resistance, which is associated to the increase of glucose, free fatty acids, insulin and IGF-1 (insulin-like growth factor 1) in the blood. These factors have been shown to increase the proliferation and reduce the apoptosis of cancerous cells [123,124].

Several *in vivo* experiments in rats have been done to show direct evidence between high-fat diet and the increase of carcinogen-induced tumors in the colon. Some of them prevailed [125-128] while some of them failed [129-134], leading to puzzling discrepancy. The latest meta-analysis study regrouping six cohort studies reported no effect of high-fat diet on colorectal carcinogenesis in humans [135].

1.2.2.2. Heterocyclic amines and polycyclic aromatic hydrocarbons

Heterocyclic amines (HCAs) and polycyclic aromatic hydrocarbons (PAHs) are carcinogenic molecules formed during the cooking of meat. HCAs are formed by pyrolysis of create(ni)ne with specific amino acids. Its formation during cooking depends on the temperature of cooking surface, the degree of browning and the length of cooking time. Since a high temperature is required, only fried, broiled, or barbecued meat contains significant amount of HCAs. The most abundant HCAs in meat are 2-amino-3,8-dimethylimidazo[4,5-f]quinoxaline (MeIQx), 2-amino-3,4,9-trimethylimidazo[4,5-f]quinoxaline (DiMeIQx) and 2-amino-1-methyl-6-phenylimidazo[4,5-b]pyridine (PhIP) [136-138]. *In vivo*, HCAs have been shown to induce colon, mammary and prostate tumors in rodents and monkeys [139]. However, the dose of HCAs used in the experiment that led to CRC in rodents and monkeys was 1,000 to 10,000 times as high as the dose found in cooked meat.

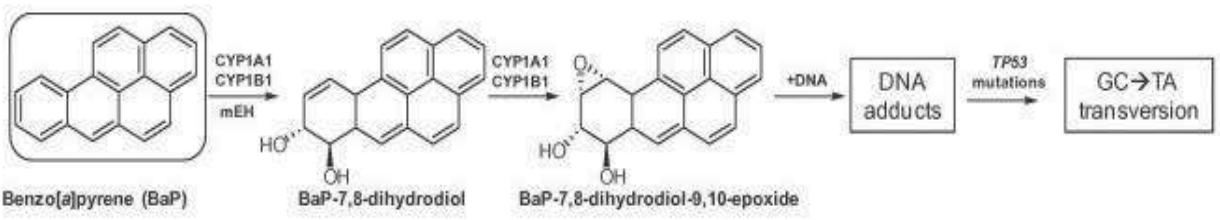

Figure 12. Metabolic activation and DNA adduct formation of benzo[a]pyrene [140].

PAHs are produced from incomplete combustion of organic compounds. Many tested PAHs, like benzo[a]pyrene (BaP), are mutagens and animal carcinogens. In humans, BaP has been shown to form DNA adducts in colon mucosa [141]. Upon phase I detoxification system by cytochromes p450 (CYP1A1 and CYP1A2) and microsomal epoxide hydrolase (mEH), transformed BaP is able to form adducts with DNA and cause a further mutation through GC→TA transversion following mutations on the tumor suppressor *p53* gene [140] (Figure 12). The main sources of PAHs for humans are cooked and smoked fish and meat (notably

barbecued meat) and tobacco smoke [142]. *In vivo* studies reported that BaP could induce the development of preneoplastic lesions in the colon of mice [143,144].

Some epidemiological studies showed the link between HCAs, PAHs and CRC in humans [145-147] while some did not [148,149]. The absence of meta-analysis makes it seem difficult to conclude the carcinogenicity of HCAs and PAHs in human CRC. Recently, specific human genotypes were shown to be critical in cooked meat-dependent colorectal carcinogenesis. They include polymorphisms on gene *NTA1* (N-acetyl transferase, a phase II enzyme) and *CYP1 A2* (cytochrome p450 1A2, a phase I enzyme) [150,151].

1.2.2.3. N-nitroso compounds

Nitrite (NO_2) is added in processed meat to ensure pink color of meat, enhance flavor and improve shelf life. N-nitroso compounds (NOCs) are produced through the reaction of nitrite and nitrogen oxides with secondary amines and N-alkylamides. They can disturb normal DNA functions through alkylation of DNA bases. Figure 13 shows an example of nitrosation of methionine that gives rise to a sulfonium ion that can methylate DNA bases. Many NOCs, including nitrosamines, nitrosamides and nitrosoguanidines, are carcinogenic in laboratory animals [152]. Human exposure to NOCs can be exogenous and endogenous. The exogenous routes include the consumption of certain processed meats (such as grilled bacon), smoked fish, cheeses or beers [153]. Endogenously, NOCs can be formed in human body through decarboxylation of amino acids by gut bacteria yielding amines and amides [152]. Heme from meat facilitates NOCs formation in human gastrointestinal tract [154]. Ascorbic acid is often added to nitrite-containing processed meat as antioxidant to prevent NOCs formation in foods and in digestive tract [155].

Animal studies reported that the intake of processed meat led to fecal excretion of NOCs, but without any evidence of CRC initiation or promotion [156-158]. Among total fecal NOCs, nitrosylated iron (FeNO) constituted about 80-90% of total NOCs found in the feces of rats fed with diet enriched in heme and NO_2 [159]. In human studies, the increase of fecal NOCs has also been observed following consumption of red meat and processed meat [152,160,161]. Furthermore, cohort studies showed that NOCs and consumption of nitrite were associated to the risk of rectal cancer [162,163]. International Agency for Research on Cancer (IARC) under World Health Organization (WHO) categorized ingested nitrite under conditions resulting in endogenous nitrosation in category 2A (probably carcinogenic to humans) [114,164].

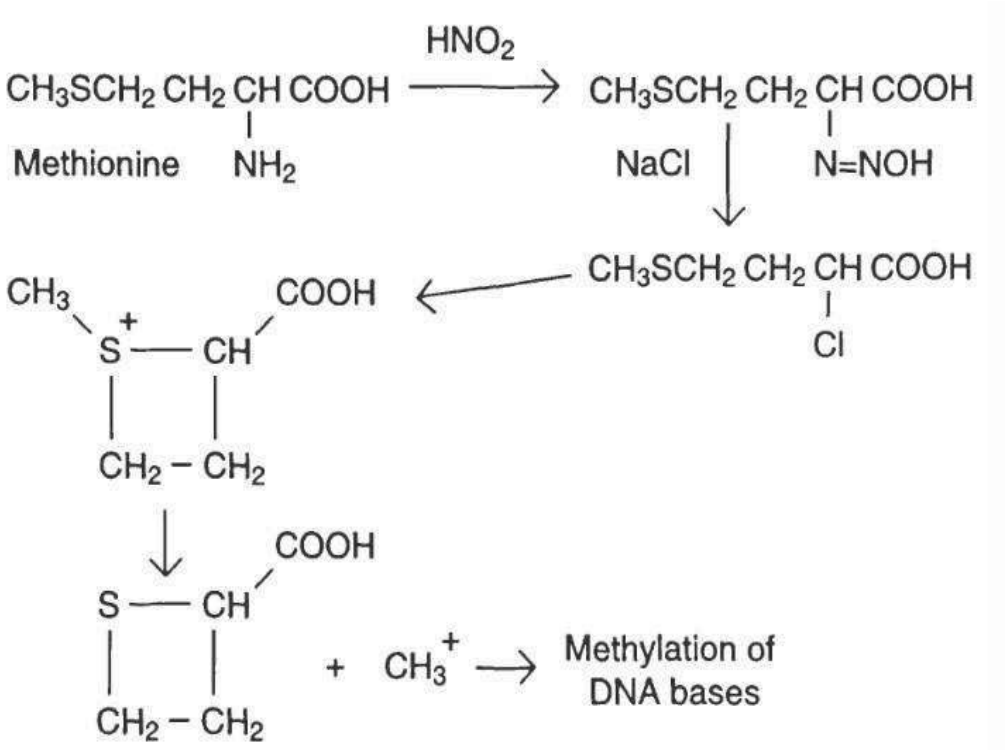

Figure 13. Nitrosation of methionine gives rise to a DNA alkylating agent [165].

1.2.2.4. N-glycolylneuraminic acid

Sialic acids are common monosaccharides that are widely expressed as outer terminal units on all vertebrate cell surfaces. They play fundamental roles in cell-cell and cell-microenvironment interactions. N-acetylneuraminic acid (NANA) and N-glycolylneuraminic acid (NGNA) are two derivatives of sialic acids. NANA can be converted to NGNA in the presence of enzyme CMP-N-acetylneuraminic acid hydroxylase (CMAH) [166,167].

NGNA is not present in humans because the human gene expressing CMAH is irreversibly mutated. This loss of CMAH was estimated to have occurred two to three millions of years ago, just before the emergence of the genus *Homo* [168]. However, NGNA is present in cells of other mammals. Despite the fact that humans are genetically unable to produce NGNA, this molecule is detectable in human epithelia and endothelia, and in higher amount in malignant tissues. Dietary intake through ingestion of mammalian tissues (such as red meat) is suspected to be the source of NGNA incorporation in human tissues. As a xenobiotic, incorporated NGNA provokes the generation of anti-NGNA "xeno-autoantibodies" that causes inflammation (called xenosialitis) [119,166]. *In vivo* studies using

human-like CMAH-KO mice showed that xenosialitis due to NGNA ingestion or injection of NGNA-expressing melanoma cell line was linked to tumor progression [119,169,170].

1.2.2.5. Heme iron

The term “heme iron” refers to iron molecule complexed with a porphyrin ring (Figure 11B). Heme iron represents 65% of total iron in human body and is present under the form of hemoglobin and myoglobin (also in certain enzymes such as cytochrome oxidase, catalase and ribonucleotide reductase) [171,172]. The role of heme iron in CRC started to be highlighted since several studies reported the cytotoxic and hyperproliferative effects of dietary heme on rat colonic epithelium [132,173]. Following the loss of *APC* gene in the colon, luminal iron level was also reported to govern intestinal tumorigenesis [174]. The latest meta-analysis study showed that a high intake of heme iron was associated with CRC risk with the relative risk of 1.15 (95% CI 1.04-1.26) [175].

A study aiming at determining at nutritional doses the relative contributions of three mechanisms involved in CRC promotion by red and processed meat (heme iron, HCAs and NOCs) has been conducted in our team. The results showed that heme iron was the only experimental factor associated with the tumor promotion in rats and Min mice without any additive or synergistic effects with HCAs or NOCs [159]. This study highlights the central role of heme iron in CRC promotion by red meat.

Three mechanisms may explain heme-mediated CRC promotion: 1) heme itself can have direct effects by generating oxidative stress, 2) heme induces lipid peroxidation in foods and in the gut, and the lipoperoxides would promote CRC, and 3) heme catalyzes the endogenous N-nitrosation that increases the formation of NOCs [120,175].

1.2.2.5.1. Direct effects of heme on carcinogenesis

Hemoglobin and hemin (heme with a chloride ligand) have been shown to be genotoxic towards human colorectal carcinoma SW480 and HT29 cells and primoculture of colonocytes [176,177]. This genotoxicity was associated with generation of free radicals [176]. In rats, cytotoxicity towards intestinal mucosa is compensated by cellular hyperproliferation that can be interpreted as a risk factor of cancer [178].

Basically, the mechanism by which heme induces carcinogenesis involves the formation of reactive oxygen species (ROS) that generate oxidative stress (Figure 14).

Uptaken heme in cells is degraded by heme oxygenase-1 (HO-1) that opens the porphyrin ring, producing biliverdin and carbon monoxide (CO) and releasing Fe^{2+}. Biliverdin is rapidly converted by cytosolic biliverdin reductase (BVR) to bilirubin that possesses powerful antioxidant activities to counteract ROS. Fe^{2+} induces the expedient production of ferritin, an antioxidant whose action is primarily mediated through the sequestration of reactive Fe^{2+} and its oxidation to less reactive ferrous ions Fe^{3+} by intrinsic ferroxidase activity. However, in case of insufficient antioxidant activity of bilirubin or ferritin, Fe^{2+} reacts with endogenous hydrogen peroxide (H_2O_2) through Fenton reaction resulting in the formation of potentially genotoxic ROS (including hydroxyl radicals •OH) that can provoke DNA damage and cell mutation [179-181]. This might be the mechanism of heme-induced CRC [182].

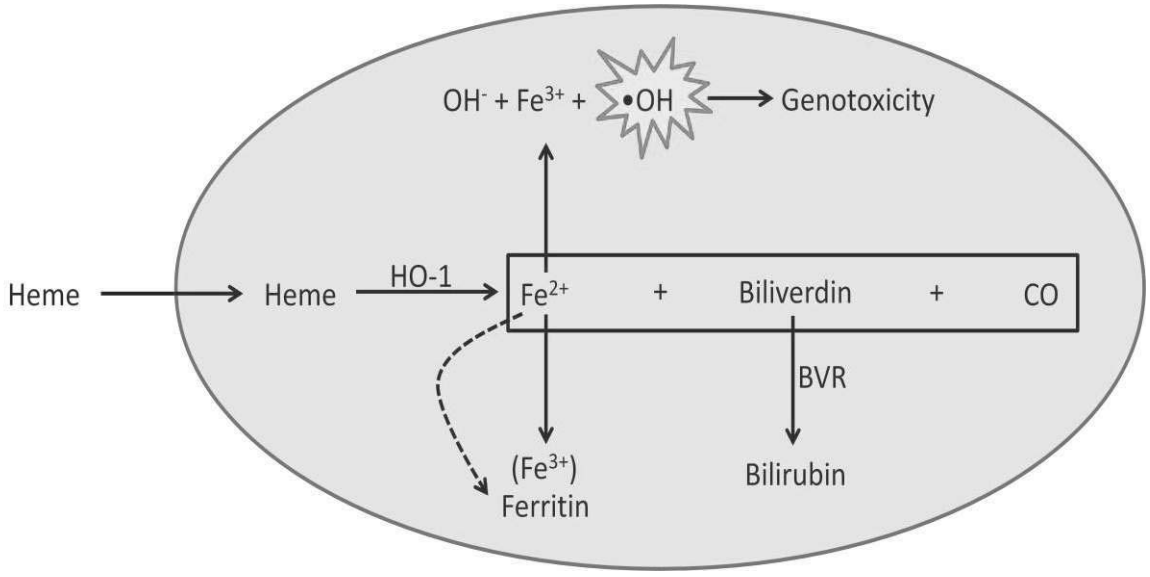

Figure 14. Model for direct effects of heme on carcinogenesis involving oxidative stress (based on [179,181]).

1.2.2.5.2. Indirect effects of heme on carcinogenesis

The indirect effects of heme on colorectal carcinogenesis involve the role of heme in catalyzing lipid peroxidation and N-nitrosation in human body. In these mechanisms, prooxidant heme in red meat (also found under nitrosylated form in processed meat) catalyzes the oxidation of unsaturated fatty acids (in lipid peroxidation) or the formation of NOCs (in N-nitrosation), leading to the formation of cytotoxic and genotoxic molecules involved in colorectal carcinogenesis (Figure 15). In general, these catalytic effects can be inhibited by calcium and chlorophyll by heme-trapping mechanism [183-187].

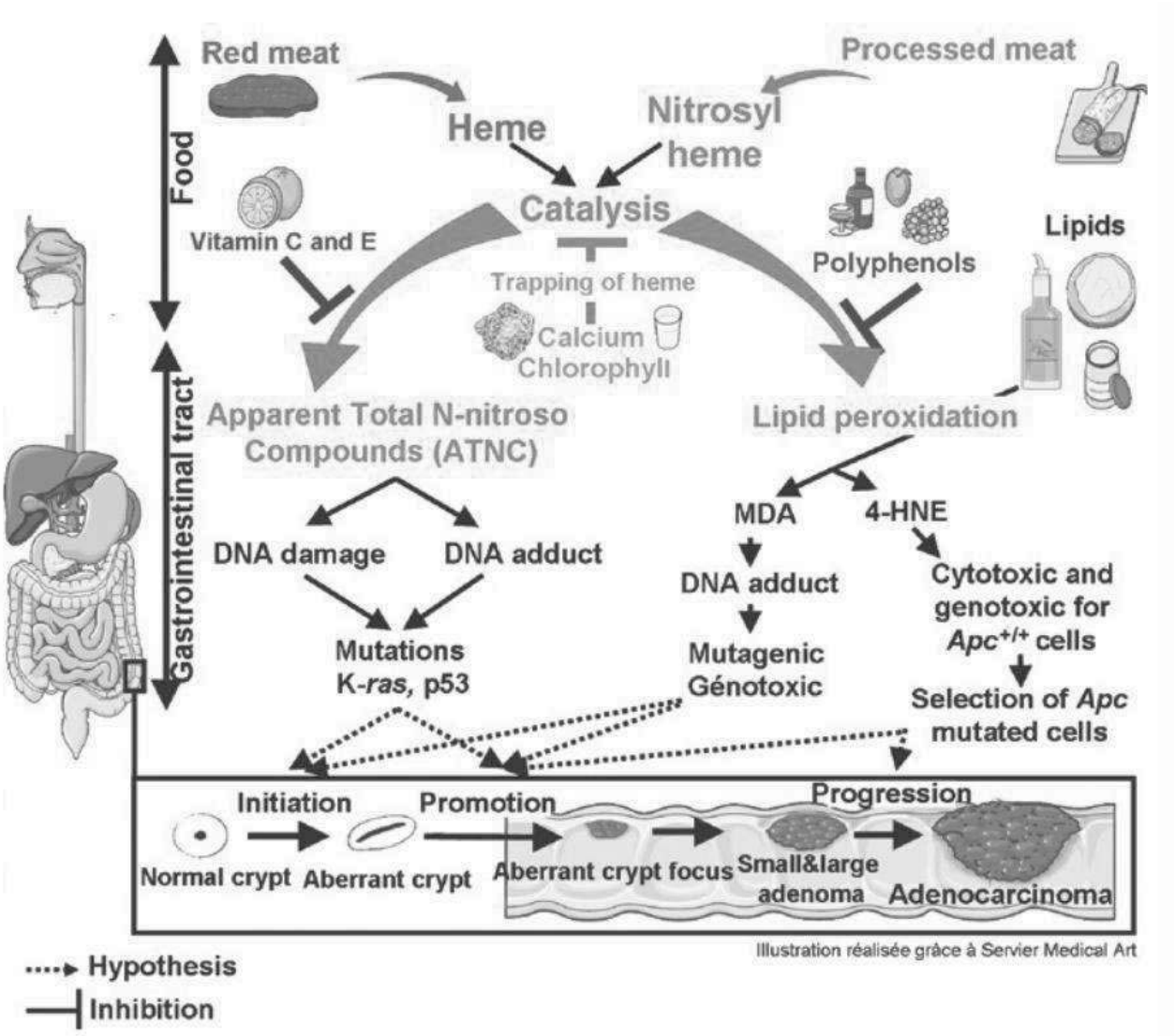

Figure 15. Indirect roles of heme iron in colorectal carcinogenesis involving catalysis of lipid peroxidation and formation of N-nitroso compounds [175].

Heme can catalyze the formation of endogenous NOCs following consumption of processed meat and this process can be inhibited by addition of vitamin C and vitamin E in processed meat [188-190]. These NOCs are also known as apparent total N-nitroso compounds (ATNCs) that include nitrosamines, nitrosamides, nitrosyl iron (FeNO) and S-nitrosothiols [191]. ATNCs have been shown to be genotoxic. Firstly, most NOCs can yield alkylating agents during metabolism and cause DNA damage. For instance, N-methyl-N-nitrosurea intrarectally perfused induced G→A transitions in oncogenic *K-RAS* in 30% of rat colon carcinoma [192]. In addition, nitrosated glycine derivatives are able to form adducts with DNA resulting in promutagenic and toxic adducts including O^6-methylguanine and O^6-carboxymethylguanine [193]. Moreover, potassium diazoacetate, a stable form of nitrosated glycine, was shown to induce tumor suppressor *p53* gene mutation in a functional yeast assay

[194]. These mutations on *K-RAS* and *p53* are involved in chromosomal instability leading to CRC development (Figure 3 and 15).

Heme also catalyzes the oxidation of polyunsaturated fatty acids (PUFAs) resulting in a variety of reactive compounds such as epoxides and aldehydes. The major aldehyde products of lipid peroxidation are malondialdehyde (MDA, derived from polyunsaturated fatty acids with two or more double bonds), 4-hydroxyhexenal (HHE, derived from n-3 fatty acids) and 4-hydroxynonenal (HNE, derived from n-6 fatty acids) [159,195,196]. An *in vivo* study investigating the role of heme iron and PUFA intake in colorectal carcinogenesis has demonstrated a 130-fold increase of urinary MDA in heme iron and fish oil-fed rats and a 300-fold increase of urinary DHN-MA (mercapturic acid of dihydroxynonane, urinary metabolite of HNE detoxification) in heme iron and safflower oil-fed rats [197]. MDA exerts genotoxicity and can form DNA adduct [198-200]. HNE appears to be the main toxic products of lipid peroxidation [159]. HNE can conduct positive selection in favor of preneoplastic colon cells harboring *APC* mutation over normal colon cells, therefore favoring CRC promotion [61,159]. The catalytic effects of heme on lipid peroxidation can be inhibited by antioxidants such as α-tocopherol and several polyphenols (quercetin and red wine polyphenols) [201-203]. Colon microbiota was also suggested to be positively involved in heme-induced lipid peroxidation [204].

1.3. 4-Hydroxynonenal and carcinogenesis

Lipid peroxidation can be described generally as a process under which oxidants such as free radicals (R•) attack lipids containing carbon-carbon double bond(s), especially PUFAs [195]. These free radicals can be generated from the mitochondrial electron transport chain, the cytochrome P450 biotransformation activities, or inflammation. Iron, through Fenton reaction with hydrogen peroxide (H_2O_2), can also catalyzes the formation of free radicals in the forms of hydroxyl radicals (•OH) or hydroperoxyl radicals (•OOH), depending on its oxidative state [205] (Figure 16A). Furthermore, these radicals can provoke lipid peroxidation through three main phases: initiation, propagation and termination [195] (Figure 16B). In the initiation phase, free radicals attack the lipids, thereby forming lipid radicals that tend to stabilize themselves by a molecular rearrangement to form a conjugated diene (step 1). In the propagation phase, lipid radicals rapidly react with oxygen to form lipid peroxy radicals (step 2) which abstract a hydrogen from other lipid molecules, thus generating new lipid radicals and lipid hydroperoxides (step 3). In the termination reaction, antioxidants (such as β-

carotene, vitamin C or vitamin E) donate a hydrogen atom to the lipid peroxy radical species resulting in the formation of nonradical products (step 4).

A

$$Fe^{2+} + H_2O_2 \rightarrow Fe^{3+} + \bullet OH + {}^{-}OH$$

$$Fe^{3+} + H_2O_2 \rightarrow Fe^{2+} + \bullet OOH + H^{+}$$

B

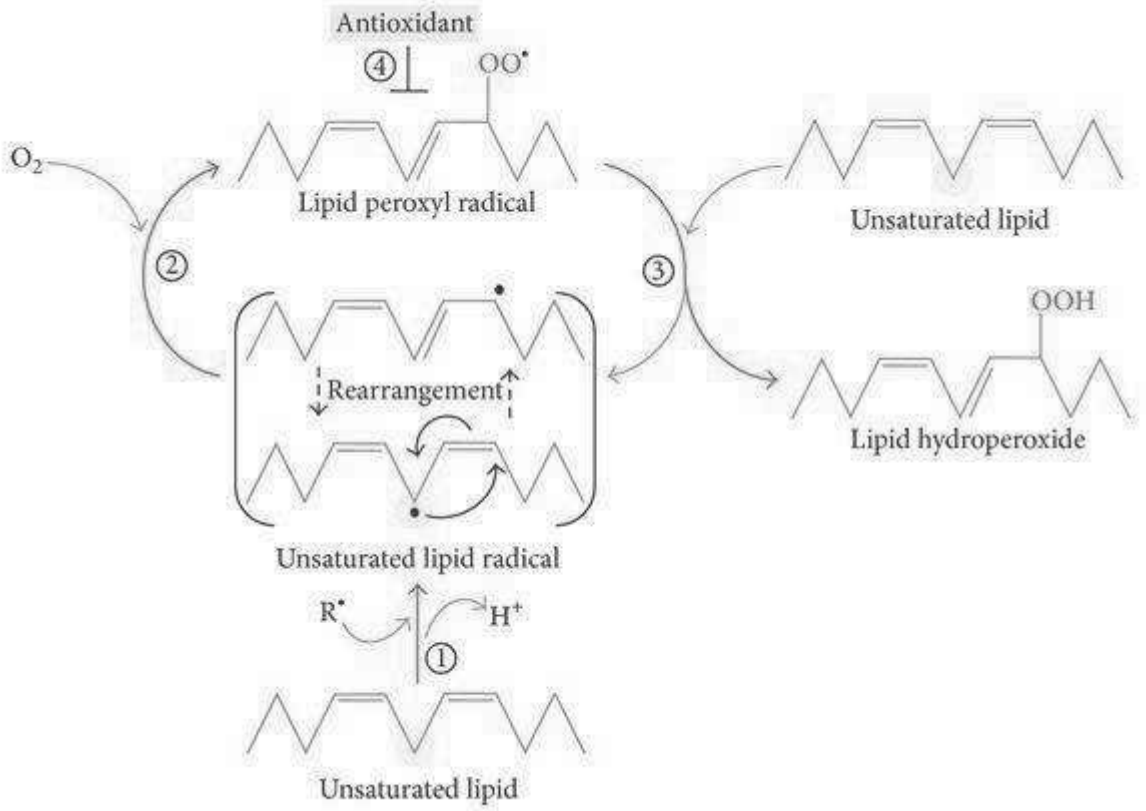

Figure 16. A) Fenton reaction involving ferrous (Fe^{2+}) and ferric (Fe^{3+}) ions resulting in hydroxyl (•OH) and hydroperoxyl (•OOH) radicals [205]. B) Lipid peroxidation consisting in initiation (step 1), propagation (steps 2-3) and termination (step 4) phases [195].

Lipid peroxidation and antioxidant status is an important parameter in CRC. Compared to healthy patients, CRC patients have been shown to exhibit higher lipid peroxidation status in their blood and lower level of serum antioxidants (vitamin C and E) [206]. Consumption of α-tocopherol was also reported to reduce biomarkers of lipid peroxidation in human stools following cured meat consumption [207]. However, the most

recent meta-analysis study found no sufficient evidence of vitamin E role for decreasing CRC [208].

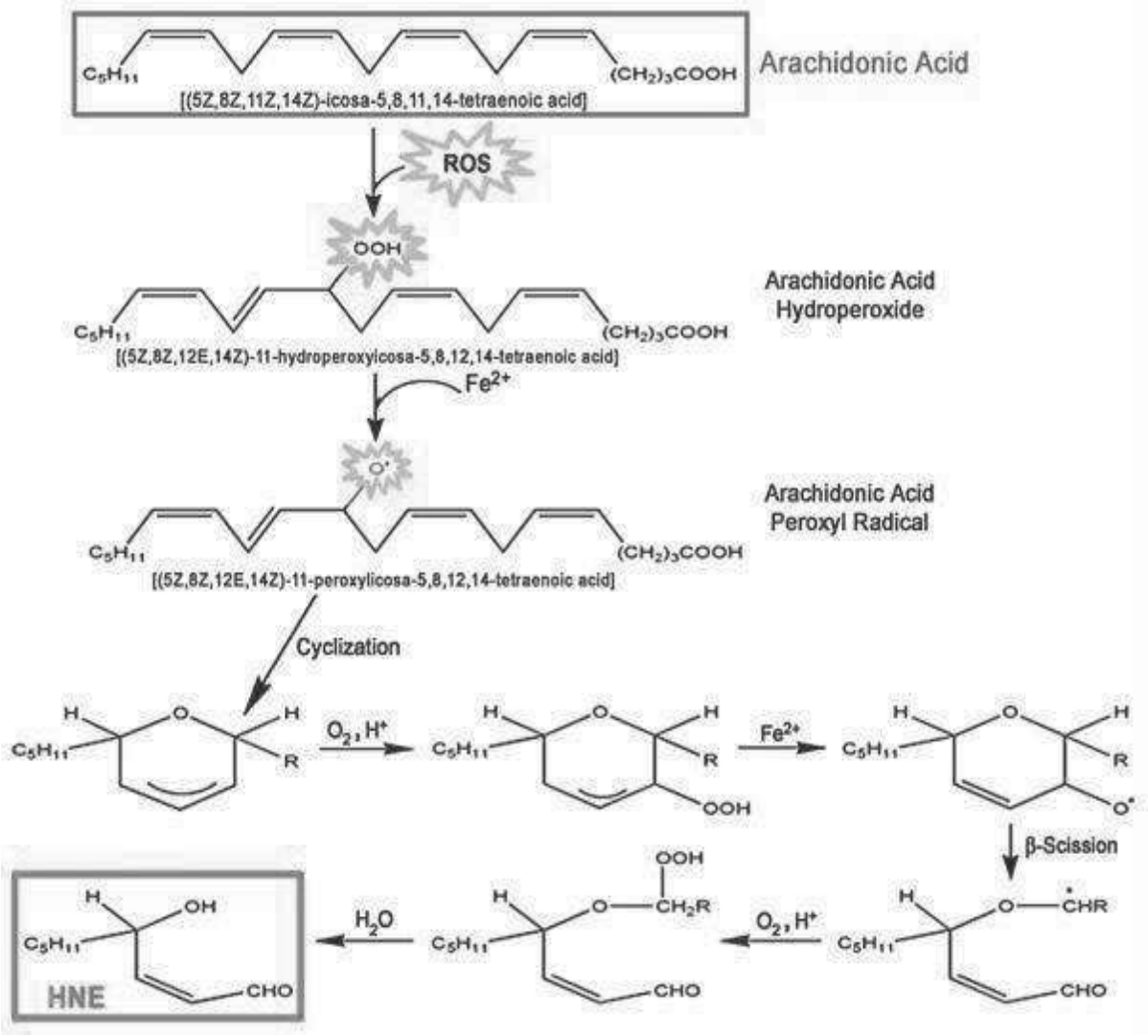

Figure 17. Formation of HNE from arachidonic acid trigerred by free radicals [209].

4-hydroxynonenal (HNE, $C_9H_{16}0_2$) is a major end product derived from the oxidation of n-6 PUFAs such as linoleic, γ-linolenic or arachidonic acids. The formation of HNE from arachidonic acid oxidation is presented in Figure 17. Following ROS attack that generates arachidonic acid hydroperoxides, ferrous (Fe^{2+}) ion catalyzes the conversion of these molecules into arachidonic acid peroxyl radicals. The highly reactive peroxyl radicals cause a molecular arrangement which cyclizes these radicals. Further oxidation and Fenton reactions result in the β-scission of the cyclized intermediate, causing the eventual formation of HNE [209]. HNE can be formed endogenously under physiological conditions through the

production of free radicals that trigger lipid peroxidation. Exogenously, HNE can enter human body through consumption of foods containing HNE, for example HNE that is formed in red meat following PUFAs oxidation catalyzed by heme iron. In this case, intestinal cells are the most susceptible to HNE-containing food because they can be directly exposed to high concentrations of HNE [210-213].

HNE has been shown to be involved in numerous pathologies, such as Alzheimer's disease, Parkinson's disease, atherosclerosis, metabolic syndrome, liver diseases and cancer. Its action in exacerbating these diseases is focused on its ability to modify protein, induce inflammation, provoke oxidative stress, cause mutations on genes, or disturb homeostasis [210]. In cancer, HNE status remains unclear but its level has been observed to be higher or lower in tumor tissues compared to healthy tissues [214-219]. Blood profiling revealed higher HNE level in CRC patients compared to healthy patients and this phenomenon was inversely correlated with their blood antioxidant status [220]. The level of HNE-protein adducts seems to be positively correlated to progression in tumor malignancy [221,222]. HNE has also been reported to bind to guanosine moiety of DNA, induce G C to T A mutations on tumor suppressor gene *p53* and inhibit DNA repair mechanisms, thereby exerting genotoxic and mutagenic potentials [223-225].

1.3.1. Reactivity of 4-hydroxynonenal

HNE possesses three reactive functions: a C2=C3 double bond, a C1=O carbonyl group and a hydroxyl group on C4 (Figure 18). Apart from possible oxidation or reduction of these reactive groups, several reactions can explain HNE ability to disrupt cellular physiology by forming adducts with DNA or protein. The C=C double bond is responsible for HNE genotoxicity through possibility of forming DNA adducts by epoxidation. The formation of protein adducts involves C2=C3 and C1=O groups. It is initiated by Michael addition that saturates C2=C3 group and enables the formation of covalent bond on C3 with amino acid residues (cysteine, histidine, or lysine). This reaction is also involved in Phase II HNE detoxification through conjugation with cysteine residue of glutathione. Following Michael addition, C1=O group reacts with lysine residue to form Schiff base to stabilize protein adducts. The formation of protein adducts can modify protein structure and activity (for instance, by forming protein cross-linking) or even inactivate it. It can also induce carbonyl stress [210,226].

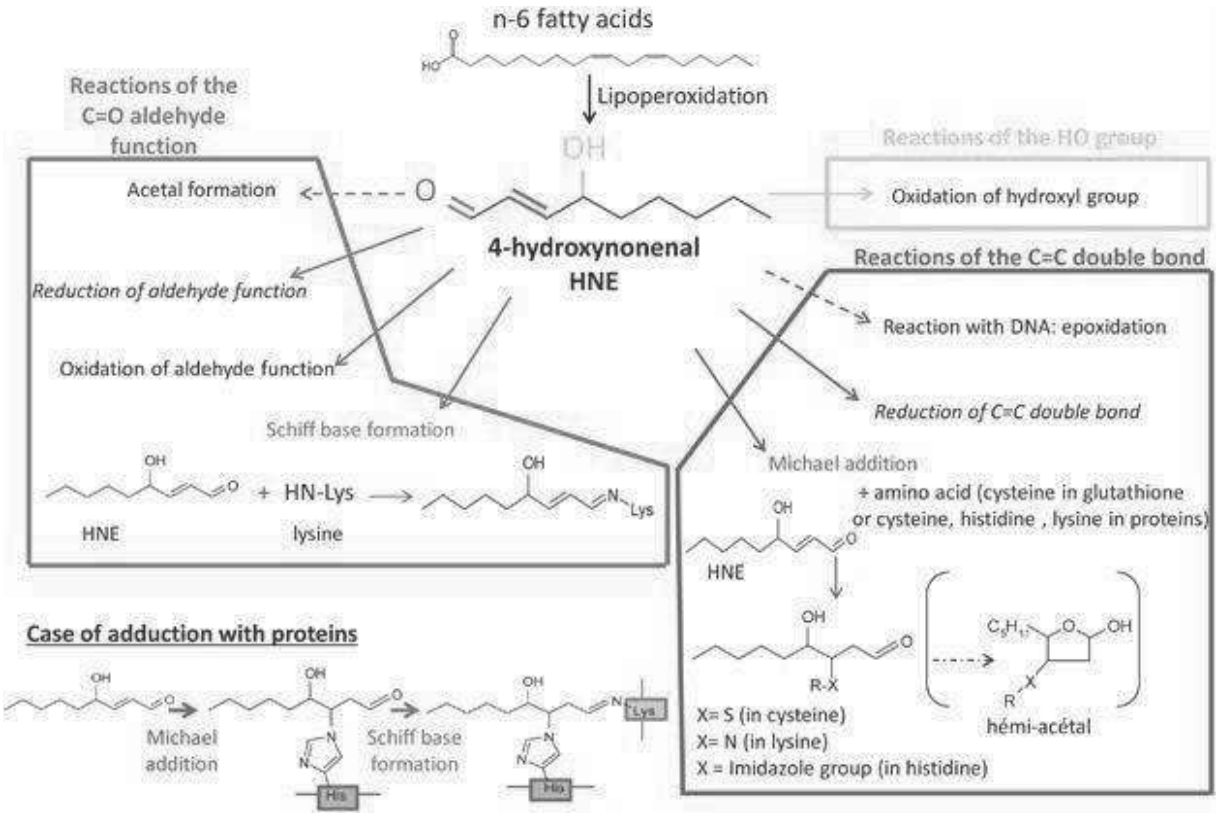

Figure 18. Reactivity of 4-hydroxynonenal
on the hydroxyl, carbonyl and C=C double bond groups [210].

1.3.2. Detoxification pathways of 4-hydroxynonenal

The half-life of HNE is less than 2 minutes. This relatively short half-life underlines the importance of HNE detoxification as a cell defense system against HNE toxicity [210]. HNE detoxification depends on cellular type. For example, colonocytes metabolize 100% of 40 µM HNE in 90 min [62] whereas hepatocytes metabolize 95% of 100 µM HNE in 3 min [227]. In radioactive HNE-fed rats, radioactivity distribution revealed that 48% of the administered radioactivity was excreted into urine and 15% into feces after 24h, while 3% were measured in intestinal contents and 2% in major organs, mostly in the liver [228]. In general, HNE detoxification pathways consist of reactivity modification of C2=C3 and C1=O groups by oxidation/reduction, saturation, or conjugation (Figure 19).

The saturation and oxidation/reduction pathways consist in hydrogenyzing double bonds C1=O and C2=C3 bond. These pathways involve three main enzymes: aldehyde dehydrogenase (ALDH), aldo-keto reductase (AKR) and alkenal/one oxidoreductase (AOR). Once enters cellular cytoplasm, HNE may undergo some possible enzymatic reactions: (1) reduction of C1=O carbonyl group by AKR resulting in 1,4-dihydroxynon-2-ene (DHN), (2)

oxidation of C1=O carbonyl group by ALDH resulting in 4-hydroxynon-2-enoic acid (HNA) and (3) hydrogenation of C2=C3 double bond by AOR resulting in 4-hydroxynonanal hemiacetal (saturated HNE), which may further be oxidized by ALDH and form 4-hydroxynonanoic acid (saturated HNA). These molecules are then released outside the cells [210].

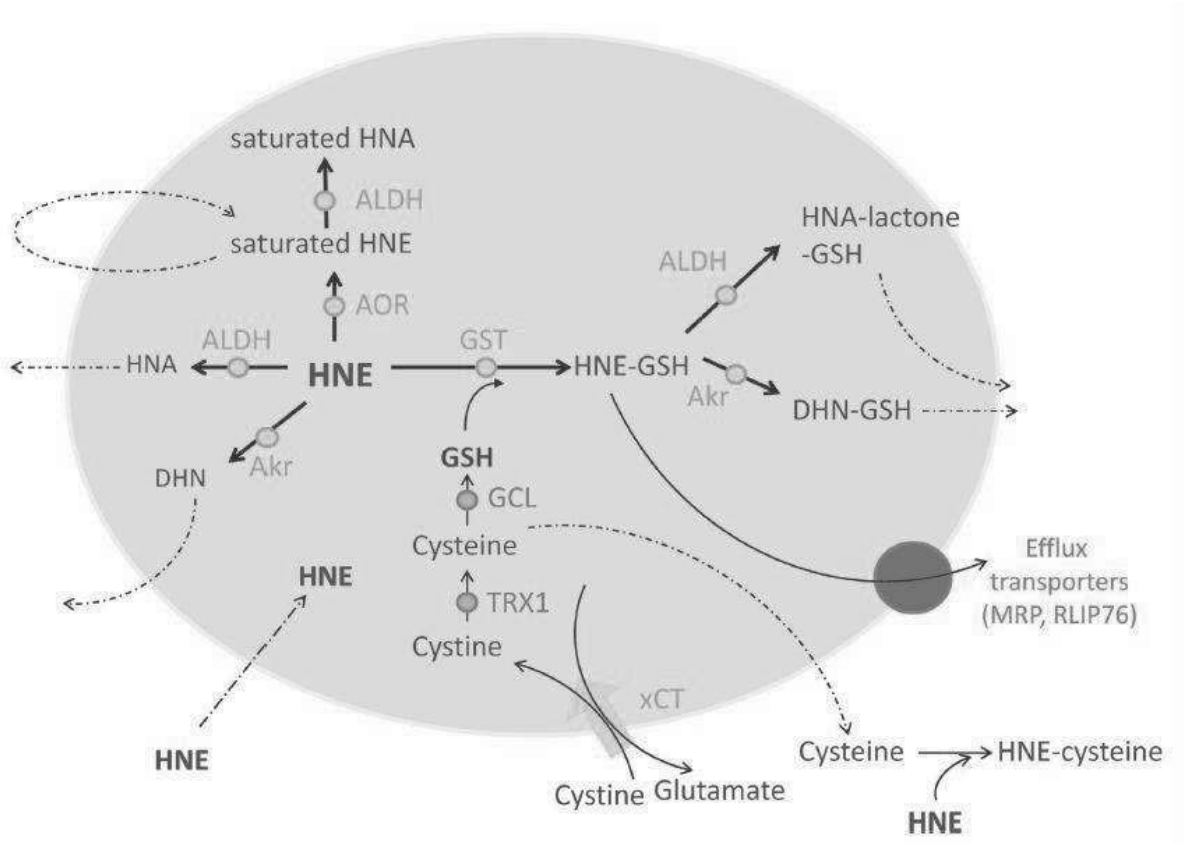

Figure 19. Putative pathways involved in the detoxification of 4-hydroxynonenal in mouse colonocytes [210].

The conjugation pathway enables detoxification of HNE through conjugation with glutathione (GSH), an antioxidant tri-peptide consisting of cysteine, glycine and glutamic acid. The production of GSH involves several proteins: (1) cystine/glutamate antiporter (xCT) embedded in cellular membrane which enables the influx of cystine (dimeric amino acid formed by two cysteine residues) into cytoplasm compensated with efflux of glutamate, (2) enzyme thioredoxin 1 (TRX1) which cleaves disulfide bond between two cysteine residues in cystine resulting in two separated cysteines and (3) enzyme glutamate cysteine ligase (GCL) which ligates cysteine and glutamate in order to form GSH. After the cleavage of disulfide bond in cystine by TRX1, cysteines can also be transferred outside the cells to capture and

inactivate extracellular HNE. Once GSH is formed, it can be conjugated with HNE in the presence of enzyme glutathione-S-transferase (GST), forming a complex HNE-GSH. This complex can be taken out directly outside the cells through membrane protein transporters such as multidrug resistance protein (MRP) and RalA-binding protein 16 encoded 76-kDa splice variant (RLIP76), or undergoes further modification catalyzed by ALDH or AKR resulting in HNA-lactone-GSH and DHN-GSH respectively before finally being released through transporters [210].

Mercapturic conjugate 1,4-dihydroxynonane mercapturic acid (DHN-MA) is known as the major urinary metabolite of HNE [213,229]. This highlights the importance of the GSH-related conjugation pathway as the major HNE detoxification pathway. A dramatical increase of urinary DHN-MA has been observed in rats fed with diets containing high heme concentration [197]. However, ω-hydroxylated metabolite of HNE 4,9-dihydroxy-2-nonenoic acid and its oxidized form 4-hydroxy-2-nonene-1,9-dicarboxylic acid have also been detected in the urine of HNE-fed mice [228]. This shows the involvement of cytochrome P450 4A in HNE detoxification pathways [230]. Urinary metabolites of HNE as thiomethyl and glucuronide conjugates were also evidenced in the urine of HNE-fed rats [228].

1.3.3. Red meat and colorectal cancer promotion: 4-hydroxynonenal in the balance

As previously mentioned, tumor heterogeneity can explain the different sensitivity of tumor cells towards cytotoxic molecules (Chapter 1.1.4) and heme iron in the red meat can provoke the formation of HNE that exerts different cytotoxicity towards normal and preneoplastic colon cells (Chapter 1.2.2.5.2). Concerning the role of HNE in CRC, heme-induced lipid peroxidation in the lumen is suggested to be involved in the promotion of colorectal carcinogenesis by generating byproducts, including HNE that triggers the positive selection of preneoplastic cells to the detriment of normal cells (Figure 20) [61]. Regarding the theory of clonal evolution of cancer (Figure 4), HNE acts as the bottleneck or selective pressure that favors the survival of preneoplastic cells over normal cells. Thus, this phenomenon might contribute to the promotion of colorectal carcinogenesis by red meat intake by positively selecting preneoplastic cells. Further studies revealed that the resistance of preneoplastic colon cells to HNE and fecal water was due to higher level of HNE detoxification enzymes (Figure 19) in preneoplastic cells compared to normal cells [62]. Interestingly, these enzymes are regulated by Nrf2 (nuclear factor (erythroid-derived 2)-like 2), a transcription factor responsible for the expression of antioxidant enzymes.

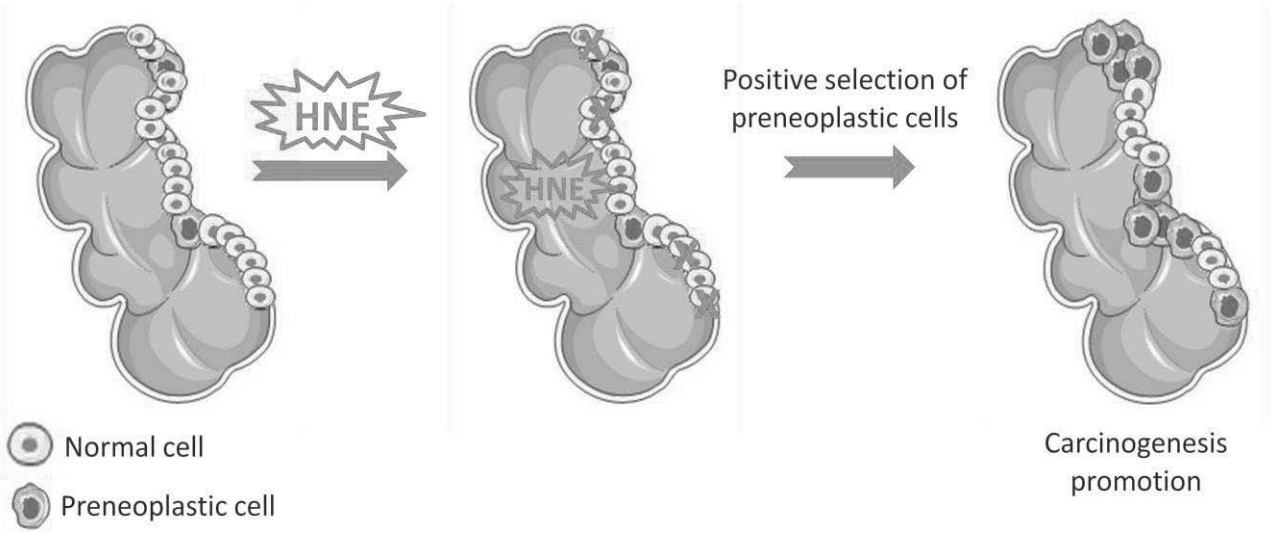

Figure 20. Model for colorectal carcinogenesis promotion based on Darwinian positive selection of preneoplastic cells over normal cells by HNE [231].

1.4. Nrf2-dependent antioxidant response

Nrf2 is a ubiquitous cytoplasmic regulatory protein acting as a transcription factor that integrates cellular stress signals and responds by directing various transcriptional programs [232]. The Nrf2-dependent antioxidant response is known as the primary cellular defense against the harmful effects of extrinsic and intrinsic insults (e.g. xenobiotics and oxidative stress) owing to its ability to activate transcription of cytoprotective genes. These genes include those expressing primary internal cellular enzymatic antioxidants, such as superoxide dismutase (SOD), catalase, GSH peroxidase (GPX) and TRX (thioredoxin) peroxidase [233]. These enzymes, known as the most important in cellular antioxidant defense system, allow to neutralize oxidative insults in the cells such as superoxide anion ($O_2^{-}\bullet$) and H_2O_2 (Figure 21). As a result, Nrf2 has traditionally been regarded as cellular main defense mechanism and a major regulator of cell survival. Activation of Nrf2-dependent antioxidant response has been shown to protect against neurodegenerative diseases, aging, diabetes, photo-oxidative stress, cardiovascular diseases, inflammation, pulmonary fibrosis, acute pulmonary injury and cancer [234-236].

Beside Nrf2, other transcription factors that are involved in cellular antioxidant response do exist, among which the most well-studied are NF-κB (nuclear factor kappa-light-chain-enhancer of activated B cells) and AP-1 (activator protein 1) composed of *jun* and *fos* gene products [237]. These transcription factors have been shown to be activated by oxidative stress and are dependent on each other [238-242]. Some antioxidant genes whose expression

is induced by these transcription factors are those expressing NQO1 (NAD(P)H quinine dehydrogenase 1), GSTs (glutathione *S*-transferases), SOD and mitochondrial PRX1 (peroxiredoxin) [237]. Nevertheless, without any intention to disregard the role of NF-κB and AP-1 in cellular response following oxidative stress, only Nrf2-dependent antioxidant response is detailed in this chapter.

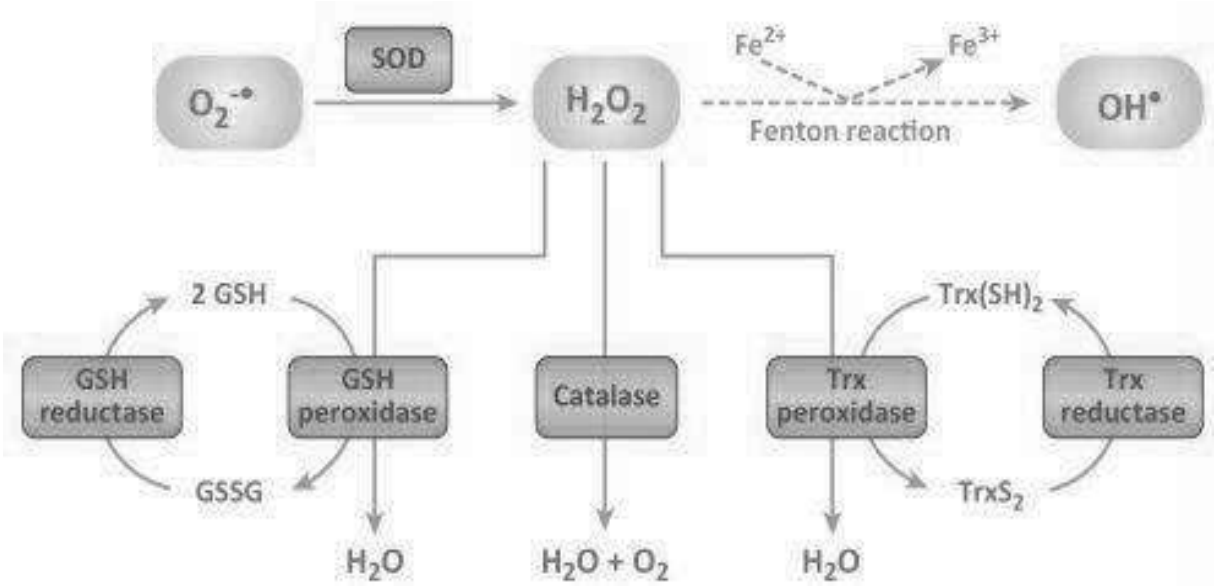

Figure 21. Important cellular antioxidant defense system involving superoxide dismutase (SOD), catalase, GSH peroxidase and TRX peroxidase ([243] with modifications).

1.4.1. Structure of Nrf2

Nrf2 contains seven functional domains, known as Neh1-Neh 7 (Figure 22). Of these, Neh2 domain, located in the N terminus of Nrf2 is the major regulatory domain. Neh2 contains seven lysine residues that are responsible for ubiquitin conjugation [244] as well as two binding sites (termed ETGE and DLG motifs) that help regulate Nrf2 stability. The ETGE and DLG motifs interact with Keap1 (Kelch-like erythroid cell-derived protein with CNC homology [ECH]-associated protein 1), which is a substrate adaptor protein for the Cullin 3 (Cul3)-dependent E3 ubiquitin ligase complex that represses Nrf2 by promoting its ubiquitination and subsequent proteasomal degradation [244-247] (Chapter 1.4.2.1).

The Neh1 and Neh6 domains are involved in the regulation of Nrf2 stability. Neh1 allows Nrf2 to bind DNA and dimerize with other transcription factors [248]. The Neh6 domain contains two binding sites (DSGIS and DSAGPS motifs) that are primordial for β-

TrCP (β-transducin repeat-containing protein)-dependent Nrf2 regulation [249-251] (Chapter 1.4.2.2).

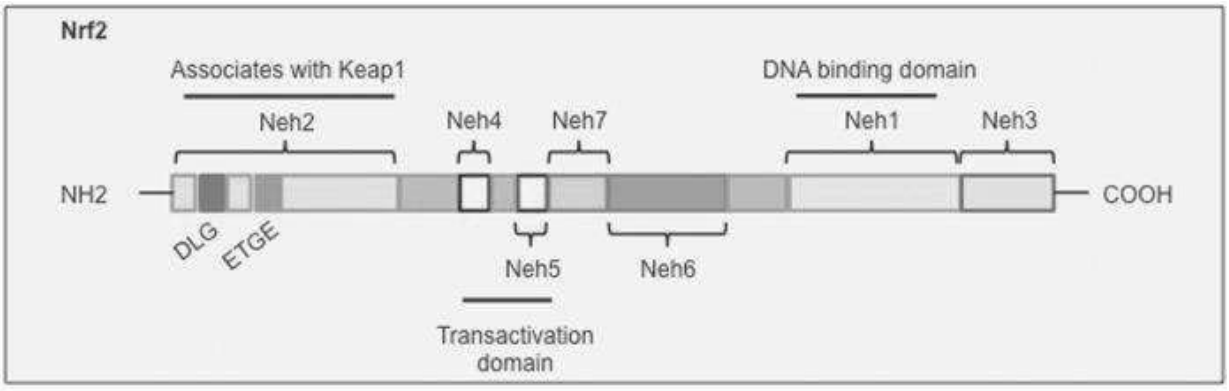

Figure 22. Structure of Nrf2 containing seven domains Neh1-Neh7 [234].

The Neh3, Neh4 and Neh5 domains interact with coactivators to enable the transactivation of Nrf2 target genes. The Neh3 domain binds to CHD6 (chromodomain helicase DNA-binding protein 6) which functions as Nrf2 transcriptional coactivator [252]. The Neh4 and Neh5 domains interact with CBP (C-AMP response element binding [CREB]-binding protein) to facilitate the transactivation of Nrf2 target genes [253,254]. Finally, the Neh7 domain is involved in Nrf2 negative regulation by interacting with RXRα (retinoic X receptor alpha), an Nrf2 repressor, and repressing the transcription of Nrf2 target genes [255].

1.4.2. Regulation of Nrf2

At the protein level, Nrf2 under basal conditions is negatively regulated by ubiquitination system aiming at degrading Nrf2. Indeed, mechanism of Nrf2 activation consists of the disruption of interaction between Nrf2 and the ubiquitination system. Before going further into details of different proteins that are involved in Nrf2 regulation by ubiquitination, the mechanism of protein degradation by ubiquitination is worth explaining (Figure 23).

Ubiquitin (Ub) is a small 8-kDa which is first transferred to the ubiquitin-activating enzyme E1 in an ATP-dependent manner. This activated ubiquitin is then transferred to ubiquitin-conjugatin enzyme E2. Finally, the ubiquitin is covalently attached to the target protein by E3 ubiquitin ligase, leading to the formation of polyubiquitin chain. The polyubiquitinated protein is recognized by the 26S proteasome and is degraded in an ATP-

dependent manner. The ubiquitins can then be recycled for other ubiquitination processes [256]. In terms of Nrf2 degradation by ubiquitination, the target protein is Nrf2 and the ubiquitination process varies in the E3 ubiquitin ligase complexes.

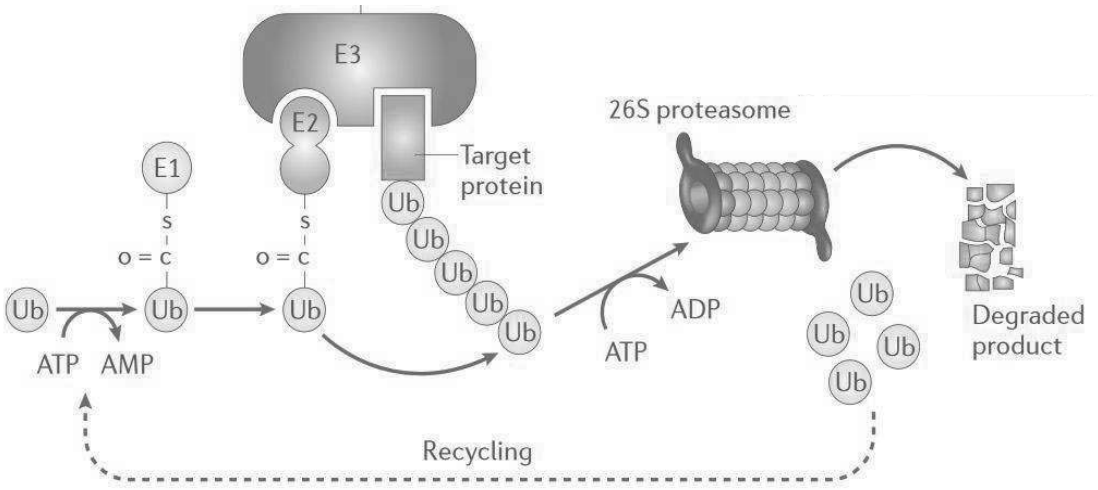

Figure 23. General mechanism of protein degradation by ubiquitination [256].

Three E3 ubiquitin ligase complexes have been reported to regulate Nrf2: 1) Keap1-Cul3-Rbx1 (ring-box 1), 2) GSK3β/β-TrCP-Skp1 (S-phase kinase-associated protein 1)-Cul1-Rbx1 and 3) Synoviolin (SYVN1 or Hrd1) (Figure 24). The mechanisms by which these complexes regulate Nrf2 are discussed in the following chapters. In addition, another mechanism of Nrf2 regulation involving p62 has been elucidated. This pathway would allow us to highlight the role of p62 in autophagy and Nrf2 signaling.

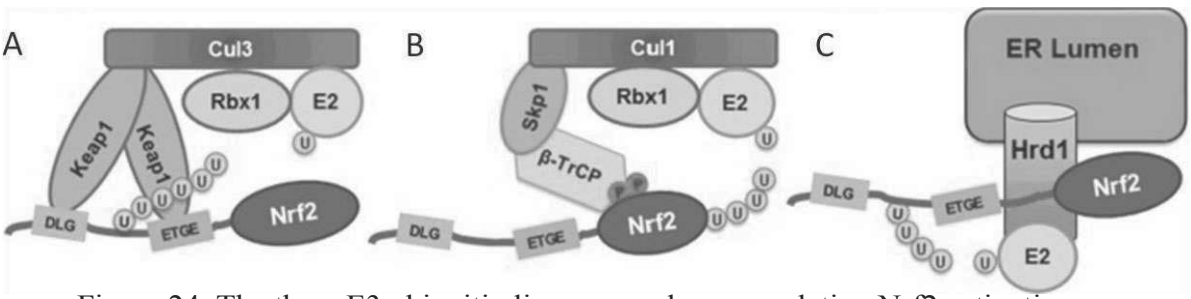

Figure 24. The three E3 ubiquitin ligase complexes regulating Nrf2 activation:
A) Keap1-Cul3-Rbx1, B) GSK3 β / β-TrCP-Skp1-Cul1-Rbx1 and C) Hrd1 [257].

1.4.2.1. Regulation of Nrf2 by Keap1-Cul3-Rbx1 E3 ubiquitin ligase

Nrf2 is primarily regulated by Keap1, a substrate adaptor that forms an E3 ubiquitin ligase with Cul3 and Rbx1. Keap1 possesses three functional domains, including a broad complex/tramtrack/bric-a-brac (BTB) domain, an intervening region (IVR, also known as linker region, LR) and a Kelch-repeat domain (Figure 25). The BTB domain is required for the formation of Keap1 homodimers as well as the recruitment of Cul3 or Rbx1 [258,259]. The Kelch-repeat domain is critical for maintaining the interaction between Keap1 and the Neh2 domain of Nrf2 [249,260]. The IVR/LR domain contains several cysteine residues that have been proposed to regulate Keap1 activity [246,261]. There are several cysteine residues functioning as sensors for electrophiles: Cys-151, Cys-226/Cys-613, Cys-273/Cys-288 and Cys-434. A disulfide bridge can be formed between Cys-226 and Cys-613 following oxidation [262].

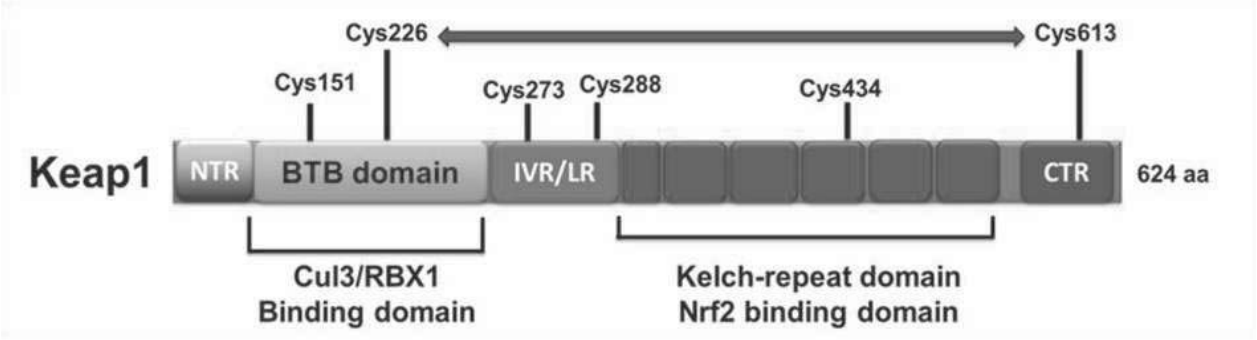

Figure 25. Structure of Keap1 containg three domains: BTB, IVR/LR and Kelch-repeat domain (NTR: N terminal region, CTR: C terminal region) [262].

Under basal conditions, Nrf2 is primarily localized in the cytoplasm and bound to Keap1 via direct protein-protein interactions between the Kelch-repeat domain of Keap1 and the ETGE and DLG motifs in the Neh2 domain of Nrf2 (Figure 24A and 26). This binding to Keap1-Cul3-Rbx1 E3 ubiquitin ligase promotes Nrf2 polyubiquitination and its subsequent proteasomal degradation by proteasome [244,263,264].

In response to a diverse array of stimuli, it has been proposed that the critical cysteine residues of Keap1, especially Cys-151, can be covalently modified, allowing Nrf2 to evade Keap1-mediated ubiquitination. The human Keap1 protein contains 27 cysteine residues that can be oxidized to sulfenic acid, form disulfides, or be covalently adducted by electrophiles [265-267]. The modification of cysteine residues on Keap1 alters its conformation and results

in the release of Nrf2 from the DLG motif to the nucleus. Another proposition for Nrf2 liberation from Keap1 involves dissociation of Cul3 that blocks ubiquitination [232]. In the nucleus, Nrf2 dimerizes with members of the masculoaponeurotic fibrosarcoma (Maf) protein family that facilitates the binding of Nrf2 to ARE (antioxidant response element), a sequence in the promoter regions of a wide variety of genes involved in cytoprotection and metabolism [268-270]. The Nrf2-Maf heterodimer recruits transcriptional coactivators that promote the transcription of numerous cytoprotective enzymes (detailed in Chapter 1.4.3). By inducing the expression of this battery of genes, Nrf2 is able to augment a wide range of cell defense processes, thereby enhancing the overall capacity of cells to detoxify potentially harmful entities. As feedback mechanism, Keap1 translocates into the nucleus to bind to Nrf2 and deregulates it *via* ubiquitination in the cytoplasm [271,272]. Regulation of Nrf2 activity involving Keap1-Cul3-Rbx1 is known as canonical pathway of Nrf2 activation.

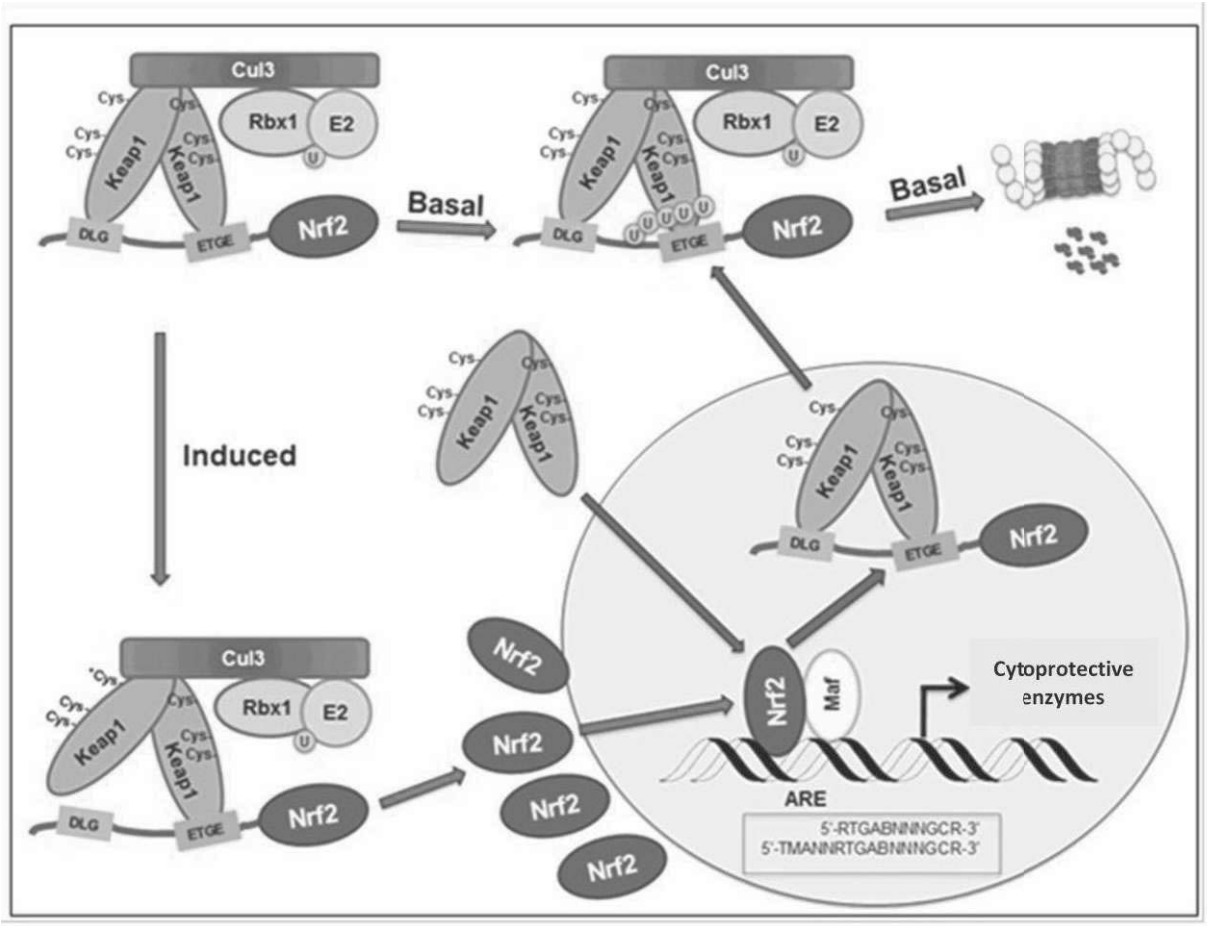

Figure 26. Nrf2-Keap1 signaling pathway ([257] with modifications).

1.4.2.2. Regulation of Nrf2 by GSK3β / β-TrCP-Skp1-Cul1-Rbx1 E3 ubiquitin ligase

Beside Keap1-Cul3-Rbx1 E3 ubiquitin ligase that has been revealed as the primary redox-sensitive regulator of Nrf2 in the Neh2 domain, a redox-insensitive degron within the Neh6 domain of Nrf2 was also reported to regulate Nrf2 ubiquitination. Subsequently, the Neh6 domain of Nrf2 contains a group of serine residues that can be phosphorylated by GSK3, a serine/threonine kinase that is also involved in APC regulation by Wnt signaling (see Chapter 1.1.5.2.1). This phosphorylation event creates a phosphorylated destruction motif (phosphodegron) which can then be recognized by the β-TrCP-Skp1-Cul1-Rbx1 E3 ubiquitin ligase complex [250] (Figure 24B). This E3 ubiquitin ligase complex ubiquitylates Nrf2 and sends it to the protasome for degradation. Two distinct motifs in the Neh6 domain of Nrf2 have been reported to be recognized by β-TrCP: DSAPGS and DSGIS. Between these two motifs, only DSGIS contains a GSK3β phosphorylation site [251].

The regulation of Nrf2 by β-TrCP-Skp1-Cul1-Rbx1 E3 ubiquitin ligase complex bridges Nrf2 activation and Wnt signaling that is activated in CRCs following APC mutation. Recently, the activation of Wnt signaling was shown to lead to Nrf2 activation in hepatocytes [273] (Figure 27). The mechanism involves Nrf2 phosphorylation by GSK3β to form a phosphodegron that is followed by β-TrCP-dependent Nrf2 degradation when no Wnt signal is detected. Upon activation of Wnt signaling, GSK3β is recruited to the membrane, along with receptors LRP5/6 and Frizzled and therefore GSK3β becomes less available to phosphorylate Nrf2.

1.4.2.3. Regulation of Nrf2 by Hrd1 E3 ubiquitin ligase

Recently, in the case of liver cirrhosis, Nrf2-mediated protective response has been reported to be suppressed during liver carcinogenesis. This finding was somehow surprising because Keap1 should be likely to be inactivated by the high levels of ROS in cirrhotic livers, leading to Nrf2 signaling by canonical mechanism [274]. Subsequently, the phenomenon of endoplasmic reticulum stress (ER stress) was pointed out to cause the suppression of Nrf2 activity during the pathogenesis of liver cirrhosis.

ER stress occurs when misfolded proteins accumulate and the unfolded protein response (UPR) is initiated. Three sensors located on the ER membrane detect the accumulation of misfolded proteins and relays signaling cascades to correct the insults: 1) inositol-requiring enzymes 1 (IRE1), 2) protein kinase RNA-like ER kinase (PERK) and 3)

activating transcription factor 6 (ATF6) [275]. Concerning IRE1, ER stress is known to enable IRE1 to homodimerize and actively splice X-box-binding protein 1 (XBP1) mRNA into a mature mRNA encoding XBP1s, a transcription factor. Hrd1 (Synovial apoptosis inhibitor 1), one of XBPs target genes, is an E3 ubiquitin ligase that is able to ubiquitylate Nrf2, leading to its degradation by proteasome [274] (Figure 24C).

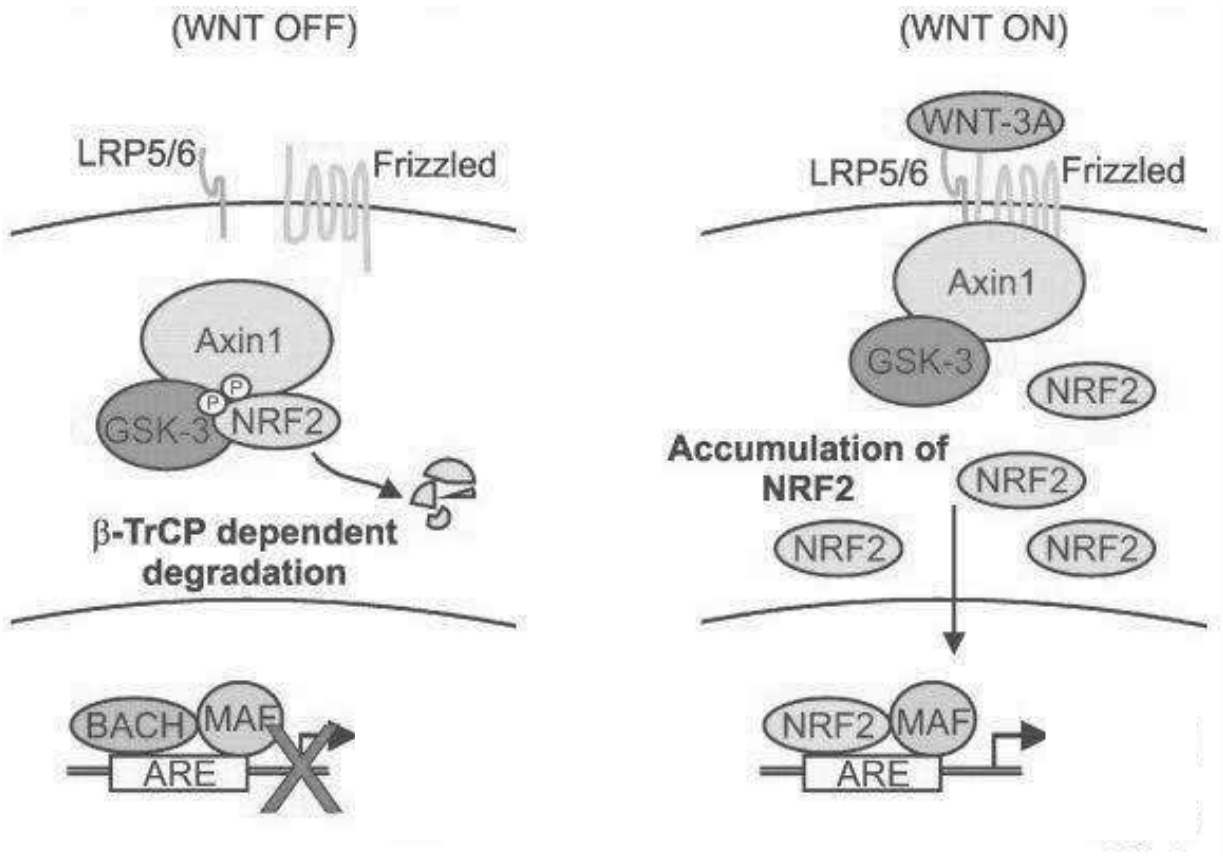

Figure 27. Mechanism of Wnt-dependent activation of Nrf2 in hepatocytes [273].

1.4.2.4. Regulation of Nrf2 by p62

Apart from negative regulation through ubiquitination involving E3 ubiquitin ligase complexes, Nrf2 is subjected to positive regulation through disruption of the Nrf2-Keap1 interaction by other proteins. Numerous proteins containing ETGE motif of Nrf2 have been identified and shown to compete with Nrf2 for Keap1 binding, thus stabilizing Nrf2 [276]. Some examples of (E/S)TGE-containing proteins include dipeptidyl peptidase 3 (DPP3), partner and localizer of breast cancer 2 (PALB2) and p62. Among these proteins, p62 is perhaps the most recognized positive regulator of Nrf2. p62 is mostly well-known for its role

as a cargo protein in autophagy machinery (Chapter 1.5.2). It possesses a Keap1-interacting region (KIR) containing STGE motif that accounts for the direct interaction between p62 and Keap1 [277]. Phosphorylation of Serine 351 residue of p62 has been shown to increase the affinity between p62 and Keap1, which resulted in Nrf2 activation through sequestration of Keap1 onto the autophagosomes for lysosomal degradation [278] (Figure 28). Recently, this phosphorylation was known to be mediated by TAK1 (TGFβ-activated kinase 1) [279]. Interestingly, p62 is also a target gene of Nrf2 [280]. This Nrf2 activation pathway was observed in arsenic-induced human lung carcinogenesis [281,282].

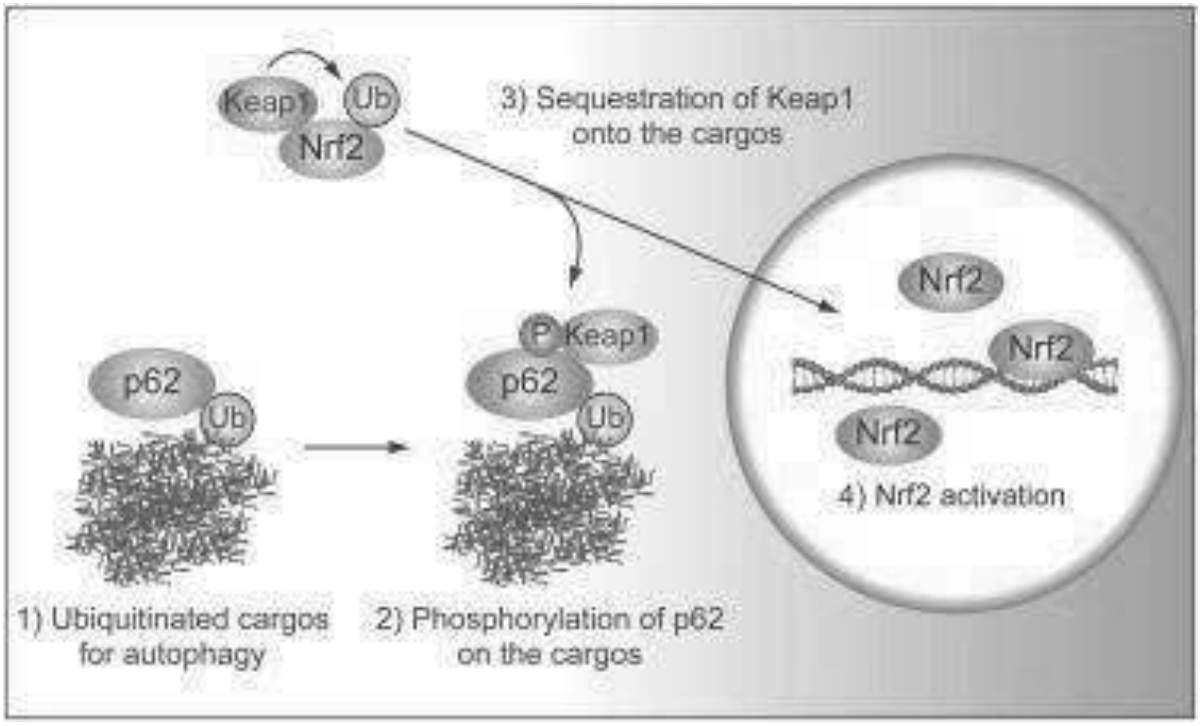

Figure 28. Regulation of Nrf2-Keap1 signaling pathway by p62 [278]

1.4.2.5. Regulation of Nrf2 at the transcriptional level by oncogenes

At the transcriptional level, Nrf2 has been reported to be up-regulated by oncogenic activation of *K-RAS*, *B-RAF* and *MYC* [283]. Colorectal carcinogenesis involves activation of these genes. *K-RAS* and *B-RAF* are mutated during transformation of early colon adenoma into intermediate adenoma, both based on chromosomal instability model and microsatellite instability model (Figure 3). *MYC* is a target gene of Wnt signaling that is continuously active following *APC* mutation in early colorectal carcinogenesis (Figure 6B). The activation of Nrf2 by the oncogenic *K-RAS* is facilitated through a TPA (12-O-Tetradecanoylphorbol-13-

acetate)-responsive element (TRE) in the regulatory region of Nrf2 [284]. Nevertheless, the precise mechanisms by which *B-RAF* and *MYC* up-regulate the transcription of Nrf2 are currently unknown.

1.4.3. Target genes of Nrf2

In general, the target genes of Nrf2 include those that are involved in: 1) Phase I-III drug detoxification, 2) thioredoxin- and glutathione-based antioxidant system, 3) carboxylate metabolism and NADPH regeneration, 4) heme and iron metabolism, 5) transcription factors and associated proteins and 6) ubiquitin ligase substrate adaptors [234,285-287] (Table 2). Interestingly, Nrf2 may perform an autoregulation by promoting the transcription of Nrf2 itself and other proteins associated in Nrf2 regulation such as Keap1 and p62 [280,287,288]. In addition, the enzymes that are involved in HNE detoxification (Figure 19) have been reported to be regulated by Nrf2 [289-292].

General biochemical function	Symbol	Name
Detoxification: Phase I drug oxidation, reduction and hydrolysis	*AKR1B1*	Aldo-keto reductase family 1, member B1 (and 1B8 and 1B10)
	AKR1C1	Aldo-keto reductase family 1, member C1 (and 1C2 and 1C3)
	ALDH3A1	Aldehyde dehydrogenase 3 family, member A1 (and 3A2)
	CBR1	Carbonyl reductase 1 (and 3)
	EPHX1	Epoxide hydrolase 1, microsomal
	PTGR1	Prostaglandin reductase 1 (also called LTB4DH)
	NQO1	NAD(P)H quinone oxidoreductase 1
Detoxification: Phase II drug conjugation	*MGST1*	Microsomal glutathione *S*-tranferase 1 (and 2)
	GSTA4	Glutathione *S*-transferase A4
	SULT1A1	Sulfotransferase family, cytosolic, 1A, member 1(2)
	UGT1A1	UDP glucuronosyltransferase 1 family,

		polypeptide A1 (and 1A6)
	UGT2B7	UDP glucuronosyltransferase 2 family, polypeptide B7 (and 2B34)
Detoxification: Phase III drug transport	*ABCB6*	ATP-binding cassette, subfamily B (MDR/TAP), member 6
	ABCC2	ATP-binding cassette, subfamily C (CFTR/MRP), member 2
	ABCC3	ATP-binding cassette, subfamily C (CFTR/MRP), member 3
Antioxidant: glutathione-based system	*GCLC*	Glutamate-cysteine ligase, catalytic subunit
	GCLM	Glutamate-cysteine ligase, modifier subunit
	GGT1	γ-glutamyltransferase 1
	GLRX	Glutaredoxin 1
	GLS	Glutaminase
	GPX2	Glutathione peroxidase 2
	GSR1	Glutathione reductase
	SLC7A11	Cystine/glutamate transporte (also called xCT)
Antioxidant: thioredoxin-based system	*PRDX1*	Peroxiredoxin 1
	PRDX6	Peroxiredoxin 6
	SRXN1	Sulfiredoxin 1
	TXN1	Thioredoxin 1
	TXNRD1	Thioredoxin reductase 1
Other antioxidant systems	*CAT*	Catalase
	SOD3	Superoxide dismutase 3
Carboxylate metabolism and NADPH regeneration	*HDK1*	Hexokinase domain containing 1
	ME1	Malic enzyme 1, $NADP^+$-dependent
	PGD	6-phosphogluconate dehydrogenase
	TALDO1	Transaldolase
	TKT	Transketolase isoform 1
	UGDH	UDP-glucose dehydrogenase
Heme and iron metabolism	*BLVRA*	Billiverdin reductase A
	BLVRB	Billiverdin reductase B
	FECH	Ferrochelatase

	FTH1	Ferritin, heavy polypeptide 1
	FTHL12	Ferritin, heavy polypeptide-like 12
	FTHL17	Ferritin, heavy polypeptide-like 17
	FTL1	Ferritin, light polypeptide
	HMOX1	Heme oxygenase 1 (also called HO1)
Transcription factors and associated proteins	*MAFG*	MafG protein
	NRF2	Nuclear factor (erythroid-derived 2)-like 2
	PPARG	Peroxisome proliferator-activated receptor γ
	PPARGC1B	Peroxisome proliferator-activated receptor γ coactivator 1β
	RXRA	Retinoid X factor α
Ubiquitin ligase substrate adaptor	*KEAP1*	Kelch-like ECH-associated protein 1

Table 2. List of genes positively regulated by Nrf2 in humans [233,287].

1.4.4. Activators and inhibitors of Nrf2

Numerous dietary phytochemicals naturally existing in vegetables, fruits and spices are considered as chemopreventive (Figure 29). These phytochemicals have been proven to activate Nrf2 [293]. For example, exposure to green tea extract containing epigallocatechin-3-gallate (EGCG) has been shown to induce and activate Phase II enzyme gene expression in HepG2 cells, as determined by the ARE reporter-gene assay [294,295]. Sulphoraphane and cinnamaldehyde, the two active phytochemicals found respectively in broccoli and cinnamon are the two well-studied Nrf2 activators. These phytochemicals are indeed electrophiles that react with Keap1-Cys^{151} and increase Nrf2 levels *via* the canonical mechanism [281,282]. Recently, rosemary extract and carnosic acid were also reported to significantly upregulate the expression of Nrf2 in colon cells and inhibit a xenograft tumor formation in mice [296].

Bardoxolone and dimethylfumarate (DMF) are two Keap1-dependent Nrf2 activators that have advanced to clinical trials for multiple sclerosis and chronic kidney diseases. Bardoxolone, a natural product derived from triterpenoid, interacts with the BTB domain of Keap1, disrupting the BTB/Cul3 interface, leading to Nrf2 activation [297]. DMF (also known as BG-12 and Tecfidera) is able to adduct Keap1 and therefore activates Nrf2

[298,299]. Recently, Keap1-independent Nrf2 activators have emerged. For example, nordihydroguaiaretic acid (NDGA) was shown to induce Nrf2 through inhibition of phosphorylation of Neh6 motif in Nrf2 by GSK3β [300]. Additionally, 4U8C and LS-102 activate Nrf2 by inhibiting IRE1 and Hrd1 respectively, thereby preventing Hrd1-dependent Nrf2 regulation [274].

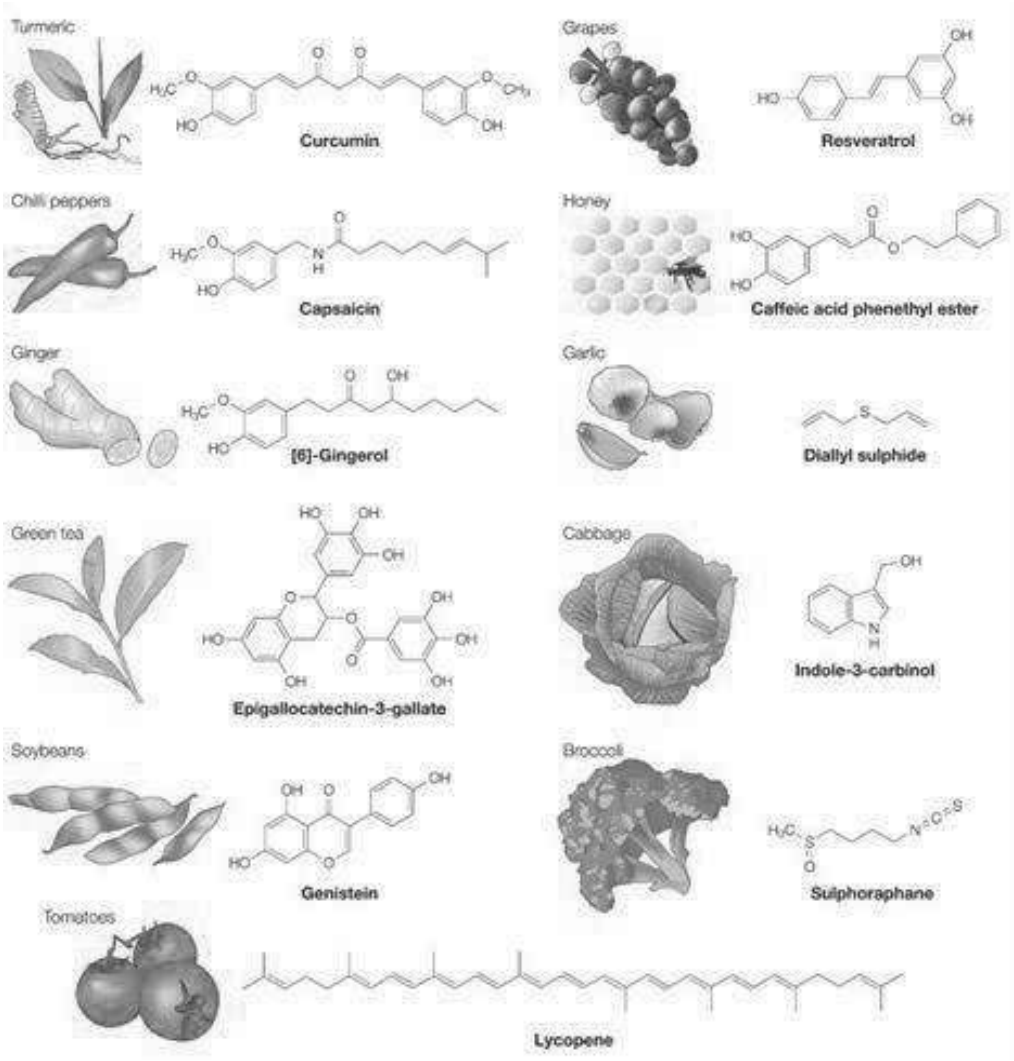

Figure 29. Representative Nrf2-activating chemopreventive phytochemicals and their dietary sources [293]

HNE has been widely reported to activate Nrf2 and contribute to the prevention of diseases like atherosclerosis, acute gastric mucosal lesions and cardiac disease [301-305]. This activation has been shown to be coordinated by activation of mitogen-activated protein kinase (MAPK) pathways, leading to nuclear translocation of Nrf2 and subsequent expression of cytoprotective enzymes [303]. However, the direct mechanism by which HNE activates

Nrf2 is still unknown. The ability of HNE to form protein adducts is suspected to be involved in Nrf2 activation by HNE through disruption of Nrf2 stability with its associated proteins [231].

Several natural phytochemicals that are present naturally in many plant extracts can exert inhibitory activities against Nrf2 activation. Trigonelline, a coffee alkaloid, efficiently decreased tertiary butylhydroquinon (tBHQ)-induced Nrf2 activity in chemoresistant pancreatic carcinoma cell lines [306]. Chrysin (5,7-dihydroxyflavone), apigenin (4',5,7-trihydroxyflavone) and luteolin (3',4',5,7-tetrahydroxyflavone) are natural flavones present in many fruits and vegetables that reduced Nrf2 expression in hepatocellular carcinoma cells [307-309]. Brusatol is a quassinoid extracted from *Brucea javanica* that reduced Nrf2 protein level in various cancer cells and sensitized them to chemotherapeutic agents [310]. Carcinogenic ochratoxin A also inhibits Nrf2 responses and this is involved in its nephrotoxicity and renal carcinogenicity [311].

1.4.5. Tumor suppressor functions of Nrf2

There are abundant evidences showing that Nrf2 activation is able to suppress carcinogenesis, especially in its early stages. Nrf2 is even considered as a major mechanism of protection against chemical and radiation capable of damaging DNA integrity and initiating carcinogenesis [312]. The role of Nrf2 in chemoprevention is mainly focused on its ability to regulate the expression and coordinated induction of genes encoding cytoprotective enzymes in reponse to chemical and radiation stress, therefore preventing further cellular damages that might occur. This leads to reduced cell death and enhanced cell survival. In addition, Nrf2 has also been reported to upregulate anti-apoptotic proteins BCL-2 (B-cell lymphoma 2) and BCL-xL (Chapter 1.5.1), favoring cell survival by preventing apoptosis [313,314].

Some diverse chemopreventive drugs, which act as Nrf2 activators, have been applied to human usage and proven to inhibit early-stage colon carcinogenesis such as sulphoraphane [315]. The same effect has also been exerted by the application of celecoxib and curcumin, other types of chemopreventive drugs [316]. In a prevention study using genetic models of carcinogenesis, synthetic oleanane triterpenoids have been reported to delay the onset of oncogene-driven tumorigenesis [317].

A study using Nrf2-knockout mice has shown that mice deficient in Nrf2 underwent increasing sensitivity to carcinogenesis and loss in chemoprotective efficacy of enzymes

inducers [318]. In addition, their susceptibility to carcinogenesis induced by colon inflammation was reported to increase [319]. These findings emphasize the potential of Nrf2 as a target for chemoprevention. However, numerous publications have revealed the potentially oncogenic activity of Nrf2 that would lead to increasing concerns about the safety of a long-term increase in Nrf2 activity.

1.4.6. Paradox of Nrf2: protective and oncogenic

As Nrf2 promotes cell survival under oxidative stress, it is logical to argue that increased Nrf2 activity could be tumor promoting by being protective to cancer cells [320]. Mutations on Keap1 or Nrf2-encoding genes have been found in several types of human cancers. These mutations disrupt Nrf2-Keap1 complex stability, leading to Nrf2 hyperactivity [234]. In the case of CRC, the promoter region of Keap1 gene is often hypermethylated. This hypermethylation inhibits Keap1 gene expression, which results in the accumulation of Nrf2 [321]. Moreover, the fact that the expression of Nrf2 is induced by oncogenes [283] provides an idea that Nrf2 is also a defense system of cancerous cells to protect themselves. Additionally, an increase in Nrf2 level has been shown in tumor cells, together with an increase in the expression of cytoprotective enzymes and in the hyperanabolism of glucose molecules [249,316]. These findings show that Nrf2 might also give protective effects favoring carcinogenesis and therefore explain the chemoresistance of tumor tissues towards chemotheraphy.

The revelation of both favorable and adverse effects of Nrf2 in carcinogenesis has raised doubts related to its potential as a target for chemoprevention. The action of Nrf2 is likened as a double-edged sword. On one hand, Nrf2 is beneficial because it may protect normal cells from oxidative stress by inducing the expression of cytoprotective enzymes. On the other hand, this protective effect may also be beneficial to the survival of cancerous cells and favor their development. These two opposing roles of Nrf2 depend on the tumor stage (Figure 30). Nrf2 activity is desirable (for the host organism) in early stages of tumorigenesis in order to enhance the endurance of normal cells towards oxidative stress and to prevent further malignancy. However, in cancerous cells, the enhancement of Nrf2 activity (caused by mutations) may confer protumorigenic metabolic alterations. For example, in skin carcinogenesis, Nrf2 activation in oncogenicly-mutated keratinocytes increased the level of NADPH, purine and glutathione levels that promoted tumor development [322]. Nrf2 activation would also protect tumors from insults generated from chemotheraphy, resulting in

its inefficiency. The importance of Nrf2 in tumor resistance concerning chemotheraphy has been highlighted in several studies, including those regarding CRCs. Knockdown of Nrf2 by siRNA (small interfering RNA) or shRNA (small hairpin RNA) enhanced the sensitivity of colon cancer cells to chemotheraphy agent 5-fluorouracil (5-FU) [323].

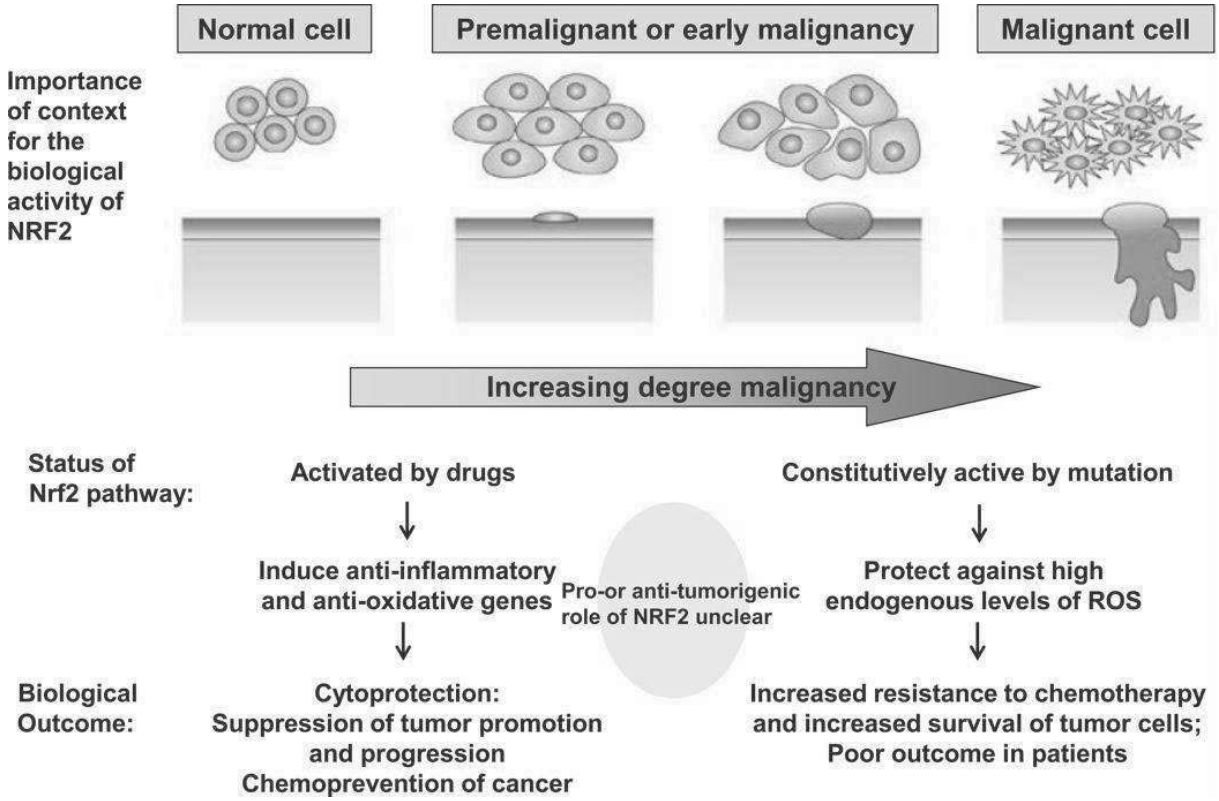

Figure 30. Model for the importance of the context of tumor stage for the biological consequences of Nrf2 activation [232]

1.5. Apoptosis and autophagy in carcinogenesis

According to cell morphological appearance, cell death can be generally classified into three types: apoptosis, autophagy and necrosis [324]. Apoptosis and autophagy (also known as Type I and Type II cell-death respectively) are both considered as programmed cell death since their enrollment is mediated by an intracellular program. Necrosis (Type III cell-death, not discussed in this manuscript) is caused by external factors such as trauma and infection, and therefore is accidental or unprogrammed. HNE has been reported to be involved in these types of cell death [210].

1.5.1. Apoptosis

Apoptosis (Figure 31) is mainly characterized by massive activity of caspases (cysteine-dependent aspartate-directed proteases) followed by cell shrinkage and fragmentation into smaller membrane-bound apoptotic bodies (membrane blebbing) before they are rapidly removed by other healthy cells through phagocytosis. The nucleus undergoes characteristic changes, including chromatin condensation and DNA breaks. Generally, apoptosis is not associated with a subsequent inflammatory response [325-327].

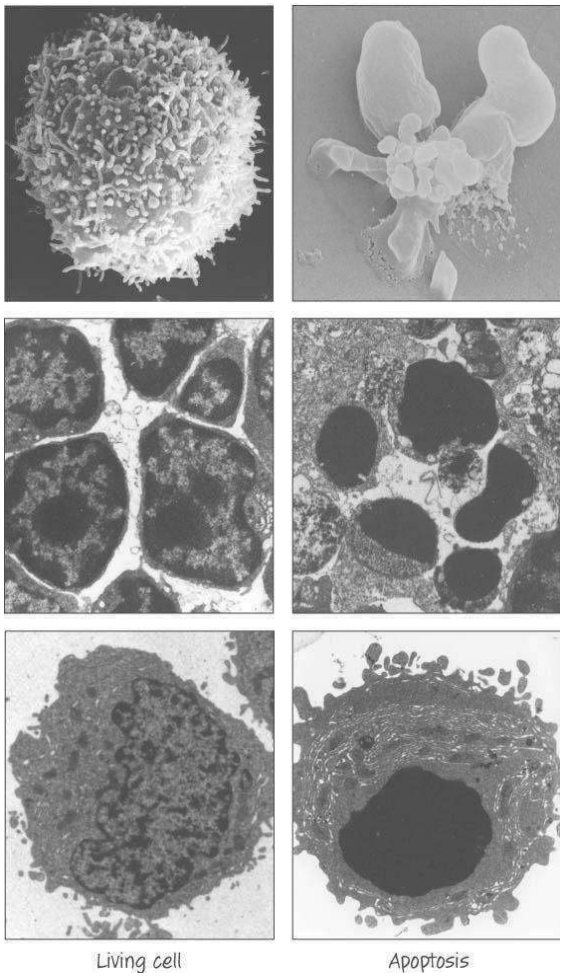

Figure 31. Apoptosis snapshots showing its characteristics including membrane blebbing and chromatin condensation [325].

Caspases (cysteine aspartate-specific proteases) are the main actors of apoptosis. Two types of caspases are involved in apoptosis mechanisms: 1) initiator caspases (such as in mammals, caspase-8 and -9) and 2) executioner caspases (in mammals, caspase-3, -6 and -7). Initiator caspases, activated by dimerization by adaptor protein, serves to activate executioner caspases that cleave cellular proteins in general, therefore conducting "cell death by thousands

of cuts". Caspases show preferences for cleaving their substrates based on peptide constitution in proteins. They generally cleave proteins after aspartate residue (coded as D in single letter amino acid code). The preferences for cleavage site of caspase-3, -6, -7, -8 and -9 are DELD, (T/V)QVD, DEVD, LETD and LEHD respectively [325,328,329].

There are two known pathways of apoptosis: 1) mitochondrial pathway (intrinsic pathway) that involves formation of mitochondrial pores and 2) death receptors-dependant pathway (extrinsic pathway) that involves ligand-mediated activation of membrane death receptors (Figure 32) [325,330]. Both pathways lead to activation of executioner caspases and have been shown to be able to interact with each other or other cell death mechanisms.

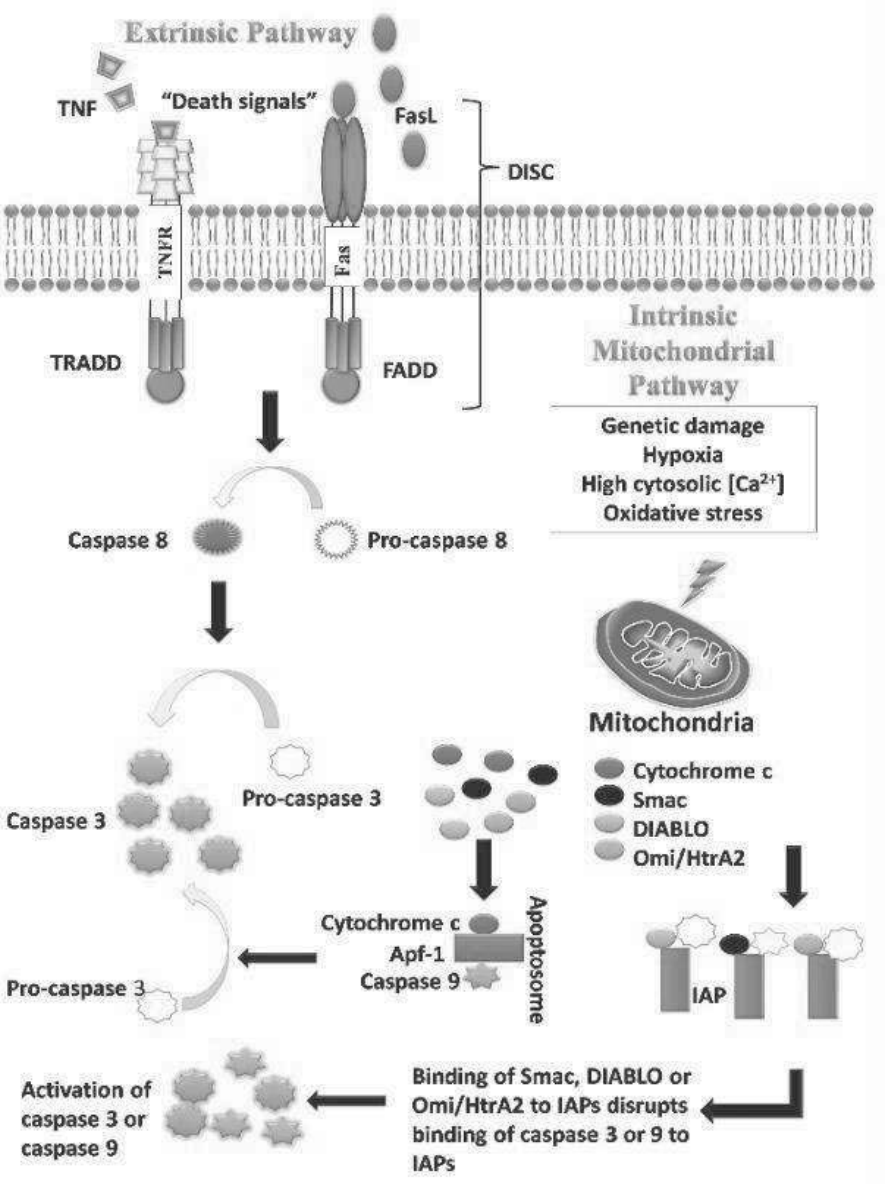

Figure 32. Model for intrinsic and extrinsic pathways of apoptosis [331].

The intrinsic apoptotic pathway involves mitochondrial outer membrane permeabilization (MOMP) following internal stimuli such as irreparable genetic damage, hypoxia, high cytosolic Ca^{2+} or severe oxidative stress [332]. This pathway is regulated by BCL-2 (B-cell lymphoma 2) family proteins that regulate the integrity of mitochondrial membrane. There are two main groups of BCL-2 proteins, namely the anti-apoptotic proteins (such as BCL-2, BCL-xL, BCL-W, BFL-1, and MCL-1) and the pro-apoptotic proteins (such as BAX, BAK, BAD, BCL-X, BID, BIK, BIM and HRK). While the anti-apoptotic proteins regulate apoptosis by blocking MOMP, the pro-apoptotic proteins promote such a permeabilization. The balance between the pro- and anti-apoptotic proteins determines apoptosis initiation. MOMP results in the release of pro-apoptotic cytochrome-c and other apoptotic factors such as apoptosis-inducing factor (AIF), second mitochondria-derived activator of caspase (Smac), direct IAP binding protein with low pI (DIABLO) and Omi/high temperature requirement protein A (HTRA2) [333]. The released cytochrome-c activates caspase-3 via the formation of a complex called apoptosome made up of cytochrome-c, APAF-1 and caspase-9. Smac/DIABLO and Omi/HTRA2 promotes caspase activation by binding to inhibitor of apoptosis proteins (IAPs) which subsequently leads to disruption in the interaction of IAPs with caspase-3 or -9 [334].

The extrinsic apoptotic pathway is triggered by the interaction of extracellular ligands with receptors on the cell surface. Although several death receptors have been described, the best known death receptors are tumor necrosis factor receptor 1 (TNFR1) and Fas (CD95) with TNF (tumor necrosis factor) and Fas ligand (FasL) as their ligands respectively [335]. These death receptors possess an intracellular death domain that recruits adapter proteins such as TNF receptor-associated death domain (TRADD) and Fas-associated death domain (FADD). Activated FADD or TRADD dimerizes and activates initiator caspase-8. The assembly of death receptor, death ligand, adapter protein and caspase-8 is called DISC (death-inducing signaling complex) and in turn activates executioner caspase-3 to carry out apoptosis [325,336]. It is noteworthy that different adaptor caspases are involved in intrinsic and extrinsic apoptotic pathway: caspase-9 in intrinsic pathway and caspase-8 in extrinsic pathway). However, the executioner caspases in both processes are caspase-3, -6 and -7.

1.5.1.1. Apoptosis and carcinogenesis

In carcinogenesis, the balance between cell proliferation and cell death is a critical factor since the disruption of this balance would drive the tendency of carcinogenesis forward

or backward [337]. Plausibly, too little cell death by apoptosis accompanied by too much cell proliferation can promote tumor formation as well as tumor progression. It is therefore not surprising that one of the characteristic features of human cancers is the inability to undergo apoptosis in response to stimuli that otherwise would trigger apoptosis in normal or sensitive cells [338]. Indeed, defective apoptosis is an acquired hallmark of cancer cells [339].

Cancer can be viewed as the result of a succession of genetic changes during which a normal cell is transformed into a malignant one while evasion of cell death is one of the essential changes in a cell that cause this malignant transformation. The defective apoptosis, which is observed in most cancer cells, is acquired through the successive mutations occurring during the carcinogenesis [340]. Through this evolutionary process, the transformed cells gain a better resistance to a certain insult compared to normal untransformed cells and this difference of resistance would favor the survival of transformed cells over normal cells, allowing further mutations and carcinogenesis [341] (Figure 4, Chapter 1.1.4). There are many ways a malignant cell can acquire apoptosis resistance. Generally, the mechanisms by which evasion of apoptosis occurs during carcinogenesis can be broadly divided into: 1) disrupted balance of pro- and anti-apoptotic proteins, 2) increased expression of anti-apoptotic factors (such as IAPs) or reduced expression of pro-apoptotic factors (such as caspases), 3) defects or mutations in apoptosis-related genes (such as pro-apoptotic p53) and 4) impaired death receptor signaling [331] (Figure 33).

1.5.1.2. APC and apoptosis

The link between APC and apoptosis is defined by armadillo repeat binding domain at N-terminal of APC protein (Figure 5) that is considered as a pro-apoptotic domain. During apoptosis, effector caspases-3 cleave APC resulting in two fragments: a fragment containing Armadillo repeat binding domain and a fragment containing β-catenin binding site [342]. The fragment with armadillo repeat binding domain then migrates to the mitochondria where it can promote cell sensitivity to apoptosis, thus exerting pro-apoptotic activity. However, this pro-apoptotic activity can be inhibited by mitochondrial 40-kDa apoptotic suppressor protein hTID-1 (human tumorous imaginal disc 1), that binds to the armadillo repeat binding domain of the cleaved APC at aa 202-512. Binding to 43-kDa isoform of hTID-1 enhanced the pro-apoptotic activity of APC fragment containing armadillo repeat binding domain [343]. Furthermore, apoptosis also allows the cleavage of β-catenin, a protein that is activated in Wnt signaling pathway (Figure 6) [342].

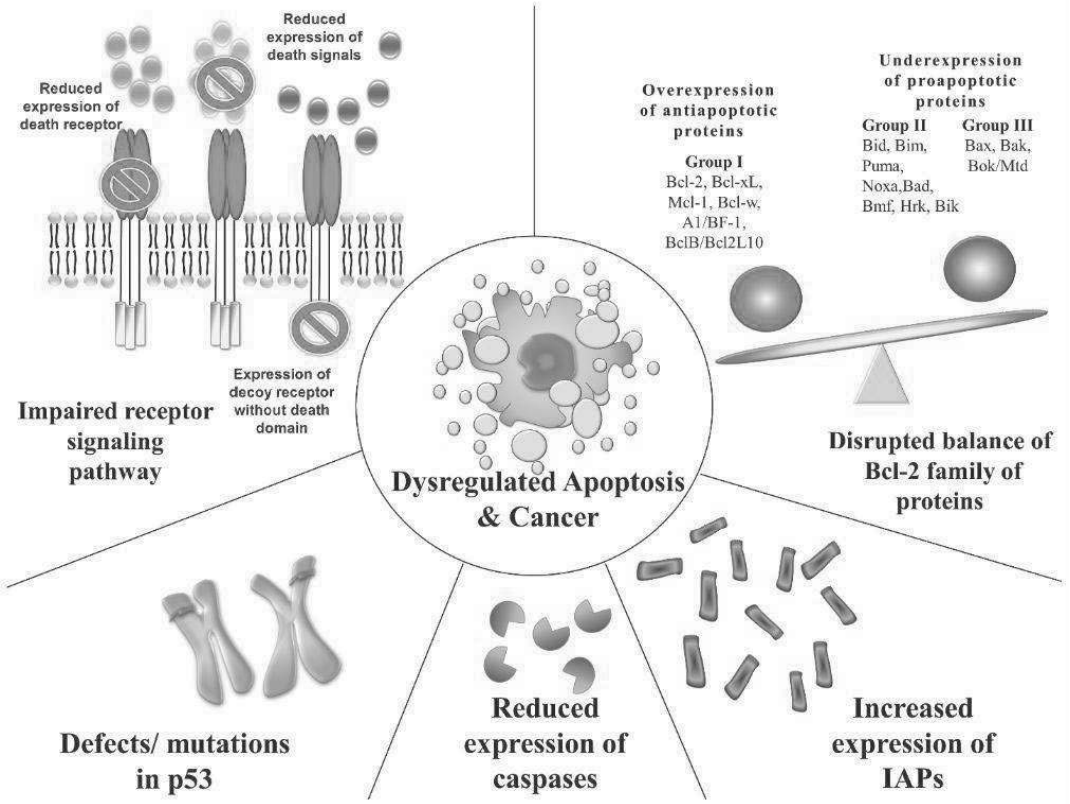

Figure 33. Mechanisms contributing to evasion of apoptosis and carcinogenesis [331].

1.5.1.3. 4-Hydroxynonenal and apoptosis

The role of HNE in intrinsic apoptotic pathway involves mitochondrial membrane disturbance, oxidative stress, p53 activation and AKT inhibition (Figure 34). Mitochondrial membrane contains a critical phospholipid called cardiolipin. Cardiolipin oxidation can generate HNE and activate MOMP [344]. HNE can also directly affect cellular redox status by depleting GSH, which can in turn induce mitochondrial crisis with mitochondrial ROS production and subsequent caspases activation [345,346]. AKT (also called protein kinase B, PKB) is a serine/threonine kinase that plays a key role in multiple cellular processes, including apoptosis. AKT regulates BCL-2 positively and BAX negatively, therefore favoring cell survival through apoptosis inhibition. Recently, HNE was shown to inhibit AKT and this inhibitory activity was related to HNE-induced apoptosis [347]. Tumor suppressor p53 is a transcription factor that regulates gene expression related to cell cycle, DNA repair and apoptosis. p53 is activated upon DNA damage and oxidative stress to protect and repair the cell, but if the stress or damage reaches a threshold, p53 triggers cell death. DNA damage or oxidative stress triggered by HNE can activate p53 which in turn will induce the expression of

proteins targeting apoptotic pathways and specifically repress the transcription of several death-inhibiting genes [348]. Some of p53 target genes that are involved in apoptosis machinery are BAX, PUMA (p53 up-regulated modulator of apoptosis) and NOXA (also known as PMAIP1, phorbol-12-myristate-13-acetate-induced protein 1) that exert pro-apoptotic activity [349-352].

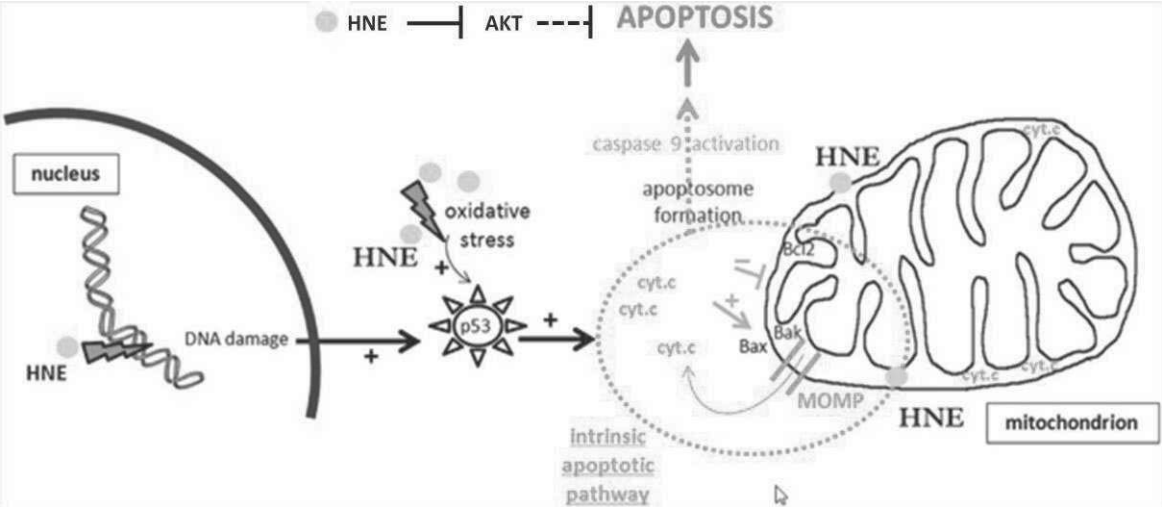

Figure 34. Role of HNE in intrinsic apoptotic pathway includes mitochondrial membrane disturbances, oxidative stress, AKT inhibition and p53 activation ([210] with modifications).

HNE has also been shown to be involved in the extrinsic apoptotic pathway (Figure 35). It promotes the expression of Fas (CD95), allowing cell sensitization to apoptosis when Fas-L is present in the microenvironment [353]. This up-regulation of Fas expression is linked to DNA damage or oxidative stress induced by HNE that activates p53 (Figure 34). Fas is a target gene of p53 and p53 is also involved in post-expressed Fas relocation to the cell surface [354,355]. The main pathway of Fas-signaling activation by HNE appears to be DISC-independent without caspase-8 and FADD. HNE can form adducts with cysteine residues of Fas resulting in Fas aggregation that could mimic ligand-cell surface receptor binding. This phenomenon results in the downstream activation of ASK1 (apoptosis signal-regulating kinase 1) and JNK (c-Jun N-terminal kinase) that can regulate apoptosis. JNK can translocate to the nucleus and phosphorylate c-Jun that will form AP-1 (activator protein 1) transcription factor with phosphorylated c-Fos. This transcription factor regulates the expression of pro-apoptotic genes [356]. JNK can also translocate to mitochondria and provoke MOMP to trigger the intrinsic apoptotic pathway [357]. Lastly, in the nucleus, HNE can create covalent links with nuclear protein Daxx (death domain-associated protein) via histidine residues and

induce Daxx export to the cytosol. Subsequently, Daxx can form a complex with Fas that exerts apoptosis negative feedback by regulating negatively JNK [358,359].

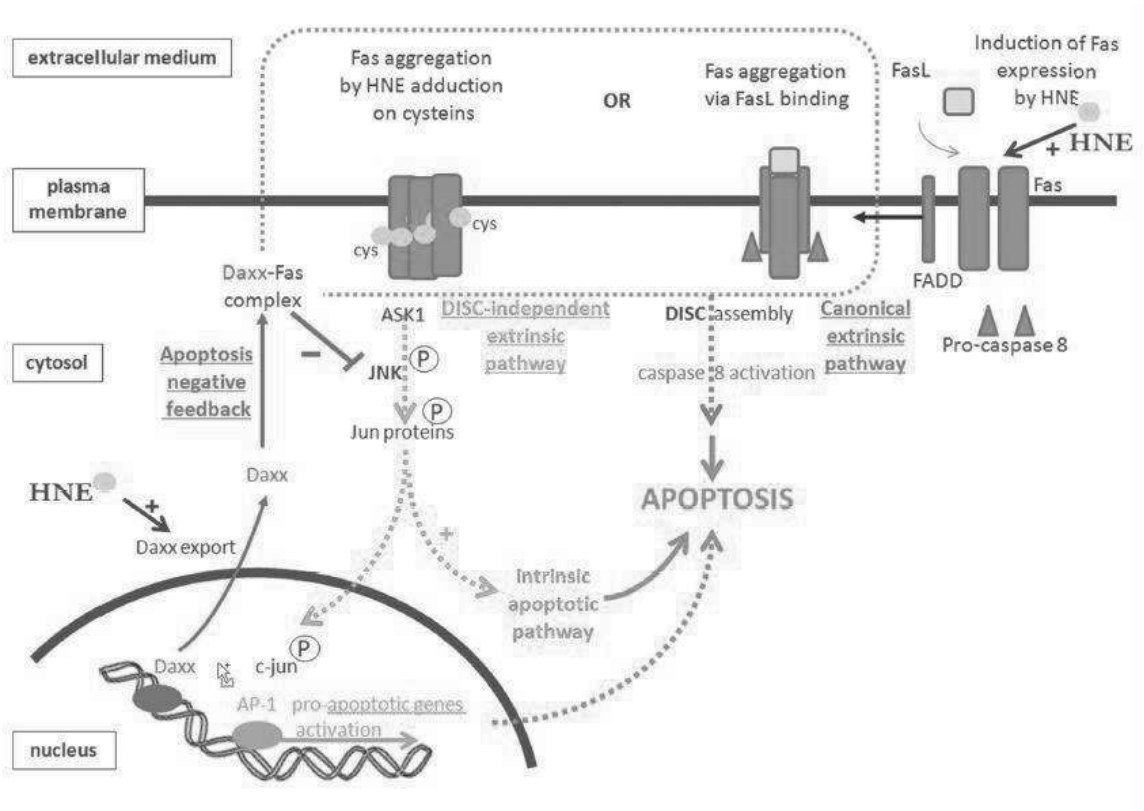

Figure 35. Role of HNE in extrinsic apoptotic pathway includes Fas aggregation-related JNK activation and induction of Daxx export to the cytosol [210].

1.5.2. Autophagy

Autophagy is defined as a lysosomal-mediated degradation activity providing an essential mechanism for recycling cellular constituents and clearance of excess or damaged lipids, proteins and organelles [360]. Cells utilize autophagy to recycle basic molecules during nutrient deprivation, to scavenge harmful or damaged organelles and to eliminate intracellular pathogens. As such, the autophagic process plays a crucial role in maintaining cellular homeostasis and also contributes to cell survival during stress [361,362]. Depending on the route of delivery to the lysosomes, three different types of autophagy are defined: 1) microautophagy, 2) chaperone-mediated autophagy and 3) macroautophagy (Figure 36).

Microautophagy describes extension and/or invagination of lysosomal membranes to engulf and degrade intracellular contents [363,364]. This process has been shown to be dependent on ATP and microfilaments and be facilitated by phospholipid-HSC70 (heat shock

cognate 70) interaction [365-367]. Chaperone-mediated autophagy involves chaperone protein HSC70 recognizing proteins with a consensus KFERQ sequence and bringing the proteins to the lysosomes *via* lysosome-associated membrane protein 2A (LAMP-2A) receptor [368]. Macroautophagy is characterized by formation of double-membrane vesicles that recognize and encircle intracellular excessive or damaged lipids, proteins and organelles. The autophagic vesicles (autophagosomes) then fuse with lysosomes (autophagolysosomes) and their contents are degraded by lysosomal enzymes [369,370]. These three types of autophagy have shared as well as independent machineries and their activities may compensate or regulate one another. This part will solely focus on macroautophagy, which is hereafter simply termed autophagy (Figure 37).

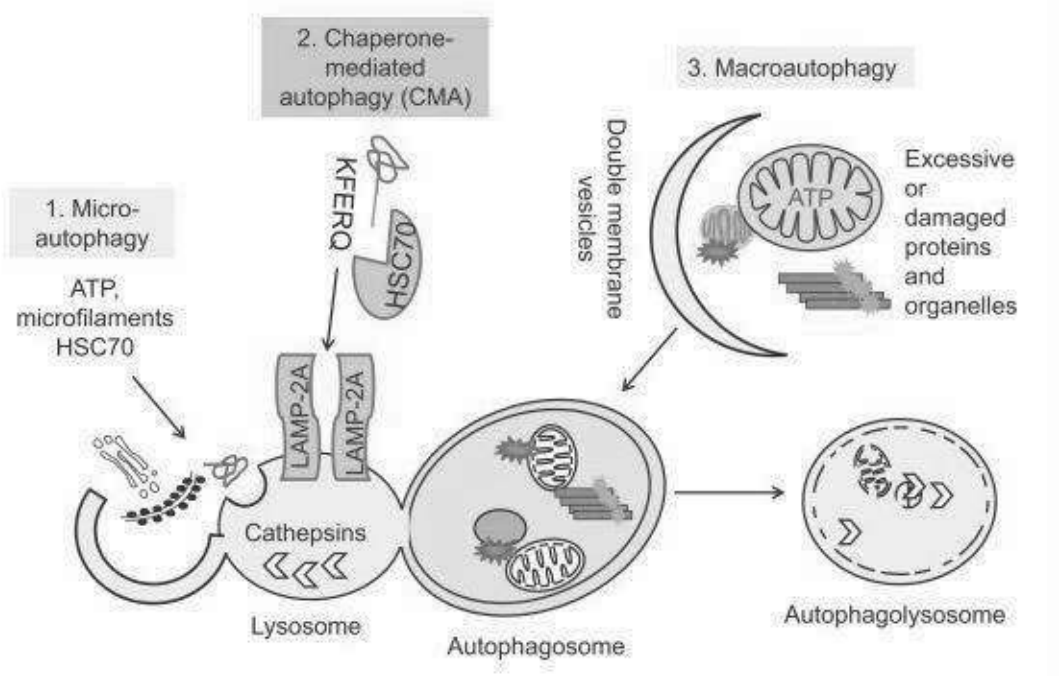

Figure 36. Three types of autophagy:
microautophagy, chaperone-mediated autophagy and macroautophagy [360].

At the beginning of its discovery, autophagy was assumed to be a bulk degradation pathway for intracellular components and therefore, was considered as a non-selective process. Recent studies, however, have highlighted the capacity of this pathway to selectively eliminate specific intracellular structures and thus better fulfil the catabolic necessities of the cell. Non-selective bulk autophagy, characterized by indiscriminate sequestration of cytosolic cargos to autophagosomes, is believed to ensue as a response to nutrient deprivation. This process mediated the recycling and global turnover of cytoplasmic materials. In contrast,

selective autophagy consists of the removal of specific cargos (including unfolded or aggregated proteins, several organelles and intracellular pathogens). Several types of selective autophagy have been identified and these processes turn over specificly a type of organelles. Cargo-specific names have been given to distinguish the various selective pathways, including the ER (reticulophagy), peroxisomes (pexophagy), mitochondria (mitophagy), lipid droplets (lipophagy), secretory granules (zymophagy), parts of the nucleus (nucleophagy), pathogens (xenophagy) and ribosomes (ribophagy) [371,372].

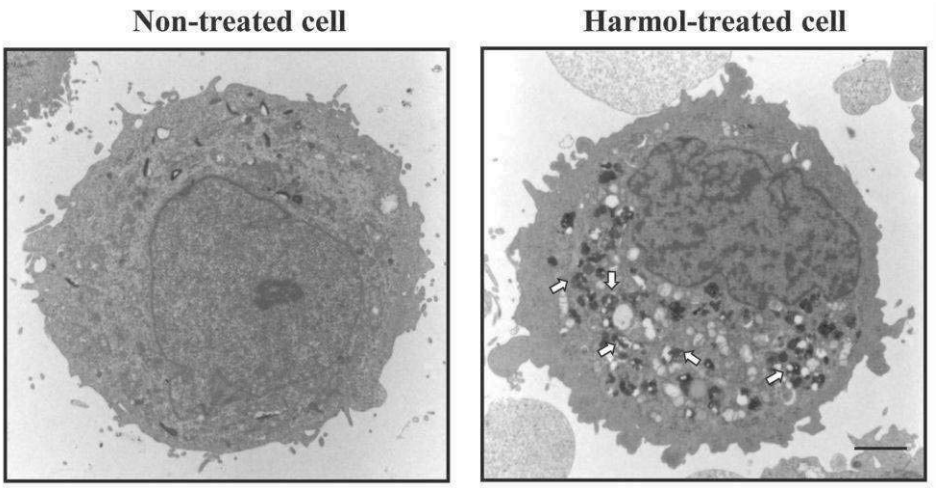

Figure 37. Electron micrographs showing macroautophagy (autophagy) in harmol-treated U251MG human glioma cells (100 μM, 12 h). The white arrows point to autophagosomes and autolysosomes (scale bar, 2 μm) [373].

The key players in selective autophagy are the so-called autophagy receptors. These play an important role in selective autophagy by allowing the recognition of cargos to be engulfed by the autophagosomes. Autophagy receptors connect the cargos to the autophagosomal membrane. The lipidated proteins light chain 3 (LC3)-II present in the inner and outer leaflets of autophagosomal membrane are the targets of autophagy receptors for cargo recognition (Figure 38). In general, autophagy receptors possess two important domains called LC3-interacting region (LIR) and ubiquitin-binding domain (UBD) that allow them to bridge LC3-II proteins in the autophagosomal membrane and the ubiquitylated cargos respectively [374]. p62/sequestosome 1 (SQSTM1) was the first selective autophagy receptor described in mammalian cells. So far, four human ubiquitin-binding autophagy receptors have been identified and are classified in a group named sequestosome 1-like receptors (SLRs): p62, NBR1 (neighbor of breast cancer early-onset 1 gene 1), NDP52 (nuclear dot protein 52) and OPTN (optineurin) [375].

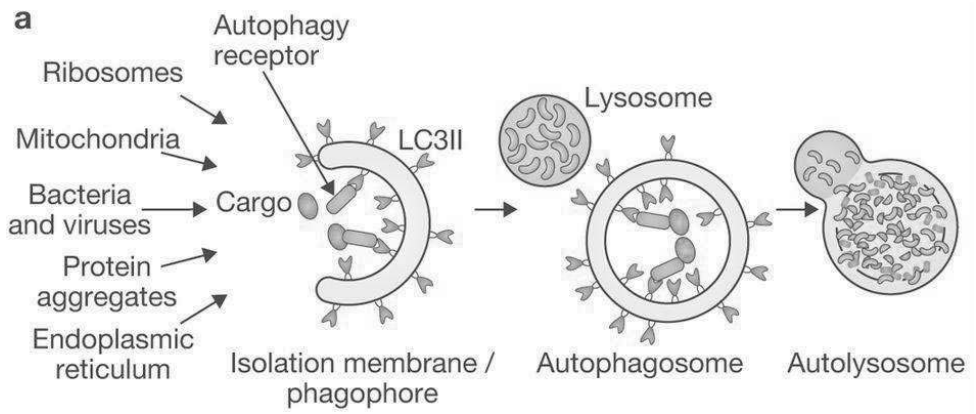

Figure 38. Autophagy receptor recognizes cargos and allows their recruitment to the autophagosomal membrane [375].

Autophagy machinery consists of more than 30 proteins and regulators that are involved in the signaling for autophagy stimulation and the formation of autophagosomes. The main regulatory pathway involves: 1) initiation of autophagy regulated by mTOR (mammalian target of rapamycin) inhibition, 2) nucleation of autophagic vesicles, 3) extension of autophagosomal membranes by ubiquitin-like conjugation pathways as well as LC3-II insertion into autophagosomal membranes and 4) cargo recognition, including p62 binding to both ubiquitinated proteins and LC3-II (Figure 39).

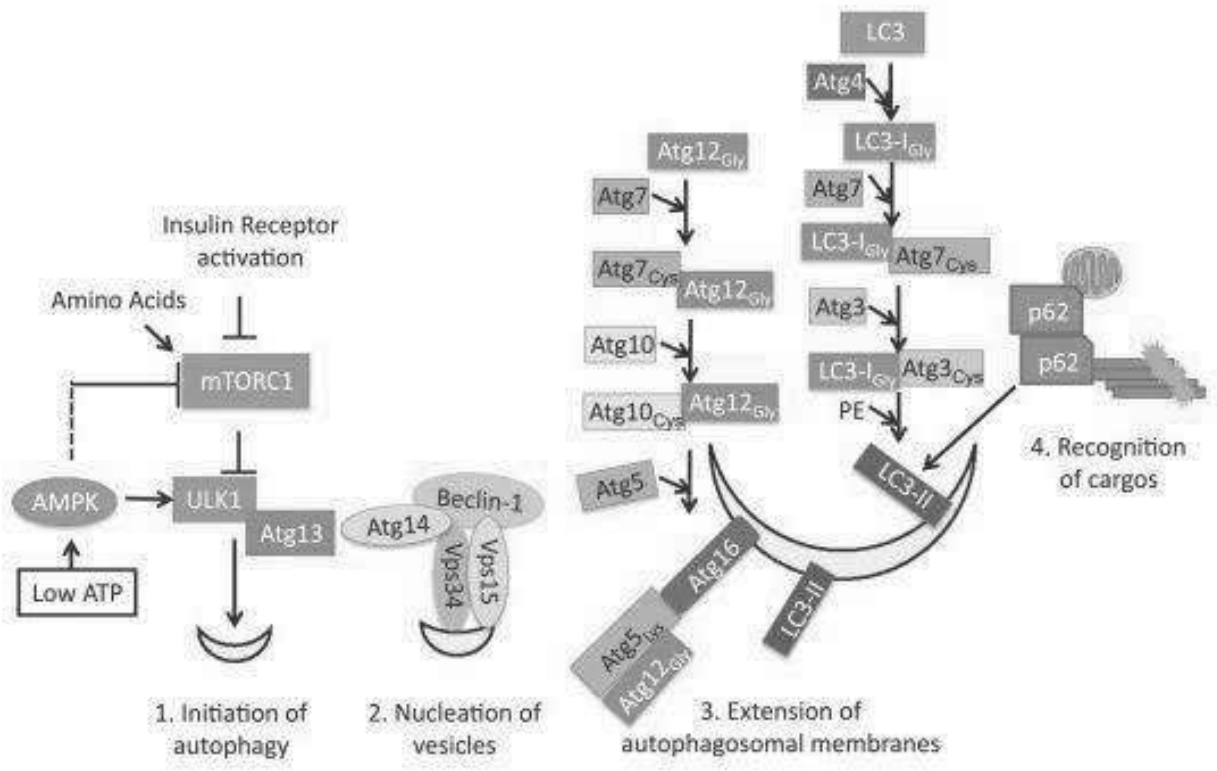

Figure 39. Proteins involved in autophagy machinery [360].

mTOR (mammalian target of rapamycin) is the key regulator of autophagy and its activity depends on nutrient availability. When nutrients or amino acids are plentiful, mTOR is active; cells grow and autophagy is inhibited. However, when energy levels are low, AMP (adenosine monophosphate) accumulates and this activates a kinase, AMPK (AMP kinase), that inhibits mTOR, and therefore autophagy is engaged. mTOR is also inhibited in response to insulin receptor withdrawal. The drug rapamycin is a potent inhibitor of mTOR and the addition of this drug to cells induces autophagy [325].

Autophagy in mammals is initiated by the ATG13 (AuTophaGy-related gene 13) complex containing a kinase called ULK1 (unc-51-like autophagy activating kinase 1), ATG13, ATG101 and FIP200. When autophagy is activated, this complex dissociates, ULK1 activates ATG13 by phosphorylation and ATG13 recruits the next complex in the pathway for nucleation of vesicles. This complex contains Beclin-1, ATG14, VPS34 (vacuolar protein sorting 34) and VPS15. During the extension of autophagosomal membranes, ATG7 is brought in, binding ATG12 and passing it to ATG10, which then places it on another protein, ATG5 by ubiquitin-like conjugation pathways. The ATG5-ATG12 complex recruits another protein, ATG16 to form the platform for the next step in the process. This complex associates with the autophagosomal membrane at an early step and dissociates from the autophagosomes upon completion of autophagy [325,360]. The source of autophagosomal membrane has been proposed to be plasma membrane, endoplasmic reticulum, Golgi and mitochondrial membranes [376,377].

The protease ATG4 cleaves pro-LC3 into LC3-I exposing a glycine residue at the C-terminal. LC3-I is then conjugated with ATG7 then ATG3 *via* thioester bonds and with phosphatidylethanolamine (PE) through an amide bond, forming LC3-II and insertion into autophagosomal membrane. LC3-II association with the autophagosomes will be sustained until autophagosomes fuse with lysosomes. ATG4 is able to delipidate LC3-II back to LC3-I. The transfer of cargos into autophagosomes involves p62, an adaptor protein that recognizes ubiquitinated proteins [325,360]. The structure of p62 contains LC3-interacting regions (LIR) that enables it to bind to LC3-II embedded in the autophagosomal membrane, thus bridging the link between the autophagosomal membrane and to-be-degraded cargos [376,378,379].

1.5.2.1. Autophagy and oxidative stress

It is commonly accepted that the principle source of endogenous oxidative stress in the cell is the mitochondrial respiratory chain that generates ROS. Indeed, oxidative stress has

been reported to induce autophagy and antioxidant supplementation partially or completely reverted the process [380-385]. The interplay between autophagy and oxidative stress is presented in Figure 40. Superoxide (O_2^-) and H_2O_2 are the principle ROS generated by mitochondria upon nutrient deprivation. They positively regulate autophagy by means of at least three different mechanisms: 1) *S*-glutathionylation (SH→S-SG) of cysteines located in the subunits of AMPK, 2) oxidation of Cys81 (SH→Sox) of ATG4 that in turn leads to the inactivation of its 'delipidating' activity on LC3 and to the accumulation of the pro-autophagic LC3-II form and 3) wide alteration of thiol redox state (e.g., decrease of GSH/GSSG ratio and increase of oxidized thiols, Sox) that is facilitated by the release of GSH to the extracellular milieu through MRP1. Following its activation by ROS, autophagy is directed to degrade intracellular components damaged by ROS and to participate in p62-regulated Nrf2 activation through the degradation of Keap1 (Chapter 1.4.2.4).

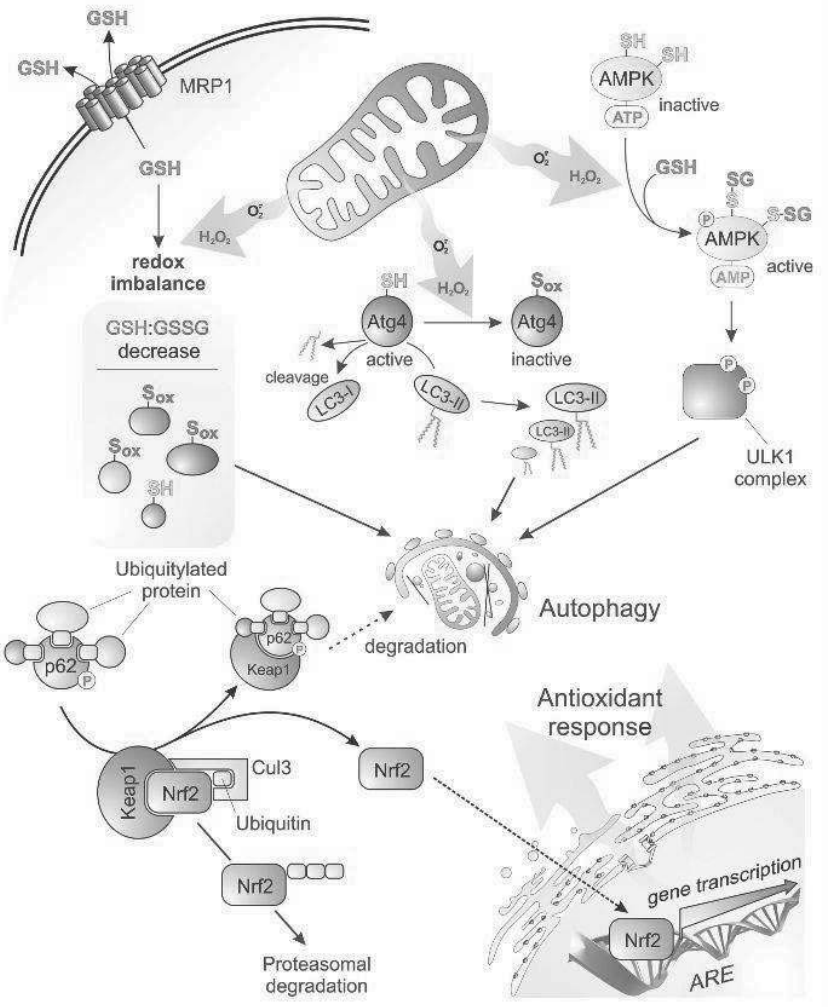

Figure 40. Interplay between autophagy and oxidative stress [386].

1.5.2.2. Autophagy and immune system

The immune system exists as a protection mechanism against diseases or other potentially damaging foreign bodies towards human body. Autophagy has been reported to be involved in such a process. At least four scopes have been identified to explain the roles of autophagy in immunity: 1) elimination of microorganisms, 2) control of pro-inflammatory signaling, 3) adaptive immunity and 4) secretion of immune mediators (Figure 41).

Autophagy is involved in the elimination of microorganisms present in the cell (Figure 41A). An incoming bacterium can induce autophagy by competing for nutrient with the host cell, thereby inhibiting mTOR. Innate immune receptors such as Toll-like receptors (TLRs) can also detect the presence of a bacterium and induce a particular type of phagocytosis mediated by LC3 called LC3-associated phagocytosis (LAP). This process is dependent on TNF receptor-associated factor 6 (TRAF6) and the formation of ROS involving NAD(P)H oxidase (NOX). Xenophagy can also take place to degrade the invading bacterium, both non-selectively (dependent on NOD2 (nucleotide-binding oligomerization domain-containing protein 2) and ATG16L1 (ATG16-like 1)) or selectively by involving autophagy receptors SLRs. Apart from detecting ubiquitins, some SLRs can also recognize galectins bound to pathogen-associated damaged vacuolar membranes. Genetic materials of a virus can also be degraded by xenophagy [387].

Autophagy is also able to control pro-inflammatory signaling (Figure 41B). Autophagy can deliver cytoplasmic pathogen-associated molecular patterns (PAMPs) to pattern recognition receptors (PRRs) such as endolytic TLRs and stimulate pro-inflammatory mediators. Failure to remove SLRs by autophagy can also increase the levels of pro-inflammatory signaling. Several phenomena can also incite inflammasome-mediated pro-inflammatory signaling by activating interleukins (IL) IL-1β and IL-18, such as leak of lysosomal protease, potassium ion (K^+) efflux and damaged mitochondria. Damaged mitochondria liberate ROS and mitochondrial DNAs into the cytoplasm that activate NLRP3 (NOD-, leucine-rich repeats (LRR)- and pyrin domain-containing protein 3) and AIM2 (absent in melanoma 2) inflammasomes. Autophagy can limit inflammasome activation by removing damaged mitochondria. In addition, autophagy proteins ATG5-ATG12 can inhibit inflammatory signaling by disrupting the interaction between RIG-I (retinoic acid-inducible gene I) and IPS1 (Interferon β promoter stimulator protein 1) that activates Type I IFN (interferon), a pro-inflammatory factor [387].

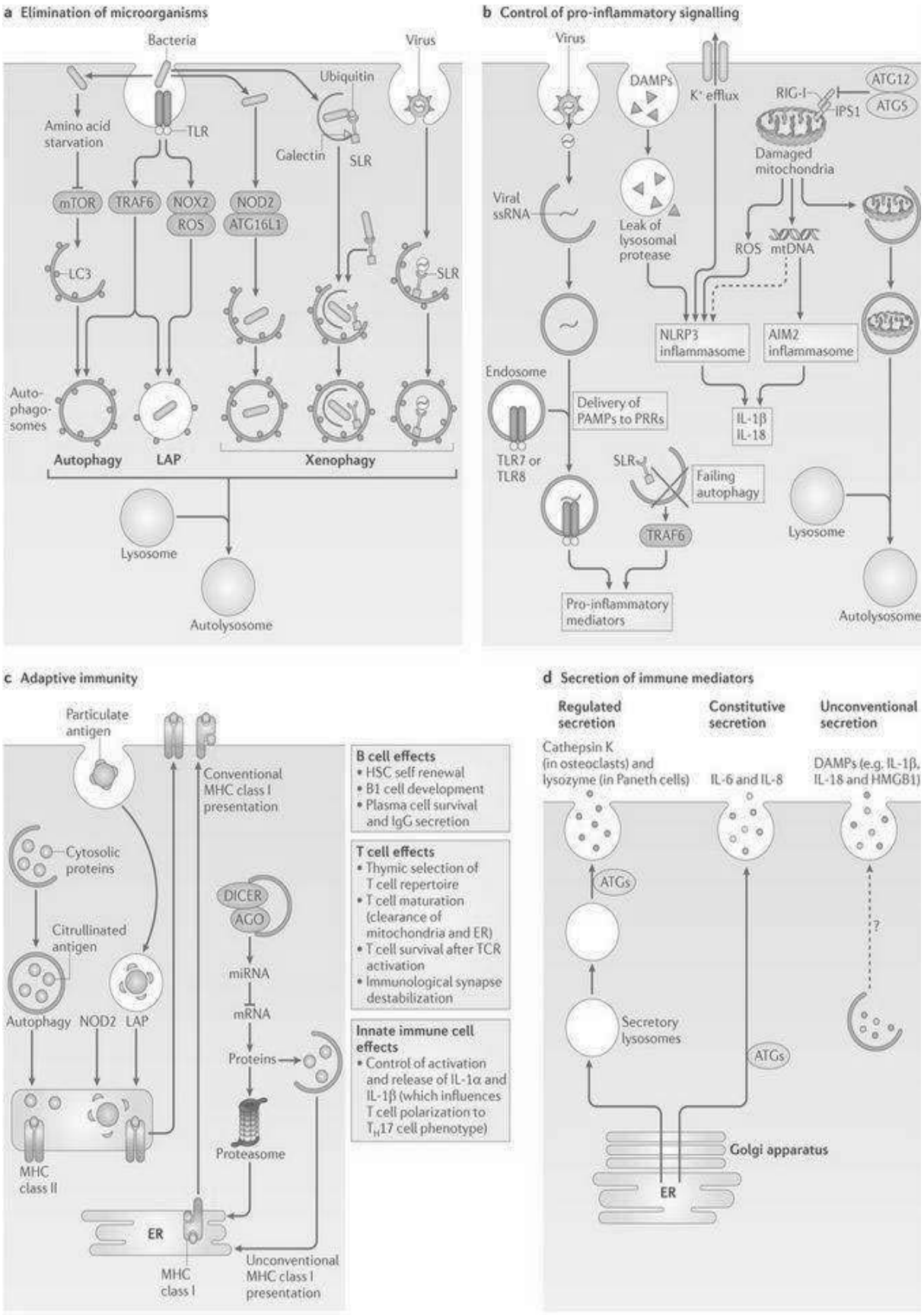

Figure 41. Principal roles of autophagy in immunity consisting of A) Elimination of microorganisms, B) Control of pro-inflammatory signaling, C) Adaptive immunity and D) Secretion of immune mediators [387].

In adaptive immunity, autophagy is involved in the antigen presentation and the homeostasis of B cells and T cells (Figure 41C). The major histocompatibility complex (MHC) is a set of cell surface proteins displaying fragments derived from pathogens (or particulate and citrullinated antigens) for recognition by T cells. Autophagy, along with NOD2 and LAP, mediate the activity of MHC class II. Autophagy affects MHC class I presentation by competing with proteasome for protein acquisition and, furthermore, by increasing the protein pools through the inhibition of micro RNA (miRNA) component machineries AGO (argonaute) and DICER. In addition, autophagy affects the self-renewal of hematopoietic stem cells (HSCs), B1 cell development, plasma cell survival and IgG secretion. Autophagy affects thymic selection of T cell repertoire, T cell maturation, T cell survival following T cell receptor (TCR) activation and immunological synapse destabilization. It also controls innate immune cell (such as macrophage) signaling through the release of IL-1α and IL-1β which influence the polarization of T cells into T helper 17 (T_H17) cells [387].

Autophagy also participates in the secretion of immune mediators (Figure 41D). Some of these mediators are stored as pre-made secretory granules that are secreted regulatedly, such as cathepsin K in osteoclasts and lysozyme in Paneth cells. Autophagy also affects the constitutive secretory pathway, which is the conventional pathway of protein secretion (such as IL-6 and IL-8) via the ER, Golgi apparatus and plasma membrane. Autophagy supports a form of unconventional pathway of protein secretion that captures cytoplasmic proteins for extracellular release independent on the ER and the Golgi apparatus. This process has been shown in the secretion of damage-associated molecular patterns (DAMPs) that promote pro-inflammatory signaling such as IL-1β, IL-18 and HMGB1 (high mobility group box 1). However, this pathway is unclear and yet to be investigated [387].

The importance of the role of autophagy in immune system and inflammation is reflected in the case of Crohn's disease. This latter is a complex and chronic disorder affecting primarily the digestive system and is characterized by abnormal inflammation in the walls of ileum and colon. It is one common form of inflammatory bowel disease (IBD) [388,389]. Genome wide association studies (GWAS) have revealed common mutations on autophagy genes found in people suffering from Crohn's disease. These genes express NOD2, ATG16L1 and IRGM (immunity-associated GTPase family M) whose role is important in xenophagy of pathogens (Figure 40A) [390,391]. IRGM is a mitochondria-associated protein

which supports autophagosome biogenesis from mitochondrial membrane upon viral infection [392]. Indeed, Crohn's disease is suggested to arise from a defective innate immune response to enteric bacteria, particularly adherent invasive *Escherichia coli* (AIEC) strains [393]. In transgenic mouse models, the invalidation of *ATG16L1* and *IRGM1* has been shown to lead to a constitutive expression of pro-inflammatory cytokines in the macrophages [394,395]. In relation to CRC, Crohn's disease has been identified as a risk factor of CRC with a relative risk of 2.5 (95% CI 1.3-4.7) according to the most recent meta-anaysis study [14].

1.5.2.3. APC and autophagy

The link between APC and autophagy is established mostly through *in vivo* studies using Min mice. However, the studies on autophagy and intestinal tumorigenesis in Min mice showed different findings. In 2012, autophagy was thought to be not involved in intestinal tumorigenesis in Min mice [396]. Intestinal polyp regions in Min mice were reported to exert slightly higher autophagy than non-polyp regions and ATG7 invalidation in Min mice did not induce intestinal tumorigenesis. In 2015, ATG5 invalidation in Min mice was reported to induce intestinal adenoma growth [397]. Another study in 2015, that showed for the first time the status of autophagy in human CRC, proposed that autophagy was activated in intestinal tumorigenesis in Min mice and human CRC. An activation of ATG gene transcription was reported in 20% of human CRC samples [398]. Autophagy inhibition through ATG7 deletion was shown to prevent tumor initiation and suppress tumor growth in Min mice. The authors reported that autophagy inhibition in Min mice resulted in dysbiosis of gut microbiota, increasing intestinal permeability, activation of immune response *via* a greater production of IL-12 and infiltration of anti-tumor response mediated by cytotoxic $CD8^+$ T cells [399]. These phenomena contributed to inhibit tumor initiation in the intestine of Min mice.

Autophagy has been reported to negatively regulate Wnt signaling in eukaryotic cells through the degradation of disheveled (Dsh), a protein that is important in the uncoupling of β-catenin and its degradation complex (Figure 6). In human CRC, defective autophagy induced aberrant activity of Wnt signaling pathway resulting in enhanced colonic tumor formation [400]. Low-dose treatment of rapamycin, an inducer of autophagy, has been reported to inhibit intestinal tumorigenesis in Min mice [401].

1.5.2.4. 4-Hydroxynonenal and autophagy

HNE has been shown to induce autophagy in vascular smooth muscle cells, SH-SY5Y neuroblastoma cells and rat aortic smooth muscle cells [402-404]. Exposure to substances that can mediate HNE formation through lipid peroxidation, such as ferritin or drug inhibitor for Parkinson's disease GSK257815A, also provoked autophagy [405,406]. The mechanism by which HNE induces autophagy is believed to involve ER stress (discussed briefly in Chapter 1.4.2.3). HNE forms adducts and modifies proteins, and these HNE-modified proteins accumulate in the ER to trigger ER stress, which in turn is an important source of signals stimulating autophagy [407,408]. Ethanol exposure towards retinal pigment epithelium (RPE) cells induced the degradation of neoformed HNE aggresomes through autophagy [409]. Activation of autophagy following HNE-induced protein damages largely contributes to the elimination of these damaged proteins and also prevented cell death by apoptosis [403], thereby highlighting the protective role of autophagy as a cellular defense mechanism regarding HNE toxicity [410]. The liver of transgenic mice overexpressing LAMP-2A receptors accumulated fewer damaged proteins compared to wild type controls due to enhanced autophagy [411]. It also appears that inhibition of autophagy can trigger apoptosis, supporting the fact that autophagy is probably a defense system for survival. HNE-protein adducts were shown to reduce autophagy in RPE cells, leading to apoptosis induction [412].

The HNE-induced autophagy activation is also modulated by HNE detoxification enzymes, such as ALDH2 or GSTA4. In the case of myocardial ischemia-reperfusion injury, ALDH2 has appeared to exert cardioprotective effects by inhibiting HNE reactivity and suppressing autophagy or mitophagy, a selective form of autophagy targeting the lysosomal degradation of mitochondria [413-415]. The role of GSTA4 has been shown to be pivotal in alleviating obstruction-induced tubule damage and renal fibrosis by preventing HNE-induced autophagy activation [416].

Finally, not all HNE intervention induces autophagy as a clearance mechanism of HNE-damaged proteins. Intracellular proteins that are severely damaged by HNE may become undegradable by autophagy due to their aberrant covalent modifications and their deposition is potentially cytotoxic. HNE can also interfere with lysosomal protease activities and impair their functions directly or through modifications of their subsrate peptides [417]. In human RPE cells, HNE-induced lysosomal dysfunctions have been reported to reduce autophagy *in vitro* [412].

1.5.2.5. Link apoptosis-autophagy

Apoptosis and autophagy are two distinct mechanisms regulating cell death and survival. However, they are not truly independent one on another and therefore, they are linked through interaction of apoptotic and autophagic components in the cell. The interaction between BCL-2 and Beclin-1 has been well known to explain the way in which cells balance and regulate apoptosis and autophagy (Figure 42).

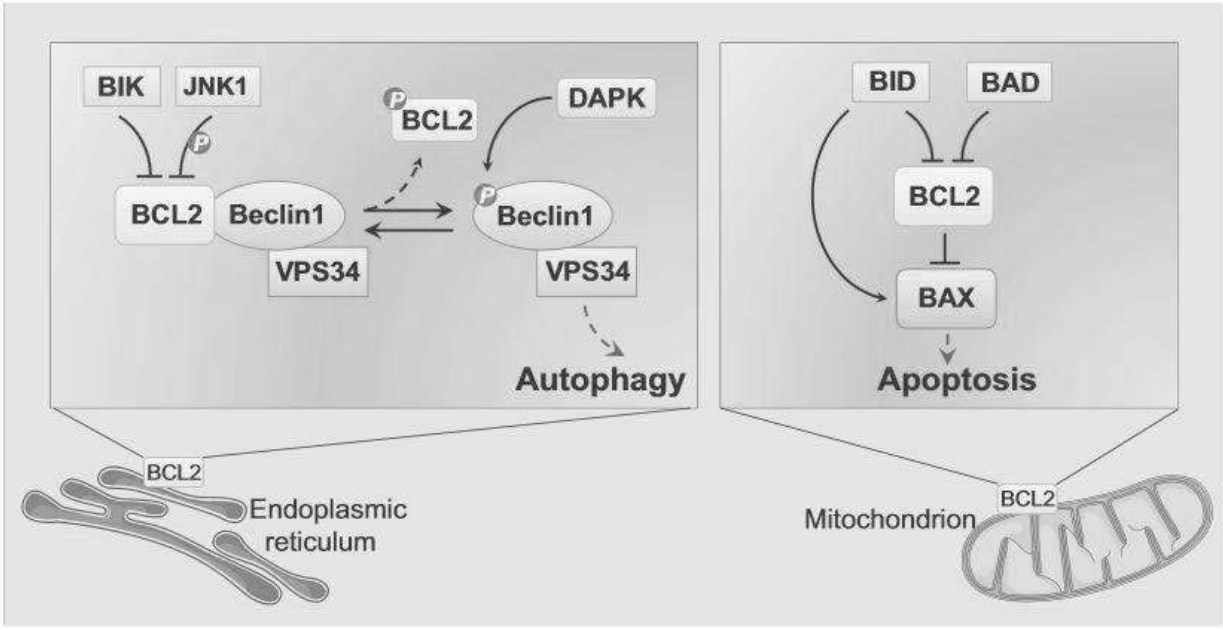

Figure 42. Interaction between BCL-2 and Beclin-1 regulates apoptosis and autophagy [362].

As previously described in Chapter 1.5.1, BCL-2 is an anti-apoptotic protein and Beclin-1 is involved in the nucleation of autophagosomes. At the endoplasmic reticulum, BCL-2 inhibits autophagy by binding to Beclin-1. This binding is regulated by several mechanisms, including competitive binding of the pro-apoptotic protein BIK to BCL-2 and phosphorylation of BCL-2 by a kinase JNK1 that will disrupt the binding and liberate Beclin-1 [418,419]. Once Beclin-1 is free, it is phosphorylated by DAPK (death-associated protein kinase) and becomes active to be involved in the formation of autophagosomes. The link between BCL-2 and Beclin-1 has also been reported to involve p62. This latter is able to directly interact with BCL-2 and disrupt the association between BCL-2 and Beclin-1 [420]. In the mitochondria, BCL-2 inhibits apoptosis by interacting with pro-apoptotic proteins BAX and BAK. Other pro-apoptotic proteins (e.g. BAD, NOXA, BID and others) activate apoptosis by inhibiting BCL-2 and its related anti-apoptotic family members [421,422]. Nevertheless, it

has been suggested that mitochondria-localized BCL-2 is also involved in inhibition of autophagy by sequestering a mitochondrial pool of AMBRA1 (activating molecule in Beclin-1 regulated autophagy protein 1), a positive regulator of Beclin-1 [423]. Caspases (caspase-3, -7 and -8) have also been reported to cleave Beclin-1, thereby destroying its pro-autophagic properties [424,425].

Another way by which apoptosis and autophagy are linked involves pro-apoptotic activity of ATG5, an autophagy protein. Following death stimuli, ATG5 is cleaved by calpain, a cytosolic calcium-activated cysteine protease, resulting in truncated ATG5 (tATG5). This latter is able to bind anti-apoptotic protein BCL-xL, leading to mitochondria-mediated apoptosis [426,427]. TNFα (tumor necrosis factor alpha), a ligand for extrinsic apoptosis pathway, has been shown to induce autophagy in cancer cell lines and this induction was repressed by activation of NF-κB (nuclear factor kappa-light-chain-enhancer of activated B cells), an important anti-apoptotic factor [428,429]. Pro-apoptotic transcription factor p53 has also been reported to regulate autophagy [430,431].

The functional relationship between apoptosis and autophagy (Figure 43) is complex in the sense that on one hand, autophagy allows a stress adaptation that avoids cell death (suppresses apoptosis) whereas on the other hand, autophagy constitutes an alternative pathway to cellular death. In general terms, it appears that similar stressors can induce either apoptosis or autophagy in a context-dependent setting. Different sensitivity thresholds would dictate whether apoptosis or autophagy will develop. The choice between apoptosis and autophagy is influenced by the fact that the two processes exhibit mutual inhibition. In some cases, a mixed phenotype of apoptosis and autophagy can be detected in a single cell. Although autophagy mostly allows cells to adapt to stress, massive autophagy can also kill cells.

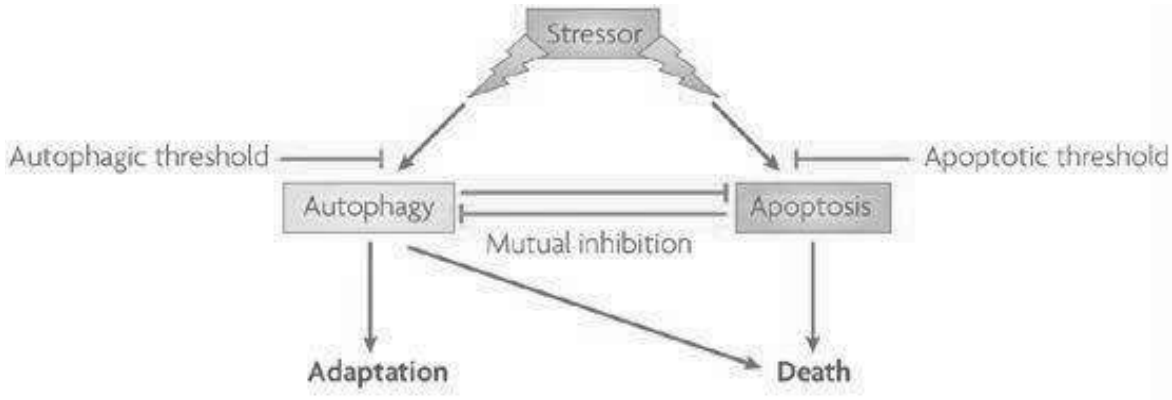

Figure 43. Relationship between apoptosis and autophagy [432].

The mutual inhibition between apoptosis and autophagy has been observed in several studies: autophagy when apoptosis is inhibited or apoptosis due to inhibited autophagy. Mouse embryonic fibroblasts (MEFs) from apoptosis-defective double-knockout $BAX^{-/-}$ $BAK^{-/-}$ mice underwent autophagy upon exposure to apoptosis inducer etoposide [433]. *In vitro*, chemical inhibition of caspases by general caspase inhibitor Z-VAD-FMK (benzyloxycarbonyl-Val-Ala-Asp (OMe) fluoromethylketone) caused autophagy in selected cell types (such as L929 mouse fibrosarcoma and human Jurkat T cell lymphoma) [434]. Autophagy inhibition in nutrient-deprived HeLa or HCT116 cancer cells resulted in apoptosis. Interestingly, the phenotype of the dying cells was influenced by the stage at which autophagy was inhibited. When autophagy was blocked at an early stage, cells underwent a typical apoptosis. However, when the fusion of autophagosomes and lysosomes was blocked by lysosomal inhibitors (such as chloroquine or bafilomycin A), autophagic vacuoles cumulated and the cells manifested a mixed of apoptotic and autophagic morphology [435,436].

1.5.2.6. Autophagy in cancer: good or bad?

Since autophagy favors cell survival upon stress, nutrition deprivation and even apoptosis triggers, it is considered as "good" in normal cells. However, one can also imagine the "bad" side of autophagy when it protects cancer cells from stress or death triggers such as chemotherapy treatment. Because of this duality, autophagy is referred as a "double-edged sword". Therefore, a question of whether the role of autophagy in cancer is good or bad submerges. The ideal condition would be to boost autophagy in normal cells to prevent cancer but inhibit it in cancer cells as part of a cancer treatment strategy [437]. The role of autophagy in cancer promotion and suppression is shown in Figure 44.

Autophagy was originally thought to be a tumor suppression mechanism due to the reported allelic loss of Beclin-1 in 40% to 75% of human breast, ovarian and prostate cancers [438,439]. In the case of breast cancer, this loss might be linked to the subsequent allelic loss of an adjacent tumor suppressor gene *BRCA1* (breast cancer 1) [440]. Indeed, *Beclin-1* and *ATG* gene deletion has been shown to favor tumor development *in vivo* and *in vitro* [441-445]. Based on these findings, autophagy deficiency is considered as a molecular event in tumor initiation (Figure 44A). Autophagy deficiency produces the accumulation of damaged proteins in the cells that causes oxidative stress, chronic inflammation, DNA damage, stem/progenitor expansion and tumor initiation [446,447].

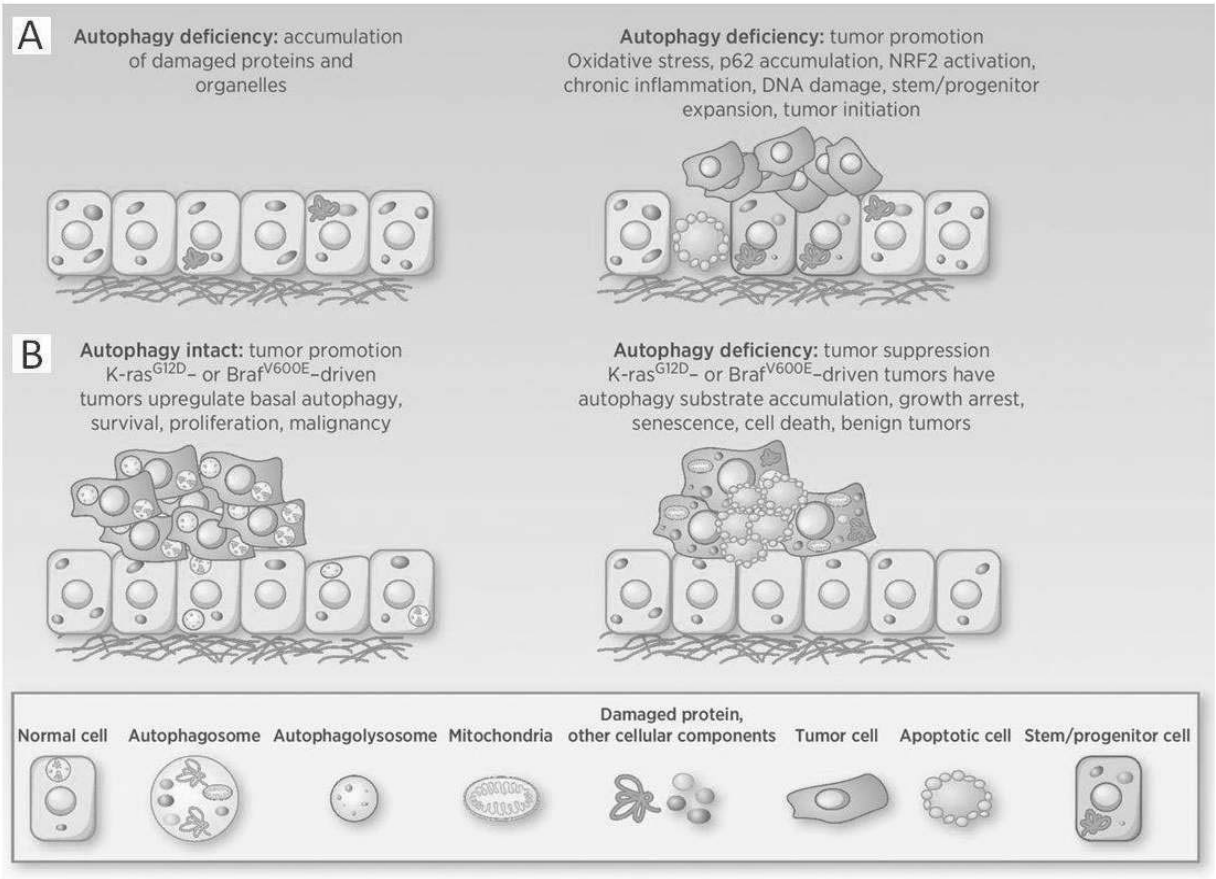

Figure 44. Role of autophagy in tumor promotion.
A) Autophagy deficiency favors tumor promotion by accumulating damaged proteins and organelles, B) Autophagy in cancer cells promotes tumor promotion by favoring survival and growth, whereas loss of autophagy restricts tumor promotion by provoking apoptosis ([447] with modifications).

Like normal cells, cancer cells also rely on autophagy to survive. For instance, CRC cells exerted autophagy as a classical way to resist nutrient deprivation [448]. Chemical inhibition of autophagy has been shown to sensitize colon cancer cells to chemotherapy agent 5-fluorouracil [449]. In many cases, cancer cells are more autophagy-dependent than normal cells. Some cancer cell lines even possess abnormally high levels of basal autophagy under fed conditions. This suggests that oncogenic events create inherent metabolic stress necessitating autophagy to sustain tumor cell survival [444,447,450,451]. Autophagy in cancer cells favors their survival, proliferation and malignancy (Figure 44B, left panel) and therefore is considered as “bad”. Impairing autophagy in cancer cells would be a plausible hypothetic way into tumor suppression. Autophagy deficiency might lead to stress caused by accumulation of defective proteins in cancer cells, growth arrest, senescence and facilitated apoptosis as cell death mechanism (Figure 44B, right panel). In the case of CRC, autophagy

impairment through inhibition of ATG7 in murine and human CRC epithelial cells prevented tumor initiation and suppressed tumor growth [398].

However, a link seems missing between the early events of tumorigenesis where autophagy is impaired and the following events that require autophagy for progression from benign to malignant tumors. Possible mechanism involving oncogenic *K-RAS* or *B-RAF* has been developed (Figure 44B). *K-RAS* and *B-RAF* genes are mutated in numerous cancers. *K-RAS*- and/or *B-RAF*-mutated cancer cells have a high dependence on autophagy and exert high level of autophagy. *K-RAS* and *B-RAF* impair acetyl-co A production and therefore prevent Krebs cycle and β-oxidation. Thus, they potentially leave cells dependent on autophagy to provide substrates, such as amino acids and fatty acids, for acetyl-co A biosynthesis.

Since the realization that autophagy is a survival pathway for tumor cells, there has been a great interest in inhibiting autophagy for cancer therapy. Indeed, numerous autophagy inducers and inhibitors have been used for treatment of almost all types of cancer [452]. These substances are whether used alone or in combination with other chemotherapy drugs. For instance, inhibition of autophagy sensitized brain tumor cells to chemotherapy [453]. Nevertheless, autophagy inhibition, especially in combination therapy, may pose cytotoxicity issues, such as to the liver and brain. Stem cells may also be more sensitive to autophagy inhibition than differentiated tissues [454]. Despite still needing developing, targeting autophagy in cancer treatment is promising to improve cancer treatment [455].

Chapter II

OBJECTIVES

My thesis was focused on mechanistic studies of the roles of heme-induced lipid peroxidation in promoting colorectal carcinogenesis, especially by provoking positive selection of preneoplastic colon cells to the detriment of normal colon cells. The base of these studies was that HNE, a product of heme-induced lipid peroxidation, induced higher mortality in mouse-origin normal cells than in preneoplastic cells harboring *APC* mutation and this phenomenon was also observed upon exposure to fecal water of heme-fed rats [61]. This difference of mortality between normal and preneoplastic cells would favor colorectal carcinogenesis promotion following the consumption heme-containing foods, such as red meat.

HNE is a molecule generated by heme-induced lipid peroxidation. Surely, there are a plethora of other molecules derived from heme-induced lipid peroxidation apart from HNE, mainly aldehydes. To study the role of lipid peroxidation in the promotion of colorectal carcinogenesis by red meat thoroughly, I used fecal water (aqueous fecal extract) of heme-fed rats obtained from *in vivo* experiments by feeding rats with standard diet supplemented with hemoglobin or beef as sources of heme iron. This fecal water represents the real biological matrix of molecules derived from luminal lipid peroxidation that are in direct contact with colon cells. Therefore, fecal water provides a complementary approach to study the effects of heme-induced lipid peroxidation on colorectal carcinogenesis promotion.

The main objectives of my thesis are (1) to compare the toxicity of purified HNE and fecal water of rats fed with purified heme or red meat, (2) to prove that lipid peroxidation-derived aldehydes are responsible for the different toxicity of fecal water of heme-fed rats in mouse-origin normal and preneoplastic cells, (3) to study the different fecal water toxicity in human colon cells and (4) to understand the mechanisms involved in this different toxicity. The hypothesis is that heme-induced lipid peroxidation is responsible for this different toxicity by preferentially inducing apoptosis in normal cells compared to preneoplastic cells. Three main questions were directed to reach the goals:

- Are **lipid peroxidation-derived aldehydes** the main compounds determining the different toxicity of fecal water of heme-fed rats in mouse-origin normal and preneoplastic cells?
- In addition to mouse cells, is this different toxicity also observed in wild type and APC knockdown **human colon cells**?
- What are the **mechanisms** involved in the resistance of preneoplastic cells upon exposure to fecal water of heme-fed rats?

Chapter III

EXPERIMENTAL MODELS

Two experimental *in vitro* models for *APC* mutation were used in this study: 1) mouse-origine APC +/+ and APC Min/+ cells [61,100] and 2) human-origin CT and CTA cells [101,102]. Both models were established to study early changes in colorectal carcinogenesis. In addition, the use of fecal water in this study is also detailed in this chapter.

3.1. Mouse-origin APC +/+ and APC Min/+ cells

The use of cells carrying only *APC* mutation would allow to investigate early phenomena that take place at the beginning of colorectal carcinogenesis. *APC* mutation is one of the earliest events that transform normal wild-type cells into early adenomas representing precancerous or preneoplastic phenotype (Figure 3). Here, my team developed mouse-origin APC +/+ and APC Min/+ (called normal and preneoplastic cells respectively) in 2003 [100]. The establishment of these cell lines consisted of mating of a heterozygous female "Immortomouse" with a male C57BL/6J mouse or with a heterozygous *APC*-mutated *Min* mouse (Figure 45). Immortomouse is transgenic mouse harboring a temperature-sensitive mutation of the simian virus 40 large T antigen gene (for cell immortalization) under the control of interferon γ which induces the promoter MHCI (major histocompatibility complex I) [456]. Large T antigen inactivates p53 and favors cellular proliferation [457].

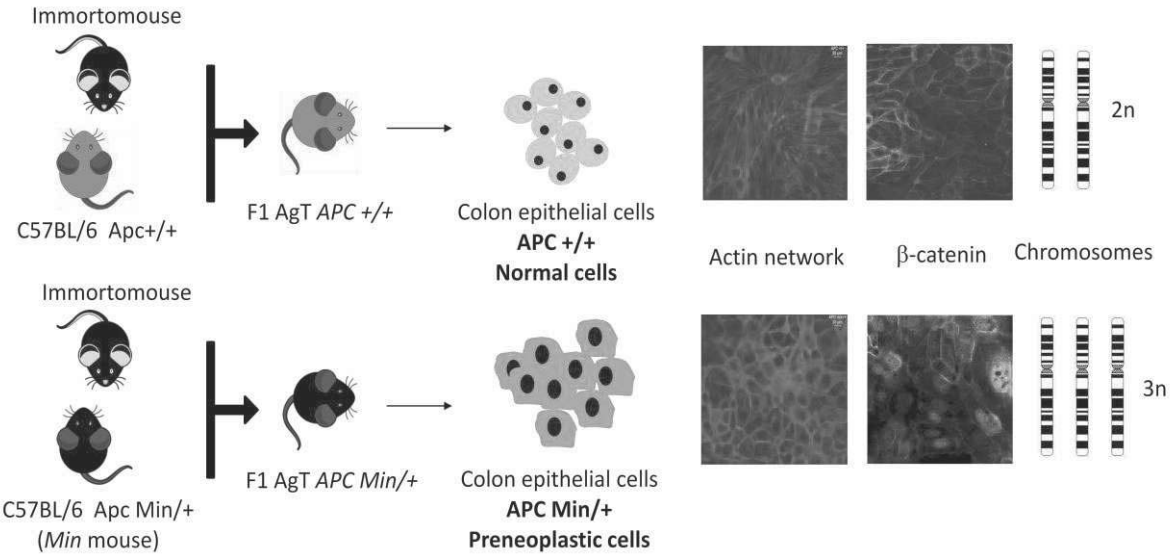

Figure 45. Establishment of mouse-origin APC +/+ and APC Min/+ cells (adapted from [100]).

The two cell lines (APC +/+ and APC Min/+) were isolated from the colon crypts of F1 progeny mice. Cultured at 33°C in the presence of interferon γ, the cells proliferate while at 37°C without interferon γ, they cease to proliferate, behaving like a primoculture. Several differences have been identified between APC +/+ and APC Min/+: 1) destructured actin network in APC Min/+ cells, 2) higher level of nuclear β-catenin in APC Min/+ cells and 3) aneuploidy in APC Min/+ cells (3n). These differences appear as the consequences of the lack of APC protein, which has substantial roles in the regulation of cytoskeletal integrity, Wnt signaling pathway and chromosome segregation.

3.2. Human-origin CT and CTA cells

The establishment of human-origin colon cells that represent *APC* mutation is very interesting in terms of early CRC-related *in vitro* studies. The precedent available human colonic epithelial cell (HCEC) lines were only of malignant origin and/or contained multiple cytogenetic changes which do not represent early colorectal carcinogenesis. In addition, for my team, this human-origin experimental model allows to approach human physiology.

Human-origin CT and CTA cells established in 2010 were obtained from biopsy samples of two healthy patients undergoing routine screening colonoscopy [101]. Following isolation and culture, these cells were immortalized by successive infections of non-oncogenic proteins *CDK4* (cyclin-dependent kinase 4) and *hTERT* (human telomerase reverse transcriptase). CDK4 is a catalytic subunit of the protein kinase complex that is important for cell cycle G1 phase progression and the loss of *CDK4* has been reported to cause cellular senescence in ARF (adenosine diphosphate ribosylation factor)/p53-independent manner [458,459]. *hTERT* is a catalytic unit of the enzyme telomerase that reverses telomere shortening during DNA replication [460]. Telomerase shortening is associated with ageing, mortality and ageing-related disease [461]. Indeed, CT stands for the initial of ***C****DK4* and *h****T****ERT*. Following introduction of shRNA against APC in CT to silence APC gene expression, CTA cells were obtained (CTA stands for ***C****DK4*, *h****T****ERT* and ***A****PC*) [102].

3.3. Fecal water of heme-fed rats

Fecal water is an aqueous extract of feces representing bioavailable parts of fecal matters. It is indeed a matrix complex containing numerous substances originated from indigested part of consumed foods, secreted molecules during digestion or neoformed compounds in the gastrointestinal tract. Components of fecal water, such as terminal

aldehydes of lipid peroxidation (MDA and HNE) or hydroperoxides (LOOH) have been demonstrated to induce apoptosis in colon normal and carcinoma cells *in vitro* [462,463]. In terms of CRC, fecal water has been widely used as a diet-related source of CRC risk biomarkers [464-468]. Red meat intake has been shown to increase the risk of CRC by increasing the fecal water activity and toxicity towards colon cells [465].

In this study, fecal water was prepared from the feces of hemoglobin (Hb)- and beef (Bf)-fed rats. Both Hb and Bf are sources of heme iron. The rats' diet was also enriched in safflower oil (rich in n-6 fatty acids) to provoke heme-catalyzed lipid peroxidation resulting in the formation of cytotoxic aldehydes. The lipid peroxidation-derived products in the fecal water can be analyzed by TBARS (Thiobarbituric acid reactive species) assay. Free HNE in the fecal water can be analyzed by mass spectrometry coupled with gas chromatography (in collaboration with *Plateforme d'Exploration du Métabolisme* (Platform for Exploration of Metabolism), Clermont-Ferrant since 2014) . To assess whether fecal aldehydes determine in part the different fecal water toxicity towards normal (APC +/+) and preneoplastic (APC Min/+) cells *in vitro*, fecal water was treated with CTR (carbonyl-trapping resin) to deplete the carbonyl compounds present in the fecal water, including aldehydes. This CTR possesses hydrazine groups that readily react with carbonyl compounds.

Chapter IV

RESULTS

The results obtained during my thesis are compiled in articles published in *Carcinogenesis* in June 2016 (Article 1), in *Cancer Research* in January 2015 (Article 2) and a manuscript in preparation for publication (Article 3). In this chapter, all articles are presented with a brief introduction resuming the principle results presented in the articles.

Article 1:

Red meat and colorectal cancer: Nrf2-dependent antioxidant response contributes to the resistance of preneoplastic colon cells to fecal water of hemoglobin- and beef-fed rats

Surya *et al.* 2016. *Carcinogenesis* 37(6):635-645.

In this study, mouse-origin APC +/+ and APC Min/+ cells (Chapter 3.1, later called normal and preneoplastic cells respectively) were used to study the effect of lipid peroxidation byproducts in early colorectal carcinogenesis *in vitro*. This study aimed at:

1) **Demonstrating that preneoplastic cells are more resistant to fecal water of heme-fed rats than normal cells and characterizing cell death**

   As previously reported [61], we observed that preneoplastic cells were more resistant to the toxicity of fecal water of heme-fed rats by executing lower level of apoptosis compared to normal cells. Following the exposure to fecal water of heme-fed rats, caspases activity appeared at a higher rate and higher final extent in normal cells than in preneoplastic cells. By analyzing apoptosis end points such as nuclear fragmentation, membrane phosphatidylserine translocation to the outer leaflet and cell membrane permeabilization after exposure to fecal water of heme-fed rats for 6 h, we generally observed higher level of apoptosis in normal cells than in preneoplastic cells.

2) **Determining the involvement of Nrf2 in such a resistance**

   We confirmed that Nrf2 was involved in the resistance of preneoplastic cells to fecal water of heme-fed rats. Basal Nrf2 activity was found to be higher in preneoplastic cells than in normal cells, shown by its nuclear colocalization. Therefore, the

expression of HNE detoxification enzymes, known to be regulated by Nrf2, was higher in preneoplastic cells than in normal cells. These conditions might give preneoplastic cells better advantages to tackle fecal water toxicity compared to normal cells. Following exposure to fecal water of heme-fed rats, Nrf2 was active in both cell lines, but the level of HNE detoxification enzymes was constantly higher in preneoplastic cells than in normal cells, potentially explaining the resistance of preneoplastic cells to fecal water toxicity. Indeed, siRNA-mediated Nrf2 silencing in preneoplastic cells sensitized them to fecal water toxicity, underlining the importance of Nrf2 in such a resistance.

3) **Proving that fecal aldehydes determine in part the different toxicity of fecal water towards normal and preneoplastic cells.**

To analyze the role of fecal aldehydes in the different toxicity of fecal water towards normal and preneoplastic cells, we optimized the depletion of carbonyl compounds in the fecal water by using carbonyl-trapping resin (CTR). We observed that the depletion of carbonyl compounds in the fecal water abolished the different fecal water toxicity in normal and preneoplastic cells. This finding underlines in part the importance of fecal aldehydes in inducing different apoptosis between normal and preneoplastic cells upon exposure to fecal water of heme-fed rats. Furthermore, CTR-treated fecal water did not induce Nrf2 activation both in normal and preneoplastic cells, leading to a constant level of HNE detoxification enzymes in normal and preneoplastic cells like under basal conditions.

Taken together, our results highlight the important role of fecal aldehydes derived from heme-induced lipid peroxidation in promoting colorectal carcinogenesis by initiating positive selection of preneoplastic cells over normal cells.

Carcinogenesis, 2016, Vol. 37, No. 6, 635–645

doi:10.1093/carcin/bgw035
Advance Access publication March 18, 2016
Original Manuscript

ORIGINAL MANUSCRIPT

Red meat and colorectal cancer: Nrf2-dependent antioxidant response contributes to the resistance of preneoplastic colon cells to fecal water of hemoglobin- and beef-fed rats

Reggie Surya[1,2], Cécile Héliès-Toussaint[1,2], Océane C. Martin[1,2], Thierry Gauthier[1,2], Françoise Guéraud[1,2], Sylviane Taché[1,2], Nathalie Naud[1,2], Isabelle Jouanin[1,2], Céline Chantelauze[3,4], Denys Durand[3,4], Charlotte Joly[5,6], Estelle Pujos-Guillot[5,6], Fabrice H. Pierre[1,2,†] and Laurence Huc[1,2,*,†]

[1]Toxalim, Université de Toulouse, INRA, INP-ENVT, INP-EI-Purpan, Université de Toulouse 3 Paul Sabatier, 180 chemin de Tournefeuille, F-31027 Toulouse, France, [2]Université de Toulouse III, INP, ENVT, UPS, TOXALIM, F-31027 Toulouse, France, [3]INRA, UMR1213 Herbivores, F-63112 Saint-Genès-Champanelle, France, [4]Université de Lyon – VetAgro Sup, UMR1213 Herbivores, F-69280 Marcy l'Etoile, France, [5]INRA, UMR1019, Plateforme d'Exploration du Métabolisme, F-63000 Clermont-Ferrand, France and [6]INRA, UMR1019, UNH, F-63000 Clermont-Ferrand, France

*To whom correspondence should be addressed. Tel: 0033 (0)5 82 06 63 20; Fax: 0033 (0)5 62 28 52 44; Email: laurence.huc@toulouse.inra.fr

†These authors contributed equally to this work.

Abstract

Epidemiological studies have associated red meat intake with risk of colorectal cancer. Experimental studies explain this positive association by the oxidative properties of heme iron released in the colon. This latter is a potent catalyst for lipid peroxidation, resulting in the neoformation of deleterious aldehydes in the fecal water of heme-fed rats. The toxicity of fecal water of heme-fed rats was associated to such lipid peroxidation. This study demonstrated that fecal water of hemoglobin- and beef-fed rats preferentially induced apoptosis in mouse normal colon epithelial cells than in those carrying mutation on *Apc* (Adenomatous polyposis coli) gene, considered as preneoplastic. Highlighting the importance of lipid peroxidation and neoformation of secondary aldehydes like 4-hydroxy-2-nonenal (HNE), we optimized the depletion of carbonyl compounds in the fecal water which turned out to abolish the differential apoptosis in both cell lines. To explain the resistance of preneoplastic cells towards fecal water toxicity, we focused on Nrf2, known to be activated by aldehydes, including HNE. Fecal water activated Nrf2 in both cell lines, associated with the induction of Nrf2-target genes related to aldehydes detoxification. However, the antioxidant defense appeared to be higher in preneoplastic cells, favoring their survival, as evidenced by Nrf2 inactivation. Taken together, our results suggest that Nrf2-dependent antioxidant response was involved in the resistance of preneoplastic cells upon exposure to fecal water of hemoglobin- and beef-fed rats. This difference could explain the promoting effect of red meat and heme-enriched diet on colorectal cancer, by initiating positive selection of preneoplastic cells.

Introduction

Colorectal cancer is the first cause of global mortality by cancer in non-smokers in affluent countries (1). Epidemiological studies proposed that physical activity and diet are important factors for colorectal cancer development (2–4). Concerning the diet, based on epidemiological and experimental studies, the International Agency for Research on Cancer (IARC) monograph

Received: September 4, 2015; **Revised:** February 10, 2016; **Accepted:** February 27, 2016

Abbreviations

ALDH3A1	aldehyde dehydrogenase 3A1
Apc	adenomatous polyposis coli
ARE	antioxidant response element
Bf	beef
CTR	carbonyl-trapping resin
GSTA4	glutathione S-transferase A4
Hb	hemoglobin
HNE	4-hydroxy-2-nonenal
HO1	heme oxygenase 1
Keap1	Kelch-like ECH-associated protein 1
MDF	mucin-depleted foci
Nrf2	nuclear factor (erythroid derived 2)-like 2
PBS	phosphate-buffered saline
TBARS	thiobarbituric acid reactive species
xCT	x-C-type cystine/glutamate antiporter

working group concluded in October 2015 that red meat is probably carcinogenic to humans (Group 2A) (5–8). Following the convincing evidence that red meat intake increases the risk of colorectal cancer, American Institute for Cancer Research (AICR) and World Cancer Research Fund (WCRF) recommended limiting red meat consumption to 300 g/week (4).

Three major mechanisms could explain the association between red meat and colorectal cancer. Firstly, potentially carcinogenic *N*-nitroso compounds can be formed in the gastrointestinal tract by N-nitrosation or nitrosylation. Secondly, cooking meat at high temperature could generate mutagenic heterocyclic amines such as 2-amino-1-methyl-6-phenylimidazo(4,5-b) pyridine (PhIP) and 2-amino-3,8-dimethylimidazo-(4,5-f)quinoxaline (MeIQx). Thirdly, epidemiological and experimental data support the hypothesis that heme iron present in red meat promotes colorectal carcinogenesis (9). In a recent study, we examined the relative contribution of these three mechanisms *in vivo* and we demonstrated that heme iron was the only experimental factor associated with the promotion of colorectal carcinogenesis in rats or mice without any additive or synergic effects with *N*-nitroso compound or heterocyclic amines (10). Furthermore, we showed that heme iron contributed to lipid peroxidation occurring in the lumen, leading to the formation of cytotoxic and genotoxic aldehydes, one of which is 4-hydroxy-2-nonenal (HNE), a secondary product of linoleic and arachidonic acid oxidation (11–13). This molecule has been reported to induce apoptosis in healthy colon cells (14). In hemoglobin (Hb)- and red meat-fed rats, we observed a significant increase of fecal thiobarbituric acid reactive species (TBARS) and urinary DHN-MA (1,4-dihydroxynonane mercapturic acid; metabolite of HNE), both are known as biomarkers of lipid peroxidation (9,15).

Numerous studies emphasized the role of fecal water and lipid peroxidation in colorectal cancer as diet-related factors (16–18). Fecal water is an aqueous extract of feces representing bioavailable parts of fecal matters. Components of fecal water, such as terminal aldehydes of lipoperoxidation (malondialdehyde and HNE) or hydroperoxides (LOOH) have been shown to induce apoptosis in colon normal and carcinoma cells *in vitro* (19,20). We previously tested *in vitro* the toxicity of fecal water of Hb- and Bf-fed rats in normal and preneoplastic immortalized mouse colonic epithelial cells derived from wild-type and *Min* mice (21). Preneoplastic cells are derived from *Min* mice and bear a mutation on the *Apc* (adenomatous polyposis coli) gene, which is a frequent and early event in human colorectal cancer (22–24). Preneoplastic cells were more resistant than normal cells upon exposure to fecal water of Hb- and Bf-fed rats (14). We thus suggest that the resistance of preneoplastic cells to the detriment of normal cells, which was associated to lipid peroxidation of fecal water, could explain the promotion of colorectal cancer following heme iron intake.

Nrf2 [nuclear factor (erythroid derived 2)-like 2] is a transcription factor that has been shown to regulate the expression of cellular detoxifying and antioxidant enzymes (including those involved in HNE detoxification) through Nrf2-Keap1-ARE signaling pathway, thus exerting cytoprotective properties against oxidative stress (25). HNE has been shown to activate Nrf2 and antioxidant genes expression (26). Our previous study revealed that different resistance between normal and preneoplastic cells upon exposure to HNE could be due to higher basal expression of HNE detoxification enzymes in preneoplastic cells compared with normal cells (27), giving preneoplastic cells a better antioxidant shield to tackle toxic effects of HNE. As the cytotoxicity of fecal water of heme-fed rats was associated to lipid peroxidation, Nrf2 could be involved in the resistance of preneoplastic cells upon exposure to fecal water.

In this study, we firstly characterized cell death type as apoptosis and compared its induction in normal and preneoplastic cells regarding fecal water of Hb- and Bf-fed rats, in comparison to HNE. After treatment with fecal water or HNE, preneoplastic cells appeared to exhibit lower level of apoptosis compared with normal cells. Moreover, HNE and fecal water activated Nrf2 in both cell lines and the depletion of carbonyl compounds in fecal water prevented this event. The resistance of preneoplastic cells was correlated to a higher Nrf2-dependent response compared with normal cells, as evidenced by Nrf2 invalidation. Thus, this study demonstrated the importance of fecal carbonylated secondary lipoperoxidation products in explaining the differential apoptosis between normal and preneoplastic cells following exposure to fecal water of Hb- and Bf-fed rats.

Materials and methods

Cell culture

Normal wild-type and *Apc*-mutated colon epithelial cells (later called normal and preneoplastic cells) were established as described previously (21). Both cell lines express the heat-labile simian virus 40 large tumor antigen gene (AgT tsA58) under the control of interferon γ and are 'immortalized', that is, they expressed active SV40 at permissive temperature (33°C). They have been tested (as published in 2014 (10)) through the characterization of *Apc* genotype (presence of *Min* mutation in preneoplastic cells), *Apc* phenotype (destructurized actin network in preneoplastic cells) and epithelial phenotype (expression of cytokeratin 18 in normal and preneoplastic cells).

Cells were cultured (approximate density 6.0×10^5 cells/cm^2) at permissive temperature of 33°C in Dulbecco-modified essential medium (DMEM) supplemented with 10% fetal calf sera, 1% penicillin/streptomycin, 2% glutamine, 10 U/ml interferon γ and 10 U/ml epidermal growth factor. All experiments were performed at non-permissive temperature of 37°C without interferon γ and epidermal growth factor to inhibit the SV40 transgene and to reach differentiated state. The treatments with HNE and fecal water were performed in serum-free DMEM containing 2% glutamine to avoid any reaction between serum and fecal water or HNE.

HNE synthesis

HNE was synthesized as described previously (28). Briefly, Grignard reaction between fumaraldehyde monoacetal and 1-pentylmagnesium bromide afforded HNE-dimethylacetal. HNE was obtained by acid hydrolysis.

Fecal samples

Feces used to generate the fecal water were obtained from two animal studies set up to explore, respectively, the effect of dietary Hb (10) and Bf on colorectal carcinogenesis (not published). Briefly, 7 days following

an injection with the carcinogen azoxymethane [Sigma Aldrich, 20 mg/kg body wt in NaCl (9 g/l)], F344 male rats were allowed free access to their respective diets for 100 days. In the first experiment, rats were fed with modified AIN-76 diet [low calcium with addition of 5% (v/w) safflower oil; control group] or with modified AIN-76 diet containing 1% (w/w) Hb (Hb-fed group) (10). In the second experiment, rats were fed with modified AIN-76 diet (control group) or with 50% modified AIN-76 diet containing 50% raw Bf sirloin. Feces were collected on the 88th and 95th day of experiment for Hb-fed and Bf-fed rats, respectively. The two studies resulted in four groups of collected feces: standard diet for Hb-fed rats, Hb-fed rats, standard diet for Bf-fed rats and Bf-fed rats. All experiment protocols were approved by the Local Animal Care and Use Committee of Institut National de la Recherche Agronomique (TOXCOM), and were conducted in accordance with the European directive 2010/63/UE and ARRIVE guidelines.

Fecal water preparation and depletion of carbonyl compounds in fecal water

Fecal water was prepared as described previously (10). Briefly, 2 g of feces was diluted with 5 ml of distilled water, ground and centrifuged. The supernatant was collected, diluted 10 times in DMEM containing glutamine 2% and sterilized by microfiltration (pore size 0.2 µm).

4-Fmoc-hydrazinobenzoyl AM NovaGel™ (Novabiochem®) is a polymeric resin grafted with fmoc-protected hydrazine functionality. Carbonyl compounds are known to readily react with hydrazine groups to yield hydrazones. Therefore, this resin, named carbonyl-trapping resin (CTR) in this work was used for carbonyl compounds depletion as described previously (10). Briefly, following activation of the resin using 500 µL of piperidine 20% (v/v) in DMSO for 5 mg of resin and repeated washes, fecal water was treated with the activated resin at 4°C for 2 h under agitation.

TBARS and free HNE assay

TBARS value was used as a global analysis of lipid peroxidation endproducts. TBARS in fecal water were analyzed as described previously (29). For free HNE assay, sample preparation was realized as described previously (30) and adapted for free HNE in fecal water. Briefly, HNE present in fecal water (400 µl) was labeled and reduced into $[^2H_1]$DHN by NaB$[^2H_4]$ (0.2 mmol) in EDTA (50 mM)/Hepes (2 mM). $[^2H_{11}]$DHN (0.8 nmol) was added as internal standard. Following reduction of double bonds in the presence of Raney nickel, HNE was extracted with ethyl acetate and dried with Na_2SO_4. Analyses (31,32) were carried out on a triple quadrupole Quattro Micro mass spectrometer (Waters Corporation, UK) coupled with a gas chromatography Agilent 6890N system (Agilent Technologies, USA).

Apoptosis detection: nuclei fragmentation, caspase activation by time-lapse microscopy and annexin V-propidium iodide (PI) staining by flow cytometry

For nuclei fragmentation assay, cells seeded in 24-well plates were incubated for 6 h of contact with HNE 40 µM and fecal water (dilution 10×) at 37°C. Cells were then fixed in paraformaldehyde 4% and stained using fluorescent dye Hoechst 33342 [Life Technologies, 0.5 ng/ml in phosphate-buffered saline (PBS)]. Apoptotic (fragmented and/or condensed) and alive nuclei were counted using fluorescence microscope (Evos fl digital inverted microscope, AMG) and expressed as percentage of total population ($n > 500$ nuclei).

For time-lapse microscopy, cells seeded in Labtek 8-well chamber 1.5 borosilicate coverglass slides were incubated under confocal microscope Leica SP8 (with micro-incubator at 37°C, 5% CO_2) with HNE 40 µM and fecal water (dilution 10×) containing Hoechst 33342 (5 µg/ml), CellEvent™ Caspase-3/7 Green Detection Reagent (Life Technologies, 2 µM) and TO-PRO®-3 Iodide (Life Technologies, 1 µM). Images were acquired using lasers 405, 488 and 638 nm under 20× magnification every 30 min for 12 h. Image analysis was performed using ImageJ software.

For flow cytometry, cells seeded in 12-well plates were incubated for 6 and 24 h in the presence of HNE 40 µM or fecal water (dilution 10×) at 37°C. Cells were then harvested and stained using APC Annexin V apoptosis detection kit with PI (BioLegend, 50 ng/ml) according to manufacturer's procedure. The flow cytometry was done using MACSQuant® Analyzer 10 and the data were analyzed using VenturiOne software (Applied Cytometry).

siRNA transfection

siRNAs were provided by Thermo Scientific Dharmacon (Courtaboeuf, France). At 37°C, medium was replaced by OptiMEM and cells were transfected overnight with 100 pmole Nrf2-specific siRNA (ON-TARGET plus SMART pool, mix of four siRNA), 100 pmole lamin-specific siRNA (siGLO LamineA/C control siRNA) as control of transfection rate or 100 pmole negative control siRNA (ON-TARGET plus siRNA Smart pool Non targeting control pool) according to manufacturer's instructions. The transfection rate was more than 75% in each cell type after 18 h of transfection. The medium was then replaced by non-permissive medium and the cells were incubated at 37°C for 24 h prior to treatments.

Immunofluorescence staining of Nrf2

Cells seeded on round coverslips (diameter 18 mm) in 12-well plates were incubated for 1 h of contact with HNE 40 µM or fecal water (dilution 10×) at 37°C. Following saturation (PBS, 0.1% Triton, 0.5% bovine serum albumin), each coverslip was incubated with primary antibodies directed against Nrf2 (Santa Cruz rabbit polyclonal IgG (33), 2.5 µg/ml in PBS, 0.1% Triton, 0.5% bovine serum albumin) for 1 h at room temperature. After washing with PBS, the cells were incubated with secondary fluorophore-labeled antibodies (Invitrogen Alexa Fluor 488 (green) donkey anti-rabbit IgG, 10 µg/ml in PBS, 0.1% Triton, 0.5% bovine serum albumin) for 1 h at room temperature. All cover slips were then sealed on microscope slides using anti-fading solution (Invitrogen Prolong Gold antifade reagent with DAPI). The slides were analyzed using confocal microscope Leica SP8 with lasers 488 nm (Alexa 488) and 405 nm (DAPI) under 63x oil immersion objective. The colocalization of Nrf2 and nuclei was observed by using fluorescence intensity graphs presenting the intensity of blue (nuclei) and green (Nrf2) fluorescence detected along determined regions of interest (ROI). Nuclear localization of Nrf2 was deduced from blue and green fluorescence pattern.

RT-qPCR

Cells were incubated for 4 h of contact with HNE 40 µM or fecal water (dilution 10×) at 37°C. RNA was isolated using Tri Reagent (Eurogenetec) according to manufacturer's instructions. Two-step RT-qPCR was performed using TBP (TATA binding protein) as the housekeeping gene. cDNA synthesis was done using the iScript cDNA Synthesis kit (Bio-Rad) with 1 µg RNA. Quantitative PCR was conducted using ViiA™ 7 Real-Time PCR System (Life Technologies), with final reaction volume of 5 µl (1 µl cDNA, 1.5 µl primers and 2.5 µL iQ SYBR Green Supermix (Bio-Rad)). Thermocycling conditions were set as following: initial denaturation at 95°C (10 min), denaturation at 95°C (15 s), annealing at 60°C (30 s) and extension at 72°C (30 s). The sequences of the primers (5′–3′) used are listed below: HO1 (F-CAA CCC CAC CAA GTT CAA ACA, R-AGG CGG TCT TAG CCT CTT CTG A), ALDH3A1 (F-AAA GTA GCC CAT GGA GGC AC, R-GTC ATT GGC TGT CAC TCC AC), xCT (F-CCT GGC ATT TGG ACG CTA CAT, R-TCA GAA TTG CTG TGA GGT TGC A), GSTA4 (F-GAA GTT CTA GTG ACA GCG TGC TTT A, R-TGT AGC TGC TGC TGT GAT TGG), TBP (F-AGA ACA ATC CAG ACT AGC AGC A, R-GGG AAC TTC ACA TCA CAG CTC).

Western blot of Nrf2

Cells were incubated for 1 h with HNE 40 µM or fecal water (dilution 10×) at 37°C. Whole cell extracts were fractionated using Nuclear Extraction kit (Active Motif). Western blot of nuclear extracts (10 µg) was performed by SDS-PAGE and blots were transferred to nitrocellulose membranes. Membranes were then saturated and incubated with primary antibodies against Nrf2 (Cell Signaling rabbit polyclonal IgG (34), dilution 1:1000) and lamin A/C (Sigma Aldrich mouse monoclonal IgG (35), dilution 1:5000) at 4°C for a night under agitation. Fluorescent secondary antibodies (Thermo Scientific Pierce DyLight 700 donkey anti-rabbit IgG and Thermo Scientific Pierce DyLight 800 donkey anti-mouse IgG, 0.25 µg/ml) were incubated for 1 h and membranes were revealed using Odyssey® CLx Li-Cor Infrared Imaging System at wavelengths of 700 and 800 nm.

Detection of HNE adducts

Cells were incubated for 6 h of contact with HNE 40 µM at 37°C. Whole cell extracts were fractionated using Nuclear Extraction kit (Active Motif). HNE-histidine adducts in cytoplasmic fraction were measured as previously described (36) using anti-HNE-his mouse monoclonal primary antibody generously given by Drs G. Waeg and N. Zarkovic (Laboratory for Oxidative Stress, Zagreb, Croatia) (37,38).

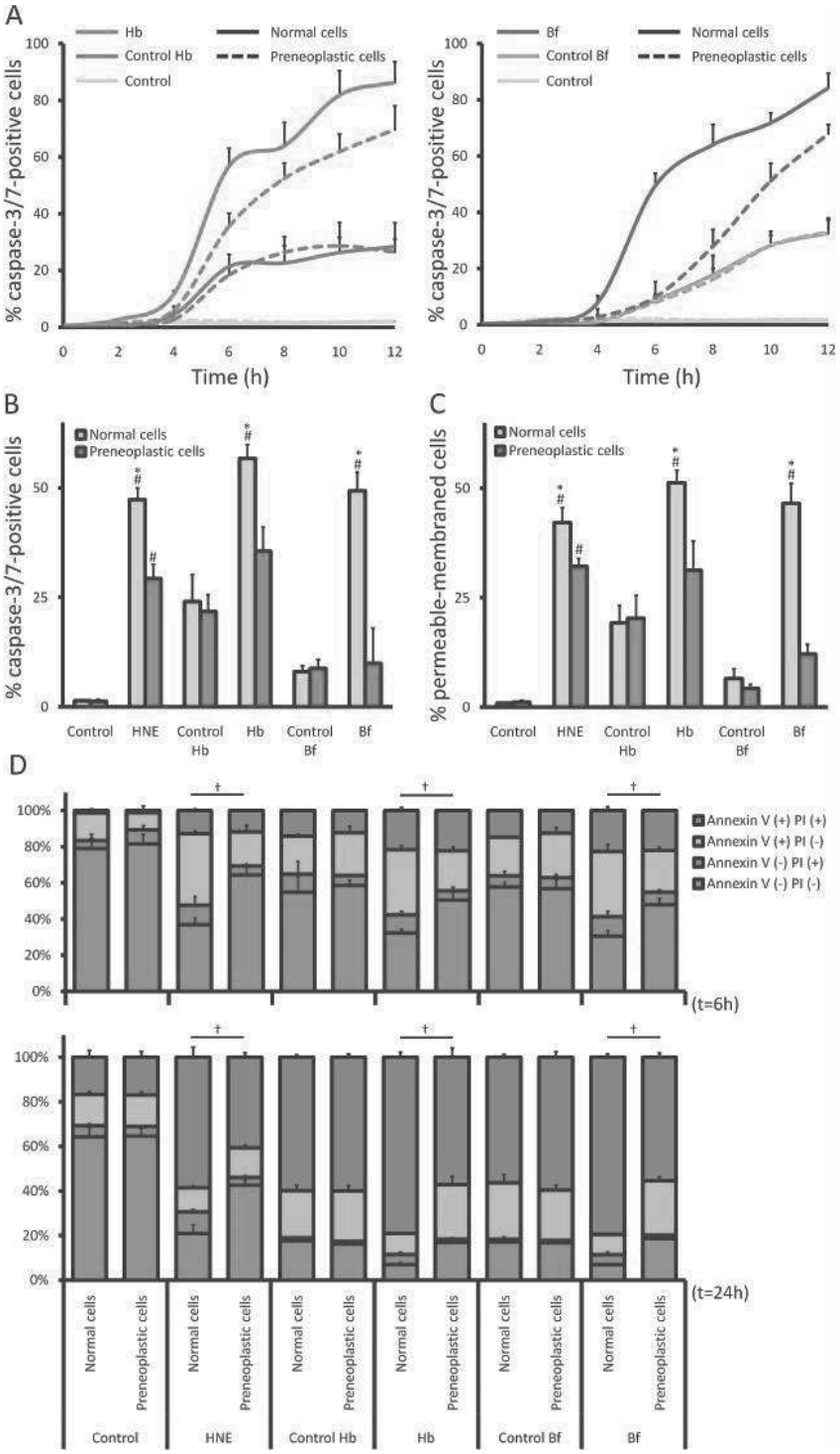

Figure 1. Fecal water of Hb- and Bf-fed rats (Hb and Bf) exerted higher toxicity towards normal cells compared with preneoplastic cells. Cells were treated with HNE 40 μM and fecal water. Control Hb and Control Bf (respective controls for Hb and Bf) were fecal water issued from standard diet-fed rats. Apoptosis was observed by detecting caspase-3/7 activity and membrane permeability using time-lapse microscopy and by APC Annexin V/propidium iodide (PI) flow cytometry. (**A**) Measures of the percentage of cells exhibiting caspase-3/7 activity upon exposure to fecal water recorded over time. (**B**) Percentage of cells with positive caspase-3/7 activity and (**C**) permeable membrane upon treatments with HNE 40 μM and fecal water ($t = 6$ h). (**D**) Repartition of cell population exhibiting positive and negative staining of APC Annexin V and PI upon treatments with HNE 40 μM and fecal water ($t = 6$ and 24 h). *Significant difference between normal and preneoplastic cells ($P < 0.05$). #Significant difference between a treatment (HNE, Hb, Bf) and its respective control (Control, Control Hb, Control Bf) ($P < 0.05$). †Significant difference between unstained (Annexin V (-) PI (-)) normal and preneoplastic cells ($P < 0.05$). Data are expressed as mean ± SD ($n = 3$).

Cystine uptake assay

L-[^{14}C]-Cystine (PerkinElmer, 100 mCi/mmol) uptake was measured according to Giraudi *et al.* with some modifications (39). Cells were seeded in a 12-well plate and incubated for 6 h of contact with fecal water (dilution 10×) at 37°C. The cells were then rinsed with warmed uptake buffer (NaCl 140 mM, HEPES 25 mM, KCl 5.4 mM, $CaCl_2$ 1.8 mM, $MgSO_4$ 0.8 mM, glucose 5 mM, pH = 7.5). Cystine uptake was started by incubating the cells in uptake buffer containing L-[^{14}C]-Cystine 0.1 µCi at room temperature for 10 min, and stopped by rinsing with ice-cold unlabelled uptake buffer. The cells were then lysed by adding NaOH 0.1 N. Lysate was mixed with scintillation cocktail (UltimaGold, PerkinElmer), protein quantification was done (Pierce bicinchoninic acid enzymatic kit) and the radioactivity was determined using a scintillation counter (Hewlett Packard). The results were expressed as nmol of incorporated cystine reported to protein content.

Statistical analysis

The results ($n \geq 3$) were analyzed using software GraphPad Prism 4 for Windows. Different responses of treatments and genotype effect were analyzed by two-way ANOVA and student's *t*-test, respectively. When ANOVA showed a statistically significant effect ($P < 0.05$), comparison among data was done using Tukey's HSD Post-hoc test. Pearson correlation test was done to analyze the correlation between the percentage of apoptotic nuclei and TBARS or free HNE concentration in fecal water.

Results

Fecal water of Hb- and Bf-fed rats induced cell death by apoptosis and preneoplastic cells exhibited higher resistance compared with normal cells

To characterize cell death, we analyzed caspase-3/7 activation, membrane phosphatidylserine translocation to the outer leaflet and cell membrane permeabilization (Figure 1A–D; Supplementary Movies 1–4, available at *Carcinogenesis* Online) in normal and preneoplastic cells following exposure to fecal water, according to the guidelines of apoptosis identification (40). Fecal water induced apoptosis in both cell lines (Figure 1A) but at a much higher extend when diets were supplemented with Hb or Bf. The differential of apoptosis in normal and preneoplastic cells was observed only upon exposure to fecal water of Hb- and Bf-fed rats, but not to the fecal water control issued from rats fed with standard diet. Compared to preneoplastic cells, normal cells exhibited earlier and higher apoptosis upon exposure to fecal water of Hb- and Bf-fed rats.

Following 6 h of exposure to fecal water of Hb- and Bf-fed rats, approximately 50% of normal cells population exhibited caspase-3/7 activation and membrane permeabilization while only approximately 30% of preneoplastic cells population exhibited the same phenomena (Figure 1B and C). The number of unstained living cells was higher in preneoplastic cells than in normal cells even at a longer incubation time of 24 h (Figure 1D). HNE was used in our experiments as positive control for apoptosis induction by lipid peroxidation byproducts. Like HNE, fecal water of Hb- and Bf-fed rats induced significantly higher apoptosis in normal cells than in preneoplastic cells ($P < 0.05$). This difference was not observed upon exposure to fecal water control.

Depletion of carbonyl compounds in fecal water of Hb- and Bf-fed rats abolished differential apoptosis in normal and preneoplastic cells

To support the fact that lipid peroxidation byproducts are involved in fecal water toxicity towards normal and preneoplastic cells, we used CTR to deplete carbonyl compounds (including

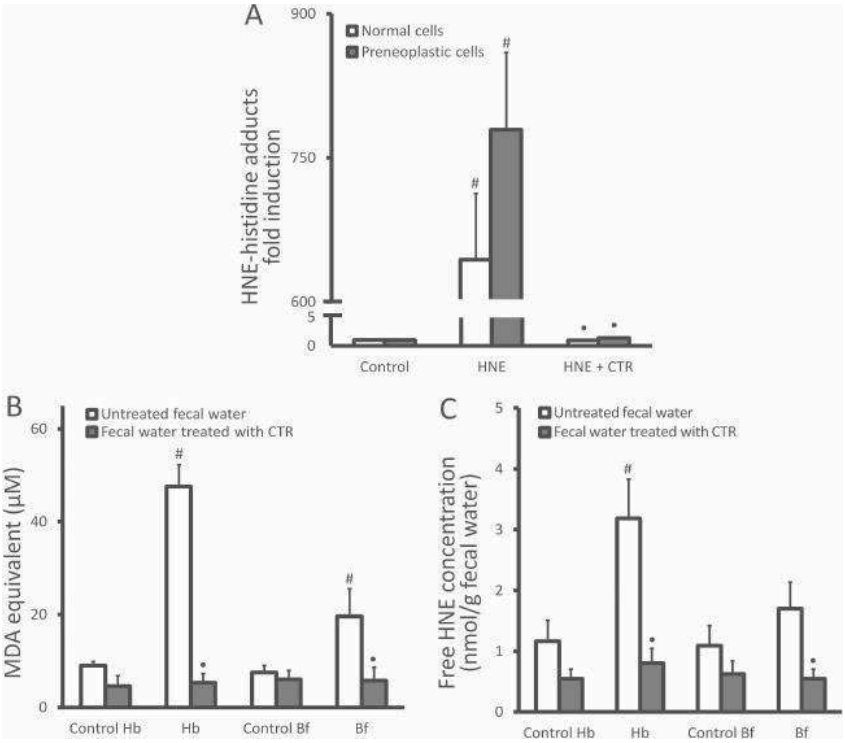

Figure 2. Carbonyl-trapping resin (CTR) was shown to be effective in depleting carbonyl compounds (including aldehydes) in fecal water of Hb- and Bf-fed rats (Hb and Bf). (**A**) HNE-histidine adducts in protein extract of cells treated with HNE 40 µM treated or not with CTR (t = 6h). (**B**) Concentration of lipid peroxidation byproducts TBARS and (C) free HNE in fecal water (Hb and Bf) and the respective controls (Control Hb and Control Bf) treated or not by CTR. # Significant difference between a treatment (HNE, Hb, Bf) and its respective control (Control, Control Hb, Control Bf) ($P < 0.05$). •Significant difference between a treatment using untreated and CTR-treated HNE or fecal water ($P < 0.05$). Data are expressed as mean ± SD ($n = 3$).

aldehydes) in fecal water. Figure 2A shows the efficacy of CTR in scavenging HNE, leading to omitted HNE-histidine adducts in the cells exposed to CTR-treated HNE. In Figure 2B and C, diet enriched in n-6 fatty acid and heme iron (under the form of Hb and Bf) led to a significant increase in fecal lipid peroxidation compared with standard diet ($P < 0.05$). Treatment by CTR was effective in reducing fecal TBARS and free HNE significantly to a concentration observed in fecal water control ($P < 0.05$).

We incubated normal and preneoplastic cells in untreated and CTR-treated fecal water to assess apoptosis by analyzing the percentage of nuclei with apoptotic appearance (fragmented or condensed) (Figure 3A), cells with positive caspase-3/7 activity (Figure 3B) and cells with permeable membrane (Figure 3C). The depletion of carbonyl compounds was shown to decrease significantly fecal water-induced apoptosis in both cell lines and abolish the differential apoptosis in normal and preneoplastic cells.

Exposure to fecal water of Hb- and Bf-fed rats induced Nrf2 activation in normal and preneoplastic cells

To analyze Nrf2 activation in normal and preneoplastic cells induced by exposure to fecal water, we investigated the nuclear localization of Nrf2. Figure 4A displays the fluorescence intensity graphs representing the localization of nuclei (blue channel) and Nrf2 (green channel) in normal and preneoplastic cells under basal conditions and upon exposure to fecal water of Hb- and Bf-fed rats. Figure 4A shows that Nrf2 was active in preneoplastic cells under basal conditions, indicated by its nuclear localization. In contrast, Nrf2 in normal cells tended to display less nuclear accumulation than preneoplastic cells. Following exposure to HNE and to fecal water of Hb- and Bf-fed rats, both normal and preneoplastic cells exhibited Nrf2 activation.

Our blot analysis of nuclear Nrf2 shows Nrf2 activation in normal and preneoplastic cells following exposure to HNE and fecal water of Hb- and Bf-fed rats, but not to fecal water control (Figure 4B and Supplementary Figure 5, available at *Carcinogenesis* Online). Interestingly, CTR-treated HNE or fecal water did not trigger Nrf2 nuclear translocation, showing the importance of carbonyl compounds in such an activation.

We analyzed the expression of heme oxygenase 1 (HO1), an Nrf2 target gene following exposure to HNE and fecal water for 4 h. Figure 4C shows higher HO1 induction in normal cells than in preneoplastic cells upon exposure to HNE and fecal water of Hb- and Bf-fed rats ($P < 0.05$). Depletion of carbonyl compounds was shown to block the upregulation of HO1 expression carried out by untreated fecal water in both cell lines.

Nrf2 was involved in the resistance of preneoplastic cells towards fecal water toxicity

To analyze whether Nrf2 is involved in the resistance of preneoplastic cells towards fecal water toxicity, we downregulated Nrf2 expression by transfecting control Nrf2-specific siRNA (siNrf2).

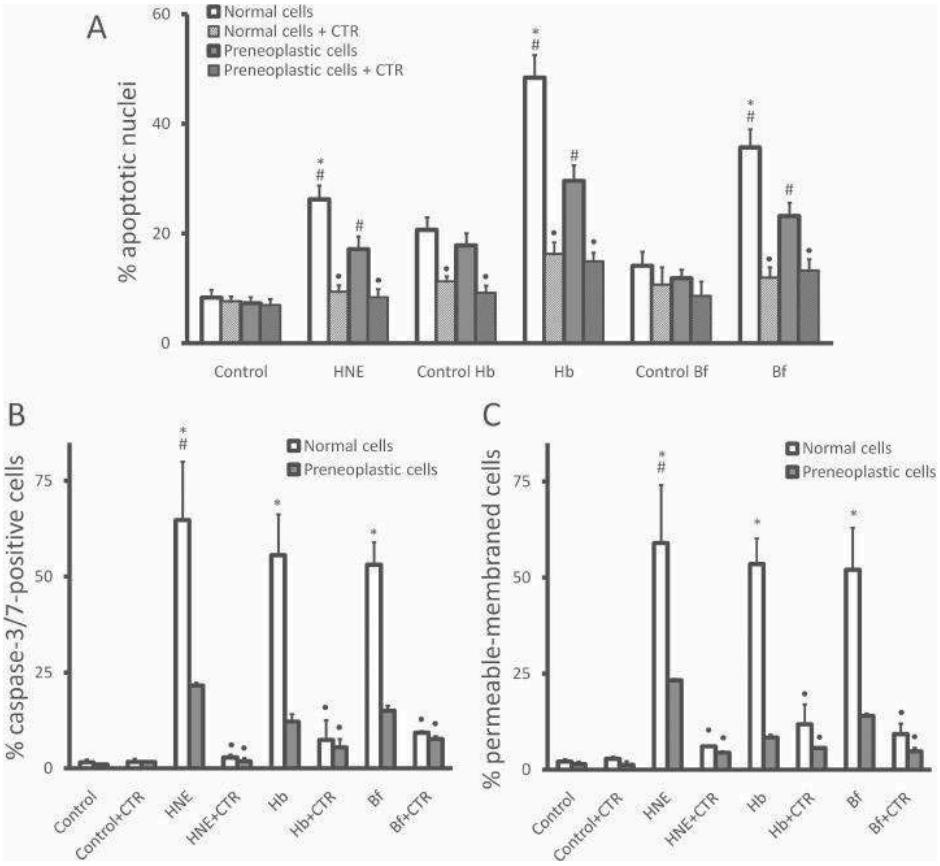

Figure 3. Depletion of carbonyl compounds (including aldehydes) in fecal water of Hb- and Bf-fed rats (Hb and Bf) abolished their differential toxicity towards normal and preneoplastic cells. (**A**) Percentage of cells exhibiting apoptotic nuclei appearance (condensed and fragmented) following exposure to HNE 40 μM and fecal water treated or not with carbonyl-trapping resin (CTR) ($t = 6$ h). (**B**) Percentage of cells with positive caspase-3/7 activity and (**C**) permeable membrane upon treatments with HNE 40 μM and fecal water treated or not with CTR ($t = 6$ h). *Significant difference between normal and preneoplastic cells ($P < 0.05$). #Significant difference between a treatment (HNE, Hb, Bf) and its respective control (Control, Control Hb, Control Bf) ($P < 0.05$). •Significant difference between a treatment using untreated and CTR-treated HNE or fecal water ($P < 0.05$). Data are expressed as mean ± SD ($n = 3$).

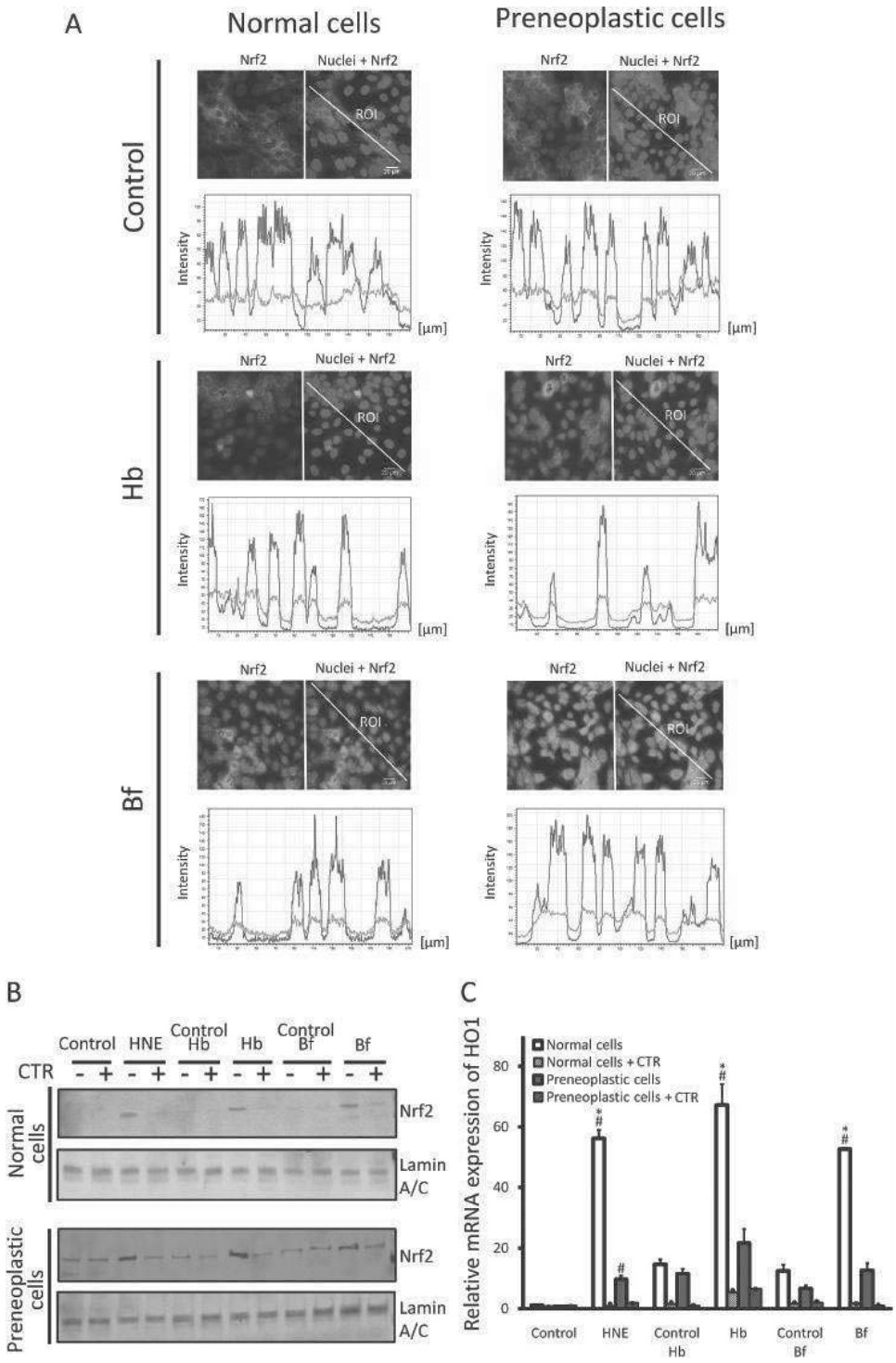

Figure 4. Nrf2 was activated in normal and preneoplastic cells upon exposure to fecal water of Hb- and Bf-fed rats (Hb and Bf). Following treatments with fecal water (t = 1 h), Nrf2 detection in cells was done by immunofluorescence and western blot. (**A**) Images of immunofluorescence analysis of fecal water-treated normal and preneoplastic cells. Blue channels indicate nuclei and green channels indicate Nrf2. The fluorescence intensity graphs represent the colocalization of blue signal (nuclei) and green signal (Nrf2) along regions of interest (ROI). The presented images are representative of three independent experiments. (**B**) Western blotting analysis of nuclear Nrf2 following exposure to HNE 40 µM and fecal water treated or not with carbonyl-trapping resin (CTR). Lamin A/C was used as loading control. The presented blots are representative of three independent experiments. (**C**) Relative mRNA expression of HO1 following exposure to HNE 40 µM and fecal water treated or not with CTR. Significant difference between normal and preneoplastic cells ($^{*}P < 0.05$). Significant difference between a treatment in a cell line (HNE, Hb, Bf) and its respective control (Control, Control Hb, Control Bf) ($^{\#}P < 0.05$). Significant difference between a treatment using untreated and CTR-treated HNE or fecal water ($^{\bullet}P < 0.05$). Data are expressed as mean ± SD ($n = 3$).

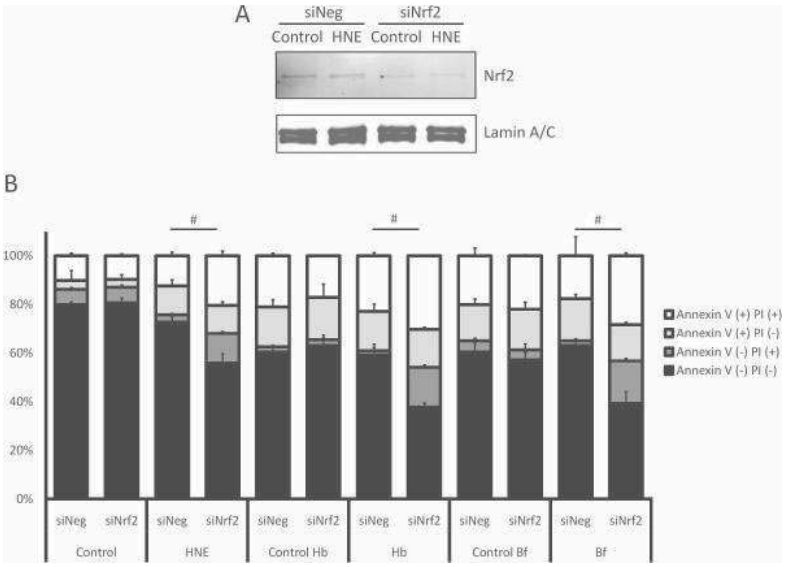

Figure 5. Nrf2 was involved in the resistance of preneoplastic cells towards the toxicity of fecal water of Hb- and Bf-fed rats (Hb and Bf). (**A**) Western blotting analysis of nuclear Nrf2 in siNeg- and siNrf2-transfected preneoplastic cells treated or not with HNE 40 μM (t = 2 h) (**B**) Repartition of siNeg- and siNrf2-transfected preneoplastic cell population exhibiting positive and negative staining of APC Annexin V and propidium iodide (PI) upon treatments with HNE 40 μM and fecal water (t = 6 h). Significant difference between unstained (Annexin V (-) PI (-)) siNeg- and siNrf2-treated preneoplastic cells ($^{\#}P < 0.05$). Data are expressed as mean ± SD ($n = 3$).

This down-regulation diminished the level of nuclear Nrf2 in preneoplastic cells both under basal conditions and upon exposure to HNE (Figure 5A). In preneoplastic cells, siNrf2 transfection reduced cell viability and increased apoptosis following 6 h of exposure to HNE and fecal water of Hb- and Bf-fed rats (Figure 5B), highlighting the importance of Nrf2 in their resistance towards fecal water toxicity. In normal cells, probably because of their high sensitivity to HNE and fecal water, no enhancement of apoptosis induction following Nrf2 invalidation was observed (Figure S6).

Exposure to fecal water of Hb- and Bf-fed rats induced higher expression of HNE detoxification enzymes in preneoplastic cells

To further investigate the role of Nrf2 in cellular response to fecal water toxicity, we analyzed the expression of three Nrf2 target genes involved in HNE detoxification: aldehyde dehydrogenase 3A1 (ALDH3A1), glutathione S-transferase A4 (GSTA4) and x-C-type cystine/glutamate antiporter (xCT). Figure 6A (left panel) shows that these genes were more expressed in preneoplastic cells than in normal cells, both under basal conditions and following exposure to HNE and fecal water of Hb- and Bf-fed rats ($P < 0.05$). Treatment with CTR set down and normalized the effects of HNE and fecal water on the expression of these genes, resulting in gene expression profiles which resemble basal conditions. Despite higher final genes expression in preneoplastic cells, we found that these genes were more upregulated in normal cells than in preneoplastic cells upon exposure to HNE and fecal water of Hb- and Bf-fed rats (Figure 6A right panel).

In accordance with the upregulation of xCT expression, we analyzed the level of cystine uptake in normal and preneoplastic cells following exposure to fecal water. Exposure to fecal water of Hb- and Bf-fed rats resulted in higher final uptake in preneoplastic cells than in normal cells (Figure 6B). Depletion of carbonyl compounds abolished the differential cystine uptake due to fecal water exposure.

Discussion

The aim of this study was to understand the mechanisms involved in the differential of fecal water toxicity prepared from Hb- or Bf-fed rats towards normal and preneoplastic mouse colonocytes. Here, we show that Nrf2 activity, *via* a higher expression of HNE-detoxification enzymes in preneoplastic cells, explains at least in part this difference. We also demonstrate that carbonyl compounds (including aldehydes) are the main agents of fecal water toxicity determining differential susceptibility of normal and preneoplastic cells.

Fecal water from Hb- and Bf-fed rats were associated to high lipid peroxidation and colorectal cancer promotion *in vivo*

Fecal water of Hb- and Bf-fed rats is a complex matrix derived from real luminal contents which is relevant for studying the effects of heme on luminal neoformation of aldehydes. In comparison with Hb- and Bf-fecal water, HNE was used as pure model molecule representative of lipid peroxidation-derived aldehydes since fecal waters were obtained from feces of rats fed with diets rich in $n - 6$ fatty acids. Indeed, HNE is an important lipoperoxidation endproduct of $n - 6$ fatty acid by heme iron, both in terms of presence and toxicity (10). The HNE concentration used in this study (40 μM) was deduced from TBARS concentration in the feces of Hb-fed rats (Figure 2B) to mimic the global level of lipoperoxidation endproducts in fecal water.

Our hypothesis on the role of lipid peroxidation in the promotion of colorectal carcinogenesis by red meat emphasizes the importance of lipid peroxidation-derived aldehydes in generating a selection of colon cells. During our *in vivo* experiments, rats were fed with standard diet enriched in safflower oil and heme under the form of Hb or raw Bf. Heme contained in Hb and raw Bf is a potent catalyst of lipid peroxidation (41,42).

As observed in Figure 2B and C, supplementation of heme under the form of Hb and Bf in rats increased fecal lipid peroxidation

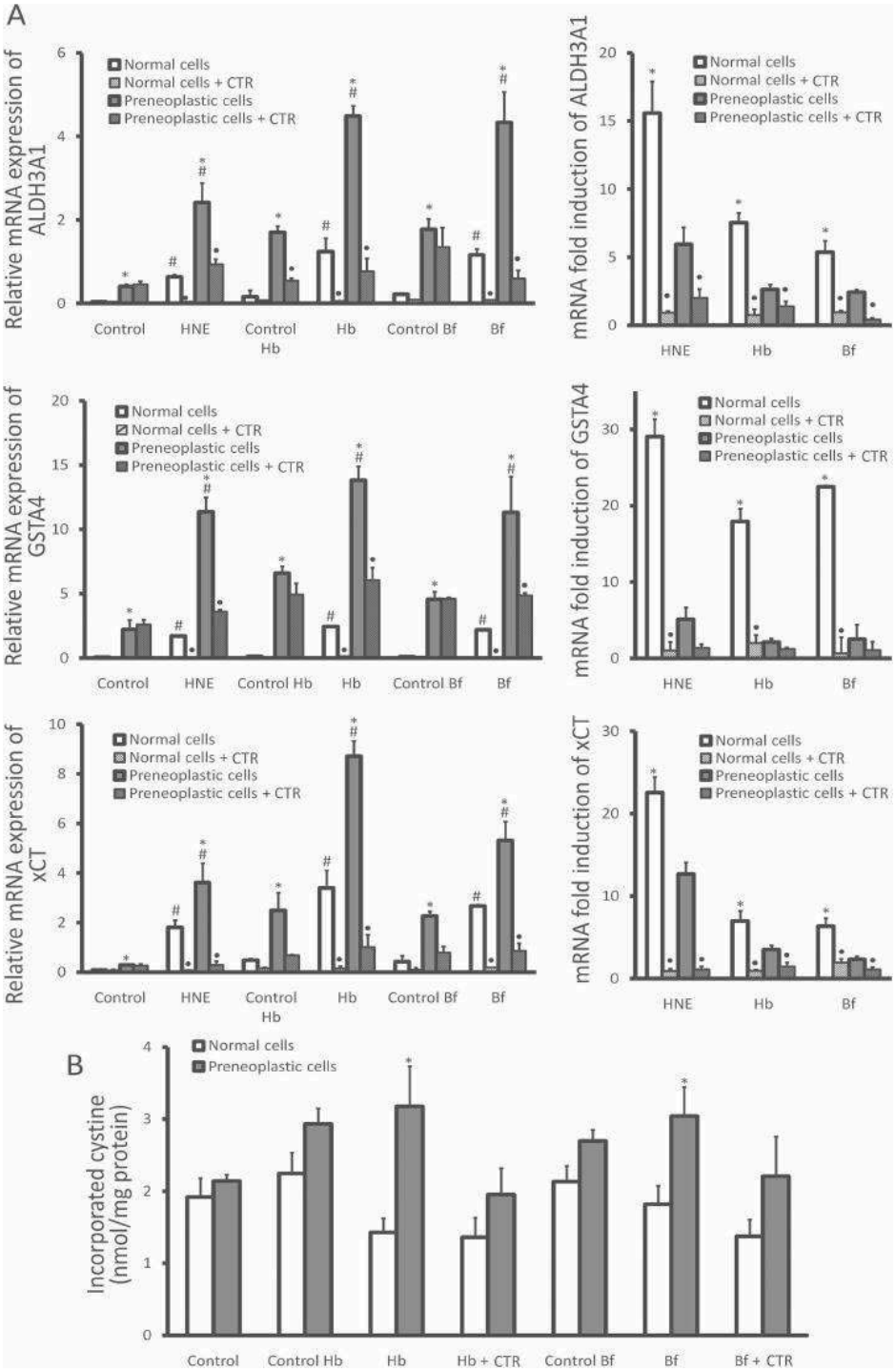

Figure 6. Preneoplastic cells expressed higher level of HNE detoxification enzymes compared with normal cells under basal conditions and upon exposure to fecal water of Hb- and Bf-fed rats (Hb and Bf). (**A**) Left panel shows the relative mRNA expression of Nrf2 downstream genes implicated in HNE detoxification (ALDH3A1, GSTA4 and xCT) in nomal and preneoplastic cells following exposure to HNE 40 μM and fecal water treated or not with carbonyl-trapping resin (CTR) (t = 4 h). Right panel shows the fold induction of mRNA expression of the genes upon exposure to HNE, Hb and Bf reported to their respective controls (Control, Control Hb and Control Bf). (**B**) Incorporated cystine reported to protein mass upon exposure to fecal water treated or not with CTR (t = 6 h). Significant difference between normal and preneoplastic cells ($^{*}P < 0.05$). Significant difference between a treatment in a cell line (HNE, Hb, Bf) and its respective control (Control, Control Hb, Control Bf) ($^{\#}P < 0.05$). Significant difference between a treatment using untreated and CTR-treated ($^{*}P < 0.05$). Data are expressed as mean ± SD (n = 3).

and HNE level correlating positively with increasing fecal toxicity towards colon cells (Figure 1). Indeed, Hb (10) and Bf supplementation (not published) increased significantly number or size of preneoplatic lesions in the colon of azoxymethane-induced rats. These lesions are mucin-depleted foci (MDF) with absent or scant mucus production (43). After 100 days, we found that the Hb-fed

rats developed significantly higher amount of MDF compared with standard diet-fed rats meat (3.4±1.2 versus 2.2±1.5 MDF per colon, respectively; $P < 0.01$) (10). Rats consuming Bf-based diet had significantly larger MDF in their colon compared with those not consuming red meat (2.6±0.6 versus 2.2±0.3 crypts by MDF, respectively; $P = 0.03$). Taken together, these results indicate that Hb or Bf consumption promoted colorectal carcinogenesis.

Higher Nrf2 activitiy in preneoplastic cells led to resistance to apoptosis towards exposure to fecal water of Hb- and Bf-fed rats

We showed that fecal water induced apoptosis in normal and preneoplastic cells through caspase-3/7 activation, membrane phosphatidylserine translocation, membrane permeabilization and finally DNA fragmentation (Figures 1 and 3). These endpoints prompted us to classify the cell death as apoptosis (40). Exposure to fecal water of Hb- and Bf-fed rats activated Nrf2 in both normal and preneoplastic cells (Figure 4). Normal cells appeared to be more responsive in upregulating HNE detoxification genes expression compared with preneoplastic cells (Figure 6A right panel). However, final expression of cytoprotective enzymes in preneoplastic cells remained higher than in normal cells, asserting that preneoplastic cells had better cellular defense towards fecal water toxicity (Figure 6A left panel). These enzymes (ALDH3A1, xCT and GSTA4) are implicated in HNE detoxification (44) and regulated by Nrf2 (45–48). Thus, preneoplastic cells were more resistant to pro-apoptotic effects of HNE and fecal water than normal cells (Figure 1). Downregulation of Nrf2 in preneoplastic cells reduced their resistance to fecal water toxicity, confirming its protective role (Figure 5).

The mechanisms by which preneoplastic cells exert higher resistance towards fecal water of Hb- and Bf-fed rats than normal cells implicate conjugation pathway with glutathione. The expression of xCT and GSTA4, two enzymes involved in glutathione conjugation pathway and cystine uptake, was higher in preneoplastic cells than in normal cells towards exposure to fecal water of Hb- and Bf-fed rats (Figure 6).

Fecal carbonyl compounds were responsible for Nrf2 activation in colon cells

We proposed that the promotion of colorectal carcinogenesis was linked to the increase of fecal lipid peroxidation level and the toxicity of fecal water. In this study, the importance of carbonyl compounds, including aldehydes derived from lipid peroxidation in fecal toxicity was clearly shown in all our results using CTR. Under activation, this latter contains reactive hydrazine derivatives which are able to scavenge carbonyl groups. Regarding its chemical specificity towards carbonyl groups under the present reaction conditions, activated CTR is very unlikely to bind other potentially cytotoxic molecules which are possibly present in fecal water such as bile acid, bilirubin and lysophospholipids.

CTR was shown to reduce the content of fecal lipid peroxidation byproducts (TBARS) and free HNE (Figure 2A–C). The percentage of apoptotic nuclei (Figure 3) was significantly correlated with the concentration of fecal TBARS ($r = 0.95$, $P < 0.01$ for normal cells; $r = 0.90$, $P < 0.01$ for preneoplastic cells) and the concentration of fecal free HNE ($r = 0.96$, $P < 0.01$ for normal cells; $r = 0.93$, $P < 0.01$ for preneoplastic cells). In our previous *in vivo* studies, we demonstrated that the limitation of lipid peroxidation was correlated to the promoting effect of heme on colorectal carcinogenesis (29,49). This protection was associated to a decrease of fecal water toxicity without causative link between lipid peroxidation and toxicity. Here, we proposed that heme-induced lipid peroxidation was at least in part responsible for the toxicity of fecal water of heme-fed rats. Indeed, as indicated above, CTR traps carbonyl compounds, including aldehydes derived from lipid peroxidation. However, other carbonyl compounds such as ketones and endogenous aldehydes can also be trapped by CTR. Therefore, our study with CTR does not demonstrate that lipid peroxidation-derived aldehydes are solely responsible for the effects of fecal water towards cells. Nevertheless, the results of free HNE trapping (Figure 2C) correlating positively with cytotoxic activity and the kinetically slower reaction of ketones towards hydrazine compounds compared to aldehydes (50) encouraged us to propose that lipid peroxidation-derived aldehydes are the main agents of fecal water toxicity.

In this study, we showed that the presence of carbonyl compounds in fecal water was potentially fundamental in determining Nrf2 activation in normal and preneoplastic cells following exposure to fecal water of Hb- and Bf-fed rats. Figure 4B indicates that Nrf2 activation stimulated by fecal water of Hb- and Bf-fed rats was nullified by depletion of carbonyl compounds. These phenomena were also observed in the expression of Nrf2 downstream genes reported in Figure 6A. In addition, we also reported that all profiles induced by treatments with HNE showed similar tendency with those induced by treatments with fecal water of Hb- and Bf-fed rats. Based on these findings, we highlight the central role of carbonyl compounds (including aldehydes) in Nrf2 activation in colon cells and in the toxicity of fecal water of heme-fed rats.

The different resistance between normal and preneoplastic cells towards exposure to fecal water of Hb- and Bf-fed rats led us to propose a mechanism of colorectal carcinogenesis through positive selection of preneoplastic cells. This phenomenon would favor the survival of preneoplastic cells and thus promote colorectal carcinogenesis.

Supplementary material

Supplementary Movies S1–S4 and Supplementary Figures 5 and 6 can be found at http://carcin.oxfordjournals.org/

Funding

This research was supported by grants from the Agence Nationale de la Recherche (ANR-10-ALIA-014 SecuriViande), the Institut National du Cancer ITMO Cancer (Plan cancer 2009–2013)/INCa/INSERM for financial support for the 'NeoMeaTox' project (ENV201213) and the Ligue Régionale contre le Cancer (Midi Pyrénées). The funders had no role in study design, data collection and analysis, the decision to publish, or preparation of the manuscript.

Acknowledgements

The authors would like to thank Technological Platform on Transcriptomics (GeT-TRiX) at INRA ToxAlim Toulouse, France for helping achieve gene expression analysis.
Conflict of Interest Statement: None declared.

References

1. Cummings, J.H. et al. (1998) Diet and the prevention of cancer. BMJ, 317, 1636–1640.
2. Watson, A.J. et al. (2011) Colon cancer: a civilization disorder. Dig. Dis., 29, 222–228.
3. Giovannucci, E. et al. (1995) Physical activity, obesity, and risk for colon cancer and adenoma in men. Ann. Intern. Med., 122, 327–334.
4. WCRF/AICR (2011) Continuous Update Project Report. Food, Nutrition, Physical Activity, and the Prevention of Colorectal Cancer. World Cancer Research Fund/American Institute for Cancer Research.
5. Norat, T. et al. (2002) Meat consumption and colorectal cancer risk: dose-response meta-analysis of epidemiological studies. Int. J. Cancer, 98, 241–256.

6. Norat, T. et al. (2005) Meat, fish, and colorectal cancer risk: the European Prospective Investigation into cancer and nutrition. J. Natl. Cancer Inst., 97, 906–916.
7. Lee, D.H. et al. (2004) Heme iron, zinc, alcohol consumption, and colon cancer: Iowa Women's Health Study. J. Natl. Cancer Inst., 96, 403–407.
8. Bouvard, V. et al. (2015) Carcinogenicity of consumption of red and processed meat. Lancet Oncol, 16, 1599–600.
9. Santarelli, R.L. et al. (2010) Meat processing and colon carcinogenesis: cooked, nitrite-treated, and oxidized high-heme cured meat promotes mucin-depleted foci in rats. Cancer Prev. Res. (Phila)., 3, 852–864.
10. Bastide, N.M. et al. (2015) A central role for heme iron in colon carcinogenesis associated with red meat intake. Cancer Res., 75, 870–879.
11. Guéraud, F. et al. (2010) Chemistry and biochemistry of lipid peroxidation products. Free Radic. Res., 44, 1098–1124.
12. Bastide, N.M. et al. (2011) Heme iron from meat and risk of colorectal cancer: a meta-analysis and a review of the mechanisms involved. Cancer Prev. Res. (Phila)., 4, 177–184.
13. Dalleau, S. et al. (2013) Cell death and diseases related to oxidative stress: 4-hydroxynonenal (HNE) in the balance. Cell Death Differ., 20, 1615–1630.
14. Pierre, F. et al. (2007) Apc mutation induces resistance of colonic cells to lipoperoxide-triggered apoptosis induced by faecal water from haem-fed rats. Carcinogenesis, 28, 321–327.
15. Pierre, F. et al. (2006) New marker of colon cancer risk associated with heme intake: 1,4-dihydroxynonane mercapturic acid. Cancer Epidemiol. Biomarkers Prev., 15, 2274–2279.
16. Lapré, J.A. et al. (1992) Diet-induced increase of colonic bile acids stimulates lytic activity of fecal water and proliferation of colonic cells. Carcinogenesis, 13, 41–44.
17. Glinghammar, B. et al. (1997) Shift from a dairy product-rich to a dairy product-free diet: influence on cytotoxicity and genotoxicity of fecal water–potential risk factors for colon cancer. Am. J. Clin. Nutr., 66, 1277–1282.
18. Klinder, A. et al. (2007) Fecal water as a non-invasive biomarker in nutritional intervention: comparison of preparation methods and refinement of different endpoints. Nutr. Cancer, 57, 158–167.
19. Awasthi, Y.C. et al. (2003) Role of 4-hydroxynonenal in stress-mediated apoptosis signaling. Mol. Aspects Med., 24, 219–230.
20. Schaeferhenrich, A. et al. (2003) Human adenoma cells are highly susceptible to the genotoxic action of 4-hydroxy-2-nonenal. Mutat. Res., 526, 19–32.
21. Forest, V. et al. (2003) Butyrate restores motile function and actin cytoskeletal network integrity in apc mutated mouse colon epithelial cells. Nutr. Cancer, 45, 84–92.
22. Nishisho, I. et al. (1991) Mutations of chromosome 5q21 genes in FAP and colorectal cancer patients. Science, 253, 665–669.
23. Markowitz, S.D. et al. (2009) Molecular origins of cancer: molecular basis of colorectal cancer. N. Engl. J. Med., 361, 2449–2460.
24. Nakamura, Y. et al. (1991) Mutations of the adenomatous polyposis coli gene in familial polyposis coli patients and sporadic colorectal tumors. Princess Takamatsu Symp., 22, 285–292.
25. Sporn, M.B. et al. (2012) NRF2 and cancer: the good, the bad and the importance of context. Nat. Rev. Cancer, 12, 564–571.
26. Siow, R.C. et al. (2007) Modulation of antioxidant gene expression by 4-hydroxynonenal: atheroprotective role of the Nrf2/ARE transcription pathway. Redox Rep., 12, 11–15.
27. Baradat, M. et al. (2011) 4-Hydroxy-2(E)-nonenal metabolism differs in Apc(+/+) cells and in Apc(Min/+) cells: it may explain colon cancer promotion by heme iron. Chem. Res. Toxicol., 24, 1984–1993.
28. Chandra, A. et al. (1997) A synthesis of 4-hydroxy-2-trans-nonenal and 4-(3H) 4-hydroxy-2-trans-nonenal. Lipids, 32, 779–782.
29. Pierre, F. et al. (2003) Meat and cancer: haemoglobin and haemin in a low-calcium diet promote colorectal carcinogenesis at the aberrant crypt stage in rats. Carcinogenesis, 24, 1683–1690.
30. Lesgards, J.F. et al. (2009) Differential distribution of 4-hydroxynonenal adducts to sulfur and nitrogen residues in blood proteins as revealed using Raney nickel and gas chromatography-mass spectrometry. Free Radic. Biol. Med., 47, 1375–1385.
31. Gladine, C. et al. (2012) Increasing intake of long-chain n-3 PUFA enhances lipoperoxidation and modulates hepatic gene expression in a dose-dependent manner. Br. J. Nutr., 107, 1254–1273.
32. Asselin, C. et al. (2006) Circulating 4-hydroxynonenal-protein thioether adducts assessed by gas chromatography-mass spectrometry are increased with disease progression and aging in spontaneously hypertensive rats. Free Radic. Biol. Med., 41, 97–105.
33. Tomasi, M.L. et al. (2014) Molecular mechanisms of lipopolysaccharide-mediated inhibition of glutathione synthesis in mice. Free Radic. Biol. Med., 68, 148–158.
34. Homma, S. et al. (2009) Nrf2 enhances cell proliferation and resistance to anticancer drugs in human lung cancer. Clin. Cancer Res., 15, 3423–3432.
35. Plasilova, M. et al. (2004) Homozygous missense mutation in the lamin A/C gene causes autosomal recessive Hutchinson-Gilford progeria syndrome. J. Med. Genet., 41, 609–614.
36. Huc, L. et al. (2012) Low concentrations of bisphenol A induce lipid accumulation mediated by the production of reactive oxygen species in the mitochondria of HepG2 cells. Toxicol. In Vitro, 26, 709–717.
37. Borovic, S. et al. (2006) Enzyme-linked immunosorbent assay for 4-hydroxynonenal-histidine conjugates. Free Radic. Res., 40, 809–820.
38. Waeg, G. et al. (1996) Monoclonal antibodies for detection of 4-hydroxynonenal modified proteins. Free Radic. Res., 25, 149–159.
39. Giraudi, P.J. et al. (2011) Functional induction of the cystine-glutamate exchanger system Xc(-) activity in SH-SY5Y cells by unconjugated bilirubin. PLoS One, 6, e29078.
40. Galluzzi, L. et al. (2009) Guidelines for the use and interpretation of assays for monitoring cell death in higher eukaryotes. Cell Death Differ., 16, 1093–1107.
41. Lorrain, B. et al. (2012) Dietary iron-initiated lipid oxidation and its inhibition by polyphenols in gastric conditions. J. Agric. Food Chem., 60, 9074–9081.
42. Roginsky, V. et al. (2007) Efficacy of metmyoglobin and hemin as a catalyst of lipid peroxidation determined by using a new testing system. J. Agric. Food Chem., 55, 6798–6806.
43. Femia, A.P. et al. (2004) Mucin-depleted foci (MDF) in the colon of rats treated with azoxymethane (AOM) are useful biomarkers for colon carcinogenesis. Carcinogenesis, 25, 277–281.
44. Baradat, M. et al. (2011) 4-Hydroxy-2(E)-nonenal metabolism differs in Apc(+/+) cells and in Apc(Min/+) cells: it may explain colon cancer promotion by heme iron. Chem. Res. Toxicol., 24, 1984–1993.
45. Hayes, J.D. et al. (2005) Glutathione transferases. Annu. Rev. Pharmacol. Toxicol., 45, 51–88.
46. Beneš, H. et al. (2013) Protection from oxidative and electrophilic stress in the Gsta4-null mouse heart. Cardiovasc. Toxicol., 13, 347–356.
47. Alnouti, Y. et al. (2008) Tissue distribution, ontogeny, and regulation of aldehyde dehydrogenase (Aldh) enzymes mRNA by prototypical microsomal enzyme inducers in mice. Toxicol. Sci., 101, 51–64.
48. Sasaki, H. et al. (2002) Electrophile response element-mediated induction of the cystine/glutamate exchange transporter gene expression. J. Biol. Chem., 277, 44765–44771.
49. Santarelli, R.L. et al. (2013) Calcium inhibits promotion by hot dog of 1,2-dimethylhydrazine-induced mucin-depleted foci in rat colon. Int. J. Cancer, 133, 2533–2541.
50. Kool, E.T. et al. (2013) Fast hydrazone reactants: electronic and acid/base effects strongly influence rate at biological pH. J. Am. Chem. Soc., 135, 17663–17666.

Supplementary Figures integrated in Article 1:

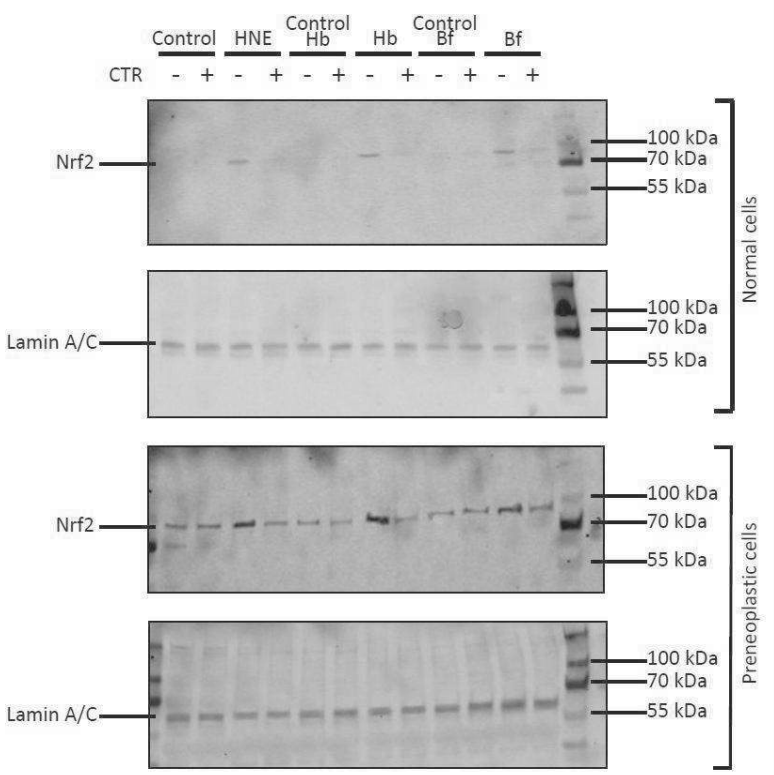

Figure S5: Exposure to HNE and fecal water of hemoglobin- and beef-fed rats (Hb and Bf) activated Nrf2 response in normal and preneoplastic cells. Uncropped full-length image with molecular weight marker of nuclear Nrf2 western blotting analysis following exposure to HNE 40 µM and fecal water treated or not with carbonyl-trapping resin (CTR) (t=1h). Lamin A/C was used as loading control. The cropped images are presented in Figure 5 in the article. The presented blots are representative of three independent experiments.

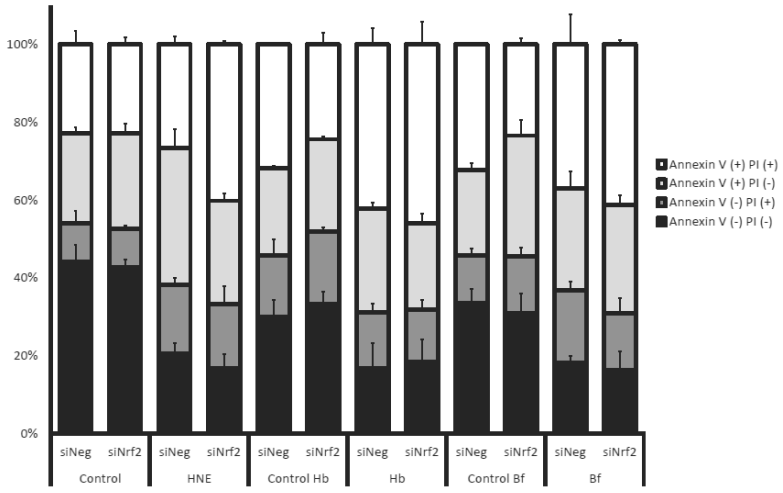

Figure S6: Normal cells did not exhibit sensitization to the toxicity of hemoglobin- and beef-fed rats (Hb and Bf) following Nrf2 inactivation. Repartition of siNeg- and siNrf2-transfected normal cell population exhibiting positive and negative staining of APC Annexin V and propidium iodide (PI) upon treatments with HNE 40 µM and fecal water (t=6 h). No significant difference was observed between unstained (Annexin V (-) PI (-)) siNeg- and siNrf2-transfected normal cells in each treatment (P>0.05). Data are expressed as Mean ± SD (n=3).

The synthesis of Article 1 is presented in Figure 46. Nrf2 activity was found to be higher in preneoplastic (APC Min/+) cells than in normal (APC +/+) cells and this resulted in higher expression of HNE detoxification enzymes in preneoplastic cells. This condition rendered preneoplastic cells more resistant than normal cells upon exposure to fecal water of heme-fed rats. Even though the expression of HNE detoxification enzymes was improved in normal cells upon exposure to fecal water of heme-fed rats, the final level of these enzymes remained higher in preneoplastic cells than in normal cells. Because of this lack of HNE detoxification enzymes in normal cells, they underwent higher level of apoptosis than preneoplastic cells following exposure to fecal water of heme-fed rats. Depletion of carbonyl compounds in the fecal water by using carbony-trapping resine (CTR) abolished the different toxicity of fecal water towards normal and preneoplastic cells.

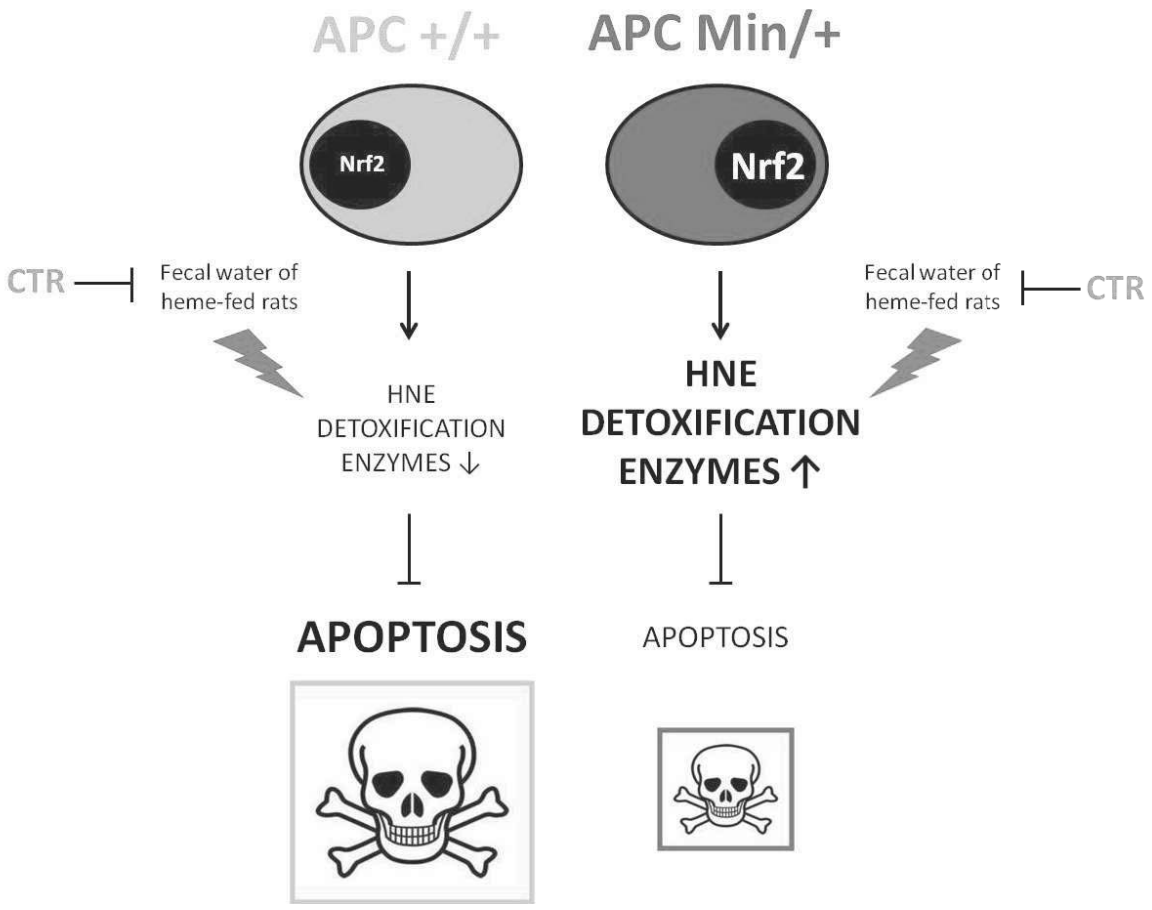

Figure 46. Schema for the role of Nrf2 in the resistance of APC Min/+ cells upon exposure to fecal water of heme-fed rats

Article 2:

A central role of heme iron in colon carcinogenesia associated with red meat intake

Bastide *et al.* 2015. *Cancer Research* 75(5):870-879.

This study, conducted by previous PhD students in the team, was focused on investigating the relative contributions of three main hypotheses on CRC and red meat intake: heme iron (Chapter 1.2.2.5), NOCs (Chapter 1.2.2.3) and HCAs (Chapter 1.2.2.2) by a 2x2x2 factorial designs in an *in vivo* experiment using azoxymethane-injected rats. I was a co-author in this study. My participation consisted in assessing the central role of aldehydes in the toxicity of fecal water of hemoglobin (Hb)-fed rats towards normal (APC +/+) and preneoplastic (APC Min/+) cells *in vitro* (results are presented in Figure 2A in the article). Briefly, the main findings presented in the article are:

1) Heme iron played a major role in the formation of colon preneoplastic lesions

In this study, to assess the relative contributions of the three potential mechanisms (heme iron, NOCs and HCAs), a 2x2x2 protocol was conducted on azoxymethane-injected rats fed with hemoglobin, HCAs (PhIP+MeIQx), or both with or without the presence of nitrite ($NaNO_2$) and nitrate ($NaNO_3$) in the drinking water to induce endogenous NOCs formation. The results showed that heme iron was the only experimental factor associated with the formation of preneoplastic lesions in the rat colon (MDF, mucin-depleted foci) without any additive or synergic effects with NOCs or HCAs. The intake of Hb-containing diet was associated with increasing formation of lipid peroxidation terminal products in the fecal water, as evidenced by the dosage of TBARS.

2) Heme iron intake induced intestinal carcinogenesis in *Min* mice and genotoxicity in normal mice

Hb-fed *Min* mice developed significantly higher load of tumor polyps compared to standard diet-fed *Min* mice and this phenomenon was associated to increasing TBARS in the feces and small intestine contents. In non-mutated C57BL/6J mice, Hb intake induced genotoxicity in small intestinal epithelium, indicating potential mutagenic effects of heme iron that might lead to carcinogenesis.

3) Preneoplastic cells were more resistant to fecal water of Hb-fed rats than normal cells: the central role of aldehydes

I participated in this part of the study. Fecal water of Hb-fed rats exerted higher cytotoxicity towards normal cells than preneoplatic cells. Depletion of carbonyl compounds in the fecal water of Hb- fed rats by carbonyl-trapping resin (CTR) appeared to reduce more than 90% of fecal TBARS and about 75% of fecal water toxicity towards normal and preneoplastic cells without any significant different toxicity observed between both cell lines ($p>0.05$). Among the three major lipid peroxidation-derived aldehydes, HNE was found to be more cytotoxic than HHE and MDA towards normal and preneoplastic cells.

Prevention and Epidemiology

Cancer Research

A Central Role for Heme Iron in Colon Carcinogenesis Associated with Red Meat Intake

Nadia M. Bastide[1,2], Fatima Chenni[1,5], Marc Audebert[1], Raphaelle L. Santarelli[1], Sylviane Taché[1], Nathalie Naud[1], Maryse Baradat[1], Isabelle Jouanin[1], Reggie Surya[1], Ditte A. Hobbs[3], Gunter G. Kuhnle[3], Isabelle Raymond-Letron[4], Françoise Gueraud[1], Denis E. Corpet[1], and Fabrice H.F. Pierre[1]

Abstract

Epidemiology shows that red and processed meat intake is associated with an increased risk of colorectal cancer. Heme iron, heterocyclic amines, and endogenous *N*-nitroso compounds (NOC) are proposed to explain this effect, but their relative contribution is unknown. Our study aimed at determining, at nutritional doses, which is the main factor involved and proposing a mechanism of cancer promotion by red meat. The relative part of heme iron (1% in diet), heterocyclic amines (PhIP + MeIQx, 50 + 25 μg/kg in diet), and NOC (induced by $NaNO_2$ + $NaNO_3$; 0.17 + 0.23 g/L of drinking water) was determined by a factorial design and preneoplastic endpoints in chemically induced rats and validated on tumors in *Min* mice. The molecular mechanisms (genotoxicity, cytotoxicity) were analyzed *in vitro* in normal and *Apc*-deficient cell lines and confirmed on colon mucosa. Heme iron increased the number of preneoplastic lesions, but dietary heterocyclic amines and NOC had no effect on carcinogenesis in rats. Dietary hemoglobin increased tumor load in *Min* mice (control diet: 67 ± 39 mm^2; 2.5% hemoglobin diet: 114 ± 47 mm^2, $P = 0.004$). *In vitro*, fecal water from rats given hemoglobin was rich in aldehydes and was cytotoxic to normal cells, but not to premalignant cells. The aldehydes 4-hydroxynonenal and 4-hydroxyhexenal were more toxic to normal versus mutated cells and were only genotoxic to normal cells. Genotoxicity was also observed in colon mucosa of mice given hemoglobin. These results highlight the role of heme iron in the promotion of colon cancer by red meat and suggest that heme iron could initiate carcinogenesis through lipid peroxidation. *Cancer Res; 75(5); 870–9. ©2015 AACR.*

Introduction

Colorectal cancer is the third most common type of cancer worldwide after lung and prostate cancer in men and after lung and breast cancer in women (1). Environmental factors, particularly diet, play roles in the development of colorectal cancer (2, 3). On the basis of epidemiologic studies, the World Cancer Research Fund panel considers the colorectal cancer risk associated with red and processed meat intake to be convincing and recommends limiting the consumption of red meat and avoiding the consumption of processed meat (2, 3). Our previous works showed that red and processed meats promote precancerous lesions (aberrant crypt foci, ACF, and mucin-depleted foci, MDF) in the colons of rats fed a low-calcium diet (4–6). These data strongly support the results from epidemiologic studies.

Three major mechanisms may explain the association between meat and colorectal cancer (7). First, potentially carcinogenic *N*-nitroso compounds can form in the gastrointestinal tract by *N*-nitrosation of peptide-derived amine or by nitrosylation yielding *S*-nitrosothiols and nitrosyl iron (FeNO). Collectively, these are measured as the apparent total *N*-nitroso compounds (ATNC; ref. 8). Second, meat cooked at high temperatures contains mutagenic heterocyclic amines (HCA) like 2-amino-1-methyl-6-phenylimidazo(4,5-b)pyridine (PhIP) and 2-amino-3,8-dimethylimidazo [4,5-f]quinoxaline (MeIQx); ref. 9]. Third, epidemiologic and experimental data support the hypothesis that heme iron present in red and processed meats promotes colorectal cancer (5–7, 10). This effect can be explained by the direct cytotoxic, genotoxic effects of heme on epithelial cells and by the catalytic effect of heme iron on the formation of ATNC and lipid peroxidation end-products like 4-hydroxynonenal (4-HNE; refs. 4, 5, 7, 11–14). Cross and colleagues investigated these 3 hypotheses in a cohort study and found a significant association between colorectal cancer and the intake of heme iron, nitrate from processed meat, and HCA (15). Nevertheless, numerous biases are possible in the determination of risk factors using epidemiologic approach, and contribution of each of these factors has never been evaluated experimentally in the same study.

The present study aimed at investigating the roles of these 3 potential mechanisms, namely heme iron, NOC, and HCA, in colorectal cancer *in vivo* at a precancerous lesion stage (MDF) in

[1]INRA UMR1331; TOXALIM (Research Center in Food Toxicology); Université de Toulouse; ENVT; INP; UPS; TOXALIM; Toulouse, France. [2]INSERM UMR-S1018; Gustave Roussy; Université Paris-Sud, Villejuif, France. [3]Department of Food and Nutritional Sciences, University of Reading, Whiteknights, Reading, United Kingdom. [4]National Veterinary School of Toulouse; Histology – Pathology; Toulouse, France. [5]Faculty of Sciences, Department of Biology, University of Djilali Liabes, Sidi Bel Abbes, Algeria.

Note: Supplementary data for this article are available at Cancer Research Online (http://cancerres.aacrjournals.org/).

N. Bastide and F. Chenni contributed equally to this article.

Corresponding Author: Fabrice Pierre, INRA UMR1331, 180 chemin de Tournefeuille, F-31027 Toulouse, France. Phone: 33-0-5-61285518; Fax: 33-0-5-61285244; E-mail: f.pierre@toulouse.inra.fr

doi: 10.1158/0008-5472.CAN-14-2554

carcinogen-induced rats (see a flowchart in Supplementary Fig. S1). Doses were chosen to mimic red meat consumption. Subsequently, the results were confirmed at the tumor stage using C57BL/6J $Apc^{Min/+}$ mice, a genetic model of colorectal cancer. The tumor incidence was associated with genotoxicity endpoints in mucosa as γH2AX and anaphase bridges. Like tumors in the majority of human colorectal cancer cases and in $Apc^{Min/+}$ mice, the preneoplastic lesion MDF in rats show activation of the Wnt signaling pathway driven by mutations in *Apc* and/or in the β-catenin gene. We also used an intestinal cellular model with normal and premalignant cells ($Apc^{+/+}$ and $Apc^{-/+}$ cells) to complement the *in vivo* studies. In combination with animal models, such cellular models allowed us (i) to understand the effect of dietary compounds on cancer promotion at early stages of carcinogenesis and (ii) to explain and further investigate the effects observed *in vivo*.

Materials and Methods

Animals and diets

Male 4-week-old F344 rats ($n = 80$; Charles Rivers), male and female 4-week-old C57BL/6J $Apc^{Min/+}$ mice (Jackson, Laboratory, $n = 35$) and $Apc^{+/+}$ mice (Charles River, $n = 33$), and male and female C57BL/6J mice ($n = 10$) were housed (2 rats per cage and 2 to 3 mice per cage) under standard laboratory conditions with free access to food and water. After acclimatization with AIN76 diet, rats were fed experimental diets for 100 days, $Apc^{Min/+}$ and $Apc^{+/+}$ mice were fed experimental diets for 49 days, and C57BL/6J mice were fed experimental diets for 14 days. Rats were killed by CO_2 asphyxiation, and mice were killed by cervical dislocation. Animal care was in accordance with the European Council and ARRIVE guidelines.

To assess the relative contributions of the 3 potential mechanisms (heme iron, NOC, and HCA), we conducted a 2 × 2 × 2 protocol on azoxymethane-induced F344 rats fed a diet containing 1% hemoglobin, HCA (PhIP, 50 μg/kg; MeIQx, 25 μg/kg), or both. To induce a strong endogenous NOC formation, drinking water was supplemented with sodium nitrate and nitrite (0.17 g/L of $NaNO_2$ and 0.23 g/L of $NaNO_3$) and compared with a nitrate-free water, according to the experimental groups described in Table 1A (16). Mice were fed a control diet or a 2.5% hemoglobin diet (Table 1B).

Azoxymethane-induced colon carcinogenesis in rat

After 1 week on the experimental diet, rats received intraperitoneal injection of azoxymethane (Sigma; 20 mg/kg body weight).

Neoplastic lesions

The large intestines of rats and large and small intestines of mice were removed and fixed in 0.05% buffered formalin (Sigma).

MDF scoring in colon of rats. MDF were scored in duplicate by 2 readers who were blinded to the origin of the colon following the high-iron diamine Alcian blue procedure (17) described by Santarelli and colleagues (4).

Tumor scoring in small intestine and colon of mice. At sacrifice, the intestinal tract from duodenum to colon was removed. Sections of duodenum, jejunum, and ileum were harvested, opened along the longitudinal axis, and washed in PBS. After fixation in 10% formalin, mouse colons were stained for 6 minutes in a 0.05% filtered methylene blue solution, and small intestines were stained for 48 hours in a 300 ppm solution of methylene blue in formalin. One reader who was blinded to the origin of the sample scored tumors and determined their diameters using a binocular microscope at 25× magnification. All tumors in each section of the intestines were counted, the smallest tumors that could be counted were approximately 0.5 mm in diameter.

Fecal assays in rat and mice

Feces were collected during the last 10 days and frozen at −20°C. Urine was collected on days 67 to 70 for rats and on days 44 to 45 for mice and frozen at −20°C before DHN-MA assay (Supplementary Materials and Methods).

Fecal water preparation. Feces of 24 hours were collected. To prepare fecal water, distilled water (1 mL for rats or 0.85 mL for mice) was added to 0.3 g of dried feces. Fecal water was prepared as described by Pierre and colleagues (5).

Heme, TBARS in fecal water of rats and mice. The heme concentration in the fecal water was measured by fluorescence according to Van den Berg and colleagues (18) and as described by Pierre and colleagues (5). To determine the lipid peroxides in the lumen, thiobarbituric acid reactive substances (TBARS) were quantified in fecal water according to the technique of Ohkawa and colleagues (19) as described previously (20). The results are expressed as the MDA equivalent.

ATNCs in fecal water of rats. ATNCs include *N*-nitroso compounds, *S*-nitrosothiols, and FeNO nitrosyl heme. They were analyzed as described previously (11) with an Ecomedics CLD Exhalyzer (Ecomedics). The values measured in 100 μL of the sample are expressed as concentration (in μmol/L).

Table 1. Experimental diets (g/100 g): study in F344 rats and in *Min* mice

	Study in F344 rats				Study in Min mice	
	Control	Heme	HCA	Heme + HCA	Control	Hemoglobin
AIN76 base	89	89	89	89	65.2	65.3
Sucrose	5.7	4.7	5.7	4.7	29.7	27.2
Casein	0.33	0.33	—	—		
Hemoglobin	—	1	—	1	—	2.5
Ferric citrate	0.015	—	0.015	—	0.035	—
PhIP + MeIQx	—	—	7.5×10^{-6}	7.5×10^{-6}		
Safflower oil	5	5	5	5	5	5

NOTE: HCA: PhIP and MeIQx were obtained from Toronto Research Chemicals. All other chemicals were analytical grade and were obtained from either Merck or Sigma. For their drinking water, each dietary group of rats was split in two subgroups. Half of them received tap water in their drinking bottle. The other half received $NaNO_2$ and $NaNO_3$ solutions in tap water. The $NaNO_2$ and $NaNO_3$ solutions were prepared with 170 mg $NaNO_2$/L water and 230 mg $NaNO_3$/L water. Water was replaced twice a week.

Cell lines

$Apc^{+/+}$ (derived from C57BL/6J mice) and $Apc^{-/+}$ (derived from C57BL/6J $Apc^{Min/+}$ mice) colon epithelial cells (21) express the heat-labile SV40 large T antigen (AgT tsa58) under the control of an IFNγ-inducible promoter. Both cell lines expressed cytokeratin 18, a marker of their epithelial phenotype (Forest 2003). Consequences of the Apc mutation were also detected in the $Apc^{-/+}$ cell line. As expected, actin network was disorganized in $Apc^{-/+}$ cells (Supplementary Fig. S2A; refs. 21, 22), accumulation of multinucleated cells was observed in $Apc^{-/+}$ cells (Supplementary Fig. S2A). As expected, the culture conditions affected cell proliferation due to the thermolabile tsA58 T antigen, which confers conditional immortalization: at 33°C with IFNγ, the large T antigen is active and drives cellular proliferation, and at 37°C, the temperature-sensitive mutation yields an inactive protein and cells act like nonproliferating epithelial cells (Supplementary Fig. S2B).

Aldehydes for cytotoxicity and genotoxicity assays

4-HNE derived from the oxidation of *n*-6 polyunsaturated fatty acids and 4-hydroxy-2-hexenal (4-HHE) derived *n*-3 polyunsaturated fatty acids were synthesized as described by Chandra and Srivastava (23). Malondialdehyde (MDA) derived from polyunsaturated fatty acids with 3 or more double bonds was prepared as described by Fenaille and colleagues (24).

Aldehyde trapping of fecal water from hemoglobin fed rats for cytotoxicity assay

Polymer resin (4-Fmoc-hydrazinobenzoyl AM NovaGel, Nobabiochem Merck Chemicals) contains hydrazine functional groups protected by Fmoc groups. To unprotect them, the resin was washed with 0.8 mL DMSO + 0.2 mL piperidine, vortexed for 1 minute, and allowed to settle for 15 minutes. The settled resin was washed twice with DMSO, 4 times with ethanol, and with distilled water. The amount of polymer resin used for each sample was based on using 100× the amount of MDA equivalents present in the fecal water sample. Polymer resin was added to fecal water, and the samples were agitated for 2 hours at 4°C. After letting the resin settle for 15 minutes, supernatant was transferred to a new tube with polymer resin and agitated for 2 hours at 4°C. After settling, the supernatant was diluted into culture medium without FCS and used for the MTT assay.

Cytotoxicity and genotoxicity assays on cell lines treated with fecal water, heme, or aldehydes

To determine cytotoxic activity of fecal water, of HNE (20 μmol/L), and of hemin (100 μmol/L), the MTT assay on $Apc^{+/+}$ and $Apc^{-/+}$ cells was used, as described previously (5). H2AX phosphorylation (γH2AX) is a rapid and sensitive cellular response to genotoxicity (25, 26). Genotoxicity and cytotoxicity of aldehydes were measured after 24 hours of treatment of $Apc^{+/+}$ and $Apc^{-/+}$ cells using a γH2AX in-cell Western blot assay according to Audebert and colleagues (27, 28). Graillot and colleagues (28) demonstrated that this assay can be used to measure cell viability via DNA quantification. Cells were seeded into 96-well plates at 5×10^3 cells per well in DMEM supplemented with 10% (v/v) FCS, 1% (v/v) penicillin/streptomycin, and 10 U/mL IFNγ at the permissive temperature of 33°C. After 72 hours, cells were transferred to 37°C without IFNγ for 24 hours and then treated with aldehyde (5, 10, and 20 μmol/L) in duplicate. Culture medium without IFNγ and FCS was used for untreated control wells. This assay was repeated 4 times.

Apoptosis assay on cell lines treated with aldehydes

Apoptosis was measured in $Apc^{+/+}$ and $Apc^{-/+}$ cells using a luminescent assay (Caspase-Glo3/7; Promega). Cells were treated with aldehydes for 6 hours. After cell lysis, plates were incubated at room temperature for 2 hours, and the luminescence intensity of each well was determined using an INFINITEM200 plate reader (TECAN). This measure was performed in triplicate with aldehydes at 2.5, 5, 10, 20, 40, and 80 μmol/L.

Histologic analyses of the small intestine of mice

Immunohistochemistry H2AX. Four-micrometer paraffin-embedded sections from formalin-fixed mouse small intestine (Swiss rolls) specimens were de-waxed in toluene and rehydrated. Sections were incubated in Dako peroxidase blocking solution (Dako S2023) and in goat serum (1:10, Dako X0907) for 20 minutes at room temperature. Sections were incubated with the rabbit polyclonal anti-γH2AX antibody (1:400, Cell Signaling Technology #9718) for 50 minutes at room temperature. The secondary antibody (biotinylated goat anti-rabbit, Thermo Scientific TR-060-BN) was applied for 30 minutes at room temperature followed by horseradish peroxidase (HRP)–streptavidin solution (DAB, Dako K0675) for 25 minutes. Peroxidase activity was revealed by DAB substrate (DAKO, K3468). Sections were counterstained with Harris hematoxylin, dehydrated, and coverslipped.

Enterocytes with nuclear γH2AX-positive foci or complete nuclear labeling were considered positive cells. Cells were assessed by counting the positive nuclei in segments of the small intestine specimen that were at least 200 glands long. The positive counts were expressed as counts per one villi-gland unit.

Anaphase bridges. Chromosomal or mitotic alterations can arise from numerous events, including errors during cell division or repair of damaged DNA. As a consequence, the separating sister chromatids are often connected by DNA bridges in anaphase. Anaphase bridges (AB) were evaluated on 4-μm paraffin-embedded sections from formalin-fixed mouse small intestine (Swiss rolls). Sections were stained with hematoxylin and eosin and AB were evaluated under light microscope using 400× magnification. Four segments from the duodenum, jejunum, and ileum that were at least 100 consecutive glands long were selected for counting. Criteria for ABs included having a well-separated parallel anaphase plate displaying a perpendicularly aligned amphophilic (stretched) connecting filament (29). The scores were expressed as number of AB per villi-gland unit.

Statistical analysis

Results were analyzed using Systat 10 software for Windows, and all data are reported as mean ± SEM. For the *in vivo* experiments on chemically induced rats, the importance of each factor was tested independently of the experimental groups (ANOVA per factor). If a significant difference was found between groups ($P < 0.05$), each experimental group was compared with the control using Dunnett test, the difference between control and hemoglobin diets effect on Min mice tumors was analyzed using the Student *t* test. For the *in vitro* study, the dose effect of aldehydes was analyzed using one-way ANOVA. If a significant difference was found between groups ($P < 0.05$), each experimental group was compared with the control treatment using Dunnett test. Second, the effect of the mutation effect at each concentration of

aldehyde was analyzed with the comparison between the $Apc^{+/+}$ and $Apc^{-/+}$ cell lines using the Student *t* test.

Results

Heme iron plays a major role in mucin-depleted foci formation

Only diets containing hemoglobin significantly increased the number of MDF per colon ($P < 0.001$) independent of the 2 other factors (Fig. 1A). Indeed, although nitrates/nitrites in drinking water induced a considerable increase in fecal ATNCs in all groups, they failed to increase the number of MDF per colon (Fig. 1A and D). Nevertheless, we noticed that the ATNC composition was different between groups, containing 30% to 80% FeNO and no *S*-nitrosothiols in the hemoglobin-fed groups compared with no FeNO and about 30% of *S*-nitrosothiols in other groups.

Diets containing hemoglobin significantly increase the amount of TBARS in fecal water (Fig. 1B) and the amount of urinary 1,4-dihydroxynonemercapturic acid (DHN-MA), a metabolite of the lipid oxidation product 4-HNE (Supplementary Fig. S3B). These oxidation biomarkers depended only on dietary and fecal heme (Supplementary Fig. S3A) and remained unchanged when the diet contained nitrates/nitrites or HCA without hemoglobin (Fig. 1B and Supplementary Fig. S3B).

Premalignant epithelial cells resist cytotoxicity induced by fecal water from heme-fed rats: the central role of aldehydes

Fecal water from rats fed hemoglobin-containing diets was more cytotoxic to the nonmutated $Apc^{+/+}$ cells than to premalignant $Apc^{-/+}$ cells (Fig. 1C). These data are consistent with previous results (20). Fecal water from rats fed HCA or nitrites/nitrates without hemoglobin was not cytotoxic to these cells (Fig. 1C).

With the trapping of aldehydes from fecal water of rats fed heme with a polymer resin with hydrazine functional groups, we found that in $Apc^{+/+}$ and $Apc^{-/+}$ cells, a 95% reduction in fecal water

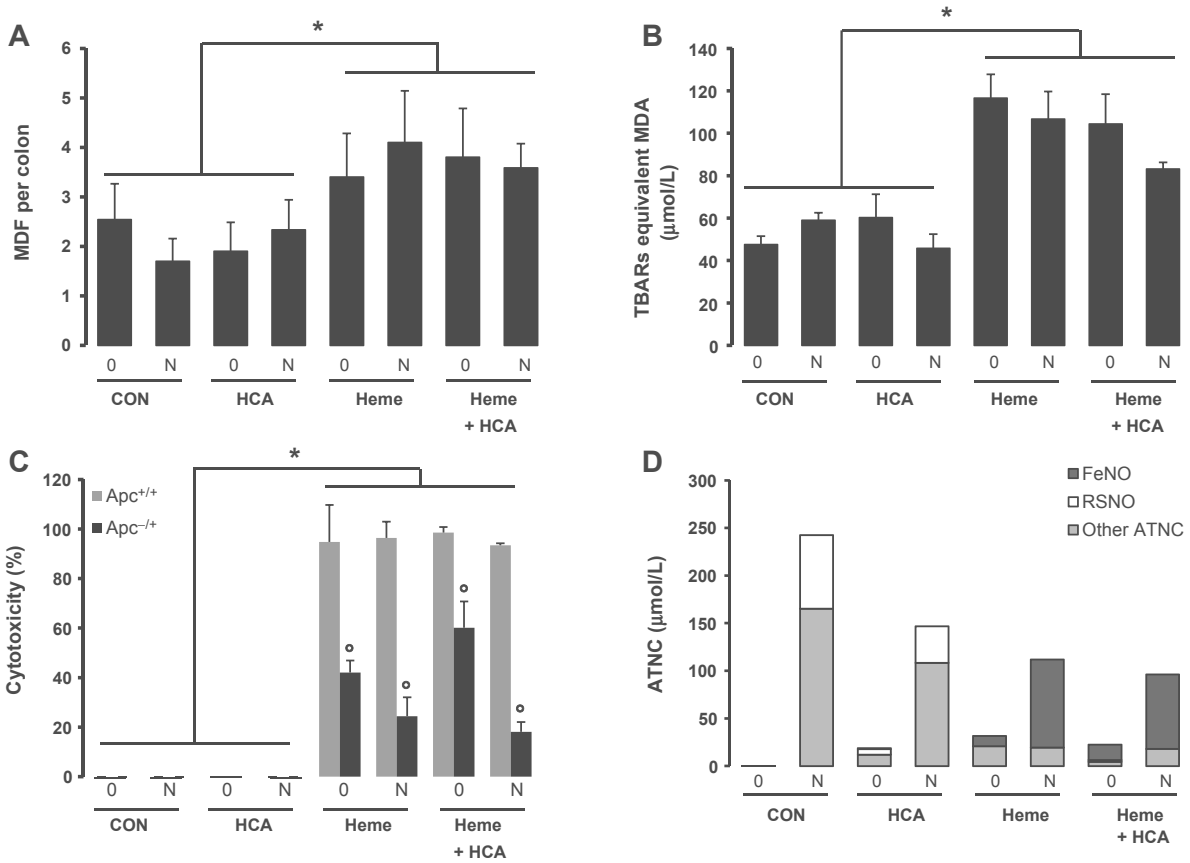

Figure 1.

Heme iron plays a major role in MDF formation in rats and is associated with fecal water lipid peroxidation biomarkers independent of the fecal concentration of ATNCs. A, the number of MDF per rat colon. A 3-factor ANOVA was used and showed only an effect of heme. B, lipid peroxidation in fecal water [measured as TBARs (MDA equivalents)]. C, fecal water cytotoxicity. The cytotoxic effects of fecal water from the 8 groups of rats on $Apc^{+/+}$ cells (gray bars) and on $Apc^{-/+}$ cells (black bars). Viability was measured by MTT assay after 24 hours of incubation with a 1:50 dilution of fecal water. D, ATNCs in fecal water shown as nitrosyl iron (FeNO), *S*-nitrosothiols (RSNO), and other ATNCs. TEM, control diet; HCA, diet with PhIP (50 μg/kg) and MeIQx (25 μg/kg); Heme, diet containing 1% hemoglobin; Heme + HCA, diet containing 1% hemoglobin, PhIP, and MeIQx: 50 + 25 μg/kg; 0, drinking water control; N, drinking water with nitrites and nitrates at 0.4 g/L. Values are means ± SEM, $n = 10$. *, significantly different from TEM and HCA, $P < 0.001$; °, significantly different from $Apc^{-/+}$ cells, $P < 0.01$.

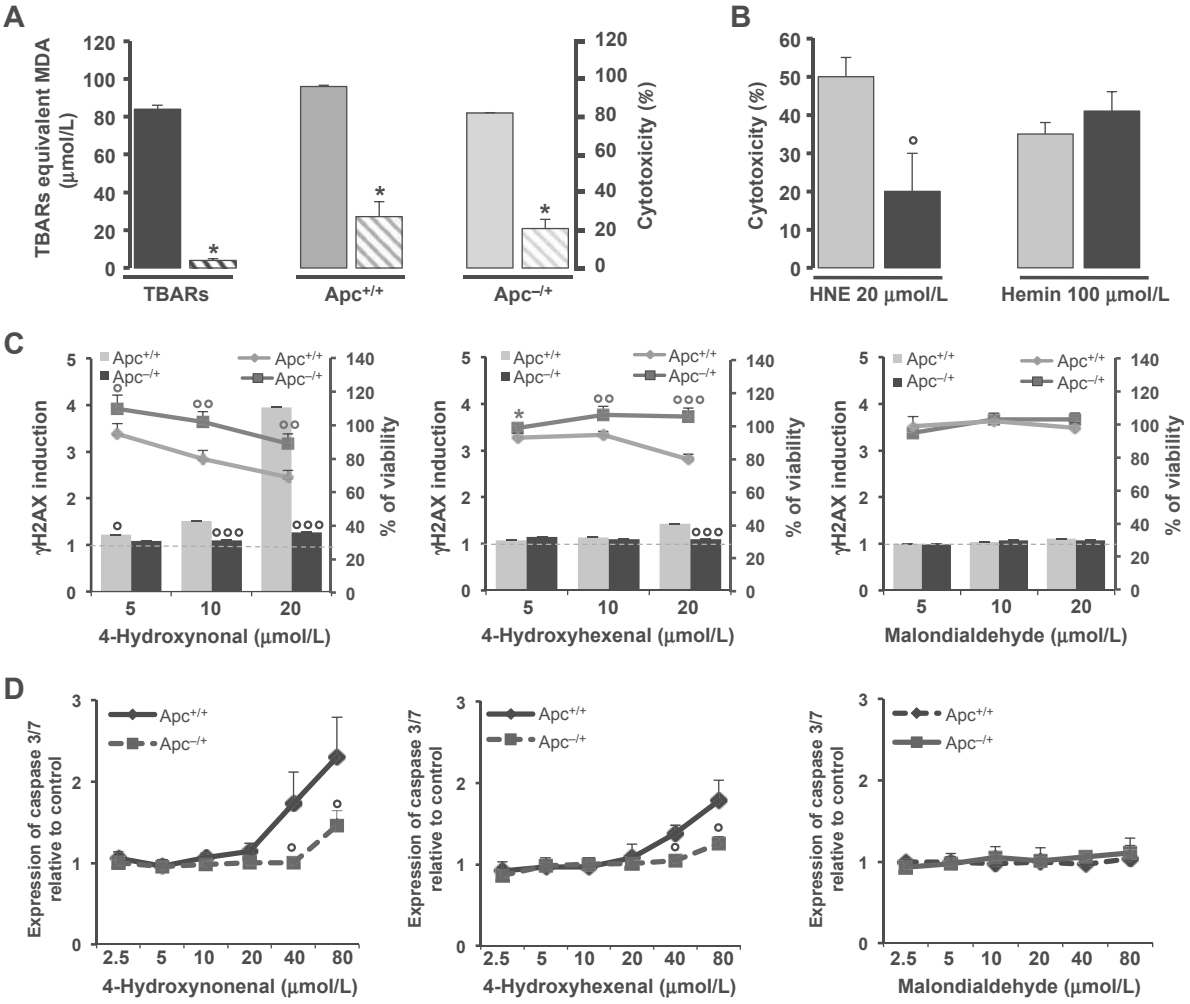

Figure 2.
The central role of aldehydes in the cytotoxic effect of fecal water of hemoglobin fed rats and the cytotoxic, genotoxic, and proapoptotic dose-dependent effects of HNE, HHE, and MDA in $Apc^{+/+}$ and $Apc^{-/+}$ cells. A, TBARS and cytotoxicity on $Apc^{+/+}$ and $Apc^{-/+}$ cells of fecal water of hemoglobin fed rats treated or not with trapping aldehydes resin. Solid bars, fecal water of hemoglobin group; hatched bars, fecal water of hemoglobin group treated with resin. Values are means ± SEM, $n = 3$. B, cytotoxicity on $Apc^{+/+}$ (gray bars) and $Apc^{-/+}$ (black bars) cells of HNE (20 µmol/L) and hemin (100 µmol/L). Values are means ± SEM, $n = 3$. C, genotoxic and cytotoxic effects of aldehydes on $Apc^{+/+}$ and $Apc^{-/+}$ cells. Values are means ± SEM, $n = 4$. D, proapoptotic dose-dependent effects of aldehydes on $Apc^{+/+}$ and $Apc^{-/+}$ cells. Values are means ± SEM, $n = 3$. *, significant difference between fecal water treated or not with resin using the Student t test (*, $P < 0.05$). °, significant difference between $Apc^{+/+}$ and $Apc^{-/+}$ using Student t test (°, $P < 0.05$; °°, $P < 0.01$; °°°, $P < 0.001$).

peroxidation was associated with a 75% reduction in cytotoxicity (Fig. 2A). Furthermore, we observed that only 4-HNE, but not heme, had differential cytotoxic effects in $Apc^{+/+}$ and $Apc^{-/+}$ cells that was similar to that observed with fecal water of rats fed heme (Fig. 2B).

We then measured the cytotoxic and genotoxic effects of 3 main lipid peroxidation end products (4-HNE, 4-HHE and MDA) on $Apc^{+/+}$ and $Apc^{-/+}$ cells using a γH2AX in-cell Western blot assay. HNE and HHE were more cytotoxic and more genotoxic to normal $Apc^{+/+}$ cells than to premalignant $Apc^{-/+}$ ones (Fig. 2C, $P < 0.05$). HNE at 10 and 20 µmol/L and HHE at 20 µmol/L were significantly more genotoxic to $Apc^{+/+}$ cells than to $Apc^{-/+}$ ones (Fig. 2C, $P < 0.05$). MDA was neither cytotoxic nor genotoxic in the tested cell lines (Fig. 2C). We confirmed these viability results with the MTT assay and with the CellTiter-Glo assay (Supplementary Fig. S4), and we used an expanded range of treatment concentrations (from 0 to 80 µmol/L) in these assays. We confirmed that HNE and HHE were more cytotoxic (from 10 to 80 µmol/L and from 40 to 80 µmol/L, respectively) to normal cells than to premalignant ones, whereas MDA had no effect (Supplementary Fig. S4).

We determined the caspase-3/7 activity and again found a significant difference between $Apc^{+/+}$ and $Apc^{-/+}$ cells after HNE and HHE treatment at 80 and 40 µmol/L, respectively

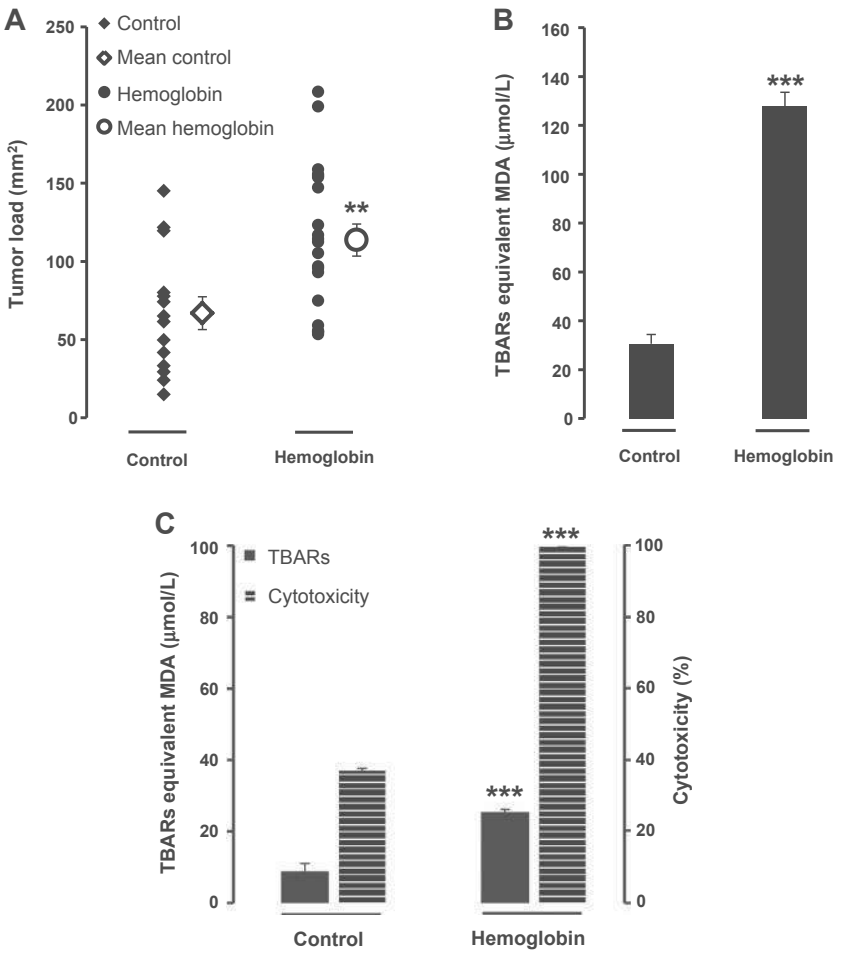

Figure 3.
The effect of hemoglobin on intestinal tumorigenesis in *Min* mice and changes in fecal and luminal biomarkers associated with this effect. A, intestinal tumor load (mm^2 per intestine). Values are means ± SEM, $n = 14$ for the control diet and $n = 21$ for the hemoglobin diet. B, lipid peroxidation in fecal water from feces [measured as TBARs (MDA equivalents)]. $n = 5$ for the control diet and $n = 7$ for the hemoglobin diet. C, cytotoxic activity and peroxidation in small intestine contents from mouse. Cytotoxicity was measured in the $Apc^{-/+}$ cell line (fecal water diluted 1:50, MTT assay). $n = 5$ for the control diet and $n = 7$ for the hemoglobin diet. ** and ***, significantly different from control diet (**, $P < 0.01$; ***, $P < 0.001$).

(Fig. 2D, $P < 0.05$). Specifically, caspase-3/7 activity was higher in $Apc^{+/+}$ cells than in $Apc^{-/+}$ cells, and MDA treatment had no effect (Fig. 2D).

Heme iron and tumoral promotion: hemoglobin increases intestinal tumorigenesis in $Apc^{Min/+}$ mice

A diet containing 2.5% hemoglobin given to $Apc^{Min/+}$ mice significantly increased the intestinal tumor load (control diet: 67 ± 39 mm^2; hemoglobin diet: 114 ± 47 mm^2, $P = 0.004$; Fig. 3A). These mice develop polyps mainly in the small intestine, and in our study, we did not observe any effects of hemoglobin diet in the colon. The hemoglobin diet also significantly increased the number of all tumors in the jejunum (Supplementary Fig. S5A). In the entire small intestine, the hemoglobin diet significantly increased the number of tumors with a diameter greater than 1 mm (1 mm < tumor size ≤ 2 mm, $P = 0.04$; 2 mm < tumor size, $P = 0.006$; Supplementary Fig. S5B). Giving the same hemoglobin diet to normal C57BL/6J $Apc^{+/+}$ mice induced no neoplasia. As observed in rats, the effect of dietary heme on mice tumors was associated with a significant increase in fecal heme (from 20 ± 22 to 198 ± 29 µmol/L) and with increases in lipoperoxidation biomarkers: fecal TBARS (Fig. 3B) and urinary DHN-MA (Supplementary Fig. S5C). We also assessed TBARS and the cytotoxicity of fecal water in the small intestine to measure biomarkers at the same location as tumors. As Min mice have a mutation in the *Apc* gene, we decided to use the mouse $Apc^{-/+}$ model to investigate the cytotoxic activity of fecal water *in vivo*. Heme diet was associated with a significant increase in fecal TBARS and cytotoxicity in the small intestine (Fig. 3C).

A heme diet is genotoxic *in vivo* in the epithelium of C57BL/6J $Apc^{+/+}$ mice

The induction of luminal lipid peroxidation by the hemoglobin diet (Fig. 3B and C) was associated with increased genotoxicity only in nonmutated C57BL/6J $Apc^{+/+}$ mice with a higher AB index in the epithelium (Fig. 4A and B). As expected the AB index was higher in C57BL/6J $Apc^{Min/+}$ mice than in C57BL/6J $Apc^{+/+}$ mice fed a control diet (Fig. 4A) because of the *Apc* mutation. In $Apc^{Min/+}$ mice, the hemoglobin diet had no additional genotoxic effect (Fig. 4A). The genotoxic effect of the hemoglobin diet in C57BL/6J $Apc^{+/+}$ was confirmed by γH2AX induction (Fig. 4C and D).

Discussion

This study examines *in vivo* the relative contributions of the 3 main factors that may explain how consumption of red and

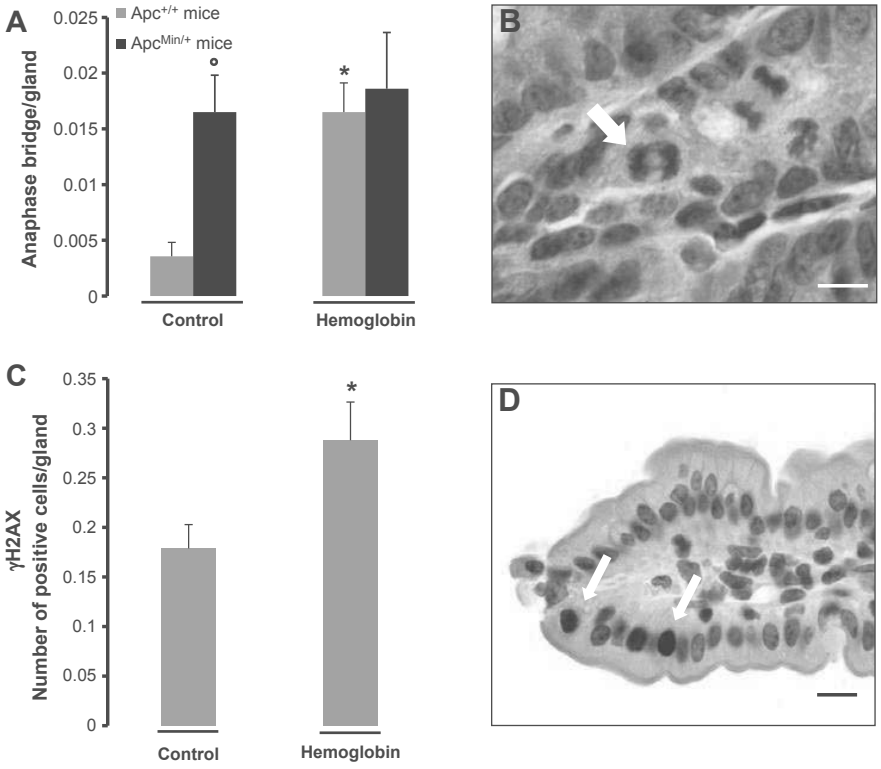

Figure 4.
The effect of a hemoglobin-containing diet on ABs and on the induction of γH2AX in the small intestinal epithelium in mice. A, the number of ABs per gland in $Apc^{Min/+}$ and $Apc^{+/+}$ mice after 50 days of the indicated experimental diet. *, significantly different from the control diet in the same genetic context; °, significantly different from $Apc^{+/+}$ mice on the same diet. B, an AB (arrow) in an $Apc^{+/+}$ mouse fed a hemoglobin diet. Scale bar, 2 μm. C, the number of γH2AX-positive cells per gland in C57BL/6J mice after 14 days on the experimental diet. D, γH2AX-positive cells (arrows) in $Apc^{+/+}$ mice fed the heme diet. Scale bar, 4 μm.

processed meat promotes colorectal cancer. Cross and colleagues showed that these factors, that is, heme, HCA, and NOC, were associated with colorectal cancer in a prospective cohort study in humans (15). However, the identification of risk factors using an epidemiologic approach has to be correlated with the experimental approach to establish the causative effect of such factors. Here, heme iron was the only experimental factor associated with a significant increase in precancerous lesions (MDF) in rats. Heme iron showed no additive or synergic effects with nitrates/nitrites or with HCA. Using a complementary approach that included 2 animal models and a cellular model, we found that heme is the determining factor in the promotion of colorectal carcinogenesis and that the selective toxicity of heme-induced alkenals to non-mutated cells seemed to play an important role in this mechanism.

HCA are complete carcinogens that induce colon, mammary, and prostate tumors in rodents and monkeys (30). The absence of effects of HCA in this study could be explained by the dose we chose, which was based on the estimated dietary exposure to HCA in a diet that is high in red meat and was relevant of the human food exposure. Indeed, carcinogenic doses of HCAs in rodents are 1,000 to 100,000 times higher than levels found in human foods (31). Nitrite undergoes an enterosalivary cycle in humans but not in rats. We hypothesized that the addition of sodium nitrates/nitrites to the rodents' drinking water, which mimics human saliva, would increase the effects of heme iron in rats by boosting nitrosation in the gut. In humans, red meat consumption increases fecal ATNC concentrations (11), as in our study with rats. Nevertheless, we could not detect any association between the ATNC level (Fig. 1D) and carcinogenesis (Fig. 1A). The highest level of ATNC was seen in the control group given nitrates/nitrites-supplemented water; this group had the fewest MDF. The lack of a relationship between ATNCs and the number of MDF does not support a strong role for ATNCs in the promotion of colon carcinogenesis by red meat.

The present results strongly suggest that at concentrations that are in line with human red meat consumption, heme iron is associated with the promotion of colon carcinogenesis at a preneoplastic stage. Most human colon cancers have an *Apc* mutation, as do MDF in humans and rats (32). To unravel the mechanisms, we used a cellular model that represented the colorectal cancer stages that we investigated *in vivo*. We chose a cellular model that mimicked the early steps of carcinogenesis. This conditionally immortalized intestinal cellular model uses premalignant $Apc^{-/+}$ cells derived from C57BL/6J $Apc^{Min/+}$ mice and "normal" $Apc^{+/+}$ cells from C57BL/6J mice (33). Characterization of both cell lines showed the expected consequences of *Apc* mutation, such as actin network disassembly, aneuploidy, and multinucleated cells (Supplementary Fig. S2). These cell lines can therefore be used to study the mechanisms involved in the early steps of colorectal cancer and thus comprise a cellular model that is a relevant complement to our *in vivo* model.

In rats, promotion of colon carcinogenesis by dietary hemoglobin was associated with changes in noninvasive biomarkers: fecal water heme iron, TBARS, and cytotoxic activity. Only the hemoglobin diet increased TBARS levels in fecal water (Fig. 1B).

We speculated that the cytotoxic effects of fecal water on normal and premalignant colonic cells *in vitro* mimic the *in vivo* situation with normal epithelium ($Apc^{+/+}$) and with *Apc*-mutated MDF. In this study, only fecal water from hemoglobin-fed rats was more cytotoxic to $Apc^{+/+}$ cells than to mutated cells (Fig. 1C). We propose that premalignant cell selection explains the heme-induced promotion of MDF. Aldehydes or heme iron itself, both present at high concentration in feces from hemoglobin-fed rats, might be responsible for this differential cytotoxicity. Using a resin to specifically trap fecal aldehydes, we showed that aldehydes alone are responsible for fecal water cytotoxicity. In addition, we observed that 4-HNE, but not heme iron, induced differential cytotoxicity in $Apc^{+/+}$ and $Apc^{-/+}$ cells similar to that observed with fecal water (Fig. 2B). Therefore, we propose that heme-induced lipid peroxidation in the gut explains the observed differential cytotoxicity and the colorectal cancer–promoting effects of heme that are observed *in vivo*.

To explore the link between aldehydes and the promotion of colon carcinogenesis, we tested the effects of 3 relevant aldehydes, 4-HNE, HHE, and MDA, in $Apc^{+/+}$ and $Apc^{-/+}$ cells. These α,β-unsaturated hydroxyalkenals are highly reactive compounds with proteins and nucleic acids (34), and they are potentially cytotoxic and genotoxic. In our cellular model, 4-HNE and HHE were more cytotoxic to normal cells than to premalignant cells and induced higher levels of apoptosis in normal cells than in premalignant cells. HNE was more cytotoxic than HHE, as reported previously (35). Furthermore, HNE, like HHE, was more genotoxic to normal cells than to premalignant ones (Fig. 2C), with a higher index of DNA double-strand breaks as revealed by the phosphorylation of histone H2AX. DNA double-strand breaks pose a critical hazard to the genome, and erroneous rejoining of DNA double-strand breaks can lead to mutation. These results thus suggest that at concentrations higher than 20 μmol/L, HNE and HHE will kill normal cells, whereas at lower concentration, they could create mutations in $Apc^{+/+}$ cells and might thus initiate carcinogenesis. Therefore, *Apc*-mutated cells are resistant to apoptosis and can survive to contact with cytotoxic and genotoxic aldehydes, which allows them to undergo further mutation and to become more malignant. Surprisingly, MDA was not toxic to the cells tested in this study but others found also that MDA had little or no toxicity in cells (35, 36). The results obtained by aldehyde trapping and *in vitro* with HNE and HHE confirmed our hypothesis that aldehydes are responsible for the differential cytotoxic effects of fecal water from heme-fed rats. Heme iron catalyzes the formation of aldehydes in the gastrointestinal tract, which would "select" premalignant cells and also increase the mutation frequency in normal cells (22).

This study shows that a hemoglobin-rich diet significantly increased the tumor load in the small intestine of $Apc^{Min/+}$ mice. In contrast, tumor load was not changed by heme diet in the colon of mice, despite the expected modulation of biochemical markers. The number of tumors in the colon of Min mice is low (<0.5 tumors per mouse), which reduces statistical power (37). These mice have a truncated *Apc* gene as in human familial adenomatous polyposis (FAP; ref. 38). Moreover, sporadic colorectal cancer tumors have the same early *Apc* mutation in 50% to 80% of cases (37). This mutation is also present in MDF (39). Our nutritional experiments in rats and mice were thus conducted in the defined genetic context of the *Apc* mutation. Promotion of carcinogenesis in rats and in $Apc^{Min/+}$ mice (Fig. 3A) was associated with 2 noninvasive biomarkers, fecal water TBARS and cytotoxic activity, in colon and in small intestine (Fig. 3B and C).

Furthermore, as we found that HNE is more genotoxic *in vitro* to wild-type cells than to $Apc^{-/+}$ cells (Fig. 2C), we decided to investigate the genotoxicity of dietary heme *in vivo* by measuring (i) the AB index in the epithelium of C57BL/6J $Apc^{+/+}$ mice and C57BL/6J $Apc^{Min/+}$ mice and (ii) by assessing γH2AX induction in the epithelium of C57BL/6J $Apc^{+/+}$ mice (Fig. 4). In these 2 studies, the induction of lipid peroxidation in the gut by heme (Fig. 3B and C) was associated with increased epithelial genotoxicity in $Apc^{+/+}$ mice but not in $Apc^{Min/+}$ mice. Together with *in vitro* data, these data show that dietary hemoglobin can induce DNA damage. We also observed ABs, which are biomarkers of chromosomal instability and a major consequence of *Apc* mutation. As expected, in mice fed the control diet, more ABs were seen in $Apc^{Min/+}$ mice than in $Apc^{+/+}$ mice (Fig. 4A). Moreover, the hemoglobin diet increased the AB index in $Apc^{+/+}$ mice (Fig. 4A). The hemoglobin diet induced the same number of ABs as the *Apc* mutation, suggesting that dietary hemoglobin generates strong initiators. Taken together, these data suggest that heme-induced aldehydes can induce mutations *in vitro* and *in vivo* and may initiate carcinogenesis.

In conclusion, we identified heme iron as the main factor responsible for the promotion of colorectal cancer by red meat and showed that aldehydes such as 4-HNE or HHE play roles in the underlying mechanism of action. Furthermore, we suggest that dietary heme could result in initiating agents in the gut. Improved dietary recommendations should focus (i) on the amount of heme iron in meat-based diets rather than on the modes of cooking or preparation and (ii) on dietary changes that could reduce the heme effect in the gut (i.e., on changes that limit the bioavailability of heme and of heme-induced peroxidation; ref. 40).

Disclosure of Potential Conflicts of Interest

No potential conflicts of interest were disclosed.

Disclaimer

The funders had no role in study design, data collection and analysis, the decision to publish, or preparation of the manuscript.

Authors' Contributions

Conception and design: N. Bastide, F. Chenni, R. Santarelli, S. Taché, D. Corpet, F. Pierre

Development of methodology: N. Bastide, R. Santarelli, S. Taché, N. Naud, M. Baradat, I. Jouanin

Acquisition of data (provided animals, acquired and managed patients, provided facilities, etc.): N. Bastide, M. Audebert, R. Santarelli, S. Taché, N. Naud, R. Surya, D.A. Hobbs, F. Gueraud

Analysis and interpretation of data (e.g., statistical analysis, biostatistics, computational analysis): N. Bastide, F. Chenni, M. Audebert, R. Santarelli, S. Taché, N. Naud, M. Baradat, R. Surya, D.A. Hobbs, G.G. Kuhnle, F. Gueraud, F. Pierre

Writing, review, and/or revision of the manuscript: N. Bastide, F. Chenni, M. Audebert, R. Santarelli, F. Gueraud, D. Corpet, F. Pierre

Administrative, technical, or material support (i.e., reporting or organizing data, constructing databases): F. Chenni, R. Santarelli, N. Naud, I. Jouanin, D.A. Hobbs, F. Pierre

Study supervision: F. Pierre

Other (histopathology): I. Raymond-Letron

Acknowledgments

The authors thank F. Blas-Y-Estrada for animal care, M.L. Jourdain for cell-cycle data, and J-Ph. Nougayrède for immunofluorescent microscopy.

Grant Support

This research was supported by grants from the French National Research Agency (ANR-06-PNRA-5E14 HemeCancer and ANR-10-ALIA-014 SecuriViande).

The costs of publication of this article were defrayed in part by the payment of page charges. This article must therefore be hereby marked *advertisement* in accordance with 18 U.S.C. Section 1734 solely to indicate this fact.

Received September 1, 2014; revised December 16, 2014; accepted December 16, 2014; published OnlineFirst January 15, 2015.

References

1. DeSantis CE, Lin CC, Mariotto AB, Siegel RL, Stein KD, Kramer JL, et al. Cancer treatment and survivorship statistics, 2014. CA Cancer J Clin 2014;64:252–71.
2. WCRF. Food, nutrition, physical activity, and the prevention of cancer: a global perspective. Washington DC: WCRF and American Institute for Cancer Research; 2007. p. 1–537.
3. WCRF. WCRF/AICR Systematic Literature Review Continuous Update Project Report: The associations between food, nutrition and physical activity and the risk of colorectal cancer. Washington DC: WCRF and American Institute for Cancer Research; 2010. p. 1–855.
4. Pierre FH, Santarelli RL, Allam O, Tache S, Naud N, Gueraud F, et al. Freeze-dried ham promotes azoxymethane-induced mucin-depleted foci and aberrant crypt foci in rat colon. Nutr Cancer 2010;62:567–73.
5. Pierre F, Freeman A, Tache S, Van der Meer R, Corpet DE. Beef meat and blood sausage promote the formation of azoxymethane-induced mucin-depleted foci and aberrant crypt foci in rat colons. J Nutr 2004;134:2711–6.
6. Corpet DE, Pierre F. Point: from animal models to prevention of colon cancer. systematic review of chemoprevention in min mice and choice of the model system. Cancer Epidemiol Biomarkers Prev 2003;12: 391–400.
7. Bastide NM, Pierre FH, Corpet DE. Heme iron from meat and risk of colorectal cancer: a meta-analysis and a review of the mechanisms involved. Cancer Prev Res (Phila) 2012;4:177–84.
8. Bingham SA, Hughes R, Cross AJ. Effect of white versus red meat on endogenous N-nitrosation in the human colon and further evidence of a dose response. J Nutr 2002;132:3522S–5S.
9. Sinha R, Knize MG, Salmon CP, Brown ED, Rhodes D, Felton JS, et al. Heterocyclic amine content of pork products cooked by different methods and to varying degrees of doneness. Food Chem Toxicol 1998;36:289–97.
10. Sesink ALA, Termont DSML, Kleibeuker JH, Vandermeer R. Red meat and colon cancer: the cytotoxic and hyperproliferative effects of dietary heme. Cancer Res 1999;59:5704–9.
11. Kuhnle GG, Story GW, Reda T, Mani AR, Moore KP, Lunn JC, et al. Diet-induced endogenous formation of nitroso compounds in the GI tract. Free Radic Biol Med 2007;43:1040–7.
12. Glei M, Klenow S, Sauer J, Wegewitz U, Richter K, Pool-Zobel BL. Hemoglobin and hemin induce DNA damage in human colon tumor cells HT29 clone 19A and in primary human colonocytes. Mutat Res 2006;594: 162–71.
13. Pierre FHF, Martin OCB, Santarelli R, Tache S, Naud N, Gueraud F, et al. Calcium and α-tocopherol suppress cured meat promotion of chemically-induced colon carcinogenesis in rats and reduce associated biomarkers in human volunteers. Am J Clin Nutr 2013;98:1255–62.
14. Santarelli RL, Naud N, Taché S, Guéraud F, Nassy G, Vendeuvre JL, et al. Calcium inhibits promotion by hot dog of 1-2-dimethylhydrazine-induced mucin-depleted foci in rat colon. Int J Cancer 2013;133:2533–41.
15. Cross AJ, Ferrucci LM, Risch A, Graubard BI, Ward MH, Park Y, et al. A large prospective study of meat consumption and colorectal cancer risk: an investigation of potential mechanisms underlying this association. Cancer Res 2010;70:2406–14.
16. Mirvish SS, Davis ME, Lisowyj MP, Gaikwad NW. Effect of feeding nitrite, ascorbate, hemin, and omeprazole on excretion of fecal total apparent N-nitroso compounds in mice. Chem Res Toxicol 2008;21:2344–51.
17. Caderni G, Femia AP, Giannini A, Favuzza A, Luceri C, Salvadori M, et al. Identification of mucin-depleted foci in the unsectioned colon of azoxymethane-treated rats: correlation with carcinogenesis. Cancer Res 2003; 63:2388–92.
18. Van den Berg JW, Koole-Lesuis R, Edixhoven-Bosdijk A, Brouwers N. Automating the quantification of heme in feces. Clin Chem 1988;34: 2125–6.
19. Ohkawa H, Ohishi N, Yagi K. Assay for lipid peroxides in animal tissues by thiobarbituric acid reaction. Anal Biochem 1979;95:351–8.
20. Pierre F, Santarelli R, Tache S, Gueraud F, Corpet DE. Beef meat promotion of dimethylhydrazine-induced colorectal carcinogenesis biomarkers is suppressed by dietary calcium. Br J Nutr 2008;99:1000–6.
21. Forest V, Pierre F, Bassonga E, Meflah K, Olivier C, Menanteau J. Apc+/min colonic epithelial cells express TNF receptors and ICAM-1 when they are co-cultured with large intestine intra-epithelial lymphocytes. Cell Immunol 2003;223:70–6.
22. Pierre F, Tache S, Guéraud F, Rerole AL, Jourdan ML, Petit C. Apc mutation induces resistance of colonic cells to lipoperoxide-triggered apoptosis induced by faecal water from haem-fed rats. Carcinogenesis 2007;28: 321–7.
23. Chandra A, Srivastava SK. A synthesis of 4-hydroxy-2-trans-nonenal and 4-(3H) 4-hydroxy-2-trans-nonenal. Lipids 1997;32:779–82.
24. Fenaille F, Mottier P, Turesky RJ, Ali S, Guy PA. Comparison of analytical techniques to quantify malondialdehyde in milk powders. J Chromatogr A 2001;921:237–45.
25. Rogakou EP, Pilch DR, Orr AH, Ivanova VS, Bonner WM. DNA double-stranded breaks induce histone H2AX phosphorylation on serine 139. J Biol Chem 1998;273:5858–68.
26. Khoury L, Zalko D, Audebert M. Validation of high-throughput genotoxicity assay screening using γH2AX in-cell western assay on HepG2 cells. Environ Mol Mutagen 2013;54:737–46.
27. Audebert M, Dolo L, Perdu E, Cravedi JP, Zalko D. Use of the gammaH2AX assay for assessing the genotoxicity of bisphenol A and bisphenol F in human cell lines. Arch Toxicol 2011;85:1463–73.
28. Graillot V, Takakura N, Hegarat LL, Fessard V, Audebert M, Cravedi JP. Genotoxicity of pesticide mixtures present in the diet of the French population. Environ Mol Mutagen 2012;53:173–84.
29. Montgomery E, Wilentz RE, Argani P, Fisher C, Hruban RH, Kern SE, et al. Analysis of anaphase figures in routine histologic sections distinguishes chromosomally unstable from chromosomally stable malignancies. Cancer Biol Ther 2003;2:248–52.
30. Sugimura T, Wakabayashi K, Nakagama H, Nagao M. Heterocyclic amines: Mutagens/carcinogens produced during cooking of meat and fish. Cancer Sci 2004;95:290–9.
31. Schwabn CE, Huber WW, Parzefall W, Hietsch G, Kassie F, SchulteHermann R, et al. Search for compoiunds that inhibit the genotoxic anc carcinogenic effects of heterocyclic aromatic amines. Crit Rev Toxicol 2000;30:1–69.
32. Femia AP, Giannini A, Fazi M, Tarquini E, Salvadori M, Roncucci L, et al. Identification of mucin depleted foci in the human colon. Cancer Prev Res (Phila) 2008;1:562–7.
33. Jamin EL, Riu A, Douki T, Debrauwer L, Cravedi JP, Zalko D, et al. Combined genotoxic effects of a polycyclic aromatic hydrocarbon (B(a) P) and an heterocyclic amine (PhIP) in relation to colorectal carcinogenesis. PLoS One 2013;8:e58591.
34. Schaur RJ. Basic aspects of the biochemical reactivity of 4-hydroxynonenal. Mol Aspects Med 2003;24:149–59.
35. Eckl PM, Ortner A, Esterbauer H. Genotoxic properties of 4-hydroxyalkenals and analogous aldehydes. Mutat Res 1993;290:183–92.
36. Fischer SM, Ogle S, Marnett LJ, Nesnow S, Slaga TJ. The lack of initiating and/or promoting activity of sodium malondialdehyde on SENCAR mouse skin. Cancer Lett 1983;19:61–6.

37. Corpet DE, Pierre F. How good are rodent models of carcinogenesis in predicting efficacy in humans? A systematic review and meta-analysis of colon chemoprevention in rats, mice and men. Eur J Cancer 2005;41:1911–22.
38. Su LK, Kinzler KW, Vogelstein B, Preisinger AC, Moser AR, Luongo C, et al. Multiple intestinal neoplasia caused by a mutation in the murine homolog of the APC gene. Science 1992;256:668–70.
39. Femia AP, Dolara P, Giannini A, Salvadori M, Biggeri A, Caderni G. Frequent mutation of Apc gene in rat colon tumors and mucin-depleted foci, preneoplastic lesions in experimental colon carcinogenesis. Cancer Res 2007;67:445–9.
40. Corpet DE. Red meat and colon cancer: should we become vegetarians, or can we make meat safer? Meat Sci 2011;89:310–6.

Article 3:

Red meat and colorectal cancer: 4-Hydroxy-2-nonenal (HNE) induces different apoptosis, autophagy and Nrf-2-related responses in normal and APC knockdown human colon epithelial cells

Surya *et al*. 2016. Manuscript to be submitted

In this study, we used human-origin experimental models HCECs (human colonic epithelial cells): CT and CTA cells to approach human physiology (Chapter 3.2). This study was directed to investigate whether *APC* invalidation in HCECs led to better detoxifying and survival ability upon exposure to HNE and fecal water of heme-fed rats. The main results obtained in this study are:

1) **CTA cells are more resistant to HNE and fecal water of heme-fed rats than CT cells**

   We observed that CTA cells exhibited lower level of apoptosis than CT cells upon exposure to HNE and fecal water of heme-fed rats, highlighting the better resistance of CTA cells to such an exposure. Following the exposure to HNE or fecal water of heme-fed rats, caspases activity appeared at a higher rate and higher final extent in CT cells than in CTA cells. By analyzing apoptosis end points such as nuclear fragmentation, cleavage of caspase-3 and PARP and cell membrane permeabilization after exposure to HNE or fecal water of heme-fed rats for 6 h, we observed higher level of apoptosis in CT cells than in CTA cells.

2) **Autophagy is involved in such a resistance.**

   CTA cells exhibited autophagy under basal conditions, shown by the formation of LC3 puncta and the lipidation of LC3-I. Following exposure to HNE and fecal water of heme-fed rats, CTA cells underwent autophagy at higher rate and extent than CT cells, probably as a defense mechanism against HNE and fecal water-induced apoptosis. To analyze the importance of autophagy in the resistance of CTA cells towards HNE or fecal water of heme-fed rats, we modulated autophagy in CT and CTA cells by using rapamycin or wortmannin to induce and inhibit autophagy respectively. Indeed, chemical inhibition of autophagy sensitized CTA cells to HNE

whereas chemical stimulation of autophagy improved the resistance of CT cells to HNE. These findings highlighted the potentially protective role of autophagy in CTA cells towards the toxicity of HNE and fecal water of heme-fed rats.

3) Nrf2, mediated by p62, is involved in such a resistance

Nrf2 was present at a higher basal activity in CTA cells than in CT cells and this led to higher expression of HNE detoxification enzymes (AKR1B1, AKR1B10 and GCLM) in CTA cells compared to CT cells. Basal Nrf2 activity in CTA cells was mediated by autophagic protein p62. We suggested that the higher p62 level in CTA cells would allow them to evacuate autophagy and activate Nrf2 more responsively than CT cells upon exposure to HNE or fecal water of heme-fed rats.

Prior to this study, the studies within the team using mouse-origin APC +/+ and APC Min/+ cells showed that *APC* mutation improved cell resistance towards HNE and fecal water of heme-fed rats (Article 1 and 2). In this study, we reported for the first time the extrapolation of cell resistance regarding *APC* invalidation to human cells. Taken together, our results revealed autophagy and Nrf2 as potential mechanisms underlying the resistance of CTA cells to the toxicity of HNE or fecal water of heme-fed rats. This study opens a perspective to modulate autophagy and Nrf2 responses during early colorectal carcinogenesis by improving the resistance of normal cells or sensitizing preneoplastic cells to the toxicity of HNE or fecal water of heme-fed rats.

Research Article

Red meat and colorectal cancer:

4-Hydroxy-2-nonenal (HNE) induces different apoptosis, autophagy and Nrf2-related responses in normal and Apc knockdown human colon epithelial cells

R Surya[1,2], J Dupuy[1,2], T Gauthier[1,2], O Martin[1,2], I Jouanin[1,2], N Naud[1,2], S Taché[1,2], Jerry W. Shay[3,4], FHF Pierre[1,2], L Huc[1,2*]

1- INRA; TOXALIM (Research Centre in Food Toxicology); 180 chemin de Tournefeuille, F-31027 Toulouse, France
2- Université de Toulouse III; INP; ENVT, UPS; TOXALIM; F-31027 Toulouse, France
3- Department of Cell Biology, The University of Texas Southwestern Medical Center, Dallas, TX, USA
4- Center for Excellence in Genomics Medicine Research, King Abdulaziz University, Jeddah, Saudi Arabia

* Corresponding author. E-mail: laurence.huc@toulouse.inra.fr

Abbreviations

3-MA : 3-methyladenine

AKR1B1 : Aldo-keto reductase family 1 member B1

AKR1B10 : Aldo-keto reductase family 1 member B10

Apc : Adenomatous polyposis coli

ARE : Antioxidant response element

BCL-2 : B-cell lymphoma 2

Bf : Beef

Caspase : Cysteine aspartate-specific protease

CDK4 : Cyclin-dependent kinase 4

CRC : Colorectal cancer

CypA : Cyclophilin A

DHN-MA : 1,4-dihydroxynonane mercapturic acid

GCLM : Glutamate-cysteine ligase, modifier subunit

Hb : Hemoglobin

HCEC : Human colon epithelial cell

HNE : 4-hydroxy-2-nonenal

HO-1 : Heme oxygenase 1

HPRT : Hypoxanthine-guanine phosphoribosyltransferase

Keap1 : Kelch-like ECH-associated protein 1

LC3 : Light chain 3

Nrf2 : Nuclear factor (erythroid derived 2)-like 2

PARP : Poly (ADP-ribose) polymerase 1

PI3K : Phosphoinositide 3-kinase

RPLP0 : Large ribosomal protein

Ser : Serine

TBARS : Thiobarbituric acid reactive species

Z-VAD-FMK : Benzyloxycarbonyl-Val-Ala-Asp (OMe) fluoromethylketone

Abstract

Red meat is a factor risk for colorectal cancer, considered as probably carcinogenic to human. Experimental studies explain the association between red meat and colorectal cancer by the oxidative properties of heme iron released in the colon. This latter is a potent catalyst for lipid peroxidation, resulting in the neoformation of cytotoxic aldehydes present in the fecal water of heme-fed rats, including 4-hydroxy-2-nonenal (HNE). In this study, we compared two isogenic non-transformed human colonic epithelial cell (HCEC) lines termed CT (normal HCECs) and CTA (HCECs with shRNA-mediated invalidation of *APC* gene, representing preneoplastic phenotype). This study demonstrates that HNE and fecal water of heme-fed rats preferentially induced apoptosis in CT cells than in CTA cells. CTA cells exerted autophagy at higher rate and extent than CT cells. Indeed, chemical inhibition of autophagy sensitized CTA cells to HNE whereas chemical stimulation of autophagy rendered CT cells more resistant to HNE, suggesting that autophagy would be a defense mechanism against HNE and fecal water-induced apoptosis. To further study the resistance of CTA cells to HNE and fecal water, we focused on Nrf2, known to be activated by HNE and promote the expression of HNE detoxification enzymes (AKR1B1, AKR1B10 and GCLM). Nrf2 was present at a higher basal activity in CTA cells than in CT cells and this activity was mediated by autophagic protein p62. The higher level of p62 in CTA cells also allowed them to evacuate autophagy and activate Nrf2 more responsively than CT cells. Taken together, our results suggest that different apoptosis, autophagy and Nrf2 responses may explain the different resistance of CT and CTA cells upon exposure to HNE or fecal water of heme-fed rats. This difference could explain the promoting effect of red meat on colorectal cancer, by initiating positive selection of cells with preneoplastic phenotypes.

Introduction

Colorectal cancer (CRC) is a major worldwide heath problem, being the third most commonly diagnosed cancer in the world and the fourth cause of cancer death worldwide. Although most of CRC cases occurred in the developed countries, the incidence rates have been rising in developing countries [1-3]. There was convincing evidence that diet and physical activity are risk factors for CRC development [4-6]. Concerning the diet, red meat consumption has been demonstrated to increase the risk of colorectal cancer with a relative risk of 1.17 (95% CI 1.05-1.31) per 100 g/day of red meat [7]. American Institute for Cancer Research (AICR) and World Cancer Research Fund (WCRF) proposed that red meat was a convincing cause of CRC and recommended limiting red meat consumption to 300 g/week [5]. Later, The International Agency for Research on Cancer (IARC) concluded in October 2015 that red meat is probably carcinogenic to humans (Group 2A) [8].

Several carcinogenic compounds that are present in or derived from red meat have been hypothesized as culprits for CRC development, such as heme iron present in the red meat, *N*-nitroso compounds that can be formed in the gastrointestinal tract by N-nitrosation or nitrosylation and heterocyclic amines that can be generated from cooking red meat at high temperature [9]. Our team previously examined *in vivo* the relative contribution of heme iron, *N*-nitroso compounds and heterocyclic amines in CRC development and we showed that heme iron was the only experimental factor associated with the promotion of colorectal carcinogenesis in rats and *Min* mice (harboring a mutation on adenomatous polyposis coli (*APC*) gene, a frequent and early event in human CRC development [10-12]) without any additive or synergic interaction with *N*-nitroso compounds or heterocyclic amines [13]. Furthermore, we showed that heme iron exerts its carcinogenic activity by catalyzing lipid

peroxidation in the lumen that results in the formation of cytotoxic and genotoxic aldehydes, one of which is 4-hydroxy-2-nonenal (HNE), a secondary product of linoleic and arachidonic acid oxidation [14-16]. In hemoglobin (Hb)- and beef (Bf)-fed rats, we observed a significant increase of fecal thiobarbituric acid reactive species (TBARS) and urinary 1,4-dihydroxynonane mercapturic acid (DHN-MA); metabolite of HNE), both are biomarkers of lipid peroxidation [17-19].

We previously assessed HNE toxicity *in vitro* in normal and preneoplastic immortalized mouse colon epithelial cells. Preneoplastic cells were derived from *Min* mice. Interestingly, preneoplastic cells appeared to be more resistant than normal cells upon exposure to HNE [19] and this phenomenon was also observed using fecal water of Hb- and Bf-fed rats [20]. Fecal water, a bioavailable aqueous extract of feces, hereby represents a complex biological matrix containing numerous neoformed substances in gastrointestinal tract including terminal aldehydes of lipid peroxidation such as malondialdehyde and HNE [21-23]. Recently, we showed that fecal aldehydes were in part responsible for the different resistance between normal and preneoplastic cells to fecal water of Hb- and Bf-fed rats, since the depletion of carbonyl compounds in this fecal water abolished the different toxicity of fecal water observed in normal and preneoplastic cells [20]. We thus suggested that heme iron intake yields lipid peroxidation-derived cytotoxic aldehydes that generate a positive selection of preneoplastic cells over normal cells, explaining the mechanism by which heme iron intake promotes CRC.

Nuclear factor (erythroid derived 2)-like 2 (Nrf2) is a transcription factor that regulates the expression of antioxidant enzymes (including those involved in HNE detoxification) through Nrf2-Keap1-ARE signaling pathway, thus exerting cytoprotective properties against oxidative stress [24]. HNE has been shown to activate Nrf2 and antioxidant genes expression [25]. Our previous study revealed that the resistance of preneoplastic cells upon exposure to fecal water

of Hb- and Bf-fed rats is due to higher basal Nrf2 activity in preneoplastic cells compared to normal cells, thus bestowing preneoplastic cells with higher level of basal HNE detoxification enzymes that protect them from HNE toxicity [20,26].

Autophagy (macroautophagy) is an intracellular degradation system that delivers cytoplasmic constituents to the lysosomes. It is mediated by the formation of autophagosomes that engulf a to-be-degraded portion of cytoplasm [27]. Autophagy is considered as a protective mechanism in response to stress. It allows the clearance and recycling of damaged proteins and organelles following the stress [28]. It has also been shown to block cellular apoptotic responses, thus favoring cell survival [29,30]. p62/SQSTM1 (sequestosome), a cargo receptor protein for autophagic degradation, is an Nrf2 target gene and can create a positive feedback loop for Nrf2 activation following its phosphorylation at Serine 351 (Ser 351) residue by TAK1 (transforming growth factor beta-activated kinase 1) [31]. Phosphorylated p62 at Ser 351 then binds to Keap1, the Nrf2 inhibitor, for further lysosomal degradation [32,33]. Indeed, autophagy was reported to be up-regulated during colorectal carcinogenesis and this up-regulation was linked to the increasing resistance of CRC cells towards chemotherapy intervention [34-37]. As autophagy may exert protective properties to cells, it could also be involved in the different resistance of normal and preneoplastic cells upon exposure to fecal water.

In this study, we analyzed the resistance of normal and Apc knockdown human colonic epithelial cells (HCECs) [38,39] upon exposure to HNE. These isogenic cell lines represent normal and preneoplastic phenotypes of human colon cells respectively, thereby allowing the studies on different cell resistance during early events in colorectal carcinogenesis. We consider that the use of human colon cancer cell lines is not pertinent to assess early colorectal carcinogenesis since their phenotypes represent advanced or late stages of colorectal carcinogenesis. Similar to our previous findings using normal and preneoplastic

mouse colon epithelial cells [19,20], Apc knockdown cells (termed CTA), which represent preneoplastic phenotype, appeared to be more resistant towards HNE toxicity compared to normal cells (termed CT) by exhibiting lower level of apoptosis. Exposure to fecal water of Hb- and Bf-fed rats showed the same phenomenon. This higher resistance of Apc knockdown cells was linked to their higher basal Nrf2 activity. Interestingly, we observed a higher level of autophagy in Apc knockdown cells following exposure to HNE and fecal water compared to normal cells. Indeed, chemical inhibition of autophagy in Apc knockdown cells sensitized them to HNE toxicity while chemical induction of autophagy in normal cells improved their resistance towards HNE toxicity. We suggest that Apc knockdown cells relied on autophagy as a protective mechanism against HNE and fecal water toxicity. Finally, we demonstrated that higher Nrf2 activity in Apc knockdown cells implicated autophagic protein p62. Thus, this study deciphered the plausible link among apoptosis, autophagy and Nrf2-related antioxidant responses in the early stages of CRC development.

Materials and Methods

Chemicals

All chemicals used in culture cell treatment were provided by Sigma Aldrich: Z-VAD-FMK (10 μM), staurosporin (1 μM), rapamycin (500 nM), wortmannin (1 mM), E64d (5 μg/mL) and pepstatin A (5 μg/mL). All chemicals were diluted in DMSO in stock solution (maximum DMSO dilution in final solution 1/1000).

Antibodies

For immunofluorescence analysis, primary and secondary fluorophore-labeled antibodies were diluted 1:100 and 1:200 respectively in PBS containing 0.1% Triton and 0.5% BSA. The primary antibodies used were anti-LC3A (Cell Signaling, rabbit) and anti-Nrf2-C20 (Santa

Cruz, rabbit). The secondary fluorophore-labeled antibody used was Alexa Fluor 488 donkey anti-rabbit IgG (Life Technologies).

For western blot analysis, primary and fluorescent secondary antibodies were diluted 1:1000 in TBS containg 3% BSA and 0.1% Tween. The primary antibodies used were anti-PARP (Cell Signaling, rabbit), anti-cleaved caspase-3 (Asp175) (Cell Signaling, rabbit), anti-BCL-2 (Cell Signaling, rabbit), anti-Beclin 1 (Cell Signaling, rabbit), anti-p62 (Santa Cruz, goat), anti-LC3A (Cell Signaling, rabbit), anti-Nrf2 (Cell Signaling, rabbit), anti-HO-1 (Santa Cruz, goat), anti-phosphorylated p62 (Ser351) (MBL, rabbit), anti-Keap1 (Santa Cruz, goat) and anti-β-actin (Santa Cruz, mouse). The fluorescent secondary antibodies used Pierce DyLight 700 donkey anti-rabbit IgG, Pierce DyLight 800 donkey anti-goat IgG and Pierce DyLight 800 donkey anti-mouse IgG (Thermo Scientific).

Cell culture

Immortalized non-transformed human colonic epithelial cells (HCECs) termed CT ("C" for *CDK4* and "T" for telomerase) were established and provided by Pr. Jerry W. Shay [39]. An isogenic cell line derived from CT (termed CTA, the additional "A" for *APC*) was obtained by shRNA-mediated downregulation of Apc [38]. Cells were cultured (approximate density $2.5x10^4$ cells/cm^2) on Primaria^{TM} flasks in a humidified atmosphere with 5% CO_2 at 37 °C, in 4:1 Dulbecco-modified Eagle medium (DMEM)/medium 199 supplemented with fetal bovine serum (FBS 2%), epidermal growth factor (EGF 20 ng/mL), hydrocortisone (1 mg/mL), insulin (10 mg/mL), transferrin (2 mg/mL), sodium selenite (5 nM) and gentamycin sulfate (50 μg/mL). All supplements for cell culture media were provided by Sigma-Aldrich. CTA cells were selected by puromycin (1 μg/mL). All treatments with HNE and fecal water were performed in complete medium without FBS to avoid any reaction between serum and fecal water or HNE.

HNE synthesis

HNE was synthesized as previously described [40]. Briefly, Grignard reaction between fumaraldehyde monoacetal and 1-pentylmagnesium bromide afforded HNE-dimethylacetal. HNE was obtained by acid hydrolysis.

Fecal samples

Feces used to generate the fecal water were obtained from two animal studies set up to explore respectively the effect of dietary hemoglobin [13] and beef on colorectal carcinogenesis (not published). Briefly, seven days following an injection with the carcinogen azoxymethane (Sigma Aldrich, 20 mg/kg body wt in NaCl (9 g/L)), F344 male rats were allowed free access to their respective diets for 100 days. In the first experiment, rats were fed with modified AIN (American Institute of Nutrition)-76 diet (low calcium with addition of 5% (v/w) safflower oil; control group) or with modified AIN-76 diet containing 1% (w/w) Hb (Hb-fed group) [13]. In the second experiment, rats were fed with modified AIN-76 diet (control group) or with 50% modified AIN-76 diet containing 50% raw beef sirloin. Feces were collected on the 88^{th} and 95^{th} day of experiment for Hb-fed and beef-fed rats respectively. The two studies resulted in four groups of collected feces: standard diet for Hb-fed rats (Control Hb), Hb-fed rats (Hb), standard diet for beef-fed rats (Control Bf) and beef-fed rats (Bf). All experiment protocols were approved by the Local Animal Care and Use Committee of Institut National de la Recherche Agronomique (TOXCOM), and were conducted in accordance with the European directive 2010/63/UE and ARRIVE guidelines.

Fecal water preparation

Fecal water was prepared as previously described [13]. Briefly, 2 g of feces was diluted in 5 mL of distilled water, ground and centrifuged. The supernatant was collected, diluted 20 times in complete medium without FBS and sterilized by microfiltration (pore size 0.2 µm).

Viability assay

Cell viability assay was done by using cell proliferation reagent WST-1 (Roche Life Science) according to manufacturer's protocol. Briefly, cells were seeded in 96-well microtiter plates. Following treatments with HNE or fecal water, cells were incubated in WST-1 reagent for 1 h in the dark. The absorbance of each well was measured by colorimetric at measurement and reference wavelengths of 440 nm and 690 nm respectively.

Apoptosis detection: nuclei fragmentation and caspase activation by time-lapse microscopy

For nuclei fragmentation assay, cells seeded in 24-well plates were incubated for 6 h of contact with HNE 40 µM and fecal water (dilution 20x) at 37 °C. Cells were then fixed in paraformaldehyde 4% and stained using fluorescent dye Hoechst 33342 (Life Technologies, 0.5 ng/mL in PBS). Apoptotic (fragmented and/or condensed) and alive nuclei were counted using fluorescence microscope (Evos fl digital inverted microscope, AMG) and expressed as percentage of total population (n>500 nuclei).

For time-lapse microscopy, cells seeded in Labtek 8-well chamber 1.5 borosilicate coverglass slides were incubated under confocal microscope Leica SP8 (with micro-incubator at 37 °C, 5% CO_2) with HNE 20 µM and fecal water (dilution 20x) containing Hoechst 33342 (5 µg/mL), CellEvent™ Caspase-3/7 Green Detection Reagent (Life Technologies, 2 µM) and TO-PRO®-3 Iodide (Life Technologies, 1 µM). Images were acquired using lasers 405, 488 and 638 nm under 20x magnification every 30 min for 12 h. Image analysis was performed using ImageJ software.

Immunofluorescence

Cells seeded on round coverslips (diameter 18 mm) in 12-well plates were incubated for 1 or 2 h of contact with HNE 20 µM or fecal water (dilution 20x) at 37 °C. Following saturation (PBS, 0.1% Triton, 0.5% BSA), each coverslip was incubated with primary antibodies directed against LC3A or Nrf2 (dilution 100x in PBS, 0.1% Triton, 0.5% BSA) for 1 h at room temperature. After washing with PBS, the cells were incubated with secondary fluorophore-labeled antibodies (Alexa Fluor 488 donkey anti-rabbit IgG, dilution 200x in PBS, 0.1% Triton, 0.5% BSA) for 1 h at room temperature. All cover slips were then sealed on microscope slides using anti-fading solution (Invitrogen Prolong Gold antifade reagent with DAPI). The slides were analyzed using confocal microscope Leica SP8 with lasers 488 nm (Alexa 488) and 405 nm (DAPI) under 63x oil immersion objective. The formation of LC3 puncta was observed and counted (n>50 nuclei). The colocalization of Nrf2 and nuclei was observed by using fluorescence intensity graphs presenting the intensity of blue (nuclei) and green (Nrf2) fluorescence detected along determined regions of interest (ROI). Nuclear localization of Nrf2 was deduced from blue and green fluorescence pattern. Image analyses were done using Leica LAS AF software.

RT-qPCR

Cells were incubated for 5 h of contact with HNE 40 µM at 37 °C. RNA was isolated using Tri Reagent (Eurogenetec) according to manufacturer's instructions. Two-step RT-qPCR was performed using HPRT (Hypoxanthine-guanine phosphoribosyltransferase), CypA (Cyclophilin A) and RPLP0 (Large ribosomal protein) as housekeeping genes. cDNA synthesis was done using the iScript cDNA Synthesis kit (Bio-Rad) with 1 µg RNA. Quantitative PCR was conducted using ViiA^{TM} 7 Real-Time PCR System (Life Technologies), with final reaction volume of 5 µL (1 µL cDNA, 1.5 µL primers and 2.5 µL

iQ SYBR Green Supermix (Bio-Rad)). Thermocycling conditions were set as following: initial denaturation at 95 °C (10 min), denaturation at 95 °C (15 s), annealing at 60 °C (30 s) and extension at 72 °C (30 s). The sequences of the primers (5' to 3') used are listed below: AKR1B1 (F-CCA ACT TCA ACC ATC TCC AGG TG, R-GTC ACC ACG ATG CCT TTG GAC T), AKR1B10 (F-GAG GAC CTG TTC ATC GTC AGC A, R-CGT CCA GAT AGC TCA GCT TCA G), GCLM (F-TCT TGC CTC CTG CTG TGT GAT G, R-TTG GAA ACT TGC TTC AGA AAG CAG), HPRT (F-CAT TAT GCT GAG GAT TTG GAA AGG, R-CTT GAG CAC ACA GAG GGC TAC A), CypA (F- CCC ACC GTG TTC TTC GAC AT, R-TGC TGT CTT TGG GAC CTT GTC T), RPLP0 (F-TGG TCA TCC AGC AGG TGT TCG A, R-ACA GAC ACT GGC AAC ATT GCG G).

Western blot

Western blot analysis was done as previously described [20,38]. Briefly, cells were incubated for 1 or 2 or 6 h with HNE 20 µM or fecal water (dilution 20x) at 37 °C, washed in ice-cold PBS, scrapped and pelleted by centrifugation. Cell pellets were then incubated in lysis buffer and homogenized by sonication. For the detection of nuclear Nrf2, whole cell lysates were fractionated using Nuclear Extraction kit (Active Motif) according to manufacturer's protocols. Western blot of nuclear extracts (10 µg) was performed by SDS-PAGE and blots were transferred to PVDF membranes by Trans Blot Turbo Transfer System (Bio-Rad). Membranes were then saturated and incubated with primary antibodies (dilution 1000x in TBS, 3% BSA, 0.1% Tween) at 4 ^{o}C for a night under agitation. Fluorescent secondary antibodies (dilution 1000x in TBS, 3% BSA, 0.1% Tween) were incubated for 1 h and membranes were revealed using Odyssey® CLx Li-Cor Infrared Imaging System at wavelengths of 700 and 800 nm.

Statistical analysis

The results (n≥3) were analyzed using software GraphPad Prism 4 for Windows. Different responses of treatments and genotype effect were analyzed by two-way ANOVA or student's *t*-test. When ANOVA showed a statistically significant effect ($p<0.05$), comparison among data was done using Tukey's HSD Post-hoc test.

Results

Apc knockdown HCECs exhibited lower apoptosis incidence compared to normal HCECs upon exposure to HNE and fecal water of Hb- and Bf-fed rats

To characterize cell death by apoptosis in HCECs, we analyzed caspase-3/7 activation, membrane permeabilization and cleavage of PARP (poly (ADP-ribose) polymerase 1) and caspase-3 (Figure 1A-C), according to the guidelines of apoptosis identification [41]. HNE induced apoptosis in a higher rate and extent in CT cells compared to in CTA cells (Figure 1A). This difference of apoptosis in CT and CTA cells was also observed upon exposure to fecal water of Hb- and Bf-fed rats, but not to fecal water of standard diet-fed rats.

The difference of apoptosis between CT and CTA cells following exposure to HNE and fecal water of Hb- and Bf-fed rats was most considerable at 6 h, the time at which the apoptosis rate in CT cells reached its peak, with approximately 50% of CT cells exhibiting caspase-3/7 activity. At this time, the amount of cells exhibiting caspase-3/7 activity and permeable membrane was significantly higher in CT cells compared to CTA cells (Figure 1B). Fecal water of standard diet-fed rats exerted relatively low caspase-3/7 activity and membrane permeabilization (< 20%) without any significant difference between CT and CTA cells.

Apoptosis is also characterized by cleavage of PARP and caspase-3. We observed this cleavage at a higher extent in CT cells than in CTA cells following 6 h exposure to HNE and fecal water of Hb- and Bf-fed rats (Figure 1C and Supplementary Figure 1). Staurosporin was

used as a positive control for apoptosis. The expression BCL-2 (B-cell lymphoma 2), an anti-apoptotic protein, was up-regulated in CT cells upon exposure to HNE and fecal water. However, BCL-2 was constantly present at a higher concentration in CTA cells than in CT cells both under basal conditions and upon exposure to HNE and fecal water (Figure 1C and Supplementary Figure 1).

Apc knockdown HCECs demonstrated higher autophagy levels compared to normal HCECs under basal conditions and upon exposure to HNE and fecal water of Hb- and Bf-fed rats

To characterize autophagy in HCECs, we performed immunofluorescence staining to investigate the formation of LC3 (Light chain 3) puncta in CT and CTA upon exposure to HNE (Figure 2A). LC3 is a protein that is involved in the formation of autophagosomes and the formation of LC3 puncta is correlated to the formation of autophagosomes. Here, we observed that CTA cells exhibited higher autophagy levels than CT cells under basal conditions. Prolonged HNE exposure induced autophagy in CT and CTA cells, but at a higher rate and extent in CTA cells (Figure 2B). To analyze the differential of autophagy in HCECs upon exposure to HNE and fecal water, we decided to choose the exposure time of 2 h since this was the longest incubation time at which the autophagy levels in CTA cells were superior to control while the autophagy levels in CT cells did not differ from the control. Indeed, following 2 h exposure to HNE and fecal water, we observed significantly higher number of LC3 puncta in CTA cells than in CT cells ($p<0.05$) (Figure 2A, 2C and Supplementary Figure 2A). Rapamycin was used as autophagy inducer whereas wortmannin was used as autophagy inhibitor.

We also verified the expression of several proteins involved in autophagy, such as Beclin-1, p62 and LC3. To halt protein-degrading autophagic flux by inhibiting lysosomal turnover, we used a mix of lysosomal inhibitors E64d and pepstatin A. The expression levels of Beclin-1

and p62 were constantly higher in CTA cells than in CT cells under basal conditions and upon exposure to fecal water (Figure 2D and Supplementary Figure 2B). In CT cells, different from the expression level of Beclin-1 that was relatively constant following the treatments, the expression level of p62 increased upon exposure to HNE and fecal water of Hb- and Bf-fed rats. Despite this increase, the expression level of p62 in CT cells remained lower than in CTA cells. The lipidation of LC3-I into LC3-II is also a characteristic of autophagy since LC3-II is a building block of autophagosomal membranes. Here, we observed higher ratio of LC3-II/LC3-I in CTA cells compared to CT cells under basal conditions and following exposure to HNE and fecal water when autophagy flux was blocked (Figure 2D and Supplementary Figure 2B), indicating higher autophagic activity in CTA cells compared to normal cells.

Chemical modulation of autophagy regulated the sensitivity of HCECs towards HNE

To study the effect of autophagy modulation on the resistance of HCECs towards HNE, we pretreated CT and CTA cells with rapamycin (autophagy inducer) or wortmannin (autophagy inhibitor) for 2 h before exposing them to HNE. At first, we used 3-methyladenine (3-MA), an inhibitor of phosphatidylinositol 3-kinases (PI3K), to inhibit autophagy in CT and CTA cells. However, at our surprise, this molecule appeared to induce autophagy instead of inhibiting it in our isogenic cell lines (Supplementary Figure 3A-B). The efficacy of rapamycin and wortmannin in inducing and inhibiting autophagy respectively was analyzed by the ratio of LC3-II/LC3-I (Figure 3A and Supplementary Figure 4A-B). Intervention of rapamycin in HNE-treated CT cells was evidenced to induce autophagy, shown by the increase of LC3-II/LC3-I ratio and this phenomenon was accompanied by the abolition of apoptosis, observed by the disappearance of cleaved PARP and cleaved caspase-3. On the contrary, incubating HNE-treated CTA cells with wortmannin nullified autophagy and induced apoptosis. Through the quantification of apoptotic nuclei, 3-MA, that appeared to

induce autophagy in CT and CTA cells, improved the resistance of CT cells towards HNE as observed in rapamycin-treated CT cells (Supplementary Figure 3C).

By monitoring caspase-3/7 activation by time-lapse microscopy, we observed that chemical induction of autophagy by rapamycin rendered CT cells more resistant to HNE toxicity whereas chemical inhibition of autophagy by wortmannin sensitized CTA cells to HNE toxicity to a level where no difference of apoptosis was observed between CT and CTA cells (Figure 3B-C). The same phenomenon was observed by apoptotic nuclei quantification (Figure 3D).

Chemical inhibition of apoptosis did not induce autophagy in HNE-treated Apc knockdown HCECs

To investigate whether apoptosis inhibition can modulate autophagy levels in HCECs, we treated HCECs with HNE in the presence of pan caspase inhibitor Z-VAD-FMK (benzyloxycarbonyl-Val-Ala-Asp (OMe) fluoromethylketone) to inhibit apoptosis. We observed that Z-VAD-FMK improved the viability of HNE-treated CT cells (Figure 4A). We also confirmed the efficacy of Z-VAD-FMK in inhibiting apoptosis in HNE-treated CT cells, shown by the reduction of apoptotic nuclei and the reduction of cleaved PARP and caspase-3 (Figure 4B-C and Supplementary Figure 5).

By observing the formation of LC3 puncta, we observed that chemical inhibition of apoptosis by Z-VAD-FMK in HNE-treated CTA cells abolished the formation of autophagosomes (Figure 4D). However, the presence of Z-VAD-FMK alone reduced the basal level of autophagy in CTA cells. In HNE-treated CT cells, no noticeable modulation of LC3 puncta formation was observed following incubation with Z-VAD-FMK.

Nrf2 was involved in the difference of resistance between normal and Apc knockdown HCECs towards HNE and fecal water toxicity

To analyze Nrf2 activation in HCECs upon exposure to HNE and fecal water, we investigated the nuclear localization of Nrf2. Since Nrf2 is a transcription factor, its nuclear localization reflects its activity. Figure 5A and Supplementary Figure 6A display the fluorescence intensity graphs representing the localization of Nrf2 (red channel) and the nuclei (blue channel) in CT and CTA cells under basal conditions and upon exposure to HNE and fecal water of Hb- and Bf-fed rats. Curcumin, a widely-known natural Nrf2 activator, was used as a positive control. Interestingly, Nrf2 was active in CTA cells under basal conditions, shown by its nuclear localization. In contrast, CT cells displayed less Nrf2 nuclear accumulation under basal conditions. Following 1 h exposure to HNE and fecal water of Hb- and Bf-fed rats, Nrf2 was active in CT and CTA cells. Despite Nrf2 activation following exposure to HNE and fecal water of Hb- and Bf-fed rats in CT cells, nuclear Nrf2 level in CT cells remained lower than in CTA cells which demonstrated relatively constant level of nuclear Nrf2 (Figure 5B and Supplementary Figure 6B). By analyzing the expression level of HO-1 (heme oxygenase 1), a canonical gene of Nrf2, we observed similar tendencies. Upon exposure to HNE and fecal water of Hb- and Bf-fed rats, HO-1 level was relatively constant in CTA cells but increased significantly in CT cells ($p<0.05$) (Figure 5B and Supplementary Figure 6B). Fecal water of standard diet-fed rats did not activate Nrf2 nor increase HO-1 level in CT cells. We also analyzed the expression of three Nrf2 target genes involved in HNE detoxification: aldo-keto reductase family 1 member B1 (AKR1B1), aldo-keto reductase family 1 member B10 (AKR1B10) and glutamate-cysteine ligase modifier subunit (GCLM). These genes were found to be more expressed in CTA cells than in CT cells under basal conditions (Figure 5C). Following exposure to HNE, the expression of these genes was up-regulated in CT cells.

Finally, to further investigate the mechanisms of Nrf2 activation by HNE and fecal water of Hb- and Bf-fed rats, we analyzed the expression of p62 (total and phosphorylated at Ser 351) and Keap1. In general, the level of p62 (total and phosphorylated) and Keap1 was higher in CTA cells than in CT cells under basal conditions (Figure 6A and Supplementary Figure 7A). Interestingly, basal autophagy in CTA cells under basal conditions (as previously shown in Figure 2A-D) was correlated with the degradation of p62 and Keap1, indicated by the increasing level of these proteins when autophagic flux was inhibited by E64d and pepstatin A. Upon exposure to HNE, the expression of p62 increased notably in CT cells, but the level of phosphorylated p62 remained relatively constant in CT and CTA cells. Keap1 was degraded by autophagy in CTA cells but not in CT cells following HNE exposure. However, the expression of Keap1 did not seem to be modulated by HNE in CT and CTA cells. The expression of Nrf2 increased following HNE exposure in CT cells but remained relatively constant and higher in CTA cells, independently on autophagic flux. By using fecal water of Hb- and Bf-fed rats, we observed similar findings regarding the expression level of total and phosphorylated p62 (Figure 6B and Supplementary Figure 7B). When the autophagic flux was blocked by E64d and pepstatin A, the increase of total p62 expression was observed only in CT cells and not in CTA cells upon exposure to fecal water of Hb- and Bf-fed rats. However, this increase of p62 in CT cells was not accompanied by the increase of p62 phosphorylation at Ser 351. Keap1 and Nrf2 were constantly present at higher amount in CTA cells than in CT cells upon exposure to fecal water. Nevertheless, we noticed an induction of Nrf2 expression in CT cells following exposure to fecal water of Hb- and Bf-fed rats.

Discussion

The aim of this study was to assess whether Apc down-regulation modulated the resistance of HCECs towards HNE and to understand the involved mechanisms. Here, we show that HNE

induced apoptosis preferentially in normal HCECs (termed CT) than in Apc knockdown HCECs (termed CTA) and this difference could at least be explained in part by higher cellular defense capacity in CTA cells through autophagy and Nrf2 activity. We also demonstrate that like HNE, fecal water of Hb- and Bf-fed rats exerted cell death rate in CT cells than in CTA cells.

Higher resistance of Apc knockdown HCECs towards the toxicity of HNE and fecal water of Hb- and Bf-fed rats may explain the mechanism of colorectal carcinogenesis

HNE is an important endproduct of n-6 fatty acid peroxidation by heme iron, both in terms of presence and toxicity [13]. Prior to this study, we evaluated the differential of resistance between mouse-origin normal and preneoplastic colon cells upon exposure to HNE. We demonstrated that preneoplastic cells were more resistant to HNE toxicity than normal cells [19] and we proposed that this positive selection of preneoplastic cells by HNE could be involved in the promotion of colorectal carcinogenesis. In this hypothesis, HNE applies a selective pressure in the colon that bottlenecks preneoplastic cells over normal cells, thus favoring cancer development.

In this study, to have a better approach of human physiology, we used two isogenic lines of immortalized HCECs: CT and CTA cells. The concentration of HNE used in this study (20 µM) was deduced from the TBARS level present in the feces of Bf-fed rats [(19.68±5.34) µM] [20] to mimic the global level of lipid peroxidation end products in feces. We exposed these cells to HNE 20 µM and found that CTA cells demonstrated a better resistance to HNE toxicity than CT cells by exhibiting less apoptotic properties such as caspase-3/7 activity, membrane permeabilization, DNA fragmentation and cleavage of PARP and caspase-3 (Figure 1A-C, Figure 3D and Supplementary Figure 1). These results were in accordance with

our previous finding using mouse-origin colon cells [19], highlighting the role of Apc dysregulation in rendering colon cells more resistant to HNE toxicity.

Fecal water of Hb- and Bf-fed rats, a complex matrix derived from luminal contents, is relevant for studying the effects of heme iron on luminal formation of aldehydes. We previously reported that Hb and Bf supplementation in rat diet increased drastically the TBARS and free HNE level in their fecal water ($p<0.05$) [20]. Like HNE, fecal water of Hb- and Bf-fed rats also induced higher apoptosis in mouse-origin normal cells compared to preneoplastic cells and this difference of toxicity was abolished when aldehydes were depleted from the fecal water [20]. In this study, by using human-origin cells, we verified that Apc invalidation improved the resistance of colon cells to HNE and fecal water of Hb- and Bf-fed rats, regardless of cells' origin. Taken together, our findings suggested that Hb and Bf supplementation in diet results in lipid peroxidation end products that provoke a positive selection of colon cells at early stages of carcinogenesis over the normal ones. Such phenomenon may favor the development of colorectal carcinogenesis that should be validated in animal models.

Autophagy potentially protects Apc knockdown HCECs from the toxicity of HNE and fecal water of Hb- and Bf-fed rats

Numerous studies have shown the oncogenic roles of autophagy in carcinogenesis by favoring cancer cell survival upon stress, nutrient deprivation and even apoptosis triggers, therefore protecting cancer cells [42-44]. In the case of CRC, autophagy is known as a classical mechanism by which cancer cells resist nutrient deprivation and chemotherapy intervention [36,37]. Chemical inhibition of autophagy has been shown to sensitize colon cancer cells to chemotherapy agent 5-fluorouracil [45]. Autophagy impairment through inhibition of autophagic protein ATG7 (autophagy-related gene 7) in human CRC epithelial cells prevented

tumor initiation and suppressed tumor growth [35]. Despite these convincing findings on the important role of autophagy in cancer cells, studies focusing on the role of autophagy in early stages of colorectal carcinogenesis are still lacking.

Here, we reported that CTA cells but not CT cells underwent autophagy under basal conditions, evidenced by the number of LC3 puncta and the lipidation of LC3-I (Figure 2A-C). We also would like to perform electronic microscopy to observe the formation of autophagosomes in CT and CTA cells to enhance our results regarding autophagy. CTA cells also expressed higher level of basal autophagic proteins such as p62 and Beclin-1 compared to CT cells (Figure 2D and Supplementary Figure 2A-B). We suggested that this advantage would enable CTA cells to be more responsive to undergo further autophagy following exposure to HNE and fecal water of Hb- and Bf-fed rats. Interestingly, autophagy in CTA cells was likely to be linked to their resistance towards HNE and fecal water of Hb- and Bf-fed rats. Several studies have revealed that apoptosis and autophagy inhibit each other mutually. While apoptosis kills cells, autophagy can allow a stress adaptation that avoids cell death (suppresses apoptosis) [46-48]. CT cells, which possessed lower level of basal autophagic proteins and exerted autophagy at a lower rate and extent compared to CTA cells, underwent higher apoptosis level upon exposure to HNE and fecal water of Hb- and Bf-fed rats (Figure 1A-C and Supplementary Figure 1).

To prove that autophagy was involved in the resistance of CTA cells towards HNE toxicity, we optimized chemical autophagy modulation in CT and CTA cells. Indeed, inhibiting autophagy in CTA cells by wortmannin sensitized them to HNE whereas stimulating autophagy in CT cells rendered them more resistant to HNE (Figure 3A-D and Supplementary Figure 4A-B). However, this interplay between apoptosis and autophagy was not reciprocal. Inhibiting apoptosis in HNE-treated CT and CTA cells by Z-VAD-FMK did not necessarily induce autophagy (Figure 4D). Even, the treatment with Z-VAD-FMK reduced the formation

of LC3 puncta in HNE-treated CTA cells. Interestingly, Z-VAD-FMK also lowered basal autophagy level in CTA cells. We are unfortunately unable to explain this inhibitory effect of Z-VAD-FMK on basal autophagy in CTA cells. In the literature, Z-VAD-FMK has previously been shown to induce non-apoptotic cell death including autophagy [49-52].

As previously mentioned, 3-MA, a PI3K inhibitor, induced autophagy in CT and CTA cells like rapamycin (Supplementary Figure 3A-B). This finding was surprising since 3-MA has been widely used to inhibit autophagy in numerous cell lines [53]. This phenomenon might be explained by the fact that 3-MA inhibits both PI3K Class I and PI3K Class III that have different effects on autophagy [54,55]. 3-MA inhibits transiently PI3K Class III that plays an important role in the nucleation of autophagosomes, thereby inhibiting autophagy. However, 3-MA also inhibits persistently PI3K Class I that in turn will inhibit autophagy negative regulator mTOR (mammalian target of rapamycin), thus inducing autophagy. This dual role of 3-MA might suggest that caution should be exercised in the application of 3-MA in studies on autophagy. In this study, we finally used wortmannin, another PI3K inhibitor, to inhibit autophagy in CT and CTA cells.

p62-dependent Nrf2 activity in Apc knockdown HCECs is involved in their resistance to HNE and fecal water of Hb- and Bf-fed rats

The Nrf2-dependent antioxidant pathway is one of the major cellular defense mechanisms against oxidative stress. Nrf2 is often associated with cancer development since it is often up regulated during carcinogenesis and contributes to the resistance of cancer cells to chemotherapy [56-58]. Recently, our team showed that Nrf2 was involved in the resistance of mouse-origin preneoplastic colon cells to HNE and fecal water of Hb- and Bf-fed rats [20]. Here, by using HCECs, we reported similar findings. Nrf2 was active under basal conditions in CTA cells but not in CT cells (Figure 5A-B and Supplementary Figure 6A-B). This

phenomenon led to higher expression of at least three enzymes involved in HNE detoxification: AKR1B1, AKR1B10 and GCLM [26] (Figure 5C). These enzymes have been shown to be regulated by Nrf2 [59-61]. Indeed, we previously reported that mouse-origin preneoplastic colon cells expressed higher level of HNE detoxification enzymes because of its higher Nrf2 level compared to normal cells [20]. In addition to HNE detoxification enzymes, BCL-2, an anti-apoptotic protein regulated by Nrf2 [62], was also more expressed in CTA cells than in CT cells (Figure 1C). Higher expression of these cytoprotective proteins in CTA cells would give them advantages to better tackle oxidative stress and other insults, thus enabling them to resist and survive. Following exposure to HNE and fecal water of Hb- and Bf-fed rats, Nrf2 was activated in CT cells, shown by its nuclear translocation and the increase of HNE detoxification proteins (Figure 5A-C and Supplementary Figure 6A-B). Despite this activation, nuclear Nrf2 was constantly present at a lower level in CT cells compared to CTA cells.

Several regulation mechanisms of Nrf2 activation have been studied and discussed. The most well-known canonical regulation of Nrf2 involves the disruption of Nrf2-Keap1 interaction. Keap1 is a member of an E3 ubiquitin ligase that constantly ubiquitinates Nrf2 for further degradation by proteasome. Oxidative stress or drug intervention can disrupt the link between Nrf2 and Keap1, leading to Nrf2 liberation and translocation into the nucleus to promote gene expression [24]. Lately, non-canonical mechanisms of Nrf2 regulation have been identified, including the involvement of autophagic protein p62 as a positive regulator of Nrf2. Phosphorylation of Ser 351 residue of p62 has been shown to increase the affinity between p62 and Keap1, which resulted in Nrf2 activation through sequestration of Keap1 onto the autophagosomes for lysosomal degradation [33]. Interestingly, p62 is also a target gene of Nrf2 [32]. Therefore, p62 can create a positive feedback loop for Nrf2 activation.

Under basal conditions, we observed higher expression of total and phosphorylated p62 (Ser 351) in CTA cells compared to CT cells (Figure 6A and Supplementary Figure 7A). Interestingly, in CTA cells, we observed an autophagic flux of total and phosphorylated p62, indicating that p62 was constantly degraded under basal conditions. Combined with the autophagic flux observed on Keap1, we concluded that Nrf2 activity in CTA cells under basal conditions was mediated by p62. To assess whether this phenomenon is linked to Nrf2 activation in CTA cells, we would perform western blotting of nuclear Nrf2 in function of autophagic flux. In CT cells, the level of phosphorylated p62 (Ser351) did not vary even upon exposure to HNE. However, the level of total p62 increased upon exposure to HNE. This phenomenon might be due to HNE-related Nrf2 activation in CT cells that promoted the expression of p62 as one of Nrf2 target genes.

Like HNE, fecal water of Hb- and Bf-fed rats induced total p62 expression in CT cells, but the level was always lower than in CTA cells (Figure 6B and Supplementary Figure 7B). Exposure to HNE and fecal water did not induce p62 phosphorylation (Ser351) in both CT and CTA cells, indicating that the p62/Nrf2 pathway was not the main mechanism of HNE-induced Nrf2 activation. This mechanism is more likely to be the canonical Nrf2/Keap1/ARE mechanism considering HNE ability to form protein adducts, including with cysteine residues of Keap1. Based on our findings, we proposed that the p62 galore in CTA cells enabled p62-mediated basal activation of Nrf2 and also provided free p62 for the cells to undergo autophagy as a defense mechanism upon insults. However, in CT cells, p62 was present in relatively low level. Therefore, to undergo autophagy following exposure to HNE or fecal water, CT cells had to express p62 till a sufficient amount, with the help of HNE-mediated Nrf2 activation that promoted p62 expression. Therefore, the cellular defense mechanism in CT cells appeared to be late compared to CTA cells. This might explain the mechanisms by which CTA cells were more resistant than CT cells to the toxicity of HNE and fecal water.

Finally, realizing the potential importance of p62 in basal Nrf2 activation in CTA cells, we would carry out siRNA-mediated p62 invalidation in CTA cells to assess whether this would sensitize them to the toxicity of HNE and fecal water.

References

1. Favoriti, P.*, et al.* (2016) Worldwide burden of colorectal cancer: a review. *Updates Surg*.
2. Torre, L.A.*, et al.* (2015) Global Cancer Incidence and Mortality Rates and Trends-An Update. *Cancer Epidemiol Biomarkers Prev*, **25**, 16-27.
3. Ferlay, J.*, et al.* (2010) Estimates of worldwide burden of cancer in 2008: GLOBOCAN 2008. *Int J Cancer*, **127**, 2893-917.
4. Watson, A.J.*, et al.* (2011) Colon cancer: a civilization disorder. *Dig Dis*, **29**, 222-8.
5. WCRF/AICR (2011) Continuous Update Project Report. Food, Nutrition, Physical Activity, and the Prevention of Colorectal Cancer. World Cancer Research Fund / American Institute for Cancer Research.
6. Giovannucci, E.*, et al.* (1995) Physical activity, obesity, and risk for colon cancer and adenoma in men. *Ann Intern Med*, **122**, 327-34.
7. Chan, D.S.*, et al.* (2011) Red and processed meat and colorectal cancer incidence: meta-analysis of prospective studies. *PLoS One*, **6**, e20456.
8. Bouvard, V.*, et al.* (2015) Carcinogenicity of consumption of red and processed meat. *Lancet Oncol*, **16**, 1599-600.
9. Santarelli, R.L.*, et al.* (2008) Processed meat and colorectal cancer: a review of epidemiologic and experimental evidence. *Nutr Cancer*, **60**, 131-44.
10. Nishisho, I.*, et al.* (1991) Mutations of chromosome 5q21 genes in FAP and colorectal cancer patients. *Science*, **253**, 665-9.
11. Markowitz, S.D.*, et al.* (2009) Molecular origins of cancer: Molecular basis of colorectal cancer. *N Engl J Med*, **361**, 2449-60.
12. Nakamura, Y.*, et al.* (1991) Mutations of the adenomatous polyposis coli gene in familial polyposis coli patients and sporadic colorectal tumors. *Princess Takamatsu Symp*, **22**, 285-92.
13. Bastide, N.*, et al.* (2015) A central role for heme iron in colon carcinogenesis associated with red meat intake. *Cancer Res*, **75**, 870-9
14. Gueraud, F.*, et al.* (2010) Chemistry and biochemistry of lipid peroxidation products. *Free Radic Res*, **44**, 1098-124.
15. Bastide, N.M.*, et al.* (2011) Heme iron from meat and risk of colorectal cancer: a meta-analysis and a review of the mechanisms involved. *Cancer Prev Res (Phila)*, **4**, 177-84.
16. Dalleau, S.*, et al.* (2013) Cell death and diseases related to oxidative stress: 4-hydroxynonenal (HNE) in the balance. *Cell Death Differ*, **20**, 1615-30.
17. Santarelli, R.L.*, et al.* (2010) Meat processing and colon carcinogenesis: cooked, nitrite-treated, and oxidized high-heme cured meat promotes mucin-depleted foci in rats. *Cancer Prev Res (Phila)*, **3**, 852-64.
18. Pierre, F.*, et al.* (2006) New marker of colon cancer risk associated with heme intake: 1,4-dihydroxynonane mercapturic acid. *Cancer Epidemiol Biomarkers Prev*, **15**, 2274-9.
19. Pierre, F.*, et al.* (2007) Apc mutation induces resistance of colonic cells to lipoperoxide-triggered apoptosis induced by faecal water from haem-fed rats. *Carcinogenesis*, **28**, 321-7.
20. Surya, R.*, et al.* (2016) Red meat and colorectal cancer: Nrf2-dependent antioxidant response contributes to the resistance of preneoplastic colon cells to fecal water of hemoglobin- and beef-fed rats. *Carcinogenesis*, **37**, 635-45.

21. Lapre, J.A*., et al.* (1992) Diet-induced increase of colonic bile acids stimulates lytic activity of fecal water and proliferation of colonic cells. *Carcinogenesis*, **13**, 41-4.
22. Glinghammar, B*., et al.* (1997) Shift from a dairy product-rich to a dairy product-free diet: influence on cytotoxicity and genotoxicity of fecal water--potential risk factors for colon cancer. *Am J Clin Nutr*, **66**, 1277-82.
23. Klinder, A*., et al.* (2007) Fecal water as a non-invasive biomarker in nutritional intervention: comparison of preparation methods and refinement of different endpoints. *Nutr Cancer*, **57**, 158-67.
24. Sporn, M.B*., et al.* (2012) NRF2 and cancer: the good, the bad and the importance of context. *Nat Rev Cancer*, **12**, 564-71.
25. Siow, R.C*., et al.* (2007) Modulation of antioxidant gene expression by 4-hydroxynonenal: atheroprotective role of the Nrf2/ARE transcription pathway. *Redox Rep*, **12**, 11-5.
26. Baradat, M*., et al.* (2011) 4-Hydroxy-2(E)-nonenal metabolism differs in Apc(+/+) cells and in Apc(Min/+) cells: it may explain colon cancer promotion by heme iron. *Chem Res Toxicol*, **24**, 1984-93.
27. Mizushima, N. (2007) Autophagy: process and function. *Genes Dev*, **21**, 2861-73.
28. Heymann, D. (2006) Autophagy: A protective mechanism in response to stress and inflammation. *Curr Opin Investig Drugs*, **7**, 443-50.
29. Marino, G*., et al.* (2014) Self-consumption: the interplay of autophagy and apoptosis. *Nat Rev Mol Cell Biol*, **15**, 81-94.
30. Boya, P*., et al.* (2005) Inhibition of macroautophagy triggers apoptosis. *Mol Cell Biol*, **25**, 1025-40.
31. Hashimoto, K*., et al.* (2016) TAK1 regulates the Nrf2 antioxidant system through modulating p62/ SQSTM1. *Antioxid Redox Signal*.
32. Jain, A*., et al.* (2010) p62/SQSTM1 is a target gene for transcription factor NRF2 and creates a positive feedback loop by inducing antioxidant response element-driven gene transcription. *J Biol Chem*, **285**, 22576-91.
33. Ichimura, Y*., et al.* (2013) Phosphorylation of p62 activates the Keap1-Nrf2 pathway during selective autophagy. *Mol Cell*, **51**, 618-31.
34. Burada, F*., et al.* (2015) Autophagy in colorectal cancer: An important switch from physiology to pathology. *World J Gastrointest Oncol*, **7**, 271-84.
35. Levy, J*., et al.* (2015) Intestinal inhibition of Atg7 prevents tumour initiation through a microbiome-influenced immune response and suppresses tumour growth. *Nat Cell Biol*, **17**, 1062-73.
36. Sato, K*., et al.* (2007) Autophagy is activated in colorectal cancer cells and contributes to the tolerance to nutrient deprivation. *Cancer Res*, **67**, 9677-84.
37. Sui, X*., et al.* (2013) Autophagy and chemotherapy resistance: a promising therapeutic target for cancer treatment. *Cell Death Dis*, **4**, e838.
38. Graillot, V*., et al.* (2016) Genotoxicity of Cytolethal Distending Toxin (CDT) on Isogenic Human Colorectal Cell Lines: Potential Promoting Effects for Colorectal Carcinogenesis. *Front Cell Infect Microbiol*, **6**, 34.
39. Roig, A.I*., et al.* (2010) Immortalized epithelial cells derived from human colon biopsies express stem cell markers and differentiate in vitro. *Gastroenterology*, **138**, 1012-21 e1-5.
40. Chandra, A*., et al.* (1997) A synthesis of 4-hydroxy-2-trans-nonenal and 4-(3H)-4-hydroxy-2-trans-nonenal. *Lipids*, **32**, 779-82.
41. Galluzzi, L*., et al.* (2009) Guidelines for the use and interpretation of assays for monitoring cell death in higher eukaryotes. *Cell Death Differ*, **16**, 1093-107.
42. Thorburn, A. (2014) Autophagy and its effects: making sense of double-edged swords. *PLoS Biol*, **12**, e1001967.
43. White, E. (2015) The role for autophagy in cancer. *J Clin Invest*, **125**, 42-6.
44. White, E*., et al.* (2015) Autophagy, Metabolism, and Cancer. *Clin Cancer Res*, **21**, 5037-46.

45. Li, J.*, et al.* (2009) Inhibition of autophagy by 3-MA enhances the effect of 5-FU-induced apoptosis in colon cancer cells. *Ann Surg Oncol*, **16**, 761-71.
46. Rubinstein, A.D.*, et al.* (2012) Life in the balance - a mechanistic view of the crosstalk between autophagy and apoptosis. *J Cell Sci*, **125**, 5259-68.
47. Maiuri, M.C.*, et al.* (2007) Self-eating and self-killing: crosstalk between autophagy and apoptosis. *Nat Rev Mol Cell Biol*, **8**, 741-52.
48. Gonzalez-Polo, R.A.*, et al.* (2005) The apoptosis/autophagy paradox: autophagic vacuolization before apoptotic death. *J Cell Sci*, **118**, 3091-102.
49. Herzog, C.*, et al.* (2012) zVAD-fmk prevents cisplatin-induced cleavage of autophagy proteins but impairs autophagic flux and worsens renal function. *Am J Physiol Renal Physiol*, **303**, F1239-50.
50. Martinet, W.*, et al.* (2006) Macrophages but not smooth muscle cells undergo benzyloxycarbonyl-Val-Ala-DL-Asp(O-Methyl)-fluoromethylketone-induced nonapoptotic cell death depending on receptor-interacting protein 1 expression: implications for the stabilization of macrophage-rich atherosclerotic plaques. *J Pharmacol Exp Ther*, **317**, 1356-64.
51. Martinet, W.*, et al.* (2006) z-VAD-fmk-induced non-apoptotic cell death of macrophages: possibilities and limitations for atherosclerotic plaque stabilization. *Autophagy*, **2**, 312-4.
52. Yu, L.*, et al.* (2004) Regulation of an ATG7-beclin 1 program of autophagic cell death by caspase-8. *Science*, **304**, 1500-2.
53. Klionsky, D.J.*, et al.* (2012) Guidelines for the use and interpretation of assays for monitoring autophagy. *Autophagy*, **8**, 445-544.
54. Jones, S.A.*, et al.* (2013) Autophagy and inflammatory diseases. *Immunol Cell Biol*, **91**, 250-8.
55. Wu, Y.T.*, et al.* (2010) Dual role of 3-methyladenine in modulation of autophagy via different temporal patterns of inhibition on class I and III phosphoinositide 3-kinase. *J Biol Chem*, **285**, 10850-61.
56. Wang, X.J.*, et al.* (2008) Nrf2 enhances resistance of cancer cells to chemotherapeutic drugs, the dark side of Nrf2. *Carcinogenesis*, **29**, 1235-43.
57. Lau, A.*, et al.* (2008) Dual roles of Nrf2 in cancer. *Pharmacol Res*, **58**, 262-70.
58. Jaramillo, M.C.*, et al.* (2013) The emerging role of the Nrf2-Keap1 signaling pathway in cancer. *Genes Dev*, **27**, 2179-91.
59. Jung, K.A.*, et al.* (2013) Identification of aldo-keto reductases as NRF2-target marker genes in human cells. *Toxicol Lett*, **218**, 39-49.
60. Nishinaka, T.*, et al.* (2011) Regulation of aldo-keto reductase AKR1B10 gene expression: involvement of transcription factor Nrf2. *Chem Biol Interact*, **191**, 185-91.
61. Jyrkkanen, H.K.*, et al.* (2008) Nrf2 regulates antioxidant gene expression evoked by oxidized phospholipids in endothelial cells and murine arteries in vivo. *Circ Res*, **103**, e1-9.
62. Niture, S.K.*, et al.* (2012) Nrf2 protein up-regulates antiapoptotic protein Bcl-2 and prevents cellular apoptosis. *J Biol Chem*, **287**, 9873-86.

Figure Legends

Figure 1. Apc knockdown HCECs (CTA) exhibited lower level of apoptosis compared to normal HCECs (CT) upon exposure to HNE or fecal water of Hb- and Bf-fed rats (Hb and Bf). Cells were treated with HNE 20 μM or fecal water. Control Hb and Control Bf (respective controls for Hb and Bf) were fecal water issued from standard diet-fed rats. (A) Percentage of cells exhibiting caspase-3/7 activity upon exposure to HNE or fecal water recorded over time. (B) Percentage of cells with positive caspase-3/7 activity and permeable membrane upon treatments with HNE or fecal water (t=6 h). (C) Western blotting analysis of apoptotic proteins cleaved PARP, cleaved caspase-3 and BCL-2 in HCECs following treatments with HNE or fecal water (t=6 h). Staurosporin was used as positive control for apoptosis. β-actin was used as loading control. The presented blots are representative of three independent experiments. The blot densitometry analysis is presented in Supplementary Figure 1. Data are expressed as mean ± SD (n=3).
* Significant difference between CT and CTA ($p<0.05$), student's *t*-test.
# Significant difference between a treatment in a cell line and control ($p<0.05$), two-way ANOVA, followed by Tukey's multiple comparison test.

Figure 2. Apc knockdown HCECs (CTA) exhibited higher level of autophagy compared to normal HCECs (CT) under basal conditions and upon exposure to HNE or fecal water of Hb- and Bf-fed rats (Hb and Bf). Cells were treated with HNE 20 μM or fecal water. Control Hb and Control Bf (respective controls for Hb and Bf) were fecal water issued from standard diet-fed rats. (A) Images of immunofluorescence analysis of HNE-treated cells (t=2 h). Blue channel indicates nuclei and green channel indicates LC3. The mix of E64d and pepstatin A was supplemented in the media to inhibit autophagic flux. Image extension showing cells treated with fecal water is presented in Supplementary Figure 2A. (B) Percentage of cells with LC3 puncta observed by immunofluorescence analysis upon exposure to HNE (t=1-6 h). (C) Percentage of cells with LC3 puncta observed by immunofluorescence analysis upon exposure to HNE or fecal water (t=2 h). Rapamycin and wortmannin were used as positive and negative controls of autophagy respectively. (D) Western blotting analysis of autophagic proteins Beclin1, p62, LC3-I and LC3-II in HCECs following treatments with HNE or fecal water (t=2 h). β-actin was used as loading control. The presented blots are representative of three independent experiments. The blot densitometry analysis is presented in Supplementary Figure 2B. Data are expressed as mean ± SD (n=3).
* Significant difference between CT and CTA ($p<0.05$), student's *t*-test.
# Significant difference between a treatment in a cell line and control ($p<0.05$), two-way ANOVA, followed by Tukey's multiple comparison test.

Figure 3. Chemical autophagy modulation in normal HCECs (CT) and Apc knockdown HCECs (CTA) regulated their resistance towards HNE. Cells were treated with HNE 20 μM, with or without the presence of rapamycin (RAP) or wortmannin (WOR) as positive or negative controls of autophagy respectively. (A) Western blotting analysis of LC3-I, LC3-II, cleaved PARP and cleaved caspase-3 in HCECs following treatments with HNE, with or without RAP or WORT (t=2 h). The mix of E64d and pepstatin A was used to inhibit autophagic flux. β-actin was used as loading control. The presented blots are representative of three independent experiments. The blot densitometry analysis is presented in Supplementary Figure 4A-B. (B) Percentage of cells exhibiting caspase-3/7 activity upon exposure to HNE, with or without RAP or WOR recorded over time. (C) Percentage of cells

with positive caspase-3/7 activity upon treatments with HNE, with or without RAP or WOR (t=6 h). (D) Percentage of cells exhibiting apoptotic nuclei (condensed or fragmented) upon exposure to HNE, with or without RAP or WOR (t=6 h). Data are expressed as mean ± SD (n=3).
* Significant difference between CT and CTA ($p<0.05$), student's *t*-test.
† Significant difference between a treatment in a cell line and treatment using HNE ($p<0.05$), two-way ANOVA, followed by Tukey's multiple comparison test.

Figure 4. Chemical apoptosis inhibition in normal HCECs (CT) and Apc knockdown HCECs (CTA) following HNE exposure did not induce autophagy. Cells were treated with HNE 20 µM or fecal water. Control Hb and Control Bf (respective controls for Hb and Bf) were fecal water issued from standard diet-fed rats. (A) Percentage of viable cells (WST-1 activity) upon exposure to HNE, with or without Z-VAD-FMK to inhibit apoptosis (t=6 h). Staurosporin was used as positive control for apoptosis. (B) Percentage of cells exhibiting apoptotic nuclei (condensed or fragmented) upon exposure to HNE, with or without Z-VAD-FMK (t=6 h). (C) Western blotting analysis of apoptotic proteins cleaved PARP and cleaved caspase-3 in HCECs following treatments with HNE, with or without Z-VAD-FMK (t=6 h). β-actin was used as loading control. The presented blots are representative of three independent experiments. The blot densitometry is presented in Supplementary Figure 5. (D) Images of immunofluorescence analysis and quantification of cells with LC3 puncta upon exposure to HNE, with or without Z-VAD-FMK (t=2 h). Blue channels indicate nuclei and green channels indicate LC3. The mix of E64d and pepstatin A was supplemented in the media to inhibit autophagic flux. Rapamycin was used as positive control for autophagy. Data are expressed as mean ± SD (n=3).
* Significant difference between CT and CTA ($p<0.05$), student's *t*-test.
# Significant difference between a treatment in a cell line and control ($p<0.05$), two-way ANOVA, followed by Tukey's multiple comparison test.
† Significant difference between a treatment in a cell line and treatment using HNE ($p<0.05$), two-way ANOVA, followed by Tukey's multiple comparison test.

Figure 5. Different Nrf2 activity in normal HCECs (CT) and Apc knockdown HCECs (CTA) contributed to their different resistance following exposure to HNE and fecal water of Hb- and Bf-fed rats (Hb and Bf respectively). Cells were treated with HNE 20 µM. (A) Images of immunofluorescence analysis of HNE-treated cells (t=1 h). Blue channels indicate nuclei and red channels indicate Nrf2. The fluorescence intensity graphs represent the colocalization of blue signal (nuclei) and red signal (Nrf2) along regions of interest (ROI). Image extension showing cells treated with fecal water is presented in Supplementary Figure 6A. (B) Western blotting analysis of Nrf2 (nuclear) and HO1 (total lysate) in HCECs following treatments with HNE and fecal water (t=1 h). Curcumin was used as positive control for Nrf2 activation. The blot densitometry analysis is presented in Supplementary Figure 6B. (C) Relative mRNA expression of HNE detoxification proteins AKR1B1 (Aldo-keto reductase Family 1 Member B1), AKR1B10 (Aldo-keto reductase Family 1 Member B10) and GCLM (Glutamate-cysteine ligase, modifier subunit) in HCECs following exposure to HNE (t=5 h). Data are expressed as mean ± SD (n=6).
* Significant difference between CT and CTA ($p<0.05$), student's *t*-test.
# Significant difference between a treatment in a cell line and control ($p<0.05$), student's *t*-test.

Figure 6. Different Nrf2 activity in normal HCECs (CT) and Apc knockdown HCECs (CTA) was associated to their different level of p62 expression and phosphorylation. Cells were treated with HNE 20 μM or fecal water. Control Hb and Control Bf (respective controls for Hb and Bf) were fecal water issued from standard diet-fed rats. Curcumin was used as positive control for Nrf2 activation. (A) Western blotting analysis of phosphorylated p62 (p62-P Ser 351), total p62 and Keap1 in HCECs following treatments with HNE, with or without the mix of E64d and pepstatin A to inhibit autophagic flux (t=2 h). (B) Western blotting analysis of phosphorylated p62 (p62-P Ser 351) and total p62 in HCECs following treatments with HNE or fecal water in the presence of E64d and pepstatin A to inhibit autophagic flux (t=2 h). In all blots, β-actin was used as loading control. All presented blots are representative of three independent experiments. The blot densitometry analysis is presented in Supplementary Figure 7A-B.

Supplementary Figure 1. Densitometry analysis of Figure 1C showing western blotting analysis of apoptotic proteins cleaved PARP, cleaved caspase-3 and BCL-2 in HCECs following treatments with HNE or fecal water (t=6 h). All band densities were reported to β-actin as loading control. Staurosporin was used as positive control for apoptosis. Data are expressed as mean ± SD (n=3).
* Significant difference between CT and CTA ($p<0.05$), student's *t*-test.
# Significant difference between a treatment in a cell line and control ($p<0.05$), two-way ANOVA, followed by Tukey's multiple comparison test.

Supplementary Figure 2. (A) Extension of Figure 2A. Images of immunofluorescence analysis of normal HCECs (CT) and Apc knockdown HCECs (CTA) treated with fecal water of Hb- and Bf-fed rats (Hb and Bf respectively) (t=2 h). Blue channels indicate nuclei and green channels indicate LC3. The mix of E64d and pepstatin A was supplemented in the media to inhibit autophagic flux. (B) Densitometry analysis of Figure 2D showing western blotting analysis of autophagic proteins Beclin1, p62, LC3-I and LC3-II in HCECs following treatments with HNE or fecal water, with or without the mix of E64d and pepstatin A to inhibit autophagic flux (t=2 h). All band densities were reported to β-actin as loading control. Rapamycin was used as positive control for autophagy. Data are expressed as mean ± SD (n=3).
* Significant difference between CT and CTA ($p<0.05$), student's *t*-test.
# Significant difference between a treatment in a cell line and control ($p<0.05$), two-way ANOVA, followed by Tukey's multiple comparison test.
• Significant difference between a treatment in a cell line with and without E64d/pepstatin A ($p<0.05$), two-way ANOVA, followed by Tukey's multiple comparison test.

Supplementary Figure 3. (A) Images of immunofluorescence analysis of cells treated with 3-methyladenine (3-MA) (t=2 h). Rapamycin was used as positive control for autophagy. Blue channels indicate nuclei and green channels indicate LC3. The mix of E64d and pepstatin A was supplemented in the media to inhibit autophagic flux. (B) Percentage of cells with LC3 puncta observed by immunofluorescence analysis upon exposure to 3-MA or rapamycin (t=2 h). (C) Percentage of cells exhibiting apoptotic nuclei (condensed or fragmented) upon exposure to HNE, with or without 3-MA or rapamycin (t=6 h). Data are expressed as mean ± SD (n=3).
* Significant difference between CT and CTA ($p<0.05$), student's *t*-test.
# Significant difference between a treatment in a cell line and control ($p<0.05$), two-way ANOVA, followed by Tukey's multiple comparison test.

Supplementary Figure 4. Densitometry analysis of Figure 3A showing western blotting analysis of LC3-I, LC3-II, cleaved PARP and cleaved caspase-3 in HCECs following treatments with HNE, with or without (A) rapamycin or (B) wortmannin (t=2 h). All band densities were reported to β-actin as loading control. The mix of E64d and pepstatin A was used to inhibit autophagic flux. Data are expressed as mean ± SD (n=3).
* Significant difference between CT and CTA ($p<0.05$), student's *t*-test.
# Significant difference between a treatment in a cell line and control ($p<0.05$), two-way ANOVA, followed by Tukey's multiple comparison test.
• Significant difference between a treatment in a cell line with and without E64d/pepstatin A ($p<0.05$), two-way ANOVA, followed by Tukey's multiple comparison test.
α Significant difference between a treatment in a cell line with and without rapamycin ($p<0.05$), two-way ANOVA, followed by Tukey's multiple comparison test.
β Significant difference between a treatment in a cell line with and without wortmannin ($p<0.05$), two-way ANOVA, followed by Tukey's multiple comparison test.

Supplementary Figure 5. Densitometry analysis of Figure 4C showing western blotting analysis of cleaved PARP and cleaved caspase-3 in HCECs following treatments with HNE, with or without Z-VAD-FMK to inhibit apoptosis (t=6 h). All band densities were reported to β-actin as loading control. Data are expressed as mean ± SD (n=3).
* Significant difference between CT and CTA ($p<0.05$), student's *t*-test.
γ Significant difference between a treatment in a cell line with and without Z-VAD-FMK ($p<0.05$), two-way ANOVA, followed by Tukey's multiple comparison test.

Supplementary Figure 6. (A) Extension of Figure 5A. Images of immunofluorescence analysis of normal HCECs (CT) and Apc knockdown HCECs (CTA) treated with fecal water of Hb- and Bf-fed rats (Hb and Bf respectively) (t=1 h). Blue channels indicate nuclei and red channels indicate Nrf2. The fluorescence intensity graphs represent the colocalization of blue signal (nuclei) and red signal (Nrf2) along regions of interest (ROI). (B) Densitometry analysis of Figure 5B showing western blotting analysis of Nrf2 (nuclear) and HO1 (total lysate) in HCECs following treatments with HNE or fecal water (t=1 h). Curcumin was used as positive control for Nrf2 activation. Data are expressed as mean ± SD (n=3).
* Significant difference between CT and CTA ($p<0.05$), student's *t*-test.
# Significant difference between a treatment in a cell line and control ($p<0.05$), two-way ANOVA, followed by Tukey's multiple comparison test.

Supplementary Figure 7. (A) Densitometry analysis of Figure 6A showing western blotting analysis of phosphorylated p62 (p62-P Ser 351), total p62 and Keap1 in HCECs following treatments with HNE, with or without the mix of E64d and pepstatin A to inhibit autophagic flux (t=2 h). (D) Densitometry analysis of Figure 6B showing western blotting analysis of phosphorylated p62 (p62-P Ser 351) and total p62 in HCECs following treatments with HNE or fecal water in the presence of E64d and pepstatin A to inhibit autophagic flux (t=2 h). All band densities were reported to β-actin as loading control. Data are expressed as mean ± SD (n=3).
* Significant difference between CT and CTA ($p<0.05$), student's *t*-test.
# Significant difference between a treatment in a cell line and control ($p<0.05$), two-way ANOVA, followed by Tukey's multiple comparison test.
• Significant difference between a treatment in a cell line with and without E64d/pepstatin A ($p<0.05$), two-way ANOVA, followed by Tukey's multiple comparison test.

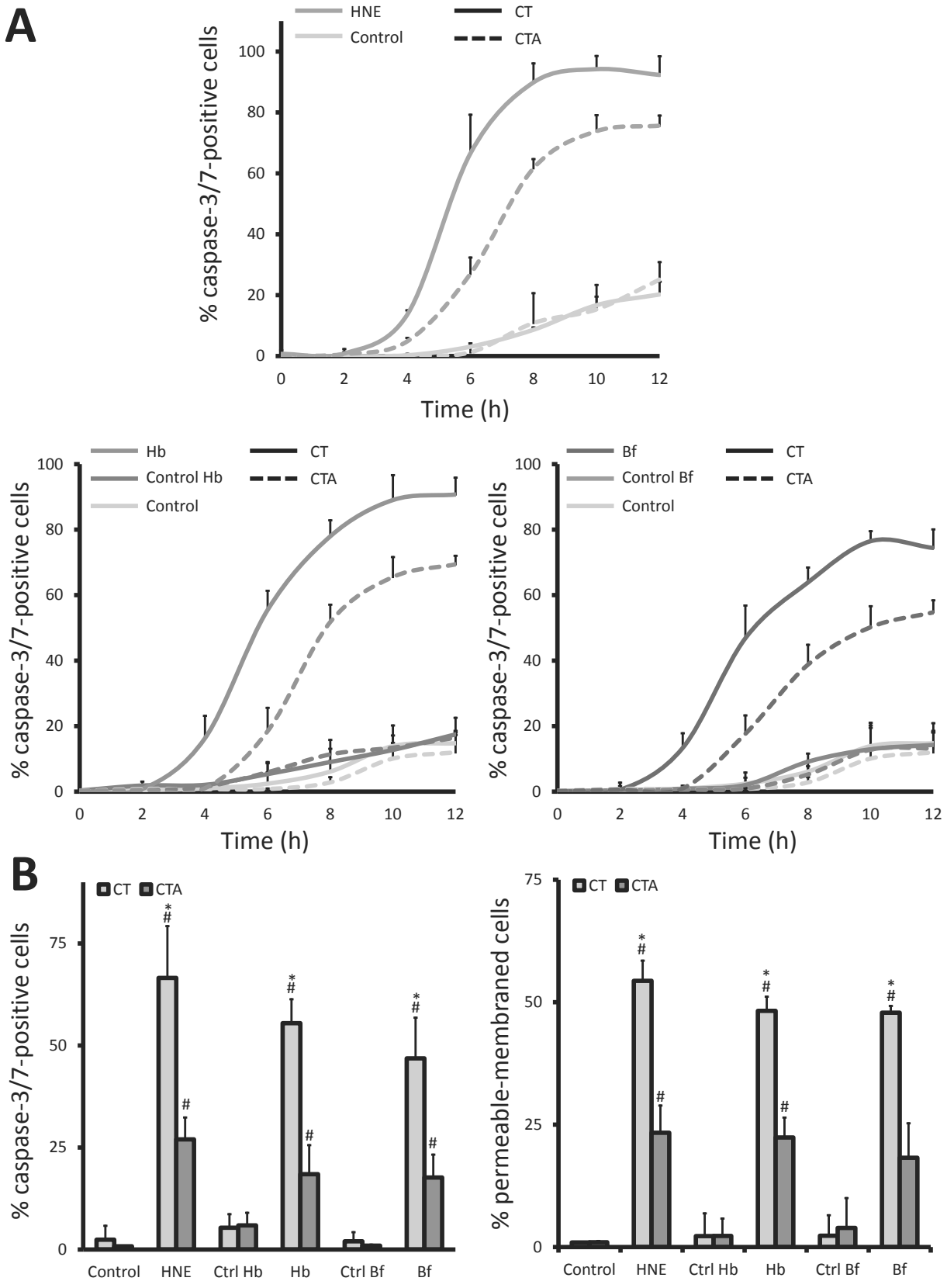
A
HNE
Control
CT
CTA
% caspase-3/7-positive cells
Time (h)
Hb
Control Hb
Control
Bf
Control Bf
B
% caspase-3/7-positive cells
% permeable-membraned cells
Control
HNE
Ctrl Hb
Hb
Ctrl Bf
Bf
C
CT
CTA
Staurosporin
PARP (116 kDa)
Cleaved PARP (89 kDa)
Cleaved caspase-3
BCL-2
B-actin

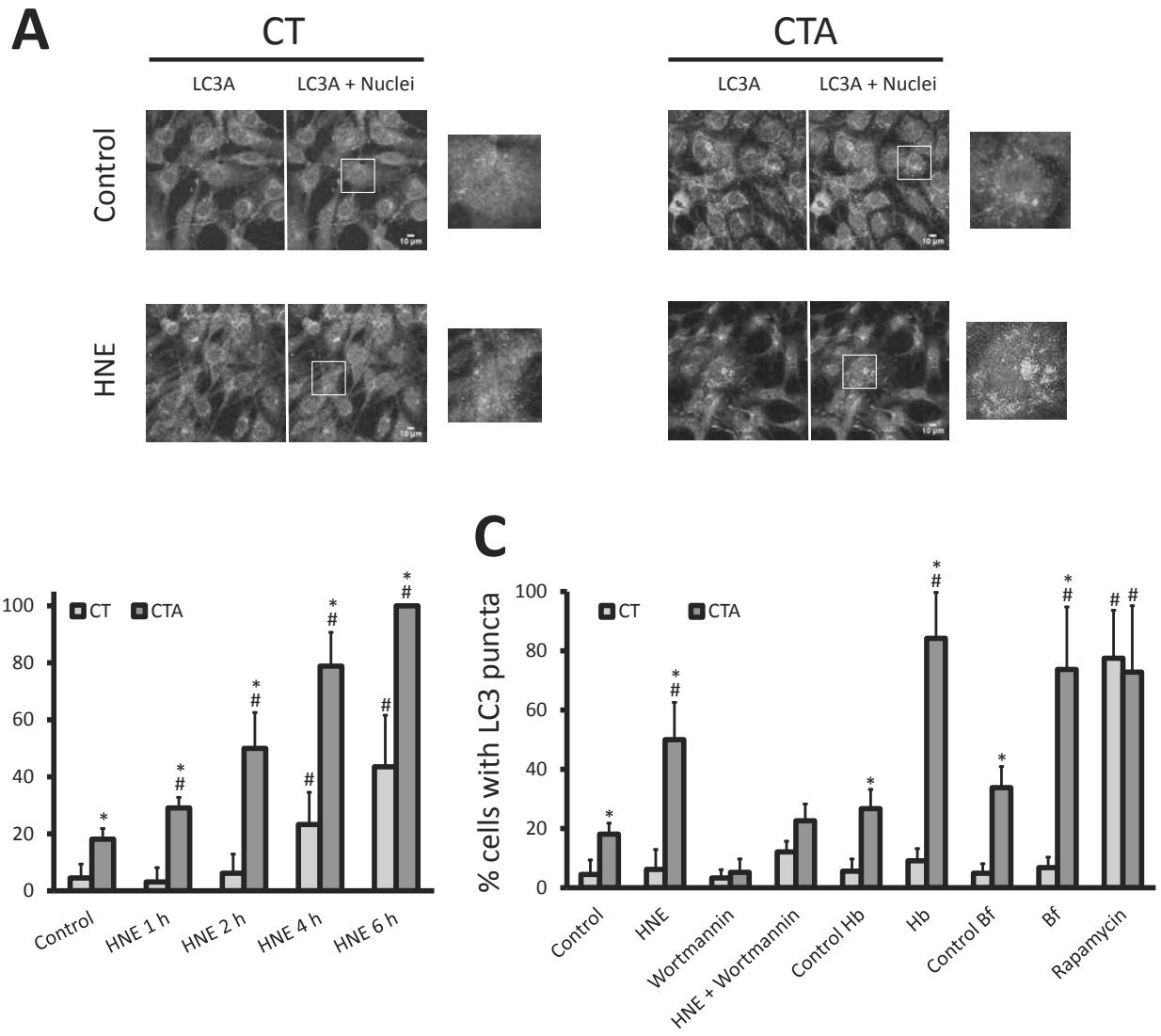
A
CT
CTA
LC3A
LC3A + Nuclei
LC3A
LC3A + Nuclei
Control
HNE
B
% cells with LC3 puncta
CT
CTA
Control
HNE 1 h
HNE 2 h
HNE 4 h
HNE 6 h
C
% cells with LC3 puncta
CT
CTA
Control
HNE
Wortmannin
HNE + Wortmannin
Control Hb
Hb
Control Bf
Bf
Rapamycin
D
CT
CTA
Control
HNE
Rapamycin
E64d + pepstatin A
Beclin1
p62
LC3A-I
LC3A-II
B-actin
Control
HNE
Control Hb
Hb
Control Bf
Bf
Rapamycin
E64d + pepstatin A
CT
CTA
Beclin1
p62
LC3A-I
LC3A-II
B-actin

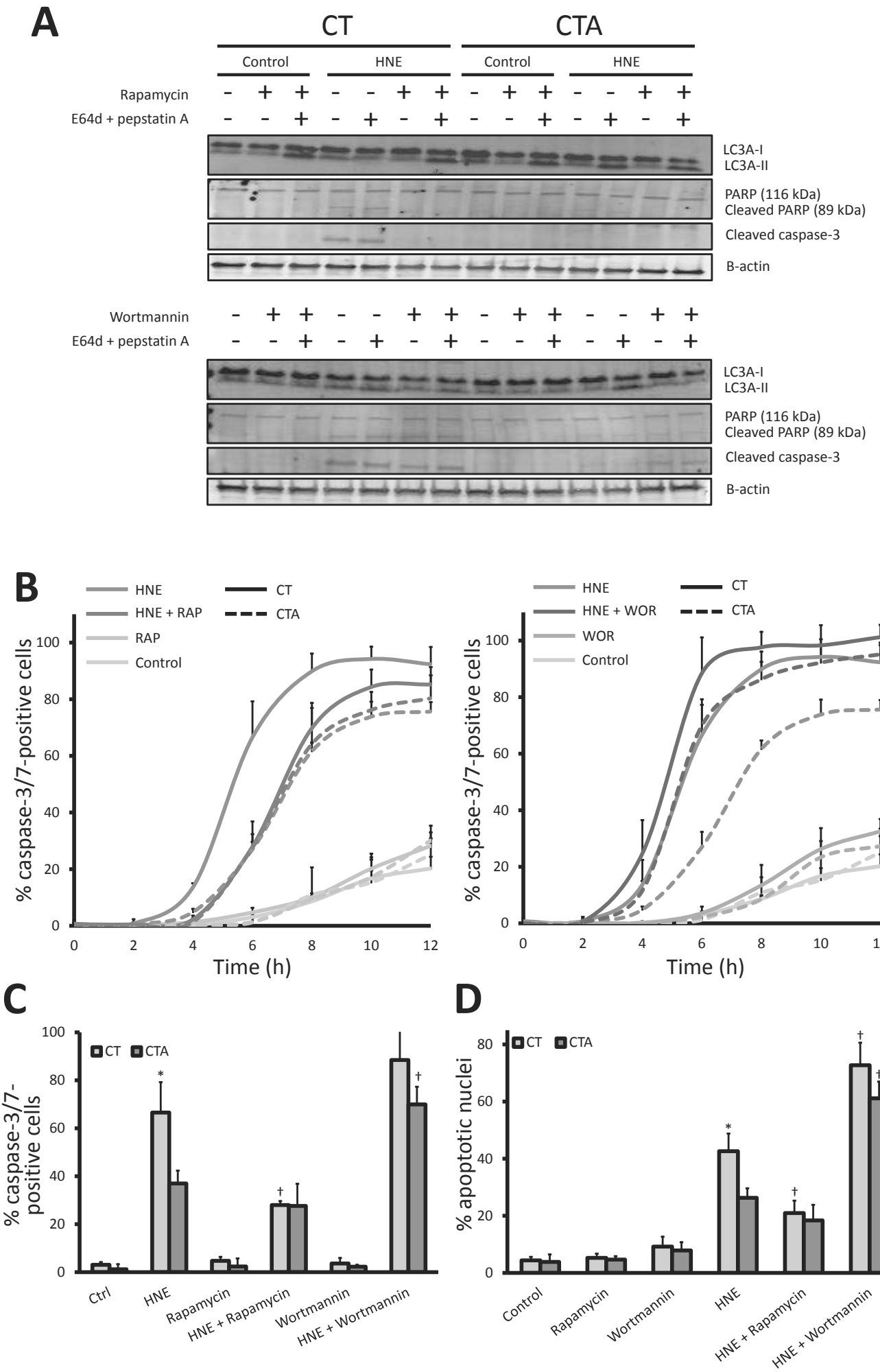
A
CT
CTA
Control
HNE
Control
HNE
Rapamycin
E64d + pepstatin A
LC3A-I
LC3A-II
PARP (116 kDa)
Cleaved PARP (89 kDa)
Cleaved caspase-3
B-actin
Wortmannin
E64d + pepstatin A
LC3A-I
LC3A-II
PARP (116 kDa)
Cleaved PARP (89 kDa)
Cleaved caspase-3
B-actin
B
HNE
HNE + RAP
RAP
Control
CT
CTA
% caspase-3/7-positive cells
Time (h)
HNE
HNE + WOR
WOR
Control
CT
CTA
% caspase-3/7-positive cells
Time (h)
C
CT
CTA
% caspase-3/7-positive cells
Ctrl
HNE
Rapamycin
HNE + Rapamycin
Wortmannin
HNE + Wortmannin
D
CT
CTA
% apoptotic nuclei
Control
Rapamycin
Wortmannin
HNE
HNE + Rapamycin
HNE + Wortmannin

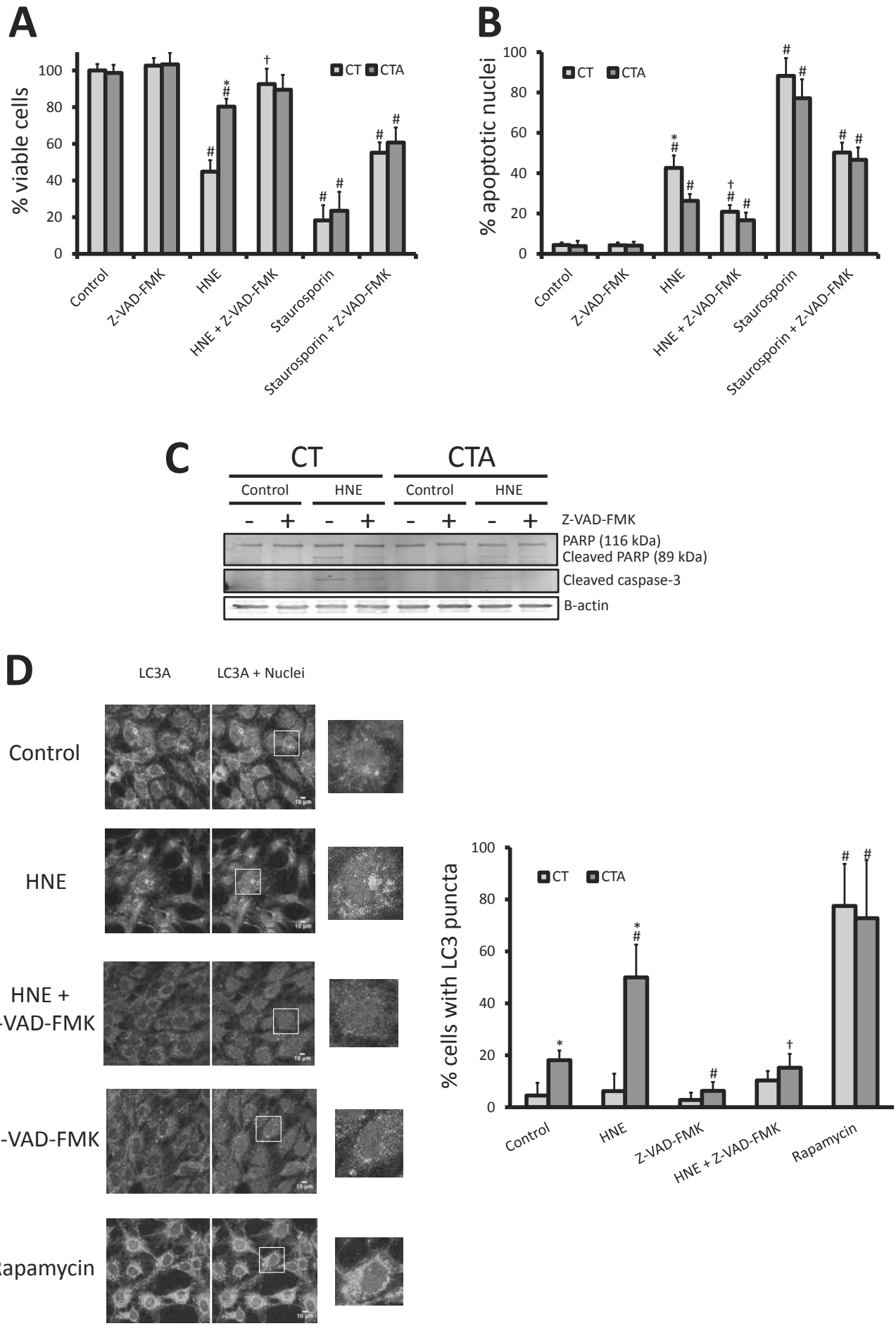
A
% viable cells
CT
CTA
Control
Z-VAD-FMK
HNE
HNE + Z-VAD-FMK
Staurosporin
Staurosporin + Z-VAD-FMK
B
% apoptotic nuclei
C
CT
CTA
Control
HNE
Z-VAD-FMK
PARP (116 kDa)
Cleaved PARP (89 kDa)
Cleaved caspase-3
B-actin
D
LC3A
LC3A + Nuclei
Control
HNE
HNE + Z-VAD-FMK
Z-VAD-FMK
Rapamycin
% cells with LC3 puncta

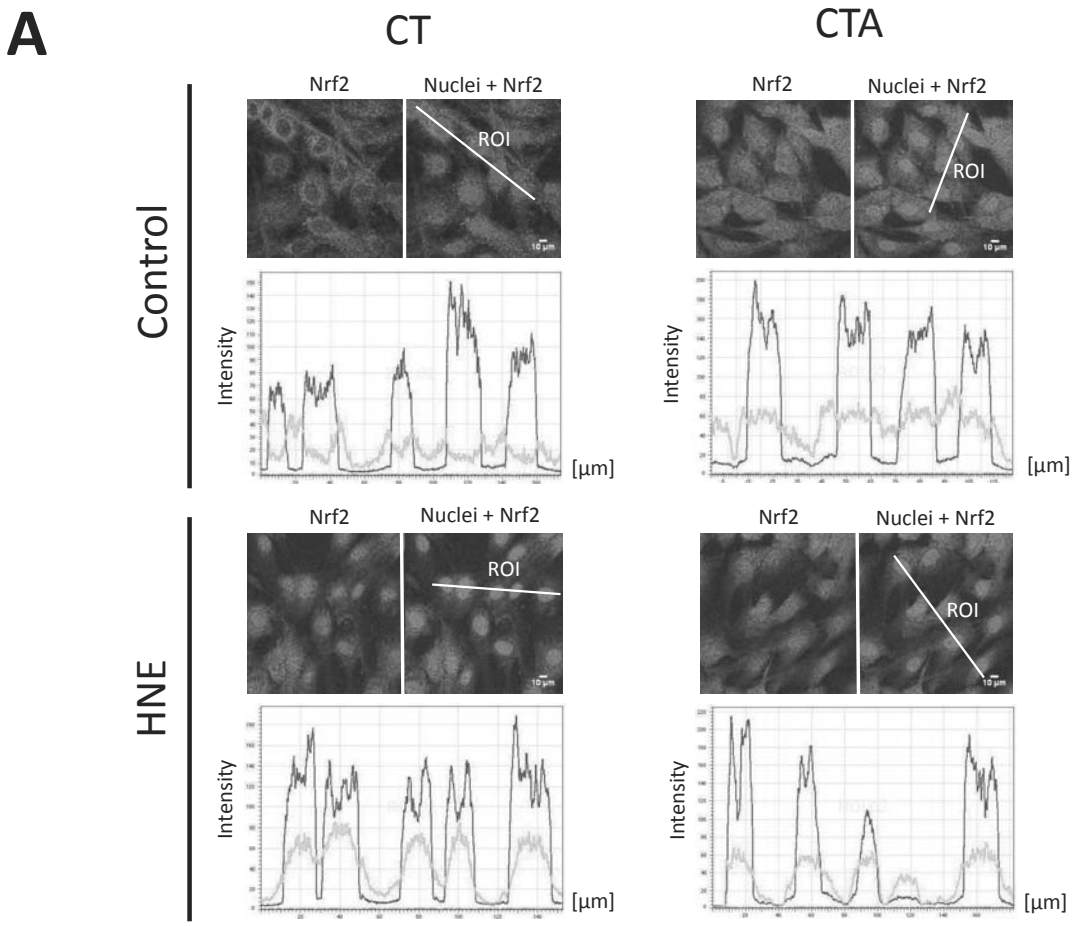
A
CT
CTA
Control
HNE
Nrf2
Nuclei + Nrf2
ROI
Intensity
[µm]

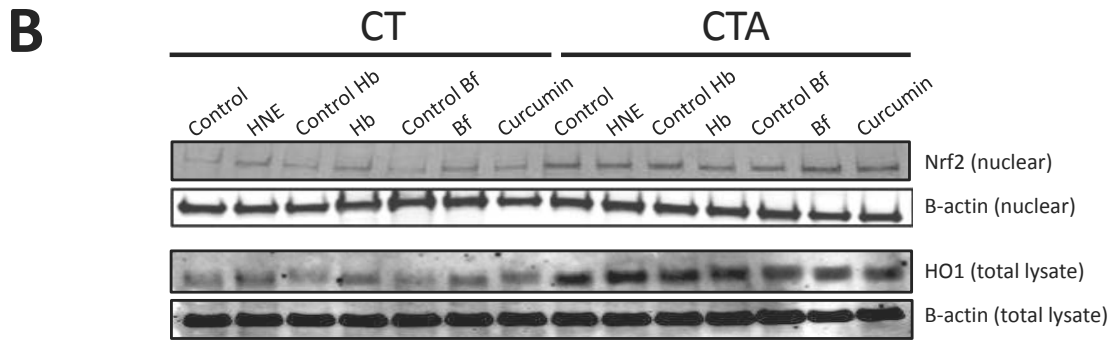
B
CT
CTA
Control
HNE
Control Hb
Hb
Control Bf
Bf
Curcumin
Nrf2 (nuclear)
B-actin (nuclear)
HO1 (total lysate)
B-actin (total lysate)

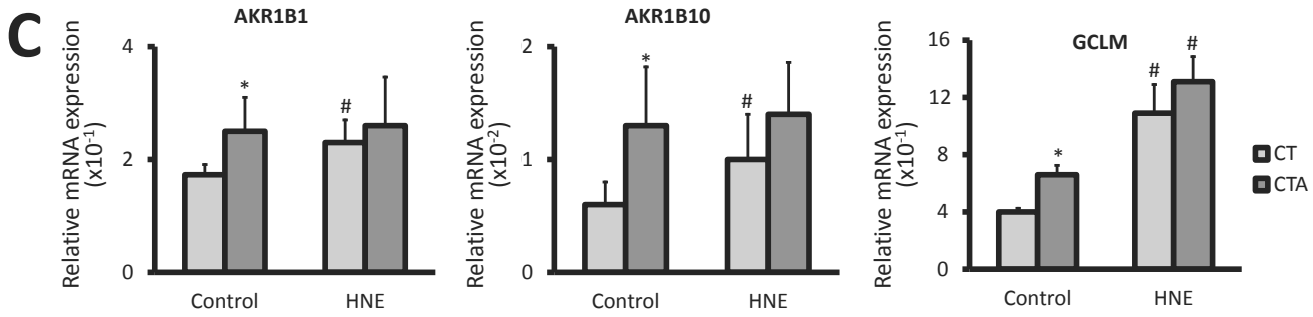
C
AKR1B1
AKR1B10
GCLM
Relative mRNA expression
(x10⁻¹)
(x10⁻²)
Control
HNE
CT
CTA

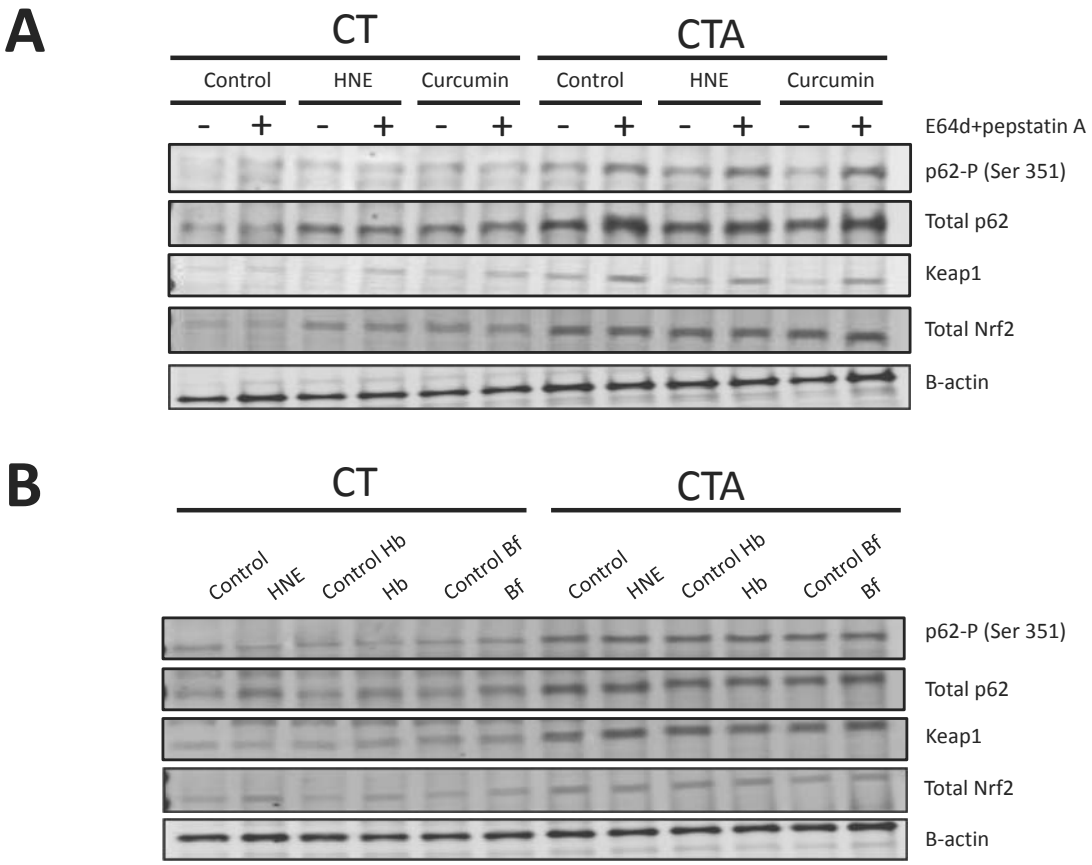
A
CT
CTA
Control
HNE
Curcumin
Control
HNE
Curcumin
- + - + - + - + - + - +
E64d+pepstatin A
p62-P (Ser 351)
Total p62
Keap1
Total Nrf2
B-actin
B
CT
CTA
Control
HNE
Control Hb
Hb
Control Bf
Bf
Control
HNE
Control Hb
Hb
Control Bf
Bf
p62-P (Ser 351)
Total p62
Keap1
Total Nrf2
B-actin

Supplementary Figure 1

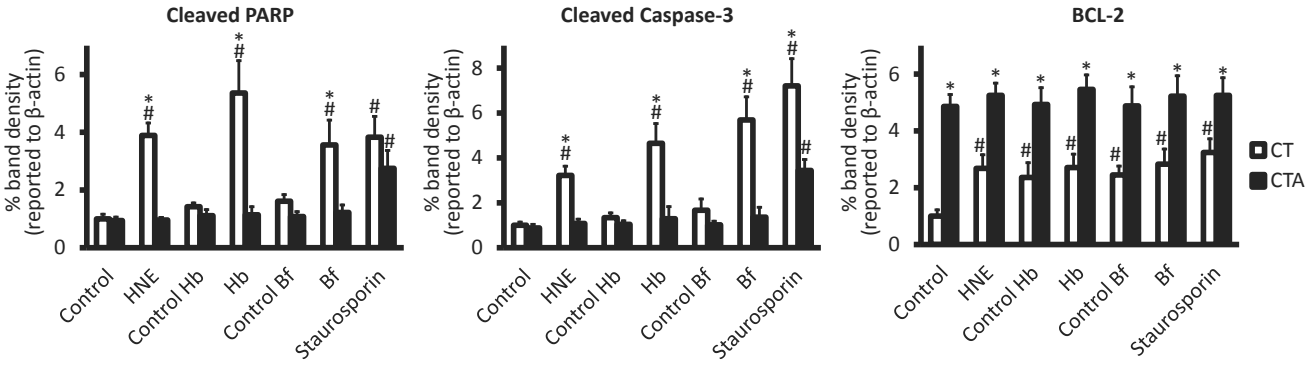

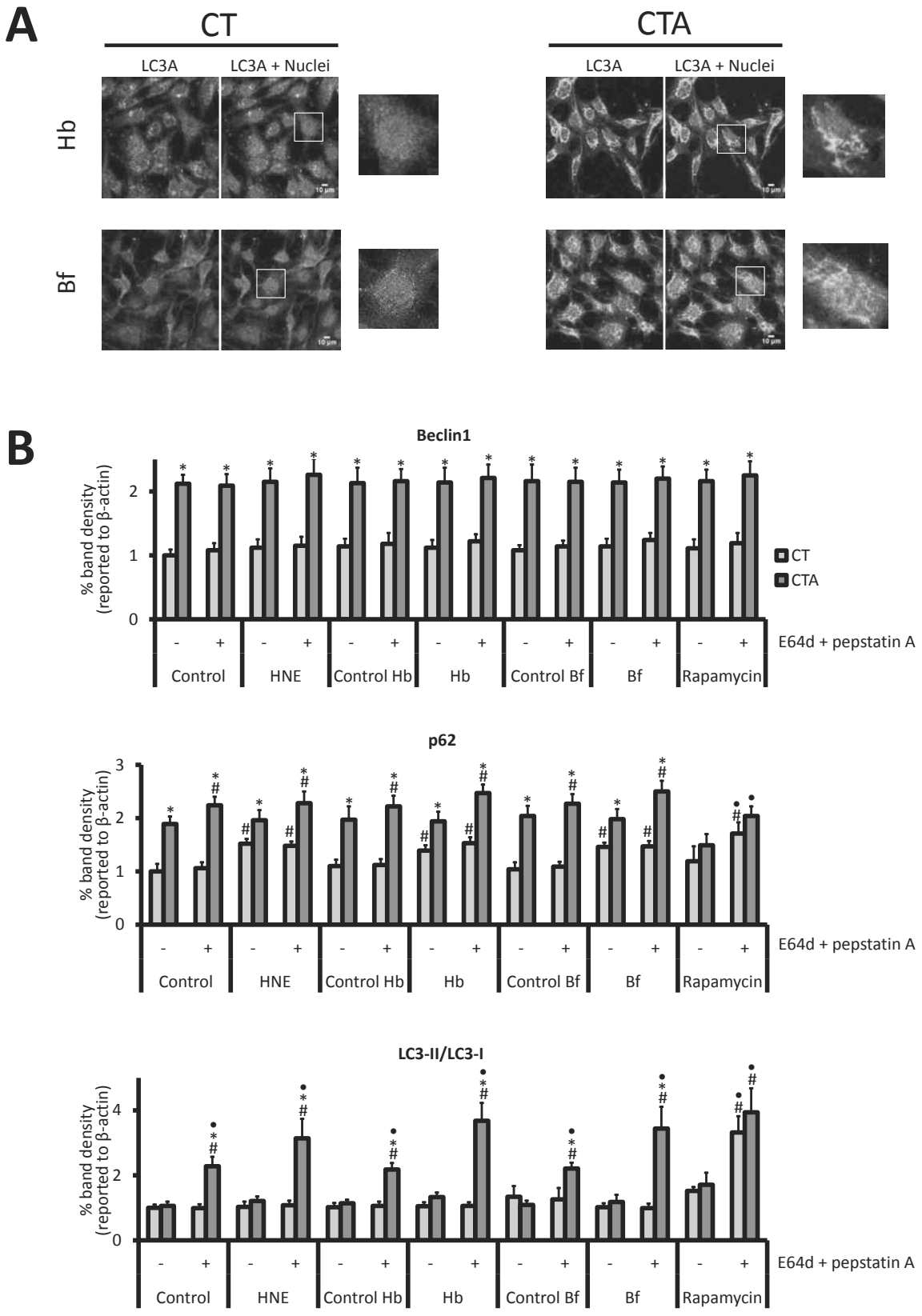
A
CT
CTA
LC3A
LC3A + Nuclei
Hb
Bf
B
Beclin1
p62
LC3-II/LC3-I
% band density (reported to β-actin)
CT
CTA
E64d + pepstatin A
Control
HNE
Control Hb
Hb
Control Bf
Bf
Rapamycin

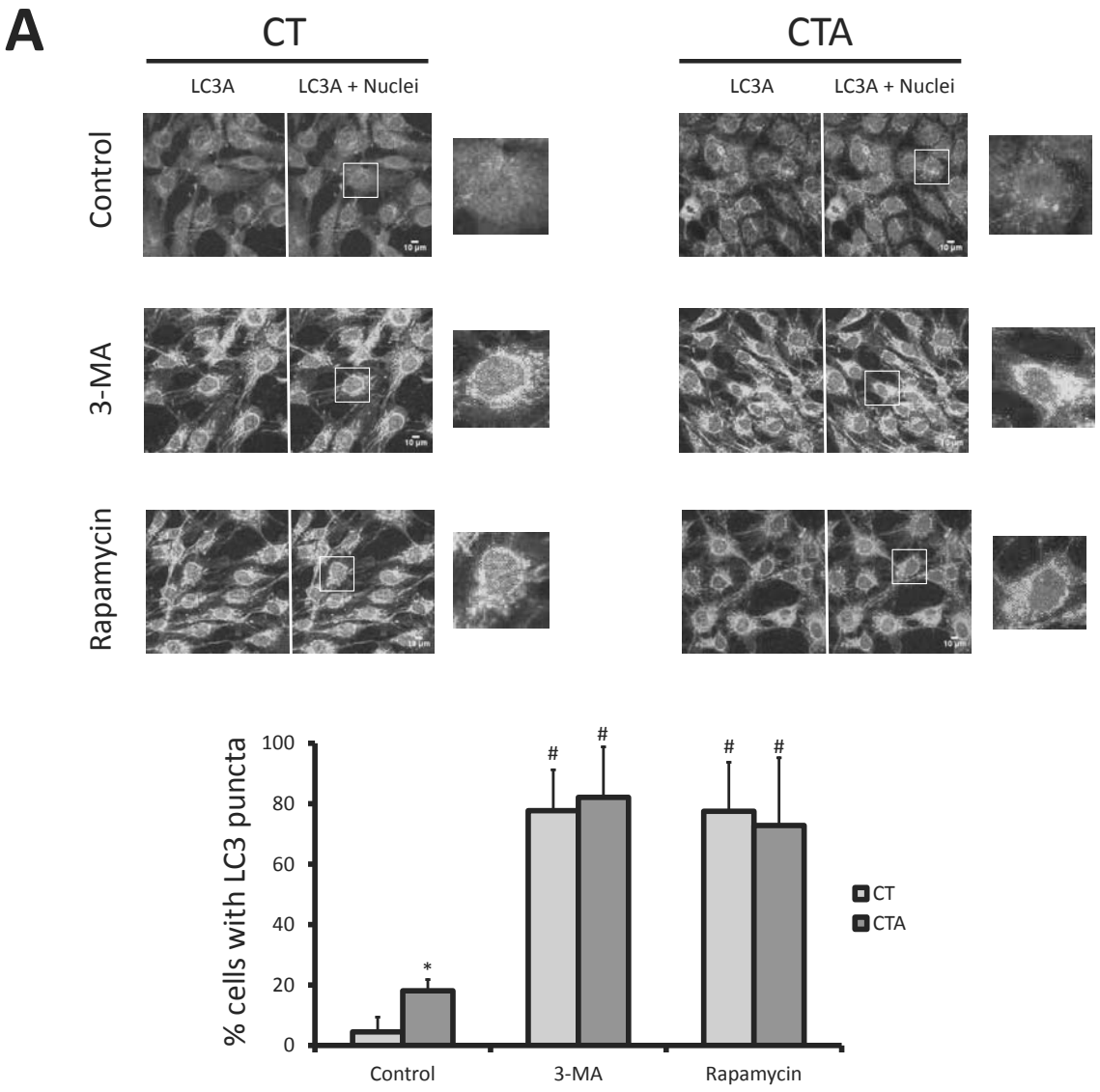
A
CT
CTA
LC3A
LC3A + Nuclei
LC3A
LC3A + Nuclei
Control
3-MA
Rapamycin
% cells with LC3 puncta
100
80
60
40
20
0
*
#
#
#
#
CT
CTA
Control
3-MA
Rapamycin
B
% apoptotic nuclei
50
25
0
*
#
#
†
†
CT
CTA
Control
Rapamycin
3-MA
HNE
HNE + Rapamycin
HNE + 3-MA

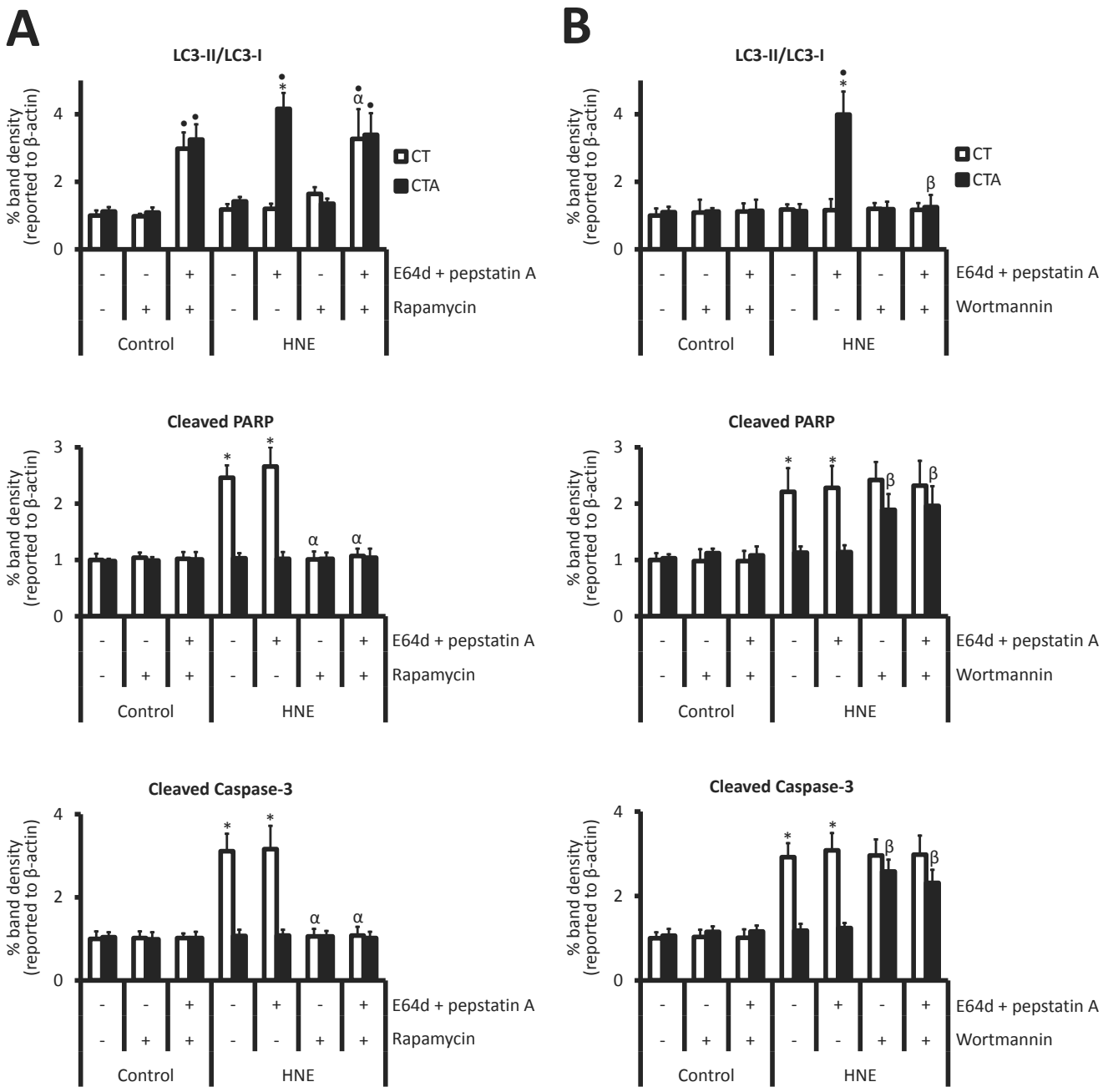
A
B
LC3-II/LC3-I
% band density (reported to β-actin)
CT
CTA
E64d + pepstatin A
Rapamycin
Wortmannin
Control
HNE
Cleaved PARP
Cleaved Caspase-3

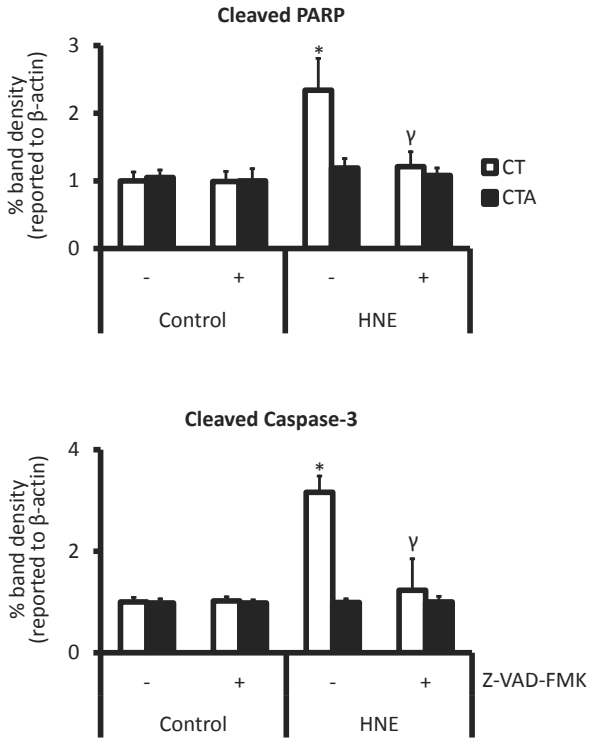
Cleaved PARP
% band density (reported to β-actin)
3
2
1
0
*
γ
CT
CTA
-
+
-
+
Control
HNE
Cleaved Caspase-3
% band density (reported to β-actin)
4
2
0
*
γ
-
+
-
+
Z-VAD-FMK
Control
HNE

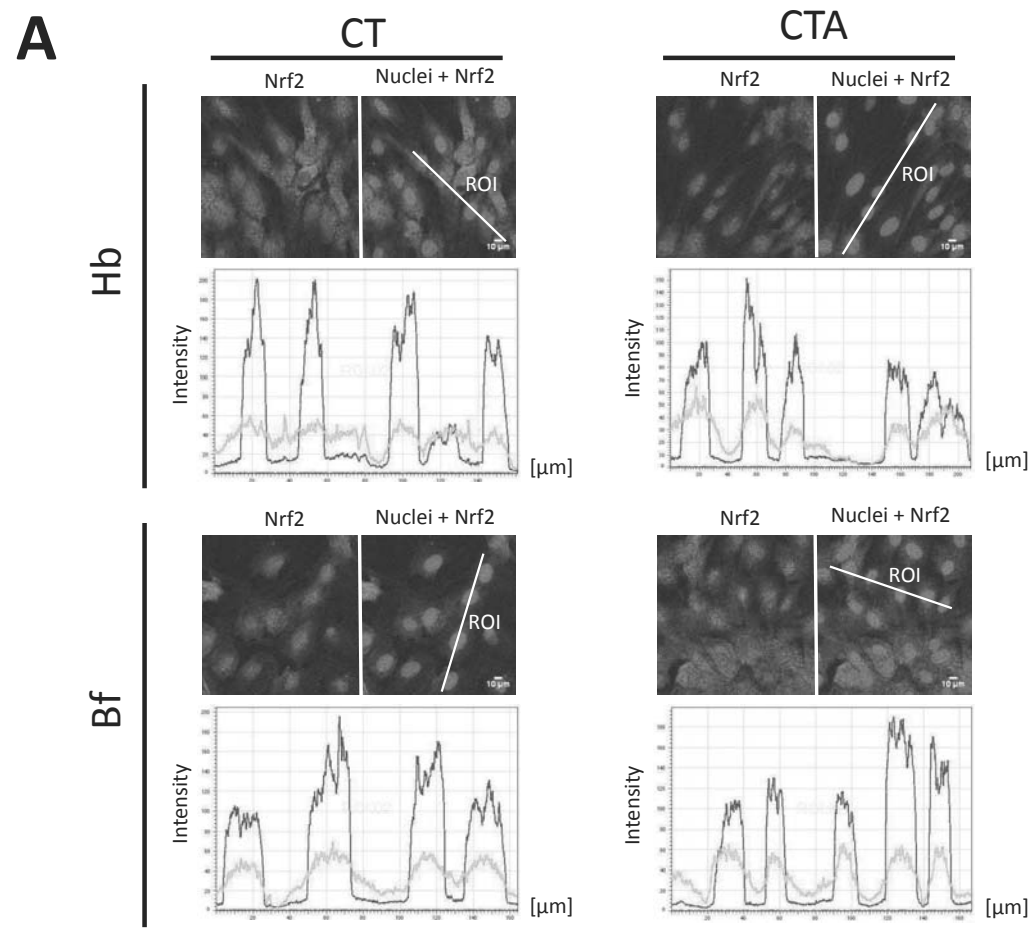
A
CT
CTA
Nrf2
Nuclei + Nrf2
ROI
Hb
Bf
Intensity
[µm]

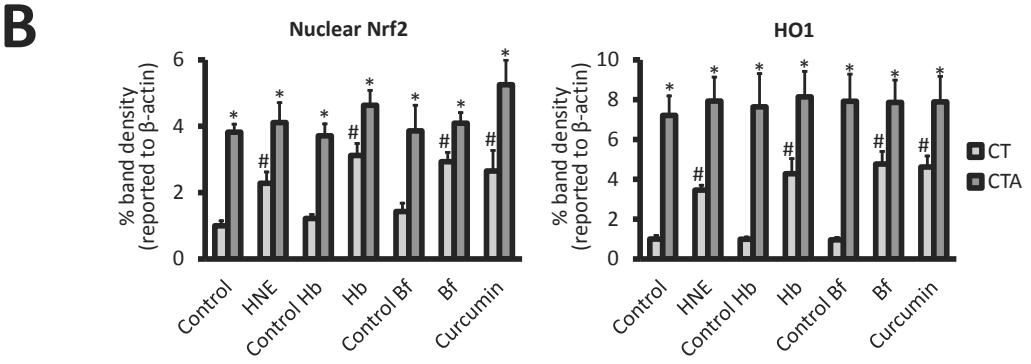
B
Nuclear Nrf2
HO1
% band density (reported to β-actin)
CT
CTA
Control
HNE
Control Hb
Hb
Control Bf
Bf
Curcumin

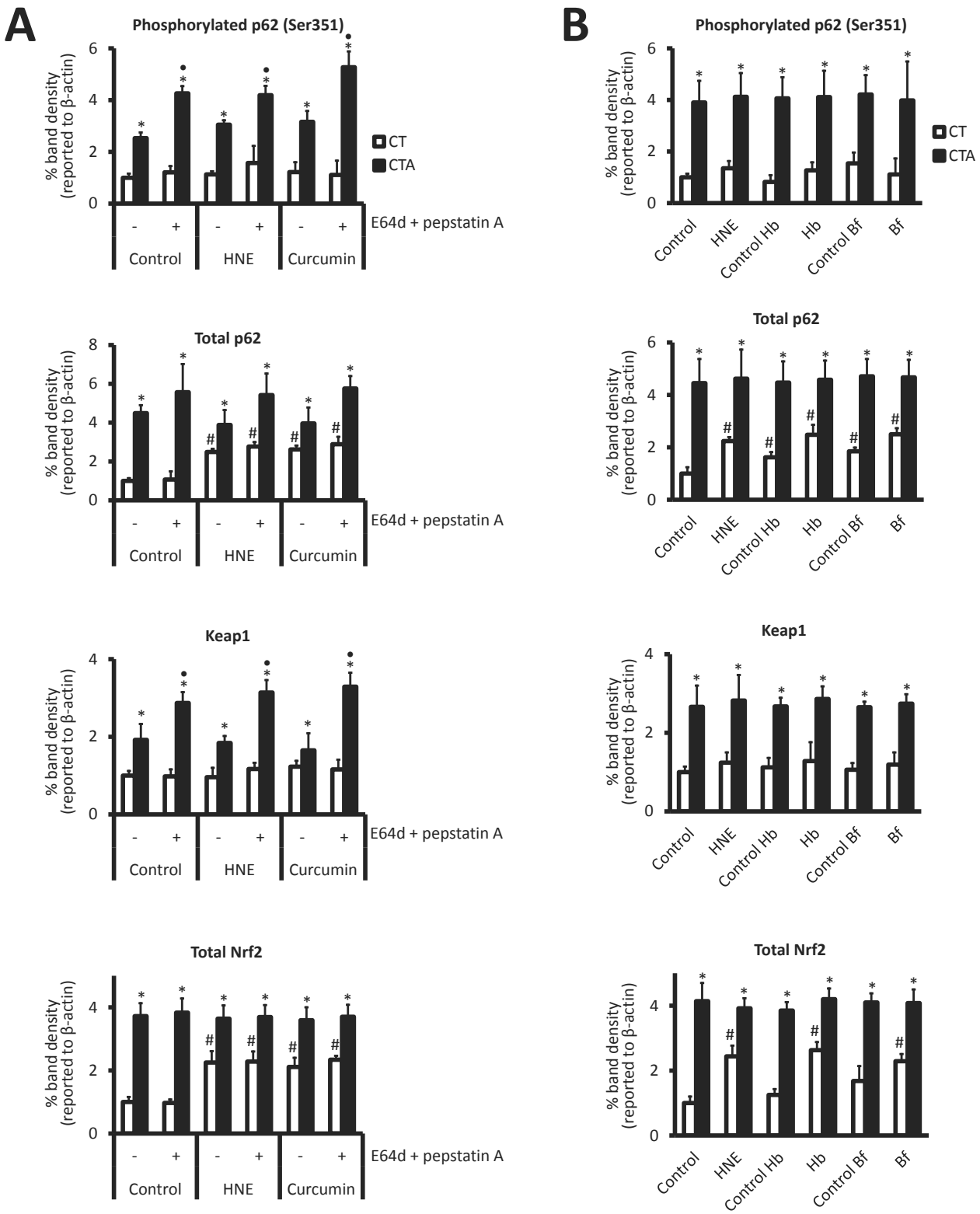
A
Phosphorylated p62 (Ser351)
% band density (reported to β-actin)
CT
CTA
E64d + pepstatin A
Control
HNE
Curcumin
Total p62
Keap1
Total Nrf2
B
Phosphorylated p62 (Ser351)
Total p62
Keap1
Total Nrf2
Control
HNE
Control Hb
Hb
Control Bf
Bf

The synthesis of Article 3 is presented in Figure 47. Nrf2 activity was found to be higher in CTA cells than in CT cells, leading to higher p62 expression in CTA cells and Nrf2 auto-activation *via* p62-dependent Keap1 degradation. Upon exposure to HNE, CTA cells exhibited higher level of autophagy than CT cells, suspected to be associated with high basal level of autophagic protein p62 in CTA cells. Autophagy was suggested to exert protective effects against HNE toxicity and therefore, apoptosis was observed in higher level in CT cells compared to CTA cells. Some of these findings have also been observed by using fecal water of heme-fed rats.

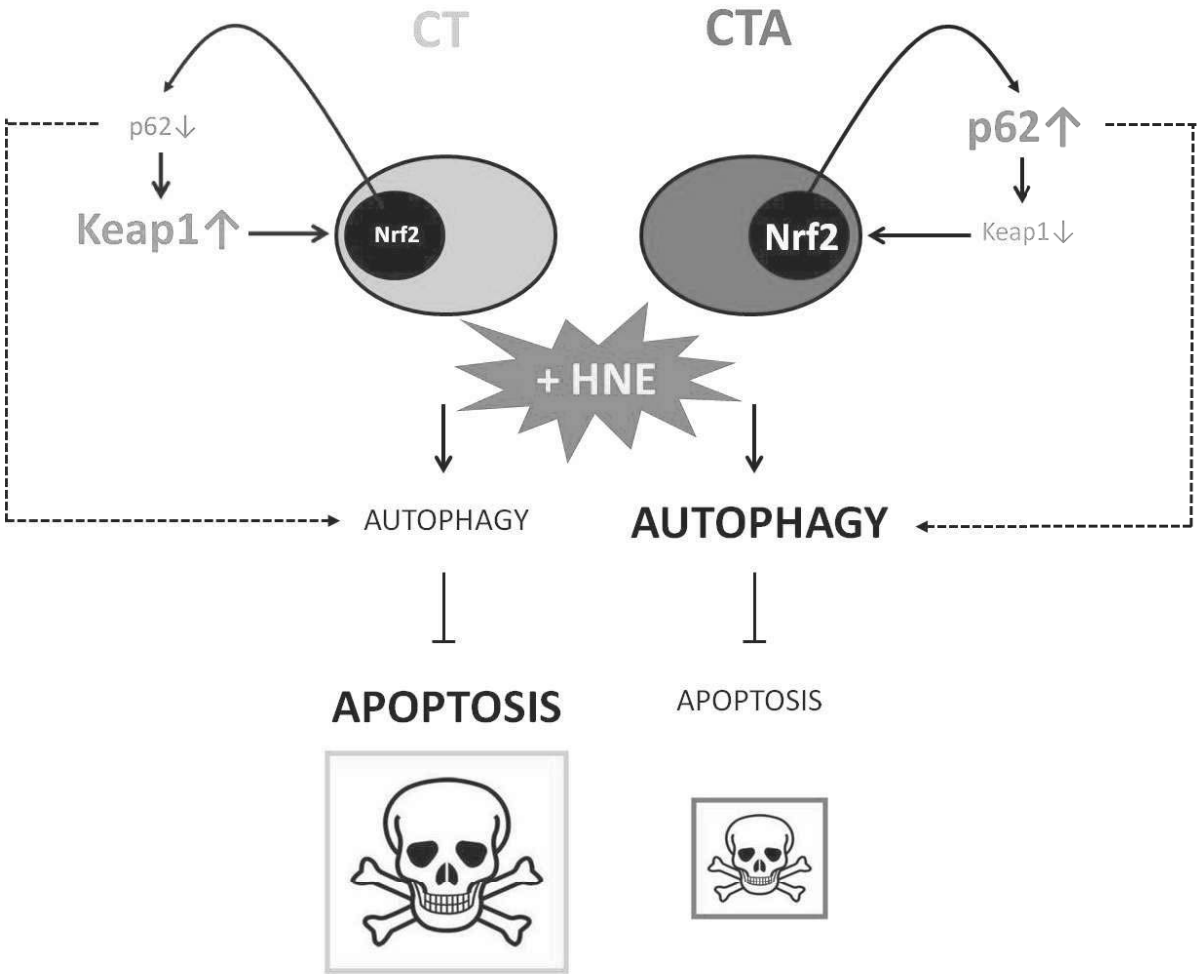

Figure 47. Schema for the role of Nrf2 and autophagy in the resistance of CTA cells upon exposure to HNE

Chapter V

DISCUSSION AND PERSPECTIVES

The principal results obtained during my thesis are that: 1) Nrf2 was involved in the resistance of mouse-origin APC Min/+ cells upon exposure to HNE or fecal water of heme-fed rats, 2) CTA cells were more resistant than CT cells towards HNE or fecal water of heme-fed rats because of their higher Nrf2 activity and autophagy level and 3) aldehydes are in part responsible for the different toxicity of fecal water towards APC +/+ and APC Min/+ cells. In this chapter, all these points are discussed in detail.

5.1. The use of HNE and fecal water of heme-fed rats represents a progressive complexification of lipid peroxidation model

The hypothesis of lipid peroxidation in colorectal carcinogenesis (Figure 15, Chapter 1.2.2.5.2) emphasizes the formation of cytotoxic aldehydes derived from heme-induced lipid peroxidation that exert higher toxicity towards normal colon cells than the preneoplastic ones, thereby generating a positive selection of preneoplastic colon cells favoring tumor development. Prior to my thesis, our team had focused on the role of HNE, a lipid peroxidation-derived aldehyde, in generating such a positive selection *in vitro* by exposing it to mouse-origin normal and preneoplastic cells. In this case, HNE was used as a pure substance synthesized in our laboratory. However, as a pure substance, HNE does not represent the complexity of intestinal contents that are directly in contact with colon cells. Therefore, the use of fecal water was suggested to better represent the complexity of intestinal contents.

Fecal water is an aqueous extract of feces representing the bioavailable parts of fecal matters. In this study, two sources of heme were fed to azoxymethane-injected rats: hemoglobin (Hb) and raw beef meat (Bf). It is noteworthy that Hb and Bf represented a complexification in the rats' diet: from Hb as a purified molecule of heme iron source to Bf as a real red meat. Fecal water of Hb- and Bf-fed rats represents a complex matrix of compounds generally excreted in the feces and substances derived from heme-induced lipid peroxidation in a biological system, including HNE but not only HNE. Therefore, fecal water of heme-fed rats is more representative to study the role of lipid peroxidation in colorectal carcinogenesis compared to HNE as a pure substance. Indeed, the use of HNE and fecal water of heme-fed

rats represents a progressive complexification of lipid peroxidation model: from HNE as a pure compound, to fecal water of rats fed with Hb as a pure compound and finally fecal water of rats fed with raw beef as a complex matrix. This progressive complexification is important to explain the importance of heme-induced lipid peroxidation in the promotion of colorectal carcinogenesis by red meat. In this study, HNE was found in general to be a representative model for heme-induced lipid peroxidation since the effects it provoked in our cellular models tended to be similar to those provoked by fecal water of heme-fed rats.

5.2. *APC* disruption improves the resistance of mouse- and human-origin colon cells towards the toxicity of HNE and fecal water of heme-fed rats

Prior to further discussion with regard to the role of *APC* disruption in cellular resistance, it appears primordial to highlight the two different experimental models used in this study: mouse-origin APC+/+ and APC Min/+ cells and human-origin CT and CTA cells. The *APC* disruption in both experimental models was obtained by different means. APC Min/+ cells exhibited *APC* mutation resulting in truncated APC protein (850 aa) whereas CT and CTA cells underwent shRNA-mediated *APC* invalidation resulting in the degradation of APC mRNA that led to lowered expression of APC protein. It is noteworthy that the truncated APC protein in APC Min/+ cells contains intact armadillo repeat binding domain (Figures 5 and 10) that suppresses tumoral incidence and is involved in apoptosis [89,342,343]. In sporadic human CRC, APC protein is often found to be truncated [469] rather than degraded as represented by CTA cells. Among the various sites in APC protein where the truncations may take place, the codon 1554 has been shown to be the "hotspot" for somatic mutation in human sporadic CRC [470]. Therefore, to approach the real characteristics of human CRC, gene cassettes may be inserted in CT cells to create *APC* mutation that results in the expression of truncated APC protein at codon 1554 as observed in human sporadic CRC.

Another important point concerns the different means of immortalization in both experimental models. In APC +/+ and APC Min/+ cells, the immortalization was achieved by using thermolabile simian virus 40 large tumor antigen gene (*AgT tsA58*) that is active only at 33 °C in the presence of interferon γ. Therefore, at treatment temperature of 37 °C without interferon γ, these cells are not immortalized and exhibit the phenotype of mouse normal colon epithelial cells. However, in CT and CTA cells, the immortalization was mediated by plasmid transfection of *CDK4* (Cyclin-dependent kinase 4) and *hTERT* (Telomerase reverse

transcriptase) genes that are integrated in the genome. Therefore, these cells are constantly immortalized at the maintenance and treatment temperature of 37 °C.

In Articles 1-3, *APC* disruption (*APC* mutation in preneoplastic APC Min/+ cells and shRNA-mediated *APC* invalidation in CTA cells) was shown to be involved in cellular resistance towards HNE or fecal water of heme-fed rats, both in mouse and human models. APC Min/+ and CTA cells underwent lower level of apoptosis following exposure to HNE or fecal water of heme-fed rats compared to wild type cells (APC +/+ and CT cells). This phenomenon might be related to Nrf2 activation in relation with *APC* disruption. *APC* disruption may activate Wnt signaling pathway that inhibits Nrf2 degradation by recruiting axin and GSK3β to the membrane (Figure 27) [273]. *In vivo*, Nrf2 knockout enhanced intestinal tumorigenesis in Min mice [471]. To assess the role of GSK3β in Nrf2 activation mediated by *APC* invalidation, I analyzed the basal expression level of GSK3β which appeared to be indifferent in CT and CTA cells (Figure 48). Following HNE exposure, the level of GSK3β diminished. We are currently unable to explain this phenomenon.

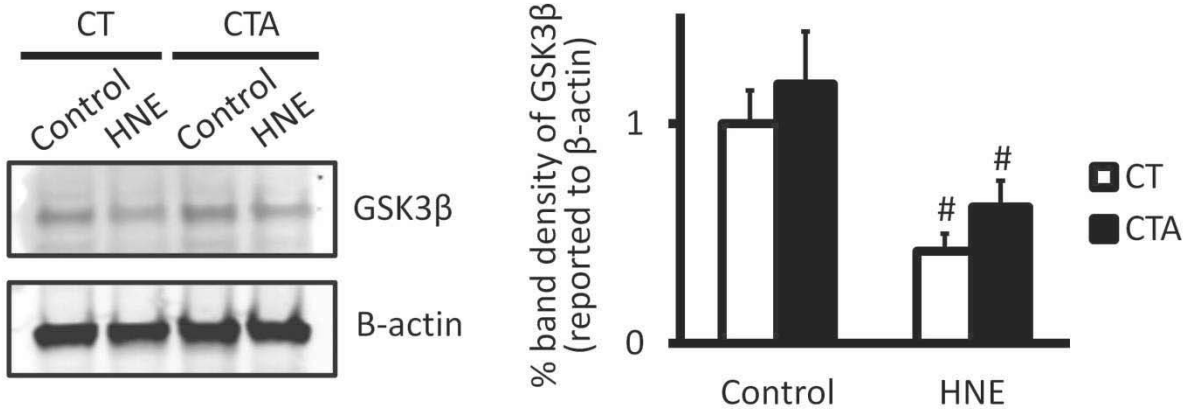

Figure 48. Western blotting analysis and densitometry of GSK3β (n=3) in CT and CTA following treatment with HNE 20 μM (t=2 h). β-actin was used as loading control. # Significant difference between HNE and Control in a cell line ($p<0.05$).

Another proposition is that Keap1, the inhibitor of Nrf2, scaffolds to the actin cytoskeleton [472] and since the cytoskeletal network is destructurized following *APC* disruption, Keap1 may be destabilized, leading to Nrf2 activation. To test these propositions, one can destructurize the actin network in APC +/+ or CT cells by cytochalasin B and observe the effects of this action in terms of Nrf2 activity and cell resistance towards HNE or fecal water.

Regarding cell resistance towards HNE or fecal water, co-culturing APC +/+ and APC Min/+ cells (or CT and CTA cells) can be considered to study and validate the Darwinian selection of preneoplastic cells over normal cells upon exposure to continuously-available HNE or fecal water *in vitro*. In this case, the two different cell lines have to be marked with two different fluorescent probes to distinguish them and the evolution of the surviving population following exposure to HNE or fecal water can be monitored by fluorescent microscopy.

To analyze cell ability to acquire tumorigenic properties, experiments on clonogenicity can be done with soft agar colony formation assay to observe the tendency of CTA cells to form colonies. This assay would allow to confirm cellular anchorage, a property of cell that is associated with the tumorigenic potential of the cultured cells. Furthermore, these colonies can be xenografted into nude mice to investigate its ability to develop CRC *in vivo*. It is to be noted that soft agar colony formation assay would not be able to be done in APC +/+ and APC Min/+ cells since these cells do not proliferate at the treatment temperature of 37 °C because of the absence of immortalization.

5.3. Different mechanisms undertaken by normal and preneoplastic cells may explain their different resistance towards HNE and fecal water of heme-fed rats

In Articles 1-3, two mechanisms were reported to be able to explain the different resistance of normal and *APC*-disrupted colon cells towards HNE and fecal water of heme-fed rats: Nrf2-dependent antioxidant response (in APC +/+ and APC Min/+ cells, also in CT and CTA cells) and autophagy (in CT and CTA cells). These mechanisms, along with other mechanisms that are suggested to be involved in such a resistance, are discussed in this chapter.

5.3.1. Higher Nrf2 activity in preneoplastic cells is associated with better ability to detoxify HNE

Nrf2-dependent antioxidant response has been reported to be up regulated in CRC [234]. A clinical study has shown that Nrf2 and its regulated enzymes were highly expressed in CRC tissues compared to adjacent non-tumor tissues [473]. Article 1 clearly shows that Nrf2 was involved in the resistance of mouse-origin preneoplastic colon cells to HNE and fecal water of heme-fed rats compared to normal cells. Nrf2 activity was found to be higher in preneoplastic cells than in normal cells under basal conditions and this phenomenon led to

higher expression of HNE detoxification enzymes in preneoplastic cells, which appeared to be regulated by Nrf2. We thus suggested that higher Nrf2 activity and expression level of HNE detoxification enzymes under basal conditions gave preneoplastic cells advantages to tackle the insults provoked by HNE or fecal water of heme-fed rats in comparison with normal cells. Following exposure to HNE or fecal water of heme-fed rats, Nrf2 was indeed activated in normal cells. However, the final level of HNE detoxification enzymes was constantly higher in preneoplastic cells, therefore suggesting the reason for which the preneoplastic cells exerted higher resistance to HNE and fecal water of heme-fed rats compared to normal cells.

As previously discussed, higher Nrf2 activity in preneoplastic cells might be due to *APC* mutation that activates Wnt signaling pathway (Figure 27) [273]. Preneoplastic cells expressed truncated APC protein at 850 aa with intact armadillo binding repeat domain but without β-catenin binding sites (Figure 5 and 10). This absence of β-catenin binding site would keep β-catenin free and thus constitutively activate Wnt signaling pathway in preneoplastic cells. The different Nrf2 activity between normal cells (expressing intact APC protein) and preneoplastic cells (expressing truncated APC protein at 850 aa) might indicate the inhibitory properties of β-catenin binding site in APC protein against Nrf2 activity or furthermore, the inducing properties of armadillo repeat binding domain regarding Nrf2 activity. Another study using cells engineered to express APC protein lacking of armadillo repeat binding domain can be conceived to analyze the role of this domain in Nrf2 activity in mouse-origin colon epithelial cells.

To investigate the important role of Nrf2 in the resistance of preneoplastic cells towards HNE or fecal water of heme-fed rats, siRNA-mediated invalidation of Nrf2 was done in normal and preneoplastic cells. In normal cells, because of their low Nrf2 activity, Nrf2 invalidation did not modulate their sensitivity towards HNE or fecal water of heme-fed rats. However, Nrf2 invalidation sensitized preneoplastic cells to HNE and fecal water of heme-fed rats, showing that Nrf2 activity was primordial in the resistance of preneoplastic cells. Furthermore, it appears interesting to analyze the decrease of HNE detoxification enzymes in Nrf2-invalidated preneoplastic cells by RT-qPCR. To establish a causal relationship regarding the importance of Nrf2 in cell resistance, our team has transfected Nrf2 over-expression vectors in normal cells and this appeared to improve their resistance towards HNE (unpublished, article submitted).

In Article 3, Nrf2 activity was also shown to contribute to the resistance of CTA cells to HNE and fecal water of heme-fed rats. Nrf2 was found in higher level in CTA cells than in CT cells under basal conditions and this phenomenon was dependent on autophagic protein p62. Three HNE detoxification enzymes were expressed in higher level in CTA cells than in CT cells under basal conditions: AKR1B1 (aldo-keto reductase family 1, member 1), AKR1B10 (aldo-keto reductase family 1, member 10) and GCLM (glutamate-cysteine ligase, modifier subunit). GCLM is an enzyme involved in the synthesis of glutathione (GSH). Since the expression level of GCLM differed in CT and CTA cells under basal conditions, we analyzed the uptake of cystine, a source of intracellular GSH synthesis, in CT and CTA cells. Our preliminary results showed that basal uptake of cystine was higher in CTA cells than in CT cells. This finding can be verified by analyzing the GSH level in CT and CTA cells. Since GCLM expression and uptake of cystine were higher in CTA cells than in CT cells, the expected results would be higher GSH level in CTA cells than in CT cells.

To verify whether Nrf2 activity is different between normal tissues and preneoplastic lesions (ACF or MDF) *in vivo*, one can separate normal and preneoplastic tissues in the colon of heme-fed rats by laser capture/cutting microdissection (LCM), a method of isolation of cells of interest from a tissue section under morphological control using laser beams [474]. Following the isolation of preneoplastic lesions from the normal tissues, the analyses of Nrf2 activity or expression of HNE detoxification enzymes can be carried out and compared in normal and preneoplastic tissues. This experiment may also be done by using sections of cut human colon samples following colorectal surgery. However, it is to be noted that colorectal surgery is normally done in patients suffering from severe or advanced CRC and therefore, the lesions found in the colon section would be more likely to be cancerous instead of preneoplastic.

In general, Nrf2 has been shown to possess a pivotal role in the resistance of preneoplastic colon cells towards HNE or fecal water of heme-fed rats. Such a resistance is believed to determine colorectal carcinogenesis. Concerning the role of Nrf2 in cancer prevention, a study within the team has revealed that treating normal APC +/+ cells with antioxidants like curcumin (bioactive compound of turmeric) or pterostilbene (bioactive compound of grapes and blueberries) enhanced their basal Nrf2 activity (unpublished, article submitted). This may give advantages to normal cells to better resist the toxicity of HNE or fecal water of heme-fed rats, thus minimizing the difference of mortality between normal and preneoplastic cells. Interestingly, curcumin and pterostilbene induced apoptosis in

preneoplastic cells but not in normal cells. Moreover, following pretreatments with curcumin or pterostilbene, normal cells underwent lower mortality than preneoplastic cells upon HNE exposure (unpublished, article submitted). This result evokes the interest of enhancing Nrf2 activity in normal cells by antioxidants to improve their resistance towards HNE exposure, thereby impairing different mortality between normal and preneoplastic cells that favors CRC promotion. In order to investigate the importance of Nrf2 in the promotion of colorectal carcinogenesis and the role of antioxidant in this process *in vivo*, experiments using Nrf2-knockout mice or rats can be conceived. Nrf2 activation by cinnamaldehyde has been reported to suppress azoxymethane/dextran sulfate sodium-induced CRC in wild type mice but not in Nrf2-knockout mice [475]. Another study has demonstrated that Nrf2-knockout mice possessed higher susceptibility to develop colitis-associated colorectal cancer than wild type mice [319]. To study the role of Nrf2 and antioxidants in red meat-associated promotion of colorectal carcinogenesis, normal and Nrf2-knockout mice or rats can be fed with sources of heme iron with/without antioxidants (curcumin or pterostilbene). The expected results would be significantly higher amount of preneoplastic lesions (ACF or MDF) found in heme-fed Nrf2-knockout mice or rats than in normal ones. Antioxidant supplementation would alleviate this effect in normal mice or rats. However, because of the absence of Nrf2, antioxidant supplementation would not exert protective effects against the promotion of colorectal carcinogenesis in Nrf2-knockout mice or rats fed with red meat.

5.3.2. Higher level of autophagy in preneoplastic cells is associated with protection against apoptosis induced by HNE or fecal water of heme-fed rats

Beside Nrf2, autophagy is also involved in the different resistance of CT and CTA cells towards HNE and fecal water of heme-fed rats, as discussed in Article 3. CTA cells underwent autophagy even under basal conditions and this was supported by higher basal expression of autophagic proteins Beclin1 and p62 in CTA cells compared to CT cells. CTA cells also demonstrated higher autophagy level than CT cells following exposure to HNE or fecal water of heme-fed rats, suggesting the potentially protective role of autophagy in inhibiting apoptosis provoked by HNE or fecal water of heme-fed rats. These findings concerning autophagy can also be verified in APC +/+ and APC Min/+ cells. Preliminary results within our group demonstrated that APC Min/+ cells expressed higher level of p62 than APC +/+ cells, as evidenced by RT-qPCR and immunofluorescence analysis (data not shown). Therefore, autophagy might also be involved in the resistance of APC Min/+ cells

upon exposure to HNE and fecal water of heme-fed rats. *In vivo*, autophagy has been shown to be involved in intestinal tumorigenesis in Min mice [397,398].

Article 3 also denotes that chemical inhibition of autophagy using wortmannin sensitized CTA cells to HNE and fecal water of heme-fed rats whereas chemical stimulation of autophagy using rapamycin improved the resistance of CT cells towards HNE and fecal water of heme-fed rats. To further study the importance of autophagy in cell resistance, siRNA-mediated invalidation of genes involved in autophagy may be considered, for example invalidation of Beclin1, ATG5 (autophagy-related gene 5) or ATG7 (autophagy-related gene 7) in CTA cells. This invalidation is expected to sensitize CTA cells to HNE or fecal water of heme-fed rats. *In vivo* studies have reported that inactivation of ATG7 or ATG5 down-regulated autophagy and suppressed tumor growth in Min or azoxymethane/dextran sodium sulfate-injected mice respectively by enhancing apoptosis in tumor cells [398,476,477].

In vivo experiments to verify the role of autophagy in colorectal carcinogenesis would also be interesting to carry out. Injection of autophagy-modulating substances (rapamycin to induce autophagy or wortmannin to inhibit autophagy) can be done in Min mice fed with sources of heme iron (hemoglobin, hemin or red meat). Afterwards, the intestinal tumorigenesis can be observed. Firstly, preliminary experiments should be conducted by injecting the mice with autophagy-modulating substances (rapamycin or wortmannin) to verify whether these substances modulate autophagy in the intestinal cells. Two studies focused on the optimization of rapamycin dosing in obtaining antiangiogenic effects against cancer in mice reported the usage of rapamycin intraperitoneal doses of 1.5 mg/kg/day and 8 mg/kg/day [478,479]. *In vivo* studies on carcinogenesis in mice demonstrated the usage of wortmannin intraperitoneal doses of 0.7 mg/kg/day and 2 mg/kg/day [480,481]. The expected results of these experiments would be that intervention of rapamycin or wortmannin would reduce the intestinal tumorigenesis in heme-fed Min mice since these substances abolished the difference of resistance between CT and CTA cells upon exposure to heme-fed rats *in vitro*. In addition, the intestinal mucosa can also be isolated for further analyses regarding immunity and inflammation, particularly the production of IL-12 and the infiltration of cytotoxic $CD8^+$ T cells. These parameters have been reported to be involved in the role of autophagy in intestinal tumorigenesis in Min mice [398,399].

Numerous studies have shown the beneficial effects of rapamycin in chemotherapy treatments against several types of cancer, including CRC. Rapamycin and its analogs have

been demonstrated to enhance therapeutic efficacy of chemotherapy agents in CRC in humans [482,483]. The mechanism by which rapamycin inhibits tumor growth is through inhibition of mTOR (mammalian target of rapamycin), a downstream target of phosphoinositide 3-kinase (PI3K)/mTOR pathway that is often activated in cancer cells and results in uncontrolled proliferation and metastasis [484,485]. Up to 2012, the use of rapamycin and its analogs in cancer treatments had been approved for renal cancer whereas its status was still under clinical trials for the application in other types of cancer [486]. As for wortmannin, this substance has also been shown to inhibit several types of cancer including breast and pancreatic cancer but the studies on CRC are still lacking [487-490]. Nevertheless, chloroquine, another autophagy inhibitor, has been reported to potentiate chemotherapy treatments in CRC, thereby highlighting the interest of inhibiting autophagy in cancer treatments [491].

Article 3 demonstrates that the superior basal expression of p62 in CTA cells compared to CT cells was involved in basal Nrf2 activation in CTA cells. Indeed, phosphorylated p62 (Ser 351) and Keap1 in CTA cells were constantly degraded under basal conditions by autophagy, indicating the occurence of p62-dependent Nrf2 activation (Chapter 1.4.2.4). This phenomenon was not observed in CT cells. To analyze whether CTA cells depend on p62 to activate Nrf2 under basal conditions, p62 can be invalidated in CTA cells by siRNA. Afterwards, we can observe whether this p62 invalidation reduces basal level of nuclear Nrf2 by immunofluorescence or western blotting. p62 invalidation can also be done to impair autophagy in CTA cells and observe whether autophagy impairment in CTA cells modulates their sensitivity to HNE or fecal water of heme-fed rats. The expected results would be that p62 invalidation reduced autophagy level in CTA cells upon exposure to HNE or fecal water of heme-fed rats. Furthermore, *in vivo* experiments using heme-fed p62-knockout mice or rats can also be done to study the role of p62 in red meat-induced colorectal carcinogenesis, especially regarding autophagy and Nrf2 status. Indeed, dysregulation of p62 has been reported to be associated with CRC proliferation [492,493]. Lastly, the role of antioxidants in modulating autophagy in CT and CTA cells would also be worth investigating. Several *in vitro* studies have reported that curcumin and pterostilbene induced autophagy in human cancer cell lines [494-497]. In terms of CRC, a study has shown that curcumin induced human CRC cell death *via* down-regulation of p62 expression [498].

5.3.3. Other mechanisms that are probably involved in the resistance of preneoplastic cells to HNE or fecal water of heme-fed rats

Beside the differential of Nrf2 and autophagy in normal and preneoplastic cells, other mechanisms are also suspected to be involved in the resistance of preneoplastic cells upon exposure to HNE or fecal water of heme-fed rats. Based on the preliminary results obtained within the team, the level of reactive oxygen species (ROS) and ER stress are suggested to be involved in such resistance.

The level of ROS has been shown to be generally more elevated in human colon tumoral tissues than in non-tumoral tissues [499-501]. Experiments within the team using H_2DCF-DA (dihydrodichlorofluorescein diacetate) to evaluate cellular oxidative status revealed that basal ROS level was higher in APC Min/+ cells than in APC +/+ cells. Higher basal ROS level in APC Min/+ and CTA cells may explain their higher basal Nrf2 activity compared to APC +/+ and CT cells, through the oxidation of the cystein residues of Keap1 and the liberation of Nrf2. In CT and CTA cells, we did not observe different basal ROS level. Nevertheless, higher basal Nrf2 activity in CTA cells compared to CT cells is suggested to be due to p62-dependent degradation of Keap1 that activates Nrf2.

ER stress is defined as disruption of ER function that causes an accumulation of misfolded and unfolded proteins in the ER lumen. In the cells, ER functions to properly fold and process secreted and transmembrane proteins. ER stress activates a signaling network called unfolded protein response (UPR) to alleviate this stress and restore ER homeostasis, promoting cell survival and adaptation. Failure of UPR promotes apoptosis [502]. ER stress is linked to Nrf2 via splicing of XBP1 and increased expression of Hrd1, an E3 ubiquitin ligase that ubiquitylates Nrf2 for further degradation by proteasome [274] (Figure 24C, Chapter 1.4.2.3). Based on my preliminary results, the expression of XBP1s (spliced XBP1) and Hrd1 tended to increase only in CT cells but not in CTA cells upon 2 h exposure to HNE (Figure 49). This indicates that HNE provokes stronger ER stress in CT cells than in CTA cells and this ER stress contributes to Hrd1-dependent negative regulation of Nrf2 in CT cells. Higher HNE-induced ER stress in CT cells might be caused by lower basal Nrf2 activity in CT cells that led to their lower expression of HNE detoxification enzymes compared to CTA cells. Indeed, HNE has been demonstrated to be able to induce ER stress based on its ability to form adducts with proteins [210,503]. For further studies regarding ER stress following HNE

exposure, ER stress in CT and CTA cells can be validated by analyzing all three pathways of ER stress: IRE1, PERK and ATF6 as discussed in Chapter 1.4.2.3.

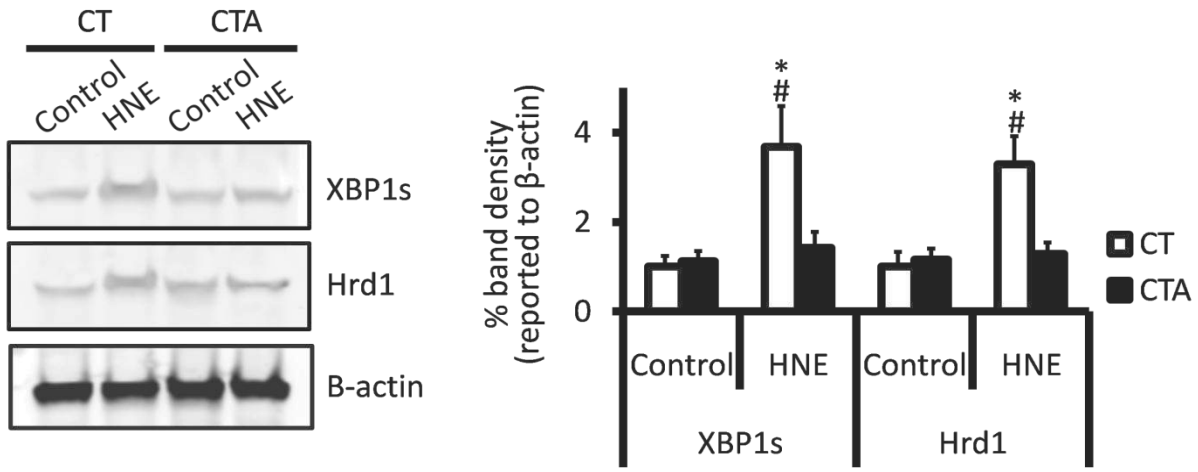

Figure 49. Western blotting analysis and densitometry of XBP1s and Hrd1 (n=3) in CT and CTA cells following treatment with HNE 20 μM (t=2 h). β-actin was used as loading control. * Significant difference between CT and CTA ($p<0.05$). # Significant difference in a cell line compared to control ($p<0.05$).

5.4. Fecal aldehydes determine in part the difference of apoptosis between normal and preneoplastic cells upon exposure to HNE or fecal water of heme-fed rats

In Articles 1 and 2, to analyze the importance of aldehydes derived from lipid peroxidation in fecal water, the depletion of fecal aldehydes was optimized by using carbonyl-trapping resin (CTR). This depletion appeared to abolish the differential of apoptosis observed in normal and preneoplastic cells upon exposure to HNE or fecal water of heme-fed rats. Supporting this finding, exposure to fecal water control obtained from standard diet-fed rats also did not provoke difference of apoptosis in normal and preneoplastic cells. These results show the importance of lipid peroxidation-derived aldehydes in the promotion of colorectal carcinogenesis by generating positive selection of preneoplastic cells over normal cells.

It is noteworthy that CTR does not only trap aldehydes in the fecal water, but all carbonyl compounds present in the fecal water. Apart from aldehydes, other carbonyl compounds that may present in the fecal water are ketones, carboxylic acids and esters. Regarding the chemical specificity of CTR towards carbonyl groups, CTR is very unlikely to bind with other potentially toxic molecules present in the fecal water, such as bile acid, bilirubin and lysophospholipids. Therefore, our study did not demonstrate that aldehydes were the sole responsible for different fecal water toxicity towards normal and preneoplastic cells.

Nevertheless, aldehydes are in part responsible for such a different fecal water toxicity since the reduction of TBARS and free HNE in CTR-treated fecal water was positively correlated with the abolition of different fecal water toxicity towards normal and preneoplastic cells.

To verify the effect of lipid peroxidation-derived aldehydes in colorectal carcinogenesis *in vivo*, especially HNE, a study using azoxymethane-injected rats fed with a precise amount of HNE is conducted in our team. The preliminary results showed that fecal water of HNE-fed rats was more cytotoxic to APC +/+ cells compared to APC Min/+ cells, as analyzed by time-lapse microscopy using fluorochrome for the detection of caspase-3/7 activity. Upon the completion of this study, the formation of preneoplastic lesions (ACF or MDF) in the colon can be observed and isolated from normal adjacent tissues by laser capture/cutting microdissection (LCM). Afterwards, the level of autophagy, Nrf2 or the expression of HNE detoxification enzymes can be analyzed and compared between the preneoplastic lesions and the normal tissues.

Since HNE is an aldehyde existing among a plethora of molecules present in fecal water of heme-fed rats, a question remains to answer: is HNE the sole agent determining the different fecal water toxicity between normal and preneoplastic cells? Or is it used only as a model for lipid peroxidation? Previously, in Articles 1 and 2, we showed that aldehydes were in part responsible for the different toxicity of fecal water of heme-fed rats in normal and preneoplastic cells. Therefore, it appears interesting to carry out studies to identify different potential aldehydes present in fecal water of heme-fed rats, especially those that are present in relatively high amount and strongly modulated by heme intake. This can be done by aldehydomics, a method for identifying aldehydes present in samples (fecal water) without “a priori” and analyzing their concentration. This method, that is developed in our team, can be done by using a probe that traps carbonyl compounds in the fecal water, followed by the analysis of the trapped carbonyl compounds by liquid chromatography coupled with high resolution mass spectrometry (LC/HRMS). Following aldehydomics, the relevant potential aldehydes can then be screened, for example in terms of their toxicity by treating epithelial colon cells with these purified aldehydes and analyzing their viability by WST-1 activity. This would allow the identification of pertinent aldehydes as fecal biomarkers of the promotion of colorectal carcinogenesis associated with red meat. In addition, aldehydomics would also allow to identify the carbonyl compounds in fecal water that are trapped by CTR because like CTR, the probe used in aldehydomics does not only trap aldehydes but all carbonyl compounds present in fecal water.

Chapter VI

CONCLUSIONS

My thesis allows to highlight the importance of heme-induced lipid peroxidation in the promotion of colorectal carcinogenesis by using biological matrix. Heme iron in hemoglobin or red meat, through its role as a potent catalyst for lipid peroxidation in the lumen of the colon, gives rise to the formation of cytotoxic aldehydes in the fecal water of heme-fed rats. One of these aldehydes is 4-hydroxy-2-nonenal (HNE), that was used in this study as a model for lipid peroxidation. HNE or fecal water of heme-fed rats exerted preferentially higher toxicity towards mouse-origin normal colon cells compared to colon cells with *APC* mutation (preneoplastic) *in vitro*. This finding was also extrapolated in human model by using human colonic epithelial cells (HCECs). *APC* knockdown HCECs (representing preneoplastic phenotype) were more resistant than wild type HCECs towards HNE or fecal water of heme-fed rats. This difference of resistance between normal and preneoplastic colon cells may explain the promotion of colorectal carcinogenesis through the positive selection of preneoplastic cells by fecal water of heme-fed rats. Fecal aldehydes were in part responsible for the different toxicity of fecal water of heme-fed rats towards normal and preneoplastic cells.

Furthermore, my thesis also points out autophagy (in human model) and Nrf2-dependent antioxidant responses (in mouse and human models) as mechanisms that are potentially involved in the resistance of preneoplastic cells to the toxicity of HNE and fecal water of heme-fed rats. Autophagy and Nrf2 were more up-regulated in preneoplastic colon cells compared to normal colon cells, both under basal conditions and upon exposure to fecal water of heme-fed rats. These mechanisms were suggested to be protective to preneoplastic cells and invalidation of these mechanisms sensitized preneoplastic cells to fecal water of heme-fed rats. In human model, high basal autophagy level in *APC* knockdown HCECs was associated with Nrf2 activation mediated by autophagic protein p62.

REFERENCES

1. WCRF/AICR (2011) Continuous Update Project Report. Food, Nutrition, Physical Activity, and the Prevention of Colorectal Cancer. World Cancer Research Fund / American Institute for Cancer Research.
2. Stewart, B.W.*, et al.* (eds.) (2014) *World Cancer Report 2014*. International Agency for Research on Cancer.
3. ACS (2015) *Global Cancer Facts and Figures*. American Cancer Society.
4. INCa (2015) *Les Cancers en France*. Institut National du Cancer.
5. NCI (2015) General information about colon cancer. http://www.cancer.gov/types/colorectal/patient/colon-treatment-pdq. Retrieved on 20 December 2015. National Cancer Institute.
6. Adelstein, B.A.*, et al.* Most bowel cancer symptoms do not indicate colorectal cancer and polyps: a systematic review. *BMC Gastroenterol*, **11**, 65.
7. Astin, M.*, et al.* The diagnostic value of symptoms for colorectal cancer in primary care: a systematic review. *Br J Gen Pract*, **61**, e231-43.
8. Cunningham, D.*, et al.* Colorectal cancer. *Lancet*, **375**, 1030-47.
9. Stein, A.*, et al.* (2011) Current standards and new trends in the primary treatment of colorectal cancer. *Eur J Cancer*, **47 Suppl 3**, S312-4.
10. Chemotherapy of metastatic colorectal cancer. *Prescrire Int*, **19**, 219-24.
11. Wasserberg, N.*, et al.* (2007) Palliation of colorectal cancer. *Surg Oncol*, **16**, 299-310.
12. Amersi, F.*, et al.* (2004) Palliative care for colorectal cancer. *Surg Oncol Clin N Am*, **13**, 467-77.
13. Jess, T.*, et al.* (2012) Risk of colorectal cancer in patients with ulcerative colitis: a meta-analysis of population-based cohort studies. *Clin Gastroenterol Hepatol*, **10**, 639-45.
14. Canavan, C.*, et al.* (2006) Meta-analysis: colorectal and small bowel cancer risk in patients with Crohn's disease. *Aliment Pharmacol Ther*, **23**, 1097-104.
15. Triantafillidis, J.K.*, et al.* (2009) Colorectal cancer and inflammatory bowel disease: epidemiology, risk factors, mechanisms of carcinogenesis and prevention strategies. *Anticancer Res*, **29**, 2727-37.
16. Krogh, D. (2010) *Biology: A Guide to the Natural World*. Benjamin-Cummings Publishing Company.
17. Hounnou, G.*, et al.* (2002) Anatomical study of the length of the human intestine. *Surg Radiol Anat*, **24**, 290-4.
18. AJCC (2009) *AJCC Cancer Staging Atlas*. American Joint Committee on Cancer.
19. ACS (2014) *Colorectal Cancer Facts and Figures 2014-2016*. American Cancer Society, Atlanta.
20. MacFarlane, A.J.*, et al.* (2007) Convergence of genetic, nutritional and inflammatory factors in gastrointestinal cancers. *Nutr Rev*, **65**, S157-66.
21. BBC (2013) How colon therapy works? http://www.bbccolonic.ca/index.php/colonic/colonic-procedure/how-colonic-works. Retrieved on 15 January 2016. Back to Balance Center.
22. Reya, T.*, et al.* (2005) Wnt signalling in stem cells and cancer. *Nature*, **434**, 843-50.
23. Humphries, A.*, et al.* (2008) Colonic crypt organization and tumorigenesis. *Nat Rev Cancer*, **8**, 415-24.
24. Baker, A.M.*, et al.* Quantification of crypt and stem cell evolution in the normal and neoplastic human colon. *Cell Rep*, **8**, 940-7.
25. Nooteboom, M.*, et al.* Age-associated mitochondrial DNA mutations lead to small but significant changes in cell proliferation and apoptosis in human colonic crypts. *Aging Cell*, **9**, 96-9.
26. Fearnhead, N.S.*, et al.* (2002) Genetics of colorectal cancer: hereditary aspects and overview of colorectal tumorigenesis. *Br Med Bull*, **64**, 27-43.
27. Heinen, C.D. (2010) Genotype to phenotype: analyzing the effects of inherited mutations in colorectal cancer families. *Mutat Res*, **693**, 32-45.

28. Jagelman, D.G.*, et al.* (1988) Upper gastrointestinal cancer in familial adenomatous polyposis. *Lancet*, **1**, 1149-51.
29. Spirio, L.*, et al.* (1993) Alleles of the APC gene: an attenuated form of familial polyposis. *Cell*, **75**, 951-7.
30. Jasperson, K.W.*, et al.* Hereditary and familial colon cancer. *Gastroenterology*, **138**, 2044-58.
31. Powell, S.M.*, et al.* (1992) APC mutations occur early during colorectal tumorigenesis. *Nature*, **359**, 235-7.
32. Smith, K.J.*, et al.* (1993) The APC gene product in normal and tumor cells. *Proc Natl Acad Sci U S A*, **90**, 2846-50.
33. Hampel, H.*, et al.* (2008) Feasibility of screening for Lynch syndrome among patients with colorectal cancer. *J Clin Oncol*, **26**, 5783-8.
34. Marra, G.*, et al.* (1995) Hereditary nonpolyposis colorectal cancer: the syndrome, the genes, and historical perspectives. *J Natl Cancer Inst*, **87**, 1114-25.
35. Vasen, H.F.*, et al.* (1999) New clinical criteria for hereditary nonpolyposis colorectal cancer (HNPCC, Lynch syndrome) proposed by the International Collaborative group on HNPCC. *Gastroenterology*, **116**, 1453-6.
36. Stoffel, E.*, et al.* (2009) Calculation of risk of colorectal and endometrial cancer among patients with Lynch syndrome. *Gastroenterology*, **137**, 1621-7.
37. Liu, B.*, et al.* (1996) Analysis of mismatch repair genes in hereditary non-polyposis colorectal cancer patients. *Nat Med*, **2**, 169-74.
38. Imai, K.*, et al.* (2008) Carcinogenesis and microsatellite instability: the interrelationship between genetics and epigenetics. *Carcinogenesis*, **29**, 673-80.
39. Fearon, E.R. Molecular genetics of colorectal cancer. *Annu Rev Pathol*, **6**, 479-507.
40. Network, C.G.A. (2012) Comprehensive molecular characterization of human colon and rectal cancer. *Nature*, **487**, 330-7.
41. Fearon, E.R.*, et al.* (1990) A genetic model for colorectal tumorigenesis. *Cell*, **61**, 759-67.
42. Vogelstein, B.*, et al.* (1993) The multistep nature of cancer. *Trends Genet*, **9**, 138-41.
43. Lengauer, C.*, et al.* (1998) Genetic instabilities in human cancers. *Nature*, **396**, 643-9.
44. Tomasetti, C.*, et al.* (2015) Only three driver gene mutations are required for the development of lung and colorectal cancers. *Proc Natl Acad Sci U S A*, **112**, 118-23.
45. Vogelstein, B.*, et al.* (1989) Allelotype of colorectal carcinomas. *Science*, **244**, 207-11.
46. Lindblom, A. (2001) Different mechanisms in the tumorigenesis of proximal and distal colon cancers. *Curr Opin Oncol*, **13**, 63-9.
47. Leggett, B.*, et al.* (2010) Role of the serrated pathway in colorectal cancer pathogenesis. *Gastroenterology*, **138**, 2088-100.
48. Weisenberger, D.J.*, et al.* (2006) CpG island methylator phenotype underlies sporadic microsatellite instability and is tightly associated with BRAF mutation in colorectal cancer. *Nat Genet*, **38**, 787-93.
49. Walther, A.*, et al.* (2009) Genetic prognostic and predictive markers in colorectal cancer. *Nat Rev Cancer*, **9**, 489-99.
50. Marusyk, A.*, et al.* (2010) Tumor heterogeneity: causes and consequences. *Biochim Biophys Acta*, **1805**, 105-17.
51. Greaves, M. (2010) Cancer stem cells: back to Darwin? *Semin Cancer Biol*, **20**, 65-70.
52. Shackleton, M.*, et al.* (2009) Heterogeneity in cancer: cancer stem cells versus clonal evolution. *Cell*, **138**, 822-9.
53. Blanco-Calvo, M.*, et al.* (2015) Colorectal Cancer Classification and Cell Heterogeneity: A Systems Oncology Approach. *Int J Mol Sci*, **16**, 13610-32.
54. Samowitz, W.S.*, et al.* (1999) Regional reproducibility of microsatellite instability in sporadic colorectal cancer. *Genes Chromosomes Cancer*, **26**, 106-14.
55. Giaretti, W.*, et al.* (1996) Intratumor heterogeneity of K-ras2 mutations in colorectal adenocarcinomas: association with degree of DNA aneuploidy. *Am J Pathol*, **149**, 237-45.
56. Nowell, P.C. (1976) The clonal evolution of tumor cell populations. *Science*, **194**, 23-8.

57. Swanton, C. (2012) Intratumor heterogeneity: evolution through space and time. *Cancer Res*, **72**, 4875-82.
58. Merlo, L.M.*, et al.* (2006) Cancer as an evolutionary and ecological process. *Nat Rev Cancer*, **6**, 924-35.
59. Gerlinger, M.*, et al.* (2012) Intratumor heterogeneity and branched evolution revealed by multiregion sequencing. *N Engl J Med*, **366**, 883-92.
60. Moreno, E. (2014) Cancer: Darwinian tumour suppression. *Nature*, **509**, 435-6.
61. Pierre, F.*, et al.* (2007) Apc mutation induces resistance of colonic cells to lipoperoxide-triggered apoptosis induced by faecal water from haem-fed rats. *Carcinogenesis*, **28**, 321-7.
62. Baradat, M.*, et al.* (2011) 4-Hydroxy-2(E)-nonenal metabolism differs in Apc(+/+) cells and in Apc(Min/+) cells: it may explain colon cancer promotion by heme iron. *Chem Res Toxicol*, **24**, 1984-93.
63. Surya, R.*, et al.* (2016) Red Meat and Colorectal Cancer: Nrf2-Dependent Antioxidant Response Contributes to the Resistance of Preneoplastic Colon Cells to Fecal Water of Hemoglobin- and Beef-Fed Rats. *Carcinogenesis*.
64. Dow, L.E.*, et al.* (2015) Apc Restoration Promotes Cellular Differentiation and Reestablishes Crypt Homeostasis in Colorectal Cancer. *Cell*, **161**, 1539-52.
65. Nelson, S.*, et al.* (2013) Interactions and functions of the adenomatous polyposis coli (APC) protein at a glance. *J Cell Sci*, **126**, 873-7.
66. Narayan, S.*, et al.* (2003) Role of APC and DNA mismatch repair genes in the development of colorectal cancers. *Mol Cancer*, **2**, 41.
67. Beroud, C.*, et al.* (1996) APC gene: database of germline and somatic mutations in human tumors and cell lines. *Nucleic Acids Res*, **24**, 121-4.
68. Miyoshi, Y.*, et al.* (1992) Germ-line mutations of the APC gene in 53 familial adenomatous polyposis patients. *Proc Natl Acad Sci U S A*, **89**, 4452-6.
69. Sansom, O.J.*, et al.* (2004) Loss of Apc in vivo immediately perturbs Wnt signaling, differentiation, and migration. *Genes Dev*, **18**, 1385-90.
70. Mao, B.*, et al.* (2001) LDL-receptor-related protein 6 is a receptor for Dickkopf proteins. *Nature*, **411**, 321-5.
71. Miller, J.R.*, et al.* (1996) Signal transduction through beta-catenin and specification of cell fate during embryogenesis. *Genes Dev*, **10**, 2527-39.
72. Dale, T.C. (1998) Signal transduction by the Wnt family of ligands. *Biochem J*, **329 (Pt 2)**, 209-23.
73. McDonald, S.A.*, et al.* (2006) Mechanisms of disease: from stem cells to colorectal cancer. *Nat Clin Pract Gastroenterol Hepatol*, **3**, 267-74.
74. Sadanandam, A.*, et al.* (2013) A colorectal cancer classification system that associates cellular phenotype and responses to therapy. *Nat Med*, **19**, 619-25.
75. Eastman, Q.*, et al.* (1999) Regulation of LEF-1/TCF transcription factors by Wnt and other signals. *Curr Opin Cell Biol*, **11**, 233-40.
76. Akiyama, T.*, et al.* (2006) Wnt signalling and the actin cytoskeleton. *Oncogene*, **25**, 7538-44.
77. Kawasaki, Y.*, et al.* (2003) Mutated APC and Asef are involved in the migration of colorectal tumour cells. *Nat Cell Biol*, **5**, 211-5.
78. Kawasaki, Y.*, et al.* (2000) Asef, a link between the tumor suppressor APC and G-protein signaling. *Science*, **289**, 1194-7.
79. Watanabe, T.*, et al.* (2004) Interaction with IQGAP1 links APC to Rac1, Cdc42, and actin filaments during cell polarization and migration. *Dev Cell*, **7**, 871-83.
80. Green, R.A.*, et al.* (2005) APC and EB1 function together in mitosis to regulate spindle dynamics and chromosome alignment. *Mol Biol Cell*, **16**, 4609-22.
81. Moss, S.F.*, et al.* (1996) Inward growth of colonic adenomatous polyps. *Gastroenterology*, **111**, 1425-32.
82. Fodde, R.*, et al.* (2001) Mutations in the APC tumour suppressor gene cause chromosomal instability. *Nat Cell Biol*, **3**, 433-8.

83. Fodde, R.*, et al.* (2001) APC, signal transduction and genetic instability in colorectal cancer. *Nat Rev Cancer*, **1**, 55-67.
84. Kaplan, K.B.*, et al.* (2001) A role for the Adenomatous Polyposis Coli protein in chromosome segregation. *Nat Cell Biol*, **3**, 429-32.
85. McCart, A.E.*, et al.* (2008) Apc mice: models, modifiers and mutants. *Pathol Res Pract*, **204**, 479-90.
86. Fodde, R.*, et al.* (1994) A targeted chain-termination mutation in the mouse Apc gene results in multiple intestinal tumors. *Proc Natl Acad Sci U S A*, **91**, 8969-73.
87. Moser, A.R.*, et al.* (1990) A dominant mutation that predisposes to multiple intestinal neoplasia in the mouse. *Science*, **247**, 322-4.
88. Su, L.K.*, et al.* (1992) Multiple intestinal neoplasia caused by a mutation in the murine homolog of the APC gene. *Science*, **256**, 668-70.
89. Crist, R.C.*, et al.* (2010) The armadillo repeat domain of Apc suppresses intestinal tumorigenesis. *Mamm Genome*, **21**, 450-7.
90. Taketo, M.M. (2006) Mouse models of gastrointestinal tumors. *Cancer Sci*, **97**, 355-61.
91. Aoki, K.*, et al.* (2003) Colonic polyposis caused by mTOR-mediated chromosomal instability in Apc+/Delta716 Cdx2+/- compound mutant mice. *Nat Genet*, **35**, 323-30.
92. Colnot, S.*, et al.* (2004) Colorectal cancers in a new mouse model of familial adenomatous polyposis: influence of genetic and environmental modifiers. *Lab Invest*, **84**, 1619-30.
93. Kuraguchi, M.*, et al.* (2006) Adenomatous polyposis coli (APC) is required for normal development of skin and thymus. *PLoS Genet*, **2**, e146.
94. Sasai, H.*, et al.* (2000) Suppression of polypogenesis in a new mouse strain with a truncated Apc(Delta474) by a novel COX-2 inhibitor, JTE-522. *Carcinogenesis*, **21**, 953-8.
95. Li, Q.*, et al.* (2005) The threshold level of adenomatous polyposis coli protein for mouse intestinal tumorigenesis. *Cancer Res*, **65**, 8622-7.
96. Quesada, C.F.*, et al.* (1998) Piroxicam and acarbose as chemopreventive agents for spontaneous intestinal adenomas in APC gene 1309 knockout mice. *Jpn J Cancer Res*, **89**, 392-6.
97. Smits, R.*, et al.* (1998) Apc1638N: a mouse model for familial adenomatous polyposis-associated desmoid tumors and cutaneous cysts. *Gastroenterology*, **114**, 275-83.
98. Cheung, A.F.*, et al.* (2010) Complete deletion of Apc results in severe polyposis in mice. *Oncogene*, **29**, 1857-64.
99. Amos-Landgraf, J.M.*, et al.* (2007) A target-selected Apc-mutant rat kindred enhances the modeling of familial human colon cancer. *Proc Natl Acad Sci U S A*, **104**, 4036-41.
100. Forest, V.*, et al.* (2003) Butyrate restores motile function and actin cytoskeletal network integrity in apc mutated mouse colon epithelial cells. *Nutr Cancer*, **45**, 84-92.
101. Roig, A.I.*, et al.* (2010) Immortalized epithelial cells derived from human colon biopsies express stem cell markers and differentiate in vitro. *Gastroenterology*, **138**, 1012-21 e1-5.
102. Graillot, V.*, et al.* (2016) Genotoxicity of Cytolethal Distending Toxin (CDT) on Isogenic Human Colorectal Cell Lines: Potential Promoting Effects for Colorectal Carcinogenesis. *Front Cell Infect Microbiol*, **6**, 34.
103. Anand, P.*, et al.* (2008) Cancer is a preventable disease that requires major lifestyle changes. *Pharm Res*, **25**, 2097-116.
104. Minamoto, T.*, et al.* (1999) Environmental factors as regulators and effectors of multistep carcinogenesis. *Carcinogenesis*, **20**, 519-27.
105. Wu, S.*, et al.* (2016) Substantial contribution of extrinsic risk factors to cancer development. *Nature*, **529**, 43-7.
106. Tomasetti, C.*, et al.* (2015) Cancer etiology. Variation in cancer risk among tissues can be explained by the number of stem cell divisions. *Science*, **347**, 78-81.
107. Haggar, F.A.*, et al.* (2009) Colorectal cancer epidemiology: incidence, mortality, survival, and risk factors. *Clin Colon Rectal Surg*, **22**, 191-7.
108. Boyle, P.*, et al.* (2000) ABC of colorectal cancer: Epidemiology. *BMJ*, **321**, 805-8.

109. Janout, V., *et al.* (2001) Epidemiology of colorectal cancer. *Biomed Pap Med Fac Univ Palacky Olomouc Czech Repub*, **145**, 5-10.
110. Johnson, I.T., *et al.* (2007) Review article: nutrition, obesity and colorectal cancer. *Aliment Pharmacol Ther*, **26**, 161-81.
111. WCRF/AICR (1997) Food, Nutrition and the Prevention of Cancer: A Global Perspective. World Cancer Research Fund/American Institute of Cancer, Washington DC.
112. WCRF/AICR (2007) Food, Nutrition, Physical Activity and the Prevention of Cancer: A Global Perspective. World Cancer Research Fund/American Institute of Cancer, Washington DC.
113. Chan, D.S., *et al.* (2011) Red and processed meat and colorectal cancer incidence: meta-analysis of prospective studies. *PLoS One*, **6**, e20456.
114. Bouvard, V., *et al.* (2015) Carcinogenicity of consumption of red and processed meat. *Lancet Oncol*, **16**, 1599-600.
115. IARC (2015) Press release. IARC Monographs evaluate consumption of red meat and processed meat. http://www.iarc.fr/en/media-centre/pr/2015/pdfs/pr240_E.pdf. Retrieved on 15 February 2016. International Agency for Research on Cancer, Lyon.
116. FAO (2015) Food balance. http://faostat3.fao.org/browse/FB/*/E. Retrieved on 15 February 2016. Food and Agricultural Organization, Rome.
117. Frauenfelder, H., *et al.* (2001) The role of structure, energy landscape, dynamics, and allostery in the enzymatic function of myoglobin. *Proc Natl Acad Sci U S A*, **98**, 2370-4.
118. Ordway, G.A., *et al.* (2004) Myoglobin: an essential hemoprotein in striated muscle. *J Exp Biol*, **207**, 3441-6.
119. Samraj, A.N., *et al.* (2015) A red meat-derived glycan promotes inflammation and cancer progression. *Proc Natl Acad Sci U S A*, **112**, 542-7.
120. Santarelli, R.L., *et al.* (2008) Processed meat and colorectal cancer: a review of epidemiologic and experimental evidence. *Nutr Cancer*, **60**, 131-44.
121. Bruce, W.R. (1987) Recent hypotheses for the origin of colon cancer. *Cancer Res*, **47**, 4237-42.
122. Larsson, S.C., *et al.* (2006) Meat consumption and risk of colorectal cancer: a meta-analysis of prospective studies. *Int J Cancer*, **119**, 2657-64.
123. Calle, E.E., *et al.* (2004) Overweight, obesity and cancer: epidemiological evidence and proposed mechanisms. *Nat Rev Cancer*, **4**, 579-91.
124. Calle, E.E., *et al.* (2004) Obesity and cancer. *Oncogene*, **23**, 6365-78.
125. Pence, B.C., *et al.* (1995) Non-promoting effects of lean beef in the rat colon carcinogenesis model. *Carcinogenesis*, **16**, 1157-60.
126. Bull, A.W., *et al.* (1979) Promotion of azoxymethane-induced intestinal cancer by high-fat diet in rats. *Cancer Res*, **39**, 4956-9.
127. Reddy, B.S., *et al.* (1976) Effect of a diet with high levels of protein and fat on colon carcinogenesis in F344 rats treated with 1,2-dimethylhydrazine. *J Natl Cancer Inst*, **57**, 567-9.
128. Kumar, S.P., *et al.* (1990) Effect of different levels of calorie restriction on azoxymethane-induced colon carcinogenesis in male F344 rats. *Cancer Res*, **50**, 5761-6.
129. Nauss, K.M., *et al.* (1983) Effect of alterations in the quality and quantity of dietary fat on 1,2-dimethylhydrazine-induced colon tumorigenesis in rats. *Cancer Res*, **43**, 4083-90.
130. Nutter, R.L., *et al.* (1983) BALB/c mice fed milk or beef protein: differences in response to 1,2-dimethylhydrazine carcinogenesis. *J Natl Cancer Inst*, **71**, 867-74.
131. Clinton, S.K., *et al.* (1992) The combined effects of dietary fat, protein, and energy intake on azoxymethane-induced intestinal and renal carcinogenesis. *Cancer Res*, **52**, 857-65.
132. Sesink, A.L., *et al.* (2000) Red meat and colon cancer: dietary haem, but not fat, has cytotoxic and hyperproliferative effects on rat colonic epithelium. *Carcinogenesis*, **21**, 1909-15.
133. Khil, J., *et al.* (2004) Beef tallow increases apoptosis and decreases aberrant crypt foci formation relative to soybean oil in rat colon. *Nutr Cancer*, **50**, 55-62.
134. Zhao, L.P., *et al.* (1991) Quantitative review of studies of dietary fat and rat colon carcinoma. *Nutr Cancer*, **15**, 169-77.

135. Alexander, D.D*., et al.* (2009) Meta-analysis of animal fat or animal protein intake and colorectal cancer. *Am J Clin Nutr*, **89**, 1402-9.
136. Sinha, R*., et al.* (1998) Heterocyclic amine content in beef cooked by different methods to varying degrees of doneness and gravy made from meat drippings. *Food Chem Toxicol*, **36**, 279-87.
137. Turesky, R.J. (2007) Formation and biochemistry of carcinogenic heterocyclic aromatic amines in cooked meats. *Toxicol Lett*, **168**, 219-27.
138. Skog, K.I*., et al.* (1998) Carcinogenic heterocyclic amines in model systems and cooked foods: a review on formation, occurrence and intake. *Food Chem Toxicol*, **36**, 879-96.
139. Sugimura, T*., et al.* (2004) Heterocyclic amines: Mutagens/carcinogens produced during cooking of meat and fish. *Cancer Sci*, **95**, 290-9.
140. Krais, A.M*., et al.* (2014) Comparison of the metabolic activation of environmental carcinogens in mouse embryonic stem cells and mouse embryonic fibroblasts. *Toxicol In Vitro*, **29**, 34-43.
141. Alexandrov, K*., et al.* (1996) Evidence of anti-benzo[a]pyrene diolepoxide-DNA adduct formation in human colon mucosa. *Carcinogenesis*, **17**, 2081-3.
142. Phillips, D.H. (1999) Polycyclic aromatic hydrocarbons in the diet. *Mutat Res*, **443**, 139-47.
143. O'Neill, I.K*., et al.* (1991) Dietary fibre, fat and beef modulation of colonic nuclear aberrations and microcapsule-trapped gastrointestinal metabolites of benzo[a]pyrene-treated C57/B6 mice consuming human diets. *Carcinogenesis*, **12**, 175-80.
144. Tudek, B*., et al.* (1989) Foci of aberrant crypts in the colons of mice and rats exposed to carcinogens associated with foods. *Cancer Res*, **49**, 1236-40.
145. Cross, A.J*., et al.* (2010) Developing a heme iron database for meats according to meat type, cooking method and doneness level. *Food Nutr Sci*, **3**, 905-913.
146. Zheng, W*., et al.* (2009) Well-done meat intake, heterocyclic amine exposure, and cancer risk. *Nutr Cancer*, **61**, 437-46.
147. Abid, Z*., et al.* (2014) Meat, dairy, and cancer. *Am J Clin Nutr*, **100 Suppl 1**, 386S-93S.
148. Ollberding, N.J*., et al.* (2012) Meat consumption, heterocyclic amines and colorectal cancer risk: the Multiethnic Cohort Study. *Int J Cancer*, **131**, E1125-33.
149. Tabatabaei, S.M*., et al.* (2010) Dietary benzo[a]pyrene intake from meat and the risk of colorectal cancer. *Cancer Epidemiol Biomarkers Prev*, **19**, 3182-4.
150. Gilsing, A.M*., et al.* (2012) Meat-related mutagen exposure, xenobiotic metabolizing gene polymorphisms and the risk of advanced colorectal adenoma and cancer. *Carcinogenesis*, **33**, 1332-9.
151. Wang, J*., et al.* (2012) Carcinogen metabolism genes, red meat and poultry intake, and colorectal cancer risk. *Int J Cancer*, **130**, 1898-907.
152. Kuhnle, G.G*., et al.* (2007) Dietary meat, endogenous nitrosation and colorectal cancer. *Biochem Soc Trans*, **35**, 1355-7.
153. Lijinsky, W. (1999) N-Nitroso compounds in the diet. *Mutat Res*, **443**, 129-38.
154. Cross, A.J*., et al.* (2003) Haem, not protein or inorganic iron, is responsible for endogenous intestinal N-nitrosation arising from red meat. *Cancer Res*, **63**, 2358-60.
155. Cross, A.J*., et al.* (2004) Meat-related mutagens/carcinogens in the etiology of colorectal cancer. *Environ Mol Mutagen*, **44**, 44-55.
156. Mirvish, S.S*., et al.* (2003) N-nitroso compounds in the gastrointestinal tract of rats and in the feces of mice with induced colitis or fed hot dogs or beef. *Carcinogenesis*, **24**, 595-603.
157. Haorah, J*., et al.* (2001) Determination of total N-nitroso compounds and their precursors in frankfurters, fresh meat, dried salted fish, sauces, tobacco, and tobacco smoke particulates. *J Agric Food Chem*, **49**, 6068-78.
158. Parnaud, G*., et al.* (2000) Endogenous N-nitroso compounds, and their precursors, present in bacon, do not initiate or promote aberrant crypt foci in the colon of rats. *Nutr Cancer*, **38**, 74-80.

159. Bastide, N.*, et al.* (2015) A central role for heme iron in colon carcinogenesis associated with red meat intake. *Cancer Res*, **75**, 870-9

160. Bingham, S.A.*, et al.* (2002) Effect of white versus red meat on endogenous N-nitrosation in the human colon and further evidence of a dose response. *J Nutr*, **132**, 3522S-3525S.
161. Joosen, A.M.*, et al.* (2009) Effect of processed and red meat on endogenous nitrosation and DNA damage. *Carcinogenesis*, **30**, 1402-7.
162. Zhu, Y.*, et al.* (2014) Dietary N-nitroso compounds and risk of colorectal cancer: a case-control study in Newfoundland and Labrador and Ontario, Canada. *Br J Nutr*, **111**, 1109-17.
163. Loh, Y.H.*, et al.* (2011) N-Nitroso compounds and cancer incidence: the European Prospective Investigation into Cancer and Nutrition (EPIC)-Norfolk Study. *Am J Clin Nutr*, **93**, 1053-61.
164. IARC (2015) IARC monographs on the evaluation of carcinogenic risks to humans. http://monographs.iarc.fr/ENG/Classification/latest_classif.php. Retrieved on 15 February 2016. International Agency for Research on Cancer, Lyon.
165. Mirvish, S.S. (1995) Role of N-nitroso compounds (NOC) and N-nitrosation in etiology of gastric, esophageal, nasopharyngeal and bladder cancer and contribution to cancer of known exposures to NOC. *Cancer Lett*, **93**, 17-48.
166. Samraj, A.N.*, et al.* (2014) Involvement of a non-human sialic Acid in human cancer. *Front Oncol*, **4**, 33.
167. Samraj, A.N.*, et al.* (2014) Corrigendum: involvement of a non-human sialic Acid in human cancer. *Front Oncol*, **4**, 83.
168. Varki, A. (2009) Multiple changes in sialic acid biology during human evolution. *Glycoconj J*, **26**, 231-45.
169. Hedlund, M.*, et al.* (2008) Evidence for a human-specific mechanism for diet and antibody-mediated inflammation in carcinoma progression. *Proc Natl Acad Sci U S A*, **105**, 18936-41.
170. Banda, K.*, et al.* (2012) Metabolism of vertebrate amino sugars with N-glycolyl groups: mechanisms underlying gastrointestinal incorporation of the non-human sialic acid xeno-autoantigen N-glycolylneuraminic acid. *J Biol Chem*, **287**, 28852-64.
171. Larsen, R.*, et al.* (2012) Heme cytotoxicity and the pathogenesis of immune-mediated inflammatory diseases. *Front Pharmacol*, **3**, 77.
172. Khan, A.A.*, et al.* (2011) Control of intracellular heme levels: heme transporters and heme oxygenases. *Biochim Biophys Acta*, **1813**, 668-82.
173. Sesink, A.L.*, et al.* (1999) Red meat and colon cancer: the cytotoxic and hyperproliferative effects of dietary heme. *Cancer Res*, **59**, 5704-9.
174. Radulescu, S.*, et al.* (2012) Luminal iron levels govern intestinal tumorigenesis after Apc loss in vivo. *Cell Rep*, **2**, 270-82.
175. Bastide, N.M.*, et al.* (2011) Heme iron from meat and risk of colorectal cancer: a meta-analysis and a review of the mechanisms involved. *Cancer Prev Res (Phila)*, **4**, 177-84.
176. Glei, M.*, et al.* (2006) Hemoglobin and hemin induce DNA damage in human colon tumor cells HT29 clone 19A and in primary human colonocytes. *Mutat Res*, **594**, 162-71.
177. Angeli, J.P.*, et al.* (2011) Lipid hydroperoxide-induced and hemoglobin-enhanced oxidative damage to colon cancer cells. *Free Radic Biol Med*, **51**, 503-15.
178. Ijssennagger, N.*, et al.* (2012) Dietary heme-mediated PPARalpha activation does not affect the heme-induced epithelial hyperproliferation and hyperplasia in mouse colon. *PLoS One*, **7**, e43260.
179. Edmunds, M.C.*, et al.* (2014) Paradoxical effects of heme arginate on survival of myocutaneous flaps. *Am J Physiol Regul Integr Comp Physiol*, **306**, R10-22.
180. Ryter, S.W.*, et al.* (2006) Heme oxygenase-1/carbon monoxide: from basic science to therapeutic applications. *Physiol Rev*, **86**, 583-650.
181. Kikuchi, G.*, et al.* (2005) Heme oxygenase and heme degradation. *Biochem Biophys Res Commun*, **338**, 558-67.

182. Ishikawa, S.*, et al.* (2010) Heme induces DNA damage and hyperproliferation of colonic epithelial cells via hydrogen peroxide produced by heme oxygenase: a possible mechanism of heme-induced colon cancer. *Mol Nutr Food Res*, **54**, 1182-91.
183. Sesink, A.L.*, et al.* (2001) Red meat and colon cancer: dietary haem-induced colonic cytotoxicity and epithelial hyperproliferation are inhibited by calcium. *Carcinogenesis*, **22**, 1653-9.
184. Pierre, F.*, et al.* (2003) Meat and cancer: haemoglobin and haemin in a low-calcium diet promote colorectal carcinogenesis at the aberrant crypt stage in rats. *Carcinogenesis*, **24**, 1683-90.
185. Pierre, F.*, et al.* (2008) Beef meat promotion of dimethylhydrazine-induced colorectal carcinogenesis biomarkers is suppressed by dietary calcium. *Br J Nutr*, **99**, 1000-6.
186. de Vogel, J.*, et al.* (2005) Natural chlorophyll but not chlorophyllin prevents heme-induced cytotoxic and hyperproliferative effects in rat colon. *J Nutr*, **135**, 1995-2000.
187. de Vogel, J.*, et al.* (2005) Green vegetables, red meat and colon cancer: chlorophyll prevents the cytotoxic and hyperproliferative effects of haem in rat colon. *Carcinogenesis*, **26**, 387-93.
188. Mirvish, S.S. (1975) Formation of N-nitroso compounds: chemistry, kinetics, and in vivo occurrence. *Toxicol Appl Pharmacol*, **31**, 325-51.
189. Mirvish, S.S. (1975) Blocking the formation of N-nitroso compounds with ascorbic acid in vitro and in vivo. *Ann N Y Acad Sci*, **258**, 175-80.
190. Mirvish, S.S. (1986) Effects of vitamins C and E on N-nitroso compound formation, carcinogenesis, and cancer. *Cancer*, **58**, 1842-50.
191. Hughes, R.*, et al.* (2001) Dose-dependent effect of dietary meat on endogenous colonic N-nitrosation. *Carcinogenesis*, **22**, 199-202.
192. Jacoby, R.F.*, et al.* (1992) K-ras oncogene mutations in rat colon tumors induced by N-methyl-N-nitrosourea. *Carcinogenesis*, **13**, 45-9.
193. Shuker, D.E.*, et al.* (1997) Nitrosated glycine derivatives as a potential source of O6-methylguanine in DNA. *Cancer Res*, **57**, 366-9.
194. Lewin, M.H.*, et al.* (2006) Red meat enhances the colonic formation of the DNA adduct O6-carboxymethyl guanine: implications for colorectal cancer risk. *Cancer Res*, **66**, 1859-65.
195. Ayala, A.*, et al.* (2014) Lipid peroxidation: production, metabolism, and signaling mechanisms of malondialdehyde and 4-hydroxy-2-nonenal. *Oxid Med Cell Longev*, **2014**, 360438.
196. Marnett, L.J. (2000) Oxyradicals and DNA damage. *Carcinogenesis*, **21**, 361-70.
197. Gueraud, F.*, et al.* (2015) Dietary polyunsaturated fatty acids and heme iron induce oxidative stress biomarkers and a cancer promoting environment in the colon of rats. *Free Radic Biol Med*, **83**, 192-200.
198. Niedernhofer, L.J.*, et al.* (2003) Malondialdehyde, a product of lipid peroxidation, is mutagenic in human cells. *J Biol Chem*, **278**, 31426-33.
199. Marnett, L.J. (1999) Lipid peroxidation-DNA damage by malondialdehyde. *Mutat Res*, **424**, 83-95.
200. Basu, A.K.*, et al.* (1983) Unequivocal demonstration that malondialdehyde is a mutagen. *Carcinogenesis*, **4**, 331-3.
201. Prasad, K.N.*, et al.* (1992) Vitamin E and cancer prevention: recent advances and future potentials. *J Am Coll Nutr*, **11**, 487-500.
202. Ross, J.A.*, et al.* (2002) Dietary flavonoids: bioavailability, metabolic effects, and safety. *Annu Rev Nutr*, **22**, 19-34.
203. Gorelik, S.*, et al.* (2008) A novel function of red wine polyphenols in humans: prevention of absorption of cytotoxic lipid peroxidation products. *FASEB J*, **22**, 41-6.
204. Martin, O.C.*, et al.* (2015) Antibiotic suppression of intestinal microbiota reduces heme-induced lipoperoxidation associated with colon carcinogenesis in rats. *Nutr Cancer*, **67**, 119-25.
205. Neyens, E.*, et al.* (2003) A review of classic Fenton's peroxidation as an advanced oxidation technique. *J Hazard Mater*, **98**, 33-50.

206. Bhagat, S.S.*, et al.* (2011) Lipid peroxidation and antioxidant vitamin status in colorectal cancer patients. *Indian J Physiol Pharmacol*, **55**, 72-6.
207. Pierre, F.H.*, et al.* (2013) Calcium and alpha-tocopherol suppress cured-meat promotion of chemically induced colon carcinogenesis in rats and reduce associated biomarkers in human volunteers. *Am J Clin Nutr*, **98**, 1255-62.
208. Arain, M.A.*, et al.* (2010) Systematic review on "vitamin E and prevention of colorectal cancer". *Pak J Pharm Sci*, **23**, 125-30.
209. Butterfield, D.A.*, et al.* (2010) Involvements of the lipid peroxidation product, HNE, in the pathogenesis and progression of Alzheimer's disease. *Biochim Biophys Acta*, **1801**, 924-9.
210. Dalleau, S.*, et al.* (2013) Cell death and diseases related to oxidative stress: 4-hydroxynonenal (HNE) in the balance. *Cell Death Differ*, **20**, 1615-30.
211. Duryee, M.J.*, et al.* (2004) Mechanisms of alcohol liver damage: aldehydes, scavenger receptors, and autoimmunity. *Front Biosci*, **9**, 3145-55.
212. Poli, G.*, et al.* (2008) 4-hydroxynonenal: a membrane lipid oxidation product of medicinal interest. *Med Res Rev*, **28**, 569-631.
213. Pierre, F.*, et al.* (2006) New marker of colon cancer risk associated with heme intake: 1,4-dihydroxynonane mercapturic acid. *Cancer Epidemiol Biomarkers Prev*, **15**, 2274-9.
214. Cheeseman, K.H.*, et al.* (1984) Lipid peroxidation and lipid antioxidants in normal and tumor cells. *Toxicol Pathol*, **12**, 235-9.
215. Tjalkens, R.B.*, et al.* (1999) Formation and export of the glutathione conjugate of 4-hydroxy-2, 3-E-nonenal (4-HNE) in hepatoma cells. *Arch Biochem Biophys*, **361**, 113-9.
216. Oberley, T.D.*, et al.* (1999) Localization of hydroxynonenal protein adducts in normal human kidney and selected human kidney cancers. *Free Radic Biol Med*, **27**, 695-703.
217. Young, O.*, et al.* (2010) Levels of oxidative damage and lipid peroxidation in thyroid neoplasia. *Head Neck*, **32**, 750-6.
218. Skrzydlewska, E.*, et al.* (2001) Antioxidant status and lipid peroxidation in colorectal cancer. *J Toxicol Environ Health A*, **64**, 213-22.
219. Karihtala, P.*, et al.* (2011) Divergent behaviour of oxidative stress markers 8-hydroxydeoxyguanosine (8-OHdG) and 4-hydroxy-2-nonenal (HNE) in breast carcinogenesis. *Histopathology*, **58**, 854-62.
220. Skrzydlewska, E.*, et al.* (2005) Lipid peroxidation and antioxidant status in colorectal cancer. *World J Gastroenterol*, **11**, 403-6.
221. Juric-Sekhar, G.*, et al.* (2009) Distribution of 4-hydroxynonenal-protein conjugates as a marker of lipid peroxidation and parameter of malignancy in astrocytic and ependymal tumors of the brain. *Tumori*, **95**, 762-8.
222. Marquez-Quinones, A.*, et al.* (2010) HNE-protein adducts formation in different pre-carcinogenic stages of hepatitis in LEC rats. *Free Radic Res*, **44**, 119-27.
223. Hu, W.*, et al.* (2002) The major lipid peroxidation product, trans-4-hydroxy-2-nonenal, preferentially forms DNA adducts at codon 249 of human p53 gene, a unique mutational hotspot in hepatocellular carcinoma. *Carcinogenesis*, **23**, 1781-9.
224. Feng, Z.*, et al.* (2003) Mutational spectrum and genotoxicity of the major lipid peroxidation product, trans-4-hydroxy-2-nonenal, induced DNA adducts in nucleotide excision repair-proficient and -deficient human cells. *Biochemistry*, **42**, 7848-54.
225. Feng, Z.*, et al.* (2004) Trans-4-hydroxy-2-nonenal inhibits nucleotide excision repair in human cells: a possible mechanism for lipid peroxidation-induced carcinogenesis. *Proc Natl Acad Sci U S A*, **101**, 8598-602.
226. Schaur, R.J. (2003) Basic aspects of the biochemical reactivity of 4-hydroxynonenal. *Mol Aspects Med*, **24**, 149-59.
227. Siems, W.G.*, et al.* (1997) Metabolic fate of 4-hydroxynonenal in hepatocytes: 1,4-dihydroxynonene is not the main product. *J Lipid Res*, **38**, 612-22.
228. Keller, J.*, et al.* (2015) "Twin peaks": searching for 4-hydroxynonenal urinary metabolites after oral administration in rats. *Redox Biol*, **4**, 136-48.

229. Alary, J.*, et al.* (1995) Mercapturic acid conjugates as urinary end metabolites of the lipid peroxidation product 4-hydroxy-2-nonenal in the rat. *Chem Res Toxicol*, **8**, 34-9.
230. Gueraud, F.*, et al.* (1999) In vivo involvement of cytochrome P450 4A family in the oxidative metabolism of the lipid peroxidation product trans-4-hydroxy-2-nonenal, using PPARalpha-deficient mice. *J Lipid Res*, **40**, 152-9.
231. Dalleau, S. (2013) Viande rouge et cancer colorectal: le 4-hydroxynonénal est-il le chaînon manquant? Université de Toulouse, Toulouse, vol. PhD, pp. 173.
232. Sporn, M.B.*, et al.* (2012) NRF2 and cancer: the good, the bad and the importance of context. *Nat Rev Cancer*, **12**, 564-71.
233. Li, N.*, et al.* (2004) Nrf2 is a key transcription factor that regulates antioxidant defense in macrophages and epithelial cells: protecting against the proinflammatory and oxidizing effects of diesel exhaust chemicals. *J Immunol*, **173**, 3467-81.
234. Jaramillo, M.C.*, et al.* (2013) The emerging role of the Nrf2-Keap1 signaling pathway in cancer. *Genes Dev*, **27**, 2179-91.
235. Al-Sawaf, O.*, et al.* (2015) Nrf2 in health and disease: current and future clinical implications. *Clin Sci (Lond)*, **129**, 989-99.
236. O'Connell, M.A.*, et al.* (2015) The Keap1/Nrf2 pathway in health and disease: from the bench to the clinic. *Biochem Soc Trans*, **43**, 687-9.
237. Espinosa-Diez, C.*, et al.* (2015) Antioxidant responses and cellular adjustments to oxidative stress. *Redox Biol*, **6**, 183-97.
238. Morgan, M.J.*, et al.* (2011) Crosstalk of reactive oxygen species and NF-kappaB signaling. *Cell Res*, **21**, 103-15.
239. Karin, M.*, et al.* (2001) AP-1: linking hydrogen peroxide and oxidative stress to the control of cell proliferation and death. *IUBMB Life*, **52**, 17-24.
240. Sen, C.K.*, et al.* (1996) Antioxidant and redox regulation of gene transcription. *FASEB J*, **10**, 709-20.
241. Fujioka, S.*, et al.* (2004) NF-kappaB and AP-1 connection: mechanism of NF-kappaB-dependent regulation of AP-1 activity. *Mol Cell Biol*, **24**, 7806-19.
242. Mercurio, F.*, et al.* (1999) NF-kappaB as a primary regulator of the stress response. *Oncogene*, **18**, 6163-71.
243. Li, H.*, et al.* (2013) Oxidative stress in vascular disease and its pharmacological prevention. *Trends Pharmacol Sci*, **34**, 313-9.
244. Zhang, D.D.*, et al.* (2004) Keap1 is a redox-regulated substrate adaptor protein for a Cul3-dependent ubiquitin ligase complex. *Mol Cell Biol*, **24**, 10941-53.
245. Cullinan, S.B.*, et al.* (2004) The Keap1-BTB protein is an adaptor that bridges Nrf2 to a Cul3-based E3 ligase: oxidative stress sensing by a Cul3-Keap1 ligase. *Mol Cell Biol*, **24**, 8477-86.
246. Kobayashi, A.*, et al.* (2004) Oxidative stress sensor Keap1 functions as an adaptor for Cul3-based E3 ligase to regulate proteasomal degradation of Nrf2. *Mol Cell Biol*, **24**, 7130-9.
247. Furukawa, M.*, et al.* (2005) BTB protein Keap1 targets antioxidant transcription factor Nrf2 for ubiquitination by the Cullin 3-Roc1 ligase. *Mol Cell Biol*, **25**, 162-71.
248. Moi, P.*, et al.* (1994) Isolation of NF-E2-related factor 2 (Nrf2), a NF-E2-like basic leucine zipper transcriptional activator that binds to the tandem NF-E2/AP1 repeat of the beta-globin locus control region. *Proc Natl Acad Sci U S A*, **91**, 9926-30.
249. McMahon, M.*, et al.* (2004) Redox-regulated turnover of Nrf2 is determined by at least two separate protein domains, the redox-sensitive Neh2 degron and the redox-insensitive Neh6 degron. *J Biol Chem*, **279**, 31556-67.
250. Rada, P.*, et al.* (2011) SCF/{beta}-TrCP promotes glycogen synthase kinase 3-dependent degradation of the Nrf2 transcription factor in a Keap1-independent manner. *Mol Cell Biol*, **31**, 1121-33.
251. Chowdhry, S.*, et al.* (2013) Nrf2 is controlled by two distinct beta-TrCP recognition motifs in its Neh6 domain, one of which can be modulated by GSK-3 activity. *Oncogene*, **32**, 3765-81.

252. Nioi, P.*, et al.* (2005) The carboxy-terminal Neh3 domain of Nrf2 is required for transcriptional activation. *Mol Cell Biol*, **25**, 10895-906.
253. Katoh, Y.*, et al.* (2001) Two domains of Nrf2 cooperatively bind CBP, a CREB binding protein, and synergistically activate transcription. *Genes Cells*, **6**, 857-68.
254. Zhu, M.*, et al.* (2001) Functional characterization of transcription regulators that interact with the electrophile response element. *Biochem Biophys Res Commun*, **289**, 212-9.
255. Wang, H.*, et al.* (2013) RXRalpha inhibits the NRF2-ARE signaling pathway through a direct interaction with the Neh7 domain of NRF2. *Cancer Res*, **73**, 3097-108.
256. Nakayama, K.I.*, et al.* (2006) Ubiquitin ligases: cell-cycle control and cancer. *Nat Rev Cancer*, **6**, 369-81.
257. Harder, B.*, et al.* (2015) Molecular mechanisms of Nrf2 regulation and how these influence chemical modulation for disease intervention. *Biochem Soc Trans*, **43**, 680-6.
258. Zipper, L.M.*, et al.* (2002) The Keap1 BTB/POZ dimerization function is required to sequester Nrf2 in cytoplasm. *J Biol Chem*, **277**, 36544-52.
259. Lo, S.C.*, et al.* (2006) Structure of the Keap1:Nrf2 interface provides mechanistic insight into Nrf2 signaling. *EMBO J*, **25**, 3605-17.
260. Itoh, K.*, et al.* (2004) Molecular mechanism activating Nrf2-Keap1 pathway in regulation of adaptive response to electrophiles. *Free Radic Biol Med*, **36**, 1208-13.
261. Ogura, T.*, et al.* (2010) Keap1 is a forked-stem dimer structure with two large spheres enclosing the intervening, double glycine repeat, and C-terminal domains. *Proc Natl Acad Sci U S A*, **107**, 2842-7.
262. Carmona-Aparicio, L.*, et al.* (2015) Overview of Nrf2 as Therapeutic Target in Epilepsy. *Int J Mol Sci*, **16**, 18348-67.
263. McMahon, M.*, et al.* (2006) Dimerization of substrate adaptors can facilitate cullin-mediated ubiquitylation of proteins by a "tethering" mechanism: a two-site interaction model for the Nrf2-Keap1 complex. *J Biol Chem*, **281**, 24756-68.
264. Tong, K.I.*, et al.* (2007) Different electrostatic potentials define ETGE and DLG motifs as hinge and latch in oxidative stress response. *Mol Cell Biol*, **27**, 7511-21.
265. Dinkova-Kostova, A.T.*, et al.* (2002) Direct evidence that sulfhydryl groups of Keap1 are the sensors regulating induction of phase 2 enzymes that protect against carcinogens and oxidants. *Proc Natl Acad Sci U S A*, **99**, 11908-13.
266. Zhang, D.D.*, et al.* (2003) Distinct cysteine residues in Keap1 are required for Keap1-dependent ubiquitination of Nrf2 and for stabilization of Nrf2 by chemopreventive agents and oxidative stress. *Mol Cell Biol*, **23**, 8137-51.
267. McMahon, M.*, et al.* (2010) Keap1 perceives stress via three sensors for the endogenous signaling molecules nitric oxide, zinc, and alkenals. *Proc Natl Acad Sci U S A*, **107**, 18838-43.
268. Nguyen, T.*, et al.* (2000) Transcriptional regulation of the antioxidant response element. Activation by Nrf2 and repression by MafK. *J Biol Chem*, **275**, 15466-73.
269. Motohashi, H.*, et al.* (2004) Small Maf proteins serve as transcriptional cofactors for keratinocyte differentiation in the Keap1-Nrf2 regulatory pathway. *Proc Natl Acad Sci U S A*, **101**, 6379-84.
270. Hirotsu, Y.*, et al.* (2012) Nrf2-MafG heterodimers contribute globally to antioxidant and metabolic networks. *Nucleic Acids Res*, **40**, 10228-39.
271. Itoh, K.*, et al.* (2003) Keap1 regulates both cytoplasmic-nuclear shuttling and degradation of Nrf2 in response to electrophiles. *Genes Cells*, **8**, 379-91.
272. Velichkova, M.*, et al.* (2005) Keap1 regulates the oxidation-sensitive shuttling of Nrf2 into and out of the nucleus via a Crm1-dependent nuclear export mechanism. *Mol Cell Biol*, **25**, 4501-13.
273. Rada, P.*, et al.* (2015) WNT-3A regulates an Axin1/NRF2 complex that regulates antioxidant metabolism in hepatocytes. *Antioxid Redox Signal*, **22**, 555-71.
274. Wu, T.*, et al.* (2014) Hrd1 suppresses Nrf2-mediated cellular protection during liver cirrhosis. *Genes Dev*, **28**, 708-22.

275. Hetz, C. (2012) The unfolded protein response: controlling cell fate decisions under ER stress and beyond. *Nat Rev Mol Cell Biol*, **13**, 89-102.
276. Hast, B.E.*, et al.* (2013) Proteomic analysis of ubiquitin ligase KEAP1 reveals associated proteins that inhibit NRF2 ubiquitination. *Cancer Res*, **73**, 2199-210.
277. Lau, A.*, et al.* (2010) A noncanonical mechanism of Nrf2 activation by autophagy deficiency: direct interaction between Keap1 and p62. *Mol Cell Biol*, **30**, 3275-85.
278. Ichimura, Y.*, et al.* (2013) Phosphorylation of p62 activates the Keap1-Nrf2 pathway during selective autophagy. *Mol Cell*, **51**, 618-31.
279. Hashimoto, K.*, et al.* (2016) TAK1 regulates the Nrf2 antioxidant system through modulating p62/ SQSTM1. *Antioxid Redox Signal*.
280. Jain, A.*, et al.* (2010) p62/SQSTM1 is a target gene for transcription factor NRF2 and creates a positive feedback loop by inducing antioxidant response element-driven gene transcription. *J Biol Chem*, **285**, 22576-91.
281. Lau, A.*, et al.* (2013) Arsenic-mediated activation of the Nrf2-Keap1 antioxidant pathway. *J Biochem Mol Toxicol*, **27**, 99-105.
282. Lau, A.*, et al.* (2013) Arsenic inhibits autophagic flux, activating the Nrf2-Keap1 pathway in a p62-dependent manner. *Mol Cell Biol*, **33**, 2436-46.
283. DeNicola, G.M.*, et al.* (2011) Oncogene-induced Nrf2 transcription promotes ROS detoxification and tumorigenesis. *Nature*, **475**, 106-9.
284. Tao, S.*, et al.* (2014) Oncogenic KRAS confers chemoresistance by upregulating NRF2. *Cancer Res*, **74**, 7430-41.
285. Zhang, Y.*, et al.* (2004) A strategy for cancer prevention: stimulation of the Nrf2-ARE signaling pathway. *Mol Cancer Ther*, **3**, 885-93.
286. Hayes, J.D.*, et al.* (2010) Cancer chemoprevention mechanisms mediated through the Keap1-Nrf2 pathway. *Antioxid Redox Signal*, **13**, 1713-48.
287. Hayes, J.D.*, et al.* (2014) The Nrf2 regulatory network provides an interface between redox and intermediary metabolism. *Trends Biochem Sci*, **39**, 199-218.
288. Lee, J.M.*, et al.* (2003) Identification of the NF-E2-related factor-2-dependent genes conferring protection against oxidative stress in primary cortical astrocytes using oligonucleotide microarray analysis. *J Biol Chem*, **278**, 12029-38.
289. Alnouti, Y.*, et al.* (2008) Tissue distribution, ontogeny, and regulation of aldehyde dehydrogenase (Aldh) enzymes mRNA by prototypical microsomal enzyme inducers in mice. *Toxicol Sci*, **101**, 51-64.
290. Boyle, J.J.*, et al.* (2011) Heme induces heme oxygenase 1 via Nrf2: role in the homeostatic macrophage response to intraplaque hemorrhage. *Arterioscler Thromb Vasc Biol*, **31**, 2685-91.
291. Maher, J.M.*, et al.* (2007) Oxidative and electrophilic stress induces multidrug resistance-associated protein transporters via the nuclear factor-E2-related factor-2 transcriptional pathway. *Hepatology*, **46**, 1597-610.
292. Sasaki, H.*, et al.* (2002) Electrophile response element-mediated induction of the cystine/glutamate exchange transporter gene expression. *J Biol Chem*, **277**, 44765-71.
293. Surh, Y.J. (2003) Cancer chemoprevention with dietary phytochemicals. *Nat Rev Cancer*, **3**, 768-80.
294. Yu, R.*, et al.* (1997) Activation of mitogen-activated protein kinases by green tea polyphenols: potential signaling pathways in the regulation of antioxidant-responsive element-mediated phase II enzyme gene expression. *Carcinogenesis*, **18**, 451-6.
295. Chen, C.*, et al.* (2000) Activation of antioxidant-response element (ARE), mitogen-activated protein kinases (MAPKs) and caspases by major green tea polyphenol components during cell survival and death. *Arch Pharm Res*, **23**, 605-12.
296. Yan, M.*, et al.* (2015) Standardized rosemary (Rosmarinus officinalis) extract induces Nrf2/sestrin-2 pathway in colon cancer cells. *Journal of Functional Food*, **13**, 137-147.

297. Cleasby, A.*, et al.* (2014) Structure of the BTB domain of Keap1 and its interaction with the triterpenoid antagonist CDDO. *PLoS One*, **9**, e98896.
298. Ellrichmann, G.*, et al.* (2011) Efficacy of fumaric acid esters in the R6/2 and YAC128 models of Huntington's disease. *PLoS One*, **6**, e16172.
299. Bomprezzi, R. (2015) Dimethyl fumarate in the treatment of relapsing-remitting multiple sclerosis: an overview. *Ther Adv Neurol Disord*, **8**, 20-30.
300. Rojo, A.I.*, et al.* (2012) Signaling pathways activated by the phytochemical nordihydroguaiaretic acid contribute to a Keap1-independent regulation of Nrf2 stability: Role of glycogen synthase kinase-3. *Free Radic Biol Med*, **52**, 473-87.
301. Ueda, K.*, et al.* (2008) Adaptive HNE-Nrf2-HO-1 pathway against oxidative stress is associated with acute gastric mucosal lesions. *Am J Physiol Gastrointest Liver Physiol*, **295**, G460-9.
302. Lopez-Bernardo, E.*, et al.* (2015) 4-Hydroxynonenal induces Nrf2-mediated UCP3 upregulation in mouse cardiomyocytes. *Free Radic Biol Med*, **88**, 427-38.
303. Siow, R.C.*, et al.* (2007) Modulation of antioxidant gene expression by 4-hydroxynonenal: atheroprotective role of the Nrf2/ARE transcription pathway. *Redox Rep*, **12**, 11-5.
304. Huang, Y.*, et al.* (2012) Anti-oxidative stress regulator NF-E2-related factor 2 mediates the adaptive induction of antioxidant and detoxifying enzymes by lipid peroxidation metabolite 4-hydroxynonenal. *Cell Biosci*, **2**, 40.
305. Dalleau, S.*, et al.* (2015) Positive selection of preneoplastic colonic cells exposed to 4-hydroxynonenal to the detriment of normal cells: involvement of Nrf2 in the promotion of colorectal cancer by meat? *Submitted to Oncogene*.
306. Arlt, A.*, et al.* (2013) Inhibition of the Nrf2 transcription factor by the alkaloid trigonelline renders pancreatic cancer cells more susceptible to apoptosis through decreased proteasomal gene expression and proteasome activity. *Oncogene*, **32**, 4825-35.
307. Gao, A.M.*, et al.* (2013) Chrysin enhances sensitivity of BEL-7402/ADM cells to doxorubicin by suppressing PI3K/Akt/Nrf2 and ERK/Nrf2 pathway. *Chem Biol Interact*, **206**, 100-8.
308. Gao, A.M.*, et al.* (2013) Apigenin sensitizes doxorubicin-resistant hepatocellular carcinoma BEL-7402/ADM cells to doxorubicin via inhibiting PI3K/Akt/Nrf2 pathway. *Carcinogenesis*, **34**, 1806-14.
309. Tang, X.*, et al.* (2011) Luteolin inhibits Nrf2 leading to negative regulation of the Nrf2/ARE pathway and sensitization of human lung carcinoma A549 cells to therapeutic drugs. *Free Radic Biol Med*, **50**, 1599-609.
310. Ren, D.*, et al.* (2011) Brusatol enhances the efficacy of chemotherapy by inhibiting the Nrf2-mediated defense mechanism. *Proc Natl Acad Sci U S A*, **108**, 1433-8.
311. Limonciel, A.*, et al.* (2014) A review of the evidence that ochratoxin A is an Nrf2 inhibitor: implications for nephrotoxicity and renal carcinogenicity. *Toxins (Basel)*, **6**, 371-9.
312. Giudice, A.*, et al.* (2006) Activation of the Nrf2-ARE signaling pathway: a promising strategy in cancer prevention. *Bioessays*, **28**, 169-81.
313. Niture, S.K.*, et al.* (2012) Nrf2 protein up-regulates antiapoptotic protein Bcl-2 and prevents cellular apoptosis. *J Biol Chem*, **287**, 9873-86.
314. Niture, S.K.*, et al.* (2012) Nrf2-induced antiapoptotic Bcl-xL protein enhances cell survival and drug resistance. *Free Radic Biol Med*, **57**, 119-31.
315. Hu, R.*, et al.* (2006) Cancer chemoprevention of intestinal polyposis in ApcMin/+ mice by sulforaphane, a natural product derived from cruciferous vegetable. *Carcinogenesis*, **27**, 2038-46.
316. Lev-Ari, S.*, et al.* (2005) Celecoxib and curcumin synergistically inhibit the growth of colorectal cancer cells. *Clin Cancer Res*, **11**, 6738-44.
317. Liby, K.T.*, et al.* (2010) Synthetic triterpenoids prolong survival in a transgenic mouse model of pancreatic cancer. *Cancer Prev Res (Phila)*, **3**, 1427-34.
318. Ramos-Gomez, M.*, et al.* (2001) Sensitivity to carcinogenesis is increased and chemoprotective efficacy of enzyme inducers is lost in nrf2 transcription factor-deficient mice. *Proc Natl Acad Sci U S A*, **98**, 3410-5.

319. Khor, T.O*., et al.* (2006) Nrf2-deficient mice have an increased susceptibility to dextran sulfate sodium-induced colitis. *Cancer Res*, **66**, 11580-4.
320. Solis, L.M*., et al.* (2010) Nrf2 and Keap1 abnormalities in non-small cell lung carcinoma and association with clinicopathologic features. *Clin Cancer Res*, **16**, 3743-53.
321. Hanada, N*., et al.* (2012) Methylation of the KEAP1 gene promoter region in human colorectal cancer. *BMC Cancer*, **12**, 66.
322. Rolfs, F*., et al.* (2015) Nrf2 Activation Promotes Keratinocyte Survival during Early Skin Carcinogenesis via Metabolic Alterations. *Cancer Res*, **75**, 4817-29.
323. Kang, K.A*., et al.* (2014) Epigenetic modification of Nrf2 in 5-fluorouracil-resistant colon cancer cells: involvement of TET-dependent DNA demethylation. *Cell Death Dis*, **5**, e1183.
324. Kroemer, G*., et al.* (2009) Classification of cell death: recommendations of the Nomenclature Committee on Cell Death 2009. *Cell Death Differ*, **16**, 3-11.
325. Green, D.R. (2011) *Means to An End: Apoptosis and Other Cell Death Mechanisms*. Cold Spring Harbor, New York.
326. Diamantis, A*., et al.* (2008) A brief history of apoptosis: from ancient to modern times. *Onkologie*, **31**, 702-6.
327. Kerr, J.F*., et al.* (1972) Apoptosis: a basic biological phenomenon with wide-ranging implications in tissue kinetics. *Br J Cancer*, **26**, 239-57.
328. Lamkanfi, M*., et al.* (2007) Caspases in cell survival, proliferation and differentiation. *Cell Death Differ*, **14**, 44-55.
329. Timmer, J.C*., et al.* (2007) Caspase substrates. *Cell Death Differ*, **14**, 66-72.
330. Galluzzi, L*., et al.* (2012) Molecular definitions of cell death subroutines: recommendations of the Nomenclature Committee on Cell Death 2012. *Cell Death Differ*, **19**, 107-20.
331. Wong, R.S. (2011) Apoptosis in cancer: from pathogenesis to treatment. *J Exp Clin Cancer Res*, **30**, 87.
332. Reed, J.C. (1997) Bcl-2 family proteins: regulators of apoptosis and chemoresistance in hematologic malignancies. *Semin Hematol*, **34**, 9-19.
333. Kroemer, G*., et al.* (2007) Mitochondrial membrane permeabilization in cell death. *Physiol Rev*, **87**, 99-163.
334. LaCasse, E.C*., et al.* (2008) IAP-targeted therapies for cancer. *Oncogene*, **27**, 6252-75.
335. Hengartner, M.O. (2000) The biochemistry of apoptosis. *Nature*, **407**, 770-6.
336. Schneider, P*., et al.* (2000) Apoptosis induced by death receptors. *Pharm Acta Helv*, **74**, 281-6.
337. Cerella, C*., et al.* (2014) From nature to bedside: pro-survival and cell death mechanisms as therapeutic targets in cancer treatment. *Biotechnol Adv*, **32**, 1111-22.
338. Fulda, S. (2009) Tumor resistance to apoptosis. *Int J Cancer*, **124**, 511-5.
339. Indran, I.R*., et al.* (2011) Recent advances in apoptosis, mitochondria and drug resistance in cancer cells. *Biochim Biophys Acta*, **1807**, 735-45.
340. Hanahan, D*., et al.* (2000) The hallmarks of cancer. *Cell*, **100**, 57-70.
341. Little, M.P. (2010) Cancer models, genomic instability and somatic cellular Darwinian evolution. *Biol Direct*, **5**, 19; discussion 19.
342. Webb, S.J*., et al.* (1999) Caspase-mediated cleavage of APC results in an amino-terminal fragment with an intact armadillo repeat domain. *FASEB J*, **13**, 339-46.
343. Qian, J*., et al.* (2010) The mitochondrial protein hTID-1 partners with the caspase-cleaved adenomatous polyposis cell tumor suppressor to facilitate apoptosis. *Gastroenterology*, **138**, 1418-28.
344. Liu, W*., et al.* (2011) Formation of 4-hydroxynonenal from cardiolipin oxidation: Intramolecular peroxyl radical addition and decomposition. *Free Radic Biol Med*, **50**, 166-78.
345. Raza, H*., et al.* (2006) 4-hydroxynonenal induces mitochondrial oxidative stress, apoptosis and expression of glutathione S-transferase A4-4 and cytochrome P450 2E1 in PC12 cells. *Toxicol Appl Pharmacol*, **216**, 309-18.

346. Liu, W.*, et al.* (2000) 4-hydroxynonenal induces a cellular redox status-related activation of the caspase cascade for apoptotic cell death. *J Cell Sci*, **113 (Pt 4)**, 635-41.
347. Ji, G.R.*, et al.* (2012) 4-Hydroxy-2-nonenal induces apoptosis by inhibiting AKT signaling in human osteosarcoma cells. *ScientificWorldJournal*, **2014**, 873525.
348. Jesenberger, V.*, et al.* (2002) Deadly encounter: ubiquitin meets apoptosis. *Nat Rev Mol Cell Biol*, **3**, 112-21.
349. Amaral, J.D.*, et al.* (2010) The role of p53 in apoptosis. *Discov Med*, **9**, 145-52.
350. Miyashita, T.*, et al.* (1995) Tumor suppressor p53 is a direct transcriptional activator of the human bax gene. *Cell*, **80**, 293-9.
351. Benchimol, S. (2001) p53-dependent pathways of apoptosis. *Cell Death Differ*, **8**, 1049-51.
352. Hemann, M.T.*, et al.* (2006) The p53-Bcl-2 connection. *Cell Death Differ*, **13**, 1256-9.
353. Li, J.*, et al.* (2006) Regulation of CD95 (Fas) expression and Fas-mediated apoptotic signaling in HLE B-3 cells by 4-hydroxynonenal. *Biochemistry*, **45**, 12253-64.
354. Kim, J.M.*, et al.* (1999) Involvement of the Fas/Fas ligand system in p53-mediated granulosa cell apoptosis during follicular development and atresia. *Endocrinology*, **140**, 2307-17.
355. Petak, I.*, et al.* (2000) p53 dependence of Fas induction and acute apoptosis in response to 5-fluorouracil-leucovorin in human colon carcinoma cell lines. *Clin Cancer Res*, **6**, 4432-41.
356. Shaulian, E.*, et al.* (2002) AP-1 as a regulator of cell life and death. *Nat Cell Biol*, **4**, E131-6.
357. Liu, J.*, et al.* (2005) Role of JNK activation in apoptosis: a double-edged sword. *Cell Res*, **15**, 36-42.
358. Salomoni, P.*, et al.* (2006) Daxx: death or survival protein? *Trends Cell Biol*, **16**, 97-104.
359. Yang, X.*, et al.* (1997) Daxx, a novel Fas-binding protein that activates JNK and apoptosis. *Cell*, **89**, 1067-76.
360. Zhang, J. (2015) Teaching the basics of autophagy and mitophagy to redox biologists--mechanisms and experimental approaches. *Redox Biol*, **4**, 242-59.
361. Levine, B.*, et al.* (2008) Autophagy in the pathogenesis of disease. *Cell*, **132**, 27-42.
362. Rubinstein, A.D.*, et al.* (2012) Life in the balance - a mechanistic view of the crosstalk between autophagy and apoptosis. *J Cell Sci*, **125**, 5259-68.
363. Mijaljica, D.*, et al.* (2011) Microautophagy in mammalian cells: revisiting a 40-year-old conundrum. *Autophagy*, **7**, 673-82.
364. Li, W.W.*, et al.* (2012) Microautophagy: lesser-known self-eating. *Cell Mol Life Sci*, **69**, 1125-36.
365. Sakai, M.*, et al.* (1982) Energy-dependent lysosomal wrapping mechanism (LWM) during autophagolysosome formation. *Histochemistry*, **76**, 479-88.
366. Sakai, M.*, et al.* (1989) Lysosomal movements during heterophagy and autophagy: with special reference to nematolysosome and wrapping lysosome. *J Electron Microsc Tech*, **12**, 101-31.
367. Sahu, R.*, et al.* (2011) Microautophagy of cytosolic proteins by late endosomes. *Dev Cell*, **20**, 131-9.
368. Kaushik, S.*, et al.* (2011) Chaperone-mediated autophagy at a glance. *J Cell Sci*, **124**, 495-9.
369. Klionsky, D.J. (2007) Autophagy: from phenomenology to molecular understanding in less than a decade. *Nat Rev Mol Cell Biol*, **8**, 931-7.
370. Zhang, J. (2013) Autophagy and Mitophagy in Cellular Damage Control. *Redox Biol*, **1**, 19-23.
371. Svenning, S.*, et al.* (2013) Selective autophagy. *Essays Biochem*, **55**, 79-92.
372. Reggiori, F.*, et al.* (2012) Selective types of autophagy. *Int J Cell Biol*, **2012**, 156272.
373. Abe, A.*, et al.* (2013) Harmol induces autophagy and subsequent apoptosis in U251MG human glioma cells through the downregulation of survivin. *Oncol Rep*, **29**, 1333-42.
374. Shaid, S.*, et al.* (2013) Ubiquitination and selective autophagy. *Cell Death Differ*, **20**, 21-30.
375. Stolz, A.*, et al.* (2014) Cargo recognition and trafficking in selective autophagy. *Nat Cell Biol*, **16**, 495-501.
376. Lamb, C.A.*, et al.* (2013) The autophagosome: origins unknown, biogenesis complex. *Nat Rev Mol Cell Biol*, **14**, 759-74.

377. Rubinsztein, D.C*., et al.* (2012) Mechanisms of autophagosome biogenesis. *Curr Biol*, **22**, R29-34.
378. Johansen, T*., et al.* (2011) Selective autophagy mediated by autophagic adapter proteins. *Autophagy*, **7**, 279-96.
379. Rogov, V*., et al.* (2014) Interactions between autophagy receptors and ubiquitin-like proteins form the molecular basis for selective autophagy. *Mol Cell*, **53**, 167-78.
380. Scherz-Shouval, R*., et al.* (2007) Oxidation as a post-translational modification that regulates autophagy. *Autophagy*, **3**, 371-3.
381. Scherz-Shouval, R*., et al.* (2007) Reactive oxygen species are essential for autophagy and specifically regulate the activity of Atg4. *EMBO J*, **26**, 1749-60.
382. Scherz-Shouval, R*., et al.* (2007) ROS, mitochondria and the regulation of autophagy. *Trends Cell Biol*, **17**, 422-7.
383. Zhang, C*., et al.* (2013) Calyxin Y induces hydrogen peroxide-dependent autophagy and apoptosis via JNK activation in human non-small cell lung cancer NCI-H460 cells. *Cancer Lett*, **340**, 51-62.
384. Levonen, A.L*., et al.* (2014) Redox regulation of antioxidants, autophagy, and the response to stress: implications for electrophile therapeutics. *Free Radic Biol Med*, **71**, 196-207.
385. Lee, J*., et al.* (2012) Autophagy, mitochondria and oxidative stress: cross-talk and redox signalling. *Biochem J*, **441**, 523-40.
386. Filomeni, G*., et al.* (2015) Oxidative stress and autophagy: the clash between damage and metabolic needs. *Cell Death Differ*, **22**, 377-88.
387. Deretic, V*., et al.* (2013) Autophagy in infection, inflammation and immunity. *Nat Rev Immunol*, **13**, 722-37.
388. Kalla, R*., et al.* (2014) Crohn's disease. *BMJ*, **349**, g6670.
389. Baumgart, D.C*., et al.* (2012) Crohn's disease. *Lancet*, **380**, 1590-605.
390. Henderson, P*., et al.* (2012) The role of autophagy in Crohn's disease. *Cells*, **1**, 492-519.
391. Nguyen, H.T*., et al.* (2013) Autophagy and Crohn's disease. *J Innate Immun*, **5**, 434-43.
392. Petkova, D.S*., et al.* (2013) IRGM in autophagy and viral infections. *Front Immunol*, **3**, 426.
393. Lapaquette, P*., et al.* (2010) Crohn's disease-associated adherent-invasive E. coli are selectively favoured by impaired autophagy to replicate intracellularly. *Cell Microbiol*, **12**, 99-113.
394. Saitoh, T*., et al.* (2008) Loss of the autophagy protein Atg16L1 enhances endotoxin-induced IL-1beta production. *Nature*, **456**, 264-8.
395. Bafica, A*., et al.* (2007) The IFN-inducible GTPase LRG47 (Irgm1) negatively regulates TLR4-triggered proinflammatory cytokine production and prevents endotoxemia. *J Immunol*, **179**, 5514-22.
396. Nishiumi, S*., et al.* (2012) Autophagy in the intestinal epithelium is not involved in the pathogenesis of intestinal tumors. *Biochem Biophys Res Commun*, **421**, 768-72.
397. Wang, L*., et al.* (2015) Heterozygous deletion of ATG5 in Apc(Min/+) mice promotes intestinal adenoma growth and enhances the antitumor efficacy of interferon-gamma. *Cancer Biol Ther*, **16**, 383-91.
398. Levy, J*., et al.* (2015) Intestinal inhibition of Atg7 prevents tumour initiation through a microbiome-influenced immune response and suppresses tumour growth. *Nat Cell Biol*, **17**, 1062-73.
399. Levy, J*., et al.* (2015) Autophagy, microbiota and intestinal oncogenesis. *Oncotarget*, **6**, 34067-8.
400. Gao, C*., et al.* (2010) Autophagy negatively regulates Wnt signalling by promoting Dishevelled degradation. *Nat Cell Biol*, **12**, 781-90.
401. Koehl, G.E*., et al.* (2010) Rapamycin inhibits oncogenic intestinal ion channels and neoplasia in APC(Min/+) mice. *Oncogene*, **29**, 1553-60.

402. Dodson, M.*, et al.* (2013) Inhibition of glycolysis attenuates 4-hydroxynonenal-dependent autophagy and exacerbates apoptosis in differentiated SH-SY5Y neuroblastoma cells. *Autophagy*, **9**, 1996-2008.
403. Hill, B.G.*, et al.* (2008) Unsaturated lipid peroxidation-derived aldehydes activate autophagy in vascular smooth-muscle cells. *Biochem J*, **410**, 525-34.
404. Haberzettl, P.*, et al.* (2013) Oxidized lipids activate autophagy in a JNK-dependent manner by stimulating the endoplasmic reticulum stress response. *Redox Biol*, **1**, 56-64.
405. Saez-Atienzar, S.*, et al.* (2014) The LRRK2 inhibitor GSK2578215A induces protective autophagy in SH-SY5Y cells: involvement of Drp-1-mediated mitochondrial fission and mitochondrial-derived ROS signaling. *Cell Death Dis*, **5**, e1368.
406. Krenn, M.A.*, et al.* (2015) Ferritin-stimulated lipid peroxidation, lysosomal leak, and macroautophagy promote lysosomal "metastability" in primary hepatocytes determining in vitro cell survival. *Free Radic Biol Med*, **80**, 48-58.
407. Csala, M.*, et al.* (2006) Endoplasmic reticulum: a metabolic compartment. *FEBS Lett*, **580**, 2160-5.
408. Mandl, J.*, et al.* (2013) Minireview: endoplasmic reticulum stress: control in protein, lipid, and signal homeostasis. *Mol Endocrinol*, **27**, 384-93.
409. Flores-Bellver, M.*, et al.* (2014) Autophagy and mitochondrial alterations in human retinal pigment epithelial cells induced by ethanol: implications of 4-hydroxy-nonenal. *Cell Death Dis*, **5**, e1328.
410. Csala, M.*, et al.* (2015) On the role of 4-hydroxynonenal in health and disease. *Biochim Biophys Acta*, **1852**, 826-38.
411. Zhang, C.*, et al.* (2008) Restoration of chaperone-mediated autophagy in aging liver improves cellular maintenance and hepatic function. *Nat Med*, **14**, 959-65.
412. Krohne, T.U.*, et al.* (2010) Effects of lipid peroxidation products on lipofuscinogenesis and autophagy in human retinal pigment epithelial cells. *Exp Eye Res*, **90**, 465-71.
413. Ma, H.*, et al.* (2011) Aldehyde dehydrogenase 2 (ALDH2) rescues myocardial ischaemia/reperfusion injury: role of autophagy paradox and toxic aldehyde. *Eur Heart J*, **32**, 1025-38.
414. Wu, B.*, et al.* (2016) Aldehyde dehydrogenase 2 activation in aged heart improves the autophagy by reducing the carbonyl modification on SIRT1. *Oncotarget*, **7**, 2175-88.
415. Ji, W.*, et al.* (2016) Aldehyde Dehydrogenase 2 Has Cardioprotective Effects on Myocardial Ischaemia/Reperfusion Injury via Suppressing Mitophagy. *Front Pharmacol*, **7**, 101.
416. Liang, A.*, et al.* (2012) Loss of glutathione S-transferase A4 accelerates obstruction-induced tubule damage and renal fibrosis. *J Pathol*, **228**, 448-58.
417. Krohne, T.U.*, et al.* (2010) Lipid peroxidation products reduce lysosomal protease activities in human retinal pigment epithelial cells via two different mechanisms of action. *Exp Eye Res*, **90**, 261-6.
418. Chang, N.C.*, et al.* (2010) Antagonism of Beclin 1-dependent autophagy by BCL-2 at the endoplasmic reticulum requires NAF-1. *EMBO J*, **29**, 606-18.
419. Wei, Y.*, et al.* (2008) JNK1-mediated phosphorylation of Bcl-2 regulates starvation-induced autophagy. *Mol Cell*, **30**, 678-88.
420. Zhou, L.*, et al.* (2013) Bcl-2-dependent upregulation of autophagy by sequestosome 1/p62 in vitro. *Acta Pharmacol Sin*, **34**, 651-6.
421. Adams, J.M.*, et al.* (2007) Bcl-2-regulated apoptosis: mechanism and therapeutic potential. *Curr Opin Immunol*, **19**, 488-96.
422. Martinou, J.C.*, et al.* (2011) Mitochondria in apoptosis: Bcl-2 family members and mitochondrial dynamics. *Dev Cell*, **21**, 92-101.
423. Strappazzon, F.*, et al.* (2011) Mitochondrial BCL-2 inhibits AMBRA1-induced autophagy. *EMBO J*, **30**, 1195-208.

424. Wirawan, E.*, et al.* (2010) Caspase-mediated cleavage of Beclin-1 inactivates Beclin-1-induced autophagy and enhances apoptosis by promoting the release of proapoptotic factors from mitochondria. *Cell Death Dis*, **1**, e18.
425. Djavaheri-Mergny, M.*, et al.* (2010) Cross talk between apoptosis and autophagy by caspase-mediated cleavage of Beclin 1. *Oncogene*, **29**, 1717-9.
426. Yousefi, S.*, et al.* (2006) Calpain-mediated cleavage of Atg5 switches autophagy to apoptosis. *Nat Cell Biol*, **8**, 1124-32.
427. Luo, S.*, et al.* (2007) Atg5 and Bcl-2 provide novel insights into the interplay between apoptosis and autophagy. *Cell Death Differ*, **14**, 1247-50.
428. Djavaheri-Mergny, M.*, et al.* (2006) NF-kappaB activation represses tumor necrosis factor-alpha-induced autophagy. *J Biol Chem*, **281**, 30373-82.
429. Djavaheri-Mergny, M.*, et al.* (2007) Regulation of autophagy by NFkappaB transcription factor and reactives oxygen species. *Autophagy*, **3**, 390-2.
430. Tasdemir, E.*, et al.* (2008) A dual role of p53 in the control of autophagy. *Autophagy*, **4**, 810-4.
431. Tasdemir, E.*, et al.* (2008) Regulation of autophagy by cytoplasmic p53. *Nat Cell Biol*, **10**, 676-87.
432. Maiuri, M.C.*, et al.* (2007) Self-eating and self-killing: crosstalk between autophagy and apoptosis. *Nat Rev Mol Cell Biol*, **8**, 741-52.
433. Shimizu, S.*, et al.* (2004) Role of Bcl-2 family proteins in a non-apoptotic programmed cell death dependent on autophagy genes. *Nat Cell Biol*, **6**, 1221-8.
434. Madden, D.T.*, et al.* (2007) A calpain-like protease inhibits autophagic cell death. *Autophagy*, **3**, 519-22.
435. Gonzalez-Polo, R.A.*, et al.* (2005) The apoptosis/autophagy paradox: autophagic vacuolization before apoptotic death. *J Cell Sci*, **118**, 3091-102.
436. Boya, P.*, et al.* (2005) Inhibition of macroautophagy triggers apoptosis. *Mol Cell Biol*, **25**, 1025-40.
437. Thorburn, A. (2014) Autophagy and its effects: making sense of double-edged swords. *PLoS Biol*, **12**, e1001967.
438. Aita, V.M.*, et al.* (1999) Cloning and genomic organization of beclin 1, a candidate tumor suppressor gene on chromosome 17q21. *Genomics*, **59**, 59-65.
439. Liang, X.H.*, et al.* (1999) Induction of autophagy and inhibition of tumorigenesis by beclin 1. *Nature*, **402**, 672-6.
440. Laddha, S.V.*, et al.* (2014) Mutational landscape of the essential autophagy gene BECN1 in human cancers. *Mol Cancer Res*, **12**, 485-90.
441. Yue, Z.*, et al.* (2003) Beclin 1, an autophagy gene essential for early embryonic development, is a haploinsufficient tumor suppressor. *Proc Natl Acad Sci U S A*, **100**, 15077-82.
442. Takamura, A.*, et al.* (2011) Autophagy-deficient mice develop multiple liver tumors. *Genes Dev*, **25**, 795-800.
443. Rosenfeldt, M.T.*, et al.* (2013) p53 status determines the role of autophagy in pancreatic tumour development. *Nature*, **504**, 296-300.
444. Yang, A.*, et al.* (2014) Autophagy is critical for pancreatic tumor growth and progression in tumors with p53 alterations. *Cancer Discov*, **4**, 905-13.
445. Qu, X.*, et al.* (2003) Promotion of tumorigenesis by heterozygous disruption of the beclin 1 autophagy gene. *J Clin Invest*, **112**, 1809-20.
446. White, E. (2015) The role for autophagy in cancer. *J Clin Invest*, **125**, 42-6.
447. White, E.*, et al.* (2015) Autophagy, Metabolism, and Cancer. *Clin Cancer Res*, **21**, 5037-46.
448. Sato, K.*, et al.* (2007) Autophagy is activated in colorectal cancer cells and contributes to the tolerance to nutrient deprivation. *Cancer Res*, **67**, 9677-84.
449. Li, J.*, et al.* (2009) Inhibition of autophagy by 3-MA enhances the effect of 5-FU-induced apoptosis in colon cancer cells. *Ann Surg Oncol*, **16**, 761-71.

450. Yang, S.*, et al.* (2011) Pancreatic cancers require autophagy for tumor growth. *Genes Dev*, **25**, 717-29.
451. Ma, X.H.*, et al.* (2011) Measurements of tumor cell autophagy predict invasiveness, resistance to chemotherapy, and survival in melanoma. *Clin Cancer Res*, **17**, 3478-89.
452. Cheong, H.*, et al.* (2012) Therapeutic targets in cancer cell metabolism and autophagy. *Nat Biotechnol*, **30**, 671-8.
453. Levy, J.M.*, et al.* (2014) Autophagy inhibition improves chemosensitivity in BRAF(V600E) brain tumors. *Cancer Discov*, **4**, 773-80.
454. Mortensen, M.*, et al.* (2011) The autophagy protein Atg7 is essential for hematopoietic stem cell maintenance. *J Exp Med*, **208**, 455-67.
455. White, E. (2013) Deconvoluting the context-dependent role for autophagy in cancer. *Nat Rev Cancer*, **12**, 401-10.
456. Smyth, M.J.*, et al.* (2001) Lymphocyte-mediated immunosurveillance of epithelial cancers? *Trends Immunol*, **22**, 409-11.
457. Dobbelstein, M.*, et al.* (1998) The large T antigen of simian virus 40 binds and inactivates p53 but not p73. *J Gen Virol*, **79 (Pt 12)**, 3079-83.
458. Zou, X.*, et al.* (2002) Cdk4 disruption renders primary mouse cells resistant to oncogenic transformation, leading to Arf/p53-independent senescence. *Genes Dev*, **16**, 2923-34.
459. Hanks, S.K. (1987) Homology probing: identification of cDNA clones encoding members of the protein-serine kinase family. *Proc Natl Acad Sci U S A*, **84**, 388-92.
460. Greider, C.W.*, et al.* (1985) Identification of a specific telomere terminal transferase activity in Tetrahymena extracts. *Cell*, **43**, 405-13.
461. Cawthon, R.M.*, et al.* (2003) Association between telomere length in blood and mortality in people aged 60 years or older. *Lancet*, **361**, 393-5.
462. Awasthi, Y.C.*, et al.* (2003) Role of 4-hydroxynonenal in stress-mediated apoptosis signaling. *Mol Aspects Med*, **24**, 219-30.
463. Schaeferhenrich, A.*, et al.* (2003) Human adenoma cells are highly susceptible to the genotoxic action of 4-hydroxy-2-nonenal. *Mutat Res*, **526**, 19-32.
464. Klinder, A.*, et al.* (2007) Fecal water as a non-invasive biomarker in nutritional intervention: comparison of preparation methods and refinement of different endpoints. *Nutr Cancer*, **57**, 158-67.
465. Pearson, J.R.*, et al.* (2009) Diet, fecal water, and colon cancer--development of a biomarker. *Nutr Rev*, **67**, 509-26.
466. Lapre, J.A.*, et al.* (1992) Diet-induced increase of colonic bile acids stimulates lytic activity of fecal water and proliferation of colonic cells. *Carcinogenesis*, **13**, 41-4.
467. Glinghammar, B.*, et al.* (1997) Shift from a dairy product-rich to a dairy product-free diet: influence on cytotoxicity and genotoxicity of fecal water--potential risk factors for colon cancer. *Am J Clin Nutr*, **66**, 1277-82.
468. Monleon, D.*, et al.* (2009) Metabolite profiling of fecal water extracts from human colorectal cancer. *NMR Biomed*, **22**, 342-8.
469. Chandra, S.H.*, et al.* (2012) A common role for various human truncated adenomatous polyposis coli isoforms in the control of beta-catenin activity and cell proliferation. *PLoS One*, **7**, e34479.
470. Rowan, A.J.*, et al.* (2000) APC mutations in sporadic colorectal tumors: A mutational "hotspot" and interdependence of the "two hits". *Proc Natl Acad Sci U S A*, **97**, 3352-7.
471. Cheung, K.L.*, et al.* (2012) Nrf2 knockout enhances intestinal tumorigenesis in Apc(min/+) mice due to attenuation of anti-oxidative stress pathway while potentiates inflammation. *Mol Carcinog*, **53**, 77-84.
472. Kang, M.I.*, et al.* (2004) Scaffolding of Keap1 to the actin cytoskeleton controls the function of Nrf2 as key regulator of cytoprotective phase 2 genes. *Proc Natl Acad Sci U S A*, **101**, 2046-51.

473. Ji, L.*, et al.* (2014) Correlation of Nrf2, NQO1, MRP1, cmyc and p53 in colorectal cancer and their relationships to clinicopathologic features and survival. *Int J Clin Exp Pathol*, **7**, 1124-31.
474. Espina, V.*, et al.* (2006) Laser capture microdissection. *Methods Mol Biol*, **319**, 213-29.
475. Long, M.*, et al.* (2015) Nrf2-dependent suppression of azoxymethane/dextran sulfate sodium-induced colon carcinogenesis by the cinnamon-derived dietary factor cinnamaldehyde. *Cancer Prev Res (Phila)*, **8**, 444-54.
476. Trivedi, P.P.*, et al.* (2016) Melatonin modulated autophagy and Nrf2 signaling pathways in mice with colitis-associated colon carcinogenesis. *Mol Carcinog*, **55**, 255-67.
477. Sakitani, K.*, et al.* (2015) Inhibition of autophagy exerts anti-colon cancer effects via apoptosis induced by p53 activation and ER stress. *BMC Cancer*, **15**, 795.
478. Guba, M.*, et al.* (2005) Dosing of rapamycin is critical to achieve an optimal antiangiogenic effect against cancer. *Transpl Int*, **18**, 89-94.
479. Woodrum, C.*, et al.* (2010) Comparison of three rapamycin dosing schedules in A/J Tsc2+/- mice and improved survival with angiogenesis inhibitor or asparaginase treatment in mice with subcutaneous tuberous sclerosis related tumors. *J Transl Med*, **8**, 14.
480. Ng, S.S.*, et al.* (2001) Wortmannin inhibits pkb/akt phosphorylation and promotes gemcitabine antitumor activity in orthotopic human pancreatic cancer xenografts in immunodeficient mice. *Clin Cancer Res*, **7**, 3269-75.
481. Ohta, T.*, et al.* (2006) Inhibition of phosphatidylinositol 3-kinase increases efficacy of cisplatin in in vivo ovarian cancer models. *Endocrinology*, **147**, 1761-9.
482. Wagner, M.*, et al.* (2009) Effective treatment of advanced colorectal cancer by rapamycin and 5-FU/oxaliplatin monitored by TIMP-1. *J Gastrointest Surg*, **13**, 1781-90.
483. Wendel, H.G.*, et al.* (2006) Determinants of sensitivity and resistance to rapamycin-chemotherapy drug combinations in vivo. *Cancer Res*, **66**, 7639-46.
484. Wang, X.W.*, et al.* (2014) Targeting mTOR network in colorectal cancer therapy. *World J Gastroenterol*, **20**, 4178-88.
485. Crunkhorn, S. (2015) Cancer: mTOR inhibition curbs colorectal cancer. *Nat Rev Drug Discov*, **14**, 14-5.
486. Zaytseva, Y.Y.*, et al.* (2012) mTOR inhibitors in cancer therapy. *Cancer Lett*, **319**, 1-7.
487. Akter, R.*, et al.* (2012) Wortmannin induces MCF-7 breast cancer cell death via the apoptotic pathway, involving chromatin condensation, generation of reactive oxygen species, and membrane blebbing. *Breast Cancer (Dove Med Press)*, **4**, 103-13.
488. Teranishi, F.*, et al.* (2009) Phosphoinositide 3-kinase inhibitor (wortmannin) inhibits pancreatic cancer cell motility and migration induced by hyaluronan in vitro and peritoneal metastasis in vivo. *Cancer Sci*, **100**, 770-7.
489. Yun, J.*, et al.* (2012) Wortmannin inhibits proliferation and induces apoptosis of MCF-7 breast cancer cells. *Eur J Gynaecol Oncol*, **33**, 367-9.
490. Li, J.*, et al.* (2012) Wortmannin reduces metastasis and angiogenesis of human breast cancer cells via nuclear factor-kappaB-dependent matrix metalloproteinase-9 and interleukin-8 pathways. *J Int Med Res*, **40**, 867-76.
491. Tang, J.C.*, et al.* (2016) Autophagy in 5-Fluorouracil Therapy in Gastrointestinal Cancer: Trends and Challenges. *Chin Med J (Engl)*, **129**, 456-463.
492. Su, Y.*, et al.* (2005) The diversity expression of p62 in digestive system cancers. *Clin Immunol*, **116**, 118-23.
493. Park, J.M.*, et al.* (2013) Prognostic impact of Beclin 1, p62/sequestosome 1 and LC3 protein expression in colon carcinomas from patients receiving 5-fluorouracil as adjuvant chemotherapy. *Cancer Biol Ther*, **14**, 100-7.
494. Zhao, G.*, et al.* (2016) Curcumin induces autophagy, inhibits proliferation and invasion by downregulating AKT/mTOR signaling pathway in human melanoma cells. *Oncol Rep*, **35**, 1065-74.
495. Guo, S.*, et al.* (2016) Curcumin activates autophagy and attenuates oxidative damage in EA.hy926 cells via the Akt/mTOR pathway. *Mol Med Rep*, **13**, 2187-93.

496. Ko, C.P.*, et al.* (2015) Pterostilbene induce autophagy on human oral cancer cells through modulation of Akt and mitogen-activated protein kinase pathway. *Oral Oncol*, **51**, 593-601.
497. Wang, Y.*, et al.* (2012) Pterostilbene simultaneously induces apoptosis, cell cycle arrest and cyto-protective autophagy in breast cancer cells. *Am J Transl Res*, **4**, 44-51.
498. Patel, M.B.*, et al.* (2012) Curcumin Induces Human Colon Cancer Cell death via p62/SQSTM1 Degradation, Phospho-ERK Up-regulation and Ceramide Generation. *Current Trends in Biotechnology and Pharmacy*, **6**, 407-417.
499. Jung, K.A.*, et al.* (2013) Enhanced 4-hydroxynonenal resistance in KEAP1 silenced human colon cancer cells. *Oxid Med Cell Longev*, **2013**, 423965.
500. Inokuma, T.*, et al.* (2009) Oxidative stress and tumor progression in colorectal cancer. *Hepatogastroenterology*, **56**, 343-7.
501. Sreevalsan, S.*, et al.* (2013) Reactive Oxygen Species and Colorectal Cancer. *Curr Colorectal Cancer Rep*, **9**, 350-357.
502. Oslowski, C.M.*, et al.* (2011) Measuring ER stress and the unfolded protein response using mammalian tissue culture system. *Methods Enzymol*, **490**, 71-92.
503. Cumaoglu, A.*, et al.* (2014) Redox status related activation of endoplasmic reticulum stress and apoptosis caused by 4-hydroxynonenal exposure in INS-1 cells. *Toxicol Mech Methods*, **24**, 362-7.